L-Università ta' Malta

Identification and Functional Characterisation of Genes Linked to Motor Neuron Disease

A dissertation submitted to the Faculty of Medicine and Surgery, University of Malta in partial fulfilment of the requirements for the degree of
Doctor of Philosophy

Rebecca Borg

2021

Supervisor:
Prof. Ruben J Cauchi, D.Phil. (Oxon).

Department of Physiology & Biochemistry
Faculty of Medicine & Surgery

Centre for Molecular Medicine & Biobanking

L-Università ta' Malta

University of Malta Library – Electronic Thesis & Dissertations (ETD) Repository

The copyright of this thesis/dissertation belongs to the author. The author's rights in respect of this work are as defined by the Copyright Act (Chapter 415) of the Laws of Malta or as modified by any successive legislation.

Users may access this full-text thesis/dissertation and can make use of the information contained in accordance with the Copyright Act provided that the author must be properly acknowledged. Further distribution or reproduction in any format is prohibited without the prior permission of the copyright holder.

To auntie Twan

forever in our hearts and memories

Acknowledgements

Foremost, I would like to express my sincere gratitude to my supervisor Prof. Ruben Cauchi. His professional advice and guidance in the completion of this dissertation have been indispensable. Furthermore, his continuous accessibility, encouragement and support have been essential for me to persevere throughout this accomplishment. I am especially grateful for his endless patience and motivation towards the final months of my PhD. Thank you for inspiring me with your immense enthusiasm, dedication and passion towards science for the last 9 years, which have without a doubt greatly influenced my scientific career so far.

I would like to express my appreciation to my colleagues and friends at the University of Malta ALS/MND lab, especially to Maia Farrugia Wismayer, Rebecca Cacciottolo and Matthew Camilleri. This project would not have been successful without their unwavering help and encouragement. Infinite thanks for shared insights, materials, tips and laughs.

I am immensely grateful to my colleagues at the Molecular Diagnostics lab, especially Dr Graziella Zahra and Team A for their support and patience especially throughout the last months.

I would like to thank my parents, loved ones and friends for their unconditional love and encouragement. Your continuous support helped me stay focused and pushed me to never give up. Lastly, I am profoundly grateful to my fiancé, Karl for always pushing me to go further, for always believing in me and for reassuring me whenever I was disheartened by this challenging achievement. I would not have come this far without you!

TABLE OF CONTENTS

List of figures:

List of Tables

List of Abbreviations

ΔΔCt	double delta Ct
AAV	adeno-associated virus
AD	autosomal-dominant
ADL	activities of daily living
Ago	argonaute
ALS	Amyotrophic Lateral Sclerosis
ALS2	alsin 2
ALSFRS-R	ALS Functional Rating Scale - Revised
ANG	angiogenin
ANXA11	annexin A11
APOE	apoliprotein E
AR	autosomal-recessive
Arp-1	actin related protein 1
ASO	antisense oligonucleotide
ATG	autophagy-related
ATP	adenosine triphosphate
ATXN2	ataxin 2
BAM	binary sequence alignment
BDNF	brain-derived neurotrophic factors
BiPAP	bilevel positive airway pressure
BMI	body mass index
C21orf2	chromosome 21 open reading frame 2
C9orf72	chromosome 9 open reading frame 72
CAPN14	calpain 14
CAP-Gly	glycine-rich cytoskeleton-associated protein
CapZ	actin-capping protein
Cas	CRISPR-associated system
CCD	coiled-coil domain
CCNF	cyclin-F
CHCHD10	coiled-coil-helix-coiled-coil-helix domain-containing protein 10
CHMP2B	charged multivesicular body protein 2B
CK	creatine kinase

CMT	Charcot-Marie-Tooth
CMT2	Charcot-Marie-Tooth type 2
CNS	central nervous system
Co-IP	co-immunoprecipitation
CRISPR	clustered regularly interspaced short palindromic repeats
CSF	cerebrospinal fluid
CT	cycle threshold
CYLD	CYLD lysine 63 deubiquitinase
DAO	d-amino acid oxidase
DCTN1	dynactin 1
DDX20	DEAD-box helicase 20
DENN	differently expressed in neoplastic versus normal cells
Dlg	discs large
DNAJC7	DnaJ heat shock protein (Hsp40) member C7
DPR	dipeptide repeat aggregates
dsRNA	double-stranded RNA
ELP3	elongator acetyltransferase complex subunit 3
EMA	European Medicines Agency
EMF	electromagnetic fields
EPHA4	ephron type-A receptor 4 precursor
ER	endoplastic reticulum
ERBB4	erb-b2 receptor tyrosine kinase 4
ESCRT-III	endosomal sorting complex required for transport III
EWSR1	ewing sarcoma breakpoint region 1
F-actin	actin filaments
fALS	familial Amyotrophic Lateral Sclerosis
FIG4	FIG4 phosphoinositide 5-phosphatase
FTD	Frontotemporal Dementia
FUS	fused in sarcoma
GATK	Genome Analysis Toolkit
gDNA	genomic DNA
GDNF	glial cell line derived neurotrophic factor
GDP	guanosine diphosphate

GDP guanosine diphoshphate
GEF guanine nucleotide exchange factor
GGNBP2 gametogenetin binding protein 2
GLE1 GLE1 RNA export mediator
GLT8D1 glycosyltransferase 8 domain containing 1
gnomAD Genome Aggregation Database
GOF gain-of-function
GPX3 glutathione peroxidase 3
GRN granulin precusor
GTP guanosine triphosphate
GWAS genome-wide association studies
Hap1 Huntington associated protein 1
HC housekeeping gene control
HE housekeeping gene experimental
HFE homeostatic iron regulator protein
HGDP Human Genome Diversity Panel
HHV Human Herpes Virus
HIV Human Immunodeficiency Virus
HNRNPA1 heterogenous nuclear ribonucleoprotein A1
HNRNPA2B1 heterogenous nuclear ribonucleoprotein A2/B1
HSP Hereditary Spastic Paraplegia
HSP6 Hereditary Spastic Paraplegia type 6
ICD inter-coiled-coil domain
IF intermediate filament
IGF-1 insulin-like growth factor 1
indel insertion/deletion
iPSCs induced pluripotent stem cells
IR inverted repeat
KIF5A kinesin family member 5A
KIFAP3 kinesin associated protein 3
LASER Locating Ancestry from SEquence Reads
LMN lower motor neuron disease
LOF loss-of-function

MAF minor allele frequency

MAPT microtubule associated protein Tau

MATR3 matrin 3

Meta-SVM meta-analytic support vector machine

miRNA microRNA

MND Motor Neuron Disease

MOBP myelin associated oligodendrocyte basic protein

MRC Medical Research Council

mRNA messenger RNA

MS mass spectroscopy

NCBI National Center for Biotechnology Information

NEFL neurofilament light

NEHL neurofilament heavy

NEFH neurofilament heavy chain

NEK1 never in mitosis gene A-related kinase 1

NES nuclear export signal

NFf-κB nuclear factor kappa-B

NFL light neurofilament

NGS next generation sequencing

NIPA1 Pradar-Willi/Angelman syndrome region protein 1 (NIPA1)

NLS nuclear localization signal

NMJ neuromuscular junction

OMIM Online Mendelian Inheritance in Man

OPTN optineurin

PAM protospacer adjacent motif

PBP progressive bulbar palsy

PBS phosphate buffered saline

PBT PBS + 0.1% Triton X-100

PC principal components

PCA principal component analysis

PD Parkinson's Disease

PFN1 profilin 1

PI(3,5)P2 phosphatidylinositol **3**,**5**-bisphosphate

PLS	Primary Lateral Sclerosis
PMA	Progressive Muscular Atrophy
PRALINE	PRofile ALIgNEment
PRPH	peripherin
PSP	Progressive Supranuclear Palsy
qPCR	quantitative polymerase chain reaction (qPCR)
RAN	repeat-associated non-AUG translation
RF	recombinant frequency
RGG	Arg-Gly-Gly
RISC	RNA-induced silencing complex
RNA	ribonucleic acid
RNAi	RNA interference
RNase A	ribonuclease A
RRMs	RNA recognition motifs
RVB	rare-variant burden analyses
S.E.M.	standard error of the mean
sALS	sporadic amyotrophic lateral sclerosis
SARM1	sterile alpha and TIR motif-containing 1
SCA2	Spinocerebellar Ataxia type 2
SCFD1	Sec1 family domain-containing protein 1
SDS-PAGE	sulfate-polyacrylamide gel electrophoresis
SETX	senataxin
shRNA	small hairpin RNA
Sig-1R	Sigma-1 receptor
SIGMAR1	sigma non-opioid intracellular receptor 1
siRNAs	small interfering RNAs
SM	SecI/Mun18
SMA	Spinal Muscular Atrophy
SMN	survival of motor neuron
SNARE	soluble N-ethlymaleimide-sensitive factor attachment protein receptors
snRNP	small nuclear ribonucleoprotein
SNV	single nucleotide variant
SOD1	superoxide dismutase 1

SPAST	spastin
SPG11	spastic paraplegia 1
SQSTM1	sequestosome 1
SS18L1	synovial sarcoma translocation gene on chromosome 18-like 1
STR	short tandem repeats
SV	structural variant
SVM	support vector machine
TAF15	TATA-box binding protein-associated factor 15
TARDBP	transactive response DNA-binding protein
TBK1	TANK-binding kinase 1
TC	tested gene control
TCA	tricarboxylic acid
TDP-43	transactive response DNA binding protein 43kDa
TE	tested gene experimental
TIA1	T-cell restricted intracellular antigen 1
TMEM106B	transmembrane protein 106B
TMV	tracheostomy mechanical ventilation
TNIP1	TNFAIP3 interacting protein 1
TUBA4A	tubulin alpha 4a
U.S. FDA	United States Food and Drug Administration
UAS	upstream activating sequence
UBA	ubiquitin-associated
UBL	ubiquitin-like
UBQLN1	ubiquilin 1
UMN	upper motor neuron
UNC13A	unc-13 homolog A
UPR	unfolded protein response
UPS	ubiquitin proteasome system
UREC	University Research Ethics Committee
UTR	untranslated regions
VAPB	vesicle-associated membrane protein associated protein B
VCF	variant call format
VCP	valosin-containing protein

VDRC	Vienna Drosophila Resource Center
VEGF	vascular endothelial growth factor A
WES	whole-exome sequencing
WGS	whole-genome sequencing
XD	X-linked-dominant
ZNF	zinc-finger motif
ZNF512B	zinc finger protein 512B

ABSTRACT

Motor neuron disorders are neurological conditions generally characterized by degeneration of motor neurons in the brain and spinal cord leading to skeletal muscle atrophy. Amyotrophic lateral sclerosis is the most common form of MND, comprising 80-90% of cases. Owing to the success of large-scale genome-wide studies and technical advances in next generation sequencing, numerous genetic associations that predispose to the disease or modify disease progression have been identified, greatly influencing our understanding of this catastrophic disorder. Malta is home to an isolated population that is genetically homogeneous, a factor that is favourable to mine for founder ALS-associated genes. To this end, a unique Malta ALS/MND Register and BioBank was set up and presently holds biological samples of Maltese ALS patients and age-sex-region-matched controls. A high percentage of ALS patients are males and a significant amount experienced occupation-associated physical exertion. Several other patient population aspects are similar to those of neighbouring European countries, however a discrepancy in the Maltese genetic architecture is evident. In effect, the Maltese ALS patient cohort was found to be negative for deleterious variants in the four major ALS genes, *C9orf72*, *SOD1*, *TARDBP* and *FUS*. However, deleterious alleles were detected in minor, ALS genes, including *ALS2*, *DAO*, *DCTN1*, *ERBB4*, *SARM1*, *SETX*, *SCFD1* and *SPG11*, genetically determining up to 40% of apparent sporadic ALS cases within the Maltese cohort. The effect of select damaging genes was analysed by generating animal models of ALS in an attempt to replicate disease phenotypes to strengthen the molecular understanding of pathogenic mechanisms associated with disease. As a result, the effects of *DCTN1* and *SCFD1* knockdown in *Drosophila* underscore a requirement of both genes for viability and normal neuromuscular function, which in part mimic the phenotypes observed in select Maltese ALS patients. Functional characterisation of population specific genes provides fundamental insights into the cellular pathways underpinning motor neuron degeneration in ALS. In turn, this facilitates the identification of therapeutic targets, particularly those directed towards personalised medicine.

CHAPTER 1

INTRODUCTION

1.1 MOTOR NEURON DISEASE

Motor neuron disease (MND) is the umbrella term for a subset of neurological disorders, which intermittently lead to progressive neuronal degeneration and atrophy of skeletal muscles. It is often challenging to distinguish between these rare, high morbidity and mortality disorders due to overlapping clinical pictures, which often lead to diagnostic dilemmas (RUTTER-LOCHER *et al.* 2016). Amyotrophic lateral sclerosis (ALS) is the most common form of MND, comprising 80-90% of cases and is characterised by loss of both upper and lower motor neurons (ROMAN 1996). Other less common sub-types are defined by the motor neurons primarily affected. Approximately 25% of MND cases are classified as progressive bulbar palsy (PBP), where symptoms are restricted to the bulbar musculature at presentation, including swallowing and speech defects (CERERO LAPIEDRA *et al.* 2002). Patients that present with pure lower motor neuron involvement are considered to have the progressive muscular atrophy (PMA) phenotype, which comprises about 10% of MND cases (VISSER *et al.* 2007). Finally, less that 5% of MND cases are classified as primary lateral sclerosis (PLS), with pure upper motor neuron involvement (PRINGLE *et al.* 1992). Nevertheless, most cases of non-ALS MND, tend to progress with additional motor neuron signs over time and eventually develop into ALS (FLOETER AND MILLS 2009; KIM *et al.* 2009; KARAM *et al.* 2010).

1.2 CLINICAL PRESENTATION

ALS has a heterogenous clinical presentation that is characterized by motor neuron degeneration which progresses with rapid muscle weakness, ultimately culminating in paralysis and most frequently respiratory failure (RAVITS AND LA SPADA 2009). Diagnosis is regularly based on conformity to revised El Escorial criteria for diagnostic certainty, which range from 'suspected ALS' to 'definite ALS' (**Table 1**) (BROOKS 1994; BROOKS *et al.* 2000). Diagnostic criteria depend on the degree and distribution of upper and lower motor neuron symptoms, complemented by neurophysiological (electromyography) and imaging data to exclude ALS mimics or variants. In line with this, ALS classification also takes into account the clinical presentation, or the phenotype, at the time of diagnosis (**Table 2**) (AL-CHALABI *et al.* 2016).

Bulbar onset typically manifests as the inability to control oropharyngeal muscles resulting in dysarthria, dysphagia and hypersalivation. In some cases, superficial neck and back muscles may also be affected. Signs of upper motor neuron involvement in this region may include facial weakness, jaw clonus and uncoordinated tongue movements (SAUNDERS 2002). Spinal onset of the disease, which is seen in the majority of cases (66%), can affect the cervical, thoracic and lumbar body regions. Most patients with sporadic onset present with symptoms in one limb, with the dominant side being commonly affected with onset in the upper limbs. The predominant symptom of spinal involvement is weakness and fatigue. Pure lower motor neuron involvement manifests with hyporeflexia and hypotonia. On the other hand, hyperreflexia and hypertonia occur with coexistence of upper motor neuron defects. Stiffness and less frequently, painful spasms may also be present in the latter. A combination of findings is a distinguishing feature of the disease and delineates a classic ALS phenotype (TALBOTT *et al.* 2016).

Degeneration of lower motor neurons in the cervical spinal cord is synonymous with hand or shoulder weakness which often hinders motor tasks associated with these regions such as hand gripping and lifting. The presence of Hoffman's sign (involuntary flexion of the thumb) as well as muscle spasticity indicate the involvement of upper motor neurons (BARMAN 2010). Lower motor neuron lesions in the thoracic spinal region leads to paraspinal muscle weakness often demonstrated by a lordotic posture and head drop (UMAPATHI *et al.* 2002). Upper motor neuron dysfunction in this area is very subtle and generally leads to loss of superficial abdominal reflexes. Lumbar lower motor neuron weakness is often characterized by footdrop and mobility difficulties, whilst upper motor neuron involvement is commonly demonstrated by a dragging gait and can be verified with a positive Babinski sign (VAN GIJN 1995). Occasionally both spinal and bulbar functions are simultaneously affected at onset. This may manifest with diaphragm weakness, resulting in respiratory dysfunction including shortness of breath and orthopnoea. Interestingly, oculomotor neurons that innervate the eye and sphincter muscles are generally spared throughout the course of the disease (BROWN AND AL-CHALABI 2017). Despite the overall predominance of spinal onset ALS, bulbar onset ALS is more prevalent in women (LONGINETTI *et al.* 2018; KORNER *et al.* 2019), patients with coexisting cognitive impairment (DE MARCHI *et al.* 2019) and old age at onset (ZHOU *et al.* 2018).

Table 1 El Escorial revised criteria for diagnosis of ALS.

	Definite ALS	Probable ALS	Laboratory-supported probable ALS	Possible ALS	Suspected ALS
El Escorial criteria -revised (BROOKS *et al.* 2000)	• UMN + LMN signs in bulbar region and at least two spinal regions • UMN + LMN signs in three spinal regions	• UMN + LMN signs in at least two regions, with some UMN signs rostral to LMN signs	• UMN + LMN signs in one region • UMN signs alone in one region and LMN signs in at least two regions as defined by electrophysiological criteria	• UMN + LMN signs found together in one region • UMN signs found alone in two regions or LMN signs rostral to UMN signs	• LMN signs only

LMN= lower motor neuron, UMN= upper motor neuron .

Table 2 Lower and upper motor neuron signs associated with ALS.

ALS Type	Region	Lower Motor Neuron signs	Upper Motor Neuron signs
Bulbar	Medulla	Dysarthria, dysphagia, hypersalivation, tongue weakness, reduced palate elevation	Hyperactive jaw jerk, jaw clonus, forced yawning, uncoordinated tongue movements, facial weakness
Spinal	Cervical spine	Flail arm, difficulty in motor tasks such as gripping and lifting	Spasticity, Hoffman's sign
	Thoracic spine	Weakness and atrophy in trunk and paraspinal muscles - head drop, lordotic posture	Subtle loss of superficial abdominal reflexes
	Lumbar spine	Distal weakness - footdrop Proximal weakness - mobility difficulty	Babinski sign, spastic dragging gait

1.3 EPIDEMIOLOGY

Globally, ALS is diagnosed in 0.6 to 3.8 individuals per 100,000 people each year. Incidence of ALS increases from 2.1 to 3.8 per 100,000 person-years when taking into consideration ALS cases in Europe only (BENJAMINSEN *et al.* 2018; LONGINETTI *et al.* 2018; ZHOU *et al.* 2018; JUN *et al.* 2019; LEIGHTON *et al.* 2019; PALESE *et al.* 2019; ROSE *et al.* 2019; TURGUT *et al.* 2019). In addition, an improved ALS ascertainment as well as an extended human lifespan that allows for increased manifestation of MND, has led to an apparent rise in ALS incidence from previous years (BENJAMINSEN *et al.* 2018; LEIGHTON *et al.* 2019; TURGUT *et al.* 2019). Several population-based studies established a prevalence of ALS between 4.1 and 8.4 cases per 100,000 people, which in some countries like the United States, may be influenced by ethnicity (MEHTA *et al.* 2018). Both incidence and prevalence of ALS increase with age.

With a peak incidence in the sixth decade, ALS is considered a mid-adulthood disorder (ROSENBOHM *et al.* 2018). Patients in Europe tend to have a later age of ALS onset when compared to other non-European countries such as China, Cuba and Uruguay (DORST *et al.* 2019; RYAN *et al.* 2019). The average lifespan following diagnosis is 2-3 years, with respiratory failure as the mode of death for most patients. However, a mean diagnostic delay of 1 year from symptom onset, uncovers the reality of more slowly progressing cases (MITCHELL *et al.* 2010b). Indeed, some forms of the disease demonstrate a protracted overall survival time that can range from a few months to decades. ALS has an overall male predisposition with a male-to-female ratio between 1 and 2 (LONGINETTI AND FANG 2019), which can increase as high as 2.9 as demonstrated by a study in Africa (LUNA *et al.* 2019).

The majority of patients with ALS (90%) are considered to be sporadic (sALS), having no affected first-degree relatives. The remaining 10% of ALS cases are familial (fALS), thus transmitted in families frequently as a dominant trait and with high penetrance (CHEN *et al.* 2013). Despite so, the classification of familial disease can be imprecise at times and may be influenced by differing interpretations of family pedigrees. In addition, being a disease of older age, may discount ALS in family members of previous generations where the cause of death might not be known. Finally, a family history of relevant diseases other than ALS is not always considered. Indeed, overlap syndromes suggest that in some cases ALS manifests with a wider spectrum of neurodegenerative symptoms. The presence of frontotemporal dementia (FTD) has been detected in up to 13% of ALS patients at time of diagnosis, whereas symptoms of behavioural dysfunction and cognitive impairment can be recognized in more than 70% of ALS cases (PHUKAN *et al.* 2012; NGUYEN *et al.* 2018). In addition, co-occurrence of genes has shown to contribute to the aetiology of both ALS and FTD suggesting the involvement of common molecular pathways. A high occurrence of psychiatric illnesses has also been demonstrated both pre- and post-ALS diagnosis. Neuropsychiatric phenotypes include those associated with depression, obsessive-compulsive disorder, bipolar affective disorder and drug dependence. Population-based studies have long corroborated a link between schizophrenia and ALS (TURNER *et al.* 2016) and a diagnosis of schizophrenia is in some instances considered as a risk factor for ALS (MCLAUGHLIN *et al.* 2017). In

support of a familial aggregation of ALS and other neurodegenerative diseases, recent findings have also demonstrated that family members of ALS patients, especially offspring, showed an increased risk of manifesting psychiatric disorders such as schizophrenia or psychosis both before and after their relative's diagnosis (LONGINETTI *et al.* 2017). In addition, a population-based study cohort revealed that the risk of developing neuropsychiatric symptoms was significantly higher in first- or second-degree relatives of ALS patients (BYRNE *et al.* 2013).

Although familial and sporadic forms of ALS are frequently perceived as two distinguishable subtypes of the disease, recent genetic insights unravelled through the large-scale efforts devoted to genome-wide association studies (GWAS) have pointed at a unifying model where both groups are shown to have common determinants (TALBOT 2011). To date, genetic associations have been identified in approximately 70% of fALS patients and 10% of sALS individuals, greatly influencing our understanding of this catastrophic disorder (RENTON *et al.* 2014). As a result, a number of molecular pathways including RNA processing, nucleocytoplasmic transport and protein homeostasis have been implicated (**Figure 1.1**); however, how motor neuron degeneration is initiated and propagated remains elusive. The new wave of gene discovery has also helped to consolidate the overlap of clinical and pathological features between ALS and other adult-onset degenerative disorders.

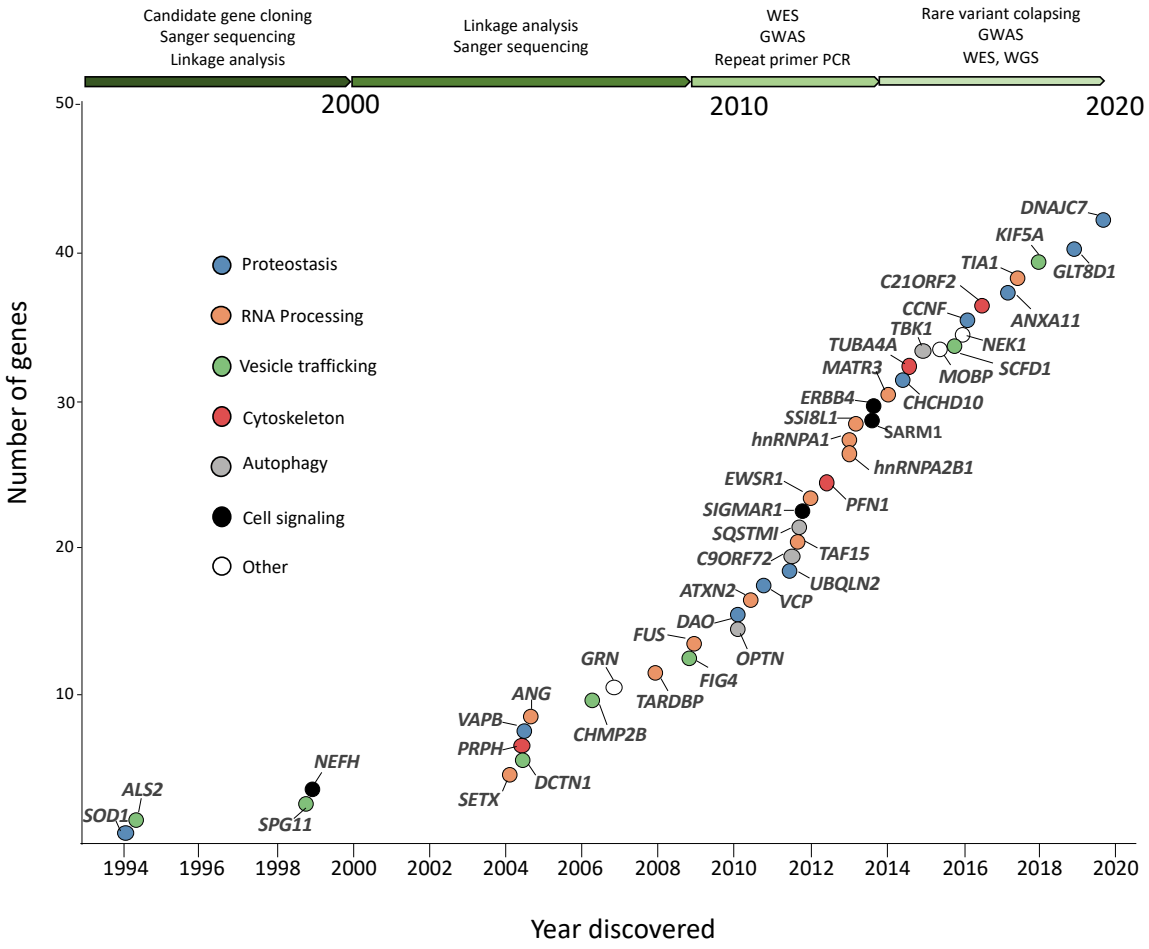

Figure 1.1 Genetics of ALS. The discovery of genes implicated in ALS has increased throughout the years. Strategies have evolved from individual gene mapping to increasingly powered technological and statistical methodologies. Since the identification of *SOD1,* more than 40 additional genes have been implicated in ALS. The genes encode proteins that have a role in protein homeostasis, interact with RNA or are important for the maintenance of cytoskeleton integrity. Other cellular processes that contribute to the pathogenesis of ALS include, vesicle trafficking, cell signalling and autophagy, among other. **GWAS**, genome-wide association studies; **WES**, whole-exome sequencing; **WGS**, whole-genome sequencing. Adapted from GREGORY 2020.

1.4 PATHOPHYSIOLOGY: GENETIC FACTORS

1.4.1 Contribution of four major genes

1.4.1.1 *SOD1*

The first attempt at understanding the genetic aetiology of ALS was achieved more than two decades ago and involved the identification of dominant missense mutations in *superoxide dismutase 1* (*SOD1*) (ROSEN 1993). More than hundred *SOD1* mutations have been reported (**Figure 1.2**) and these account for about 12-20% of fALS patients and up to 2-7% of sALS patients making *SOD1* the second most common ALS gene (ZOU *et al.* 2017). *SOD1* encodes the enzyme Cu-Zn superoxide dismutase that catalyses highly reactive superoxide radicals to oxygen and hydrogen peroxide, providing defence against oxygen toxicity. This momentous turnaround for ALS research quickly led to the development of *SOD1* transgenic mouse models (GURNEY *et al.* 1994; TURNER AND TALBOT 2008). As a result, multiple investigations demonstrated that motor neuron degeneration is driven by a plethora of toxic properties of the mutant protein that is independent of its dismutase activity (WONG *et al.* 1995; BRUIJN *et al.* 1998). It appears that ALS-causing mutant SOD1 fails to fold properly forming intracellular aggregates that result in the accumulation of misfolded SOD1 (BRUIJN *et al.* 1997). Consequently, misfolded SOD1 forms ubiquitinated cytoplasmic inclusions that are unable to be disposed of by the ubiquitin-proteasome system (UPS) and autophagy pathway, possibly contributing to toxicity in ALS (BENDOTTI *et al.* 2012; CHEN *et al.* 2012). In addition, mutant *SOD1* mouse models have also demonstrated that failure of various other cellular functions, including mitochondrial energy production and axonal transport bring about axonal retraction and denervation and, subsequently, neuronal cell death (ILIEVA *et al.* 2009).

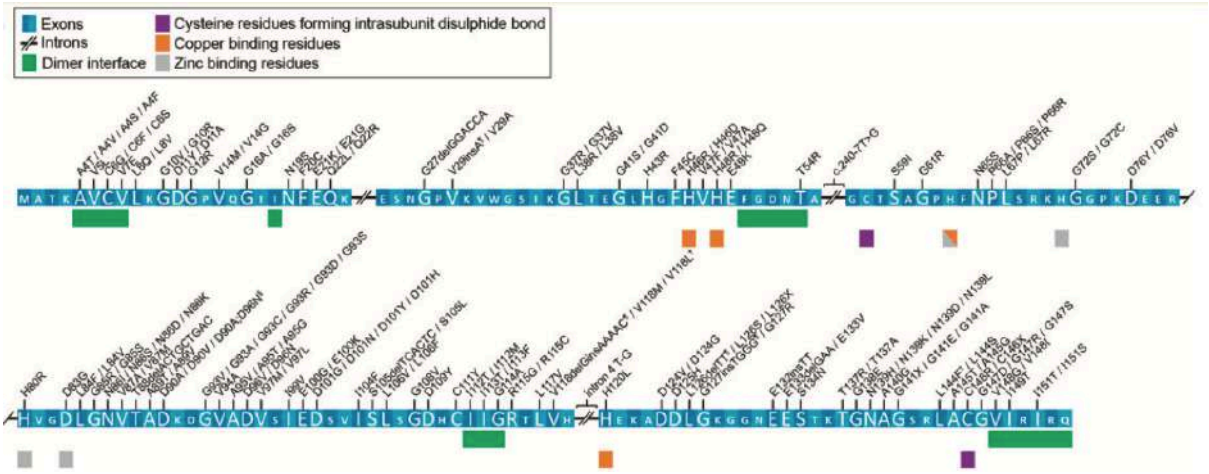

Figure 1.2 ALS-linked human *SOD1* variants. Depiction of the SOD1 amino acid sequence, including the location of introns. Over one hundred and fifty *SOD1* mutations have been described in patients with ALS, accounting for 12-20% of fALS cases and up to 7% of sALS cases. Intronic variants are not shown (SACCON *et al.* 2013).

1.4.1.2 *TARDBP*

Mutations in *transactive response DNA-binding protein* (*TARDBP)* gene, which encodes for the transactive response DNA binding protein 43kDa (TDP-43) have also been associated with neurodegenerative diseases, including ALS. Specifically, the accumulation of ubiquitinated TDP-43 inclusions in both sporadic and familial ALS cases continue to underscore the build-up of ubiquitinated aggregates as a pathological hallmark of the disease. TDP-43 deposition is also present in some forms of FTD, hinting at a common pathway (NEUMANN *et al.* 2006). The majority of *TARDBP* variants are missense mutations in the region encoding the glycine-rich C-terminal (**Figure 1.3**) and are the cause of 4-5% and 1% of fALS and sALS, respectively (RENTON *et al.* 2014). TDP-43 is a multifunctional protein that predominantly localizes to the nucleus. Amongst its many functions that encompass multiple phases of RNA processing, its role in mRNA splicing is perhaps the most prominent. One of its two RNA recognition motifs (RRMs) enables it to bind GU-rich sequences, typical features of thousands of pre-mRNAs that are consequently targeted by TDP-43 (POLYMENIDOU *et al.* 2011; LAGIER-TOURENNE *et al.* 2012). In conditions of cellular stress, TDP-43 is able to shift to the cytoplasm where it associates with stress granules, which are enriched in translation-stalled mRNAs (DEWEY *et al.* 2011; MCDONALD *et al.* 2011). Indeed, in an induced stressful scenario such

as oxidative stress, TDP-43 mainly localizes to the cytoplasm, incorporated in stress granules (COLOMBRITA *et al.* 2009).

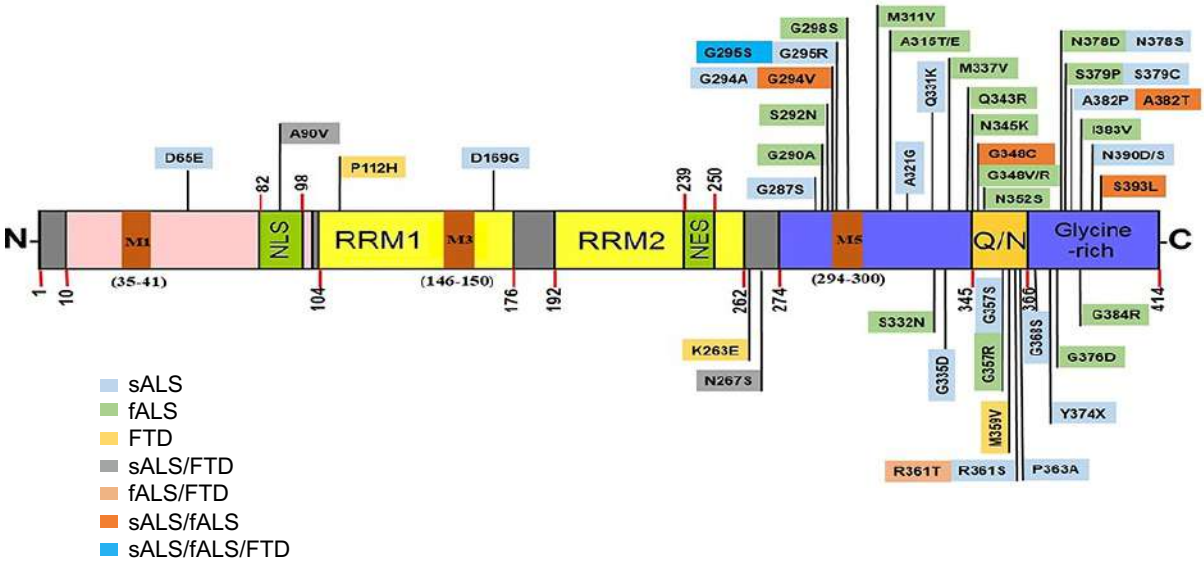

Figure 1.3 MND-associated TDP-43 variants. Domain organization of TDP-43 comprising of two RNA recognition motif (RRM) domains, a nuclear export signal (NES), a nuclear localization signal (NLS), mitochondrial localisation motifs (M1, M3 & M5) and a glycine-rich C-terminal domain. The majority of fALS and sALS mutations are located in the region encoding the glycine-rich C-terminal. A considerable degree of genetic overlap between sALS and fALS, as well as between ALS and FTD can be explained by TDP-43 mutations (PRASAD *et al.* 2019).

Based on the molecular mechanisms involving TDP-43, both loss-of-function (LOF) and gain-of-function (GOF) models of TDP-43 pathogenicity in ALS have been described. Several studies have demonstrated that loss of nuclear TDP-43 results in splicing defects in cellular and animal models (DE CONTI *et al.* 2015; LING *et al.* 2015), as well as in motor neurons of *TARDBP*-ALS patients (HIGHLEY *et al.* 2014). Furthermore, splicing defects as a result of TDP-43 repression in animal models often leads to neuronal loss, impaired axonal growth and muscle degeneration (SCHMID *et al.* 2013; VANDEN BROECK *et al.* 2013). TDP-43 aggregates could also gain a toxic function. Indeed, accumulation of TDP-43 is further facilitated by stress granule formation, enhancing TDP-43 toxicity (JOHNSON *et al.* 2009; ARNOLD *et al.* 2013) which can spread along axons and from cell to cell in a prion-like manner (FEILER *et al.* 2015). Nevertheless, the distinct possibility of pleiotropic or combined effects has been largely considered, such that, disease-associated mutations prompt the exit of TDP-43 from the nucleus, enhancing

cytoplasmic aggregation (GOF), which consequently lead to nuclear depletion of TDP-43, and in-turn contributes to abnormal RNA-processing (LOF) (LEE *et al.* 2011).

1.4.1.3 *FUS*

The idea that aberrant RNA processing contributes to ALS pathogenesis continued to gain ground upon the identification of *fused in sarcoma* (*FUS*) mutations. Presently, there are over 50 *FUS* mutations associated with ALS, accounting for 4-5% fALS and less than 1% sALS. In the majority, the inheritance pattern of these mutations is autosomal dominant and carriers have been reported in most populations, including North America, Europe, Australia and Africa. Approximately two-thirds of *FUS* variants cluster in the RNA binding domain at the C-terminus and have an increased frequency in fALS, whereas the remaining one-third are located in the N-terminus and are mainly linked to sALS (**Figure 1.4**) (KWIATKOWSKI *et al.* 2009; VANCE *et al.* 2009; DENG *et al.* 2014). FUS pathology is rare in FTD, accounting for only 5-10% of cases that are frequently characterized by young onset and hyperorality (NEUMANN *et al.* 2009; URWIN *et al.* 2010; GOWELL *et al.* 2020).

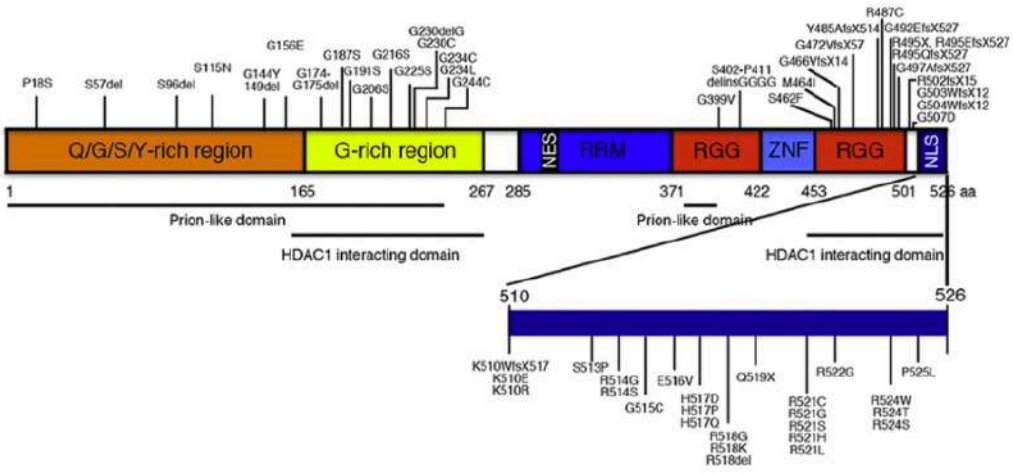

Figure 1.4 Known ALS-related *FUS* mutations. Functional domains in FUS proteins include the prion-like domain that consists of a Q/G/S/Y-rich region and a G-rich region, the Arginine-rich motif (RRM), two Arg-Gly-Gly (RGG)-repeat regions separated by a zinc-finger motif (ZNF), and a nuclear localisation signal (NLS) at the C-terminal. The majority of *FUS* variants associated with ALS cluster at the C-terminus and the G-rich region (SHANG AND HUANG 2016).

Like TDP-43, FUS protein targets numerous genes through its multiple RNA-binding domains. Similarly, it particularly binds to long intron sequences and regulates their splicing. Despite this functional similarity, mRNAs targeted by FUS are remarkably distinct from those of TDP-43 (LAGIER-TOURENNE *et al.* 2012). The majority of *FUS* mutations particularly cluster in the C-terminal nuclear localization signal (NLS)-containing domain. Mutations in this region cause FUS, a nuclear protein, to mislocalise to the cytoplasm as a result of compromised transportin-mediated nuclear import. Consequently, FUS is recruited into stress granules that are likely to form inclusions under stress conditions (DORMANN *et al.* 2010). Pathogenic toxicity associated with FUSopathies is speculated to take effect via multistep mechanisms, similar to those that underlie TDP-43 toxicity (DORMANN AND HAASS 2011).

1.4.1.4 *C9orf72*

A significant discovery that has revolutionized ALS research was the identification of a large hexanucleotide (G_4C_2) repeat expansion in the noncoding region of the gene chromosome 9 open reading frame 72 (*C9orf72*) as the most prevalent ALS/FTD-causing mutation (DEJESUS-HERNANDEZ *et al.* 2011; RENTON *et al.* 2011). Although pathogenic expansions of a similar nature in the *Ataxin-2* (*ATXN2*) gene (ELDEN *et al.* 2010) and *Pradar-Willi/Angelman syndrome region protein 1* (*NIPA1*) gene (BLAUW *et al.* 2012) have been formerly linked to ALS, their frequency is by no means comparable to that of *C9orf72* repeat expansions. The large expansion accounts for a striking 35% of fALS cases and almost 5-7% of European sALS individuals, a number that reflects more than just the occasional sporadic case. Furthermore, *C9orf72* mutations have been retrieved in a remarkable percentage of FTDs (25%) and constitute the major overlapping factor between the two distinct clinical disorders (VAN BLITTERSWIJK *et al.* 2012). *C9orf72* mutation carriers may have up to thousand non-coding G_4C_2 repeats, whilst the number of repeats generally never exceeds 24-30 in normal individuals (IACOANGELI *et al.* 2019).

The precise function of the C9orf72 protein is poorly defined. Based on its structural similarity to DENN (differentially expressed in normal and neoplastic cells)-like

proteins, it has been speculated that C9orf72 is a member of this group of GDP-GTP exchange factors for Rab-GTPases, which contribute to the coordination of membrane trafficking (LEVINE *et al.* 2013). *In vitro* studies further implicate C9orf72 protein in membrane trafficking, and suggest that the protein regulates endocytosis and autophagy. Furthermore, C9orf72 is involved in shuttling RNA-binding proteins, hnRNPA2/B1 and hnRNPA1 between the nucleus and the cytoplasm, thus it may also be implicated in RNA metabolism (FARG *et al.* 2014).

Several studies hypothesize that the resulting pathogenic effect is a result of abnormal *C9orf72* expression. A reduction of mRNA expression has been detected in patients with the *C9orf72* expansion, implicating haploinsufficiency (LOF) as a mechanism contributing to ALS (DEJESUS-HERNANDEZ *et al.* 2011). On the contrary, the C9orf72 expansion may be associated with a toxic RNA GOF mechanism as a consequence of sequestration of RNA binding proteins, production of abnormal RNA subtypes or increased DNA instability as a result of RNA-DNA hybrid structure formation (WALKER *et al.* 2017). Distinctly, aberrant protein homeostasis may occur *via* impaired autophagy or accumulation of dipeptide repeat proteins after non-ATG mediated translation (LEHMER *et al.* 2017). Nonetheless both mechanisms are not mutually exclusive and may occur simultaneously.

1.4.2 Disruption of protein quality control

Increasing evidence that defects in the protein quality control machinery are implicated in ALS pathogenesis emerged upon the identification of fALS-associated mutations in proteins that regulate the proteasome and autophagy pathways of protein degradation and clearance. In view of the fact that protein aggregation is a hallmark feature of ALS, the implication of protein degradation as a mechanism underpinning ALS pathogenesis is highly relevant. Genes that are associated with ALS and are involved in protein degradation *via* the UPS include *ubiquilin 2* (*UBQLN2*), *sequesosome 1* (*SQSTM1*) and *sigma non-opioid intracellular receptor 1* (*SIGMAR1*), whilst those involved in autophagy include *optineurin* (*OPTN*), *TANK-binding kinase* (*TKB1*) and *valosin-containing protein* (*VCP*). Finally, ALS-linked genes involved in endosomal transport include *alsin* (*ALS2*),

vesicle-associated membrane protein-associated protein B (*VAPB*), *charged multivesicular body protein b* (*CHMP2B*) and *phosphoinositide 5-phosphatase* (*FIG4*).

Rare missense mutations in the *UBQLN2* gene give rise to X-linked ALS or ALS-FTD (DENG *et al.* 2011). *UBQLN2* belongs to the family of ubiquitin-like (UBL) proteins and delivers ubiquitin-tagged proteins to the proteasome and autophagosome for degradation by virtue of its C-terminal ubiquitin-associated (UBA) domain and N-terminal UBL domain (KO *et al.* 2004). Mutations in a 12PXX tandem-repeat-containing region within the N-terminal are of particular interest, however, mutations outside this region have also been described (SYNOFZIK *et al.* 2012).

An alternative candidate ALS gene *SQSTM1*, is similar to *UBQLN2* in structure and associated inclusions are found in an array of neurodegenerative diseases (ZATLOUKAL *et al.* 2002). The protein facilitates the degradation of ubiquitinated proteins and is important for the activation of nuclear factor kappa-B (NFf-κB) (BJORKOY *et al.* 2006). Depletion of SQSTM1 levels in a zebrafish model induced motor defects as a result of impaired autophagy (LATTANTE *et al.* 2015) .

Defects in *SIGMAR1* are associated with autosomal recessive inherited ALS, characterised with juvenile onset, that predominantly manifests with upper motor neuron involvement and a slowly progressive phenotype. Sigma-1 receptor (Sig-1R) is a multifunctional ER receptor chaperone that plays a role in calcium transport between the endoplasmic reticulum (ER) and mitochondria and counteracts ER stress. Sig-1R is abundant in motor neurons at excitatory postsynaptic densities which are disrupted in sALS, most likely due to Sig-R1 accumulation in the cytoplasm (AL-SAIF *et al.* 2011).

OPTN is a multifunctional protein, though perhaps its role in membrane trafficking and chaperoning of organelles and misfolded proteins for degradation is among its most prominent. Variants of *OPTN* have been identified in both fALS and sALS patients (ZHU *et al.* 2007). The function of OPTN is regulated in part by TBK1, which has also been implicated in both fALS (FREISCHMIDT *et al.* 2015) and sALS (CIRULLI *et al.* 2015), although the frequency of *TBK1* variants is generally low. TBK1 facilitates phosphorylation of OPTN, improving its affinity to proteins required in the autophagosome. Functional

studies indicated that among some of the detrimental effects of *TBK1* variants is the loss of function of the C-terminal coiled-coil CCD2 domain, which allows TBK1 to collaborate with multiple proteins, including OPTN and SQSTM1, that are involved in key processes such as ubiquitin-mediated protein degradation, neuroinflammation and autophagy pathways (FREISCHMIDT *et al.* 2015; OAKES *et al.* 2017).

Mutations in the gene encoding VCP/p97 were identified in a small set of ALS patients by exome sequencing (JOHNSON *et al.* 2010). The multifunctional AAA+-ATPase directs ubiquitinated proteins to the proteasome and plays an important role in autophagosome maturation. The majority of mutations cluster in the N-terminal domain, which is essential for normal function of VCP (MEYER *et al.* 2012). In addition, defects in VCP were shown to result in mitochondrial uncoupling, leading to a reduction in ATP production (BARTOLOME *et al.* 2013).

Alsin, a Rab5 guanine nucleotide exchange factor (GEF) is coded by *ALS2* and is involved in regulation of endocytosis. Defects in ALS2 are thereby implicated in the dysregulation of endocytic trafficking in ALS pathogenesis (LAI *et al.* 2009). Mutations in *VAPB* are associated with a late onset, slow progressing form of ALS, which is most frequently linked to dysfunction in intracellular membrane trafficking (NISHIMURA *et al.* 2004). VAPB is a member of the VAP protein family. It is an integral ER protein that in addition to protein transport, is involved in the unfolded protein response (UPR) and the regulation of ER-mitochondria interactions (STOICA *et al.* 2014). Defects in VAPB, specifically the P56S variant, that disrupt the UPR and hinder anterograde axonal transport of mitochondria have also been implicated in ALS pathogenesis (KANEKURA *et al.* 2006; SUZUKI *et al.* 2009; MOROTZ *et al.* 2012).

CHMP2B participates in systemizing integral membrane proteins in multivesicular bodies leading to their degradation by autophagy (FILIMONENKO *et al.* 2007). CHMP2B is highly expressed throughout the CNS, where it forms part of the ESCRT-III (endosomal sorting complex required for transport III) complex, where it plays a role in the recycling or degradation of endosomal cargo in the lysosome (SKIBINSKI *et al.* 2005). Mutations in *CHMP2B* are often identified in ALS cases with a predominant lower motor

neuron phenotype, in which they likely contribute to motor neuron injury as a result of the disruption of autophagic clearance of cellular proteins (COX *et al.* 2010).

FIG4 is primarily required for normal lysosome function and for the regulation of PI(3,5)P2 phosphorylation (GARY *et al.* 2002). Mutations of *FIG4* were initially associated with a severe form of Charcot-Marie-Tooth (CMT) disease, characterized by early onset involvement of sensory and motor neurons (CHOW *et al.* 2007), but were subsequently also found in both fALS and sALS cases (CHOW *et al.* 2009). Defects in *FIG4* are thought to cause loss of function, as indicated by FIG4 knockdown-mediated neurodegeneration and motor defects in mouse and *Drosophila* models, respectively (CHOW *et al.* 2007; KYOTANI *et al.* 2016).

1.4.3 Altered homeostasis and function of RNA

The identification of ALS-causing mutations in the genes encoding TDP-43 and FUS introduced the role of dysfunctional ribostasis as a significant contributor to ALS pathogenesis. Mutations in other genes involved in RNA metabolism, including *senataxin* (*SETX*), *angiogenin* (*ANG*), *heterogenous nuclear ribonucleoprotein A1/A2B1* (*hnRNPA1/hnRNPA2B1*) and *matrin3* (*MATR3*), continue to highlight aberrant RNA metabolism as a key mechanism in disease development.

Defects in the *SETX* gene are associated with both cerebellar and motor neuron degeneration. An autosomal recessive pattern of inheritance gives rise to cerebellar ataxia syndrome, whereas an autosomal dominant inheritance leads to a slowly progressive motor neuropathy (CHEN *et al.* 2004; CHEN *et al.* 2006). SETX is a DNA/RNA helicase, that plays a critical role in transcription, R-loop resolution and DNA damage repair. The mechanism by which *SETX* variants give rise to disease is not clear, although dysfunction of helicase activity or other steps in RNA processing is speculated (BENNETT *et al.* 2018).

Angiogenin (ANG) is a multifunctional protein that forms part of the ribonuclease A (RNase A) super family. In addition to its angiogenic activity, it interacts with numerous proteins to regulate several processes including cell proliferation, apoptosis, and stress

response (APARICIO-ERRIU AND PREHN 2012; BRADSHAW *et al.* 2017). Furthermore, ANG sustains a neuroprotective function by promoting neurite growth (SUBRAMANIAN AND FENG 2007). In view of its neuroprotective properties, variants in *ANG* are significantly represented in both sALS and fALS, as well as in Parkinson's disease (PD) (GREENWAY *et al.* 2006; VAN ES *et al.* 2011).

Mutations in hnRNPA1/A2B1 were identified in less than 1% of ALS cases (KIM *et al.* 2013). In the nucleus, both proteins co-operate with distinct hnRNPs to regulate splicing (DATAR *et al.* 1993; DREYFUSS *et al.* 1993; MILI *et al.* 2001). Moreover, hnRNPA1 and hnRNPA2B1 are essential for mRNA stability, transport and miRNA processing (GUIL AND CACERES 2007; VILLARROYA-BELTRI *et al.* 2013; ALARCON *et al.* 2015). Similar to *hnRNPA1/A2B1*, *MATR3* variants account for less than 1% of ALS cases (JOHNSON *et al.* 2014; XU *et al.* 2016; MARANGI *et al.* 2017). MATR3 plays an important role in transcription regulation, RNA processing and mRNA export and stability, by binding to DNA and RNA and some RNA-binding proteins, including TDP-43 (SALTON *et al.* 2011; SKOWRONSKA-KRAWCZYK *et al.* 2014; BOEHRINGER *et al.* 2017).

1.4.4 Flaws in cytoskeletal dynamics

Adequate neuronal function relies on efficient axonal transport of organelles and vesicles between soma and synapses. Defects in the axonal pathway as a consequence of mutations in proteins involved in axonal transport machinery and cytoskeleton integrity have been documented in ALS patients (BURK AND PASTERKAMP 2019b). Genes that encode these proteins include, *dynactin subunit 1* (*DCTN1), neurofilament light* (*NEFL*), *neurofilament heavy* (*NEHL*), *peripherin* (*PRPH*), *profilin* (*PFN1*) and *tubulin alpha 4a* (*TUBA4A).*

DCTN1 or $p150^{Glued}$, is the largest subunit of the dynactin complex, which contains more than 20 subunits. DCTN1 interacts with cytoplasmic dynein 1, a motor protein that assists retrograde axonal transport (HIROKAWA *et al.* 2010). ALS-causing mutations hamper the binding of $p150^{Glued}$ to microtubules, leading to dysfunctional dynein/dynactin-mediated transport of cargos such as autophagosomes (LEVY *et al.* 2006; IKENAKA *et al.* 2013). Affected individuals are reported to either develop an early

onset, lower motor neuron neuropathy with laryngeal involvement or an ALS-FTD clinical phenotype (MUNCH *et al.* 2005).

Several intermediate filament (IF) genes code for proteins that contribute to the integrity of the cytoskeletal architecture. Mutations in the *NEFL, NEFH* and *PRPH* genes have been reported in ALS patients. The *NEFL* gene encodes light neurofilament (NFL) subunits that together with medium and heavy subunits assemble neurofilaments that are crucial for normal nerve cell function. In ALS motor neurons, *NEFL* mRNA is remarkably bound by TDP-43 and FUS and is sequestered in stress granules, resulting in a diminished expression of NFL (BERGERON *et al.* 1994; STRONG *et al.* 2007). Overexpression of NFH in transgenic mice induces neurological defects including neurofilamentous swellings that are characteristics of those observed in ALS patients (COTE *et al.* 1993). Peripherin is a component of motor neuron spheroids identified in transgenic mouse models, as well as ALS patients. Such spheroids are thought to hinder axonal transport of other IF proteins, resulting in motor neuron degeneration (BEAULIEU *et al.* 2000; ROBERTSON *et al.* 2003).

PFN1 is required for the polymerization of filamentous actin that is crucial for various cellular functions such as axon growth. ALS-linked *PFN1* variants inhibit actin binding, reducing actin polymerization, which consequently disturbs the cytoskeleton (SMITH *et al.* 2015). In addition, mutant PFN1 is seen to interact with and induce stress granule formation, linking RNA aggregation observed in ALS and cytoskeletal defects (FIGLEY *et al.* 2014). Mutations in the *PFN1* gene were identified by exome sequencing in a minor group of ALS families, primarily characterized by a lower motor neuron clinical phenotype (WU *et al.* 2012).

Microtubules form the axon cytoskeletal backbone, and are composed of multiple copies of α and β tubulin subunits. Mutations in *TUBA4A* gene, that encodes one form of α tubulin were linked to a substantial number of fALS cases. Missense mutations in the encoded protein disrupt tubulin dimerization, consequently leading to a weakened microtubule network and irregular cytoskeletal scaffolding (SMITH *et al.* 2014). A small number of *TUBA4A* mutations can be found in the protein domain that allows

interaction with other tubulin subunits as well as the axonal transport proteins dynein and kinesin (HOWES *et al.* 2014).

1.4.5 Novel genetic loci associated with ALS

Owing to the success of large-scale genome-wide studies and technical developments in next generation sequencing, increasing numbers of ALS-associated genes continue to be identified. In recent years, a number of novel genes linked to monogenic forms of ALS have been described. Despite this, little is known on the frequency data for mutations in these genes since large-scale screening of independent patient cohorts is limited (CHIA *et al.* 2018). Novel discoveries include the identification of *kinesin heavy chain isoform 5A* (*KIF5A*), *cyclin-F* (*CCNF*), *NIMA related kinase 1* (*NEK1*), *annexin A11* (*ANXA11*) and *glycosyltransferase 8 domain containing 2* (*GLT8D1*) as ALS-associated genes.

Distinct mutations in the *KIF5A* gene were previously described in hereditary spastic paraplegia (HSP) (REID *et al.* 2002), Charcot-Marie-Tooth type 2 (CMT2) (LIU *et al.* 2014) and neonatal intractable myoclonus disorders (DUIS *et al.* 2016), and recently also in ALS. Specifically, two splice-site mutations and a rare missense mutation were found in fALS patients. All LOF splice-site variants within this region targeted the C-terminal cargo-binding domain and are predicted to lead to aberrant splicing (BRENNER *et al.* 2018).

Mutations in *CCNF* were identified in families presenting with ALS, ALS with FTD and FTD alone (D'ANGIOLELLA *et al.* 2010; WILLIAMS *et al.* 2016). Such variants are likely to induce aberrant proteostasis *via* disrupted ubiquitin-dependent protein degradation. Of note, overexpression of mutant CCNF in neuronal cells results in an increase in ubiquitin-tagged proteins, including TDP-43. This suggests that abnormal proteostasis associated with abnormal CCNF might be exacerbated by TDP-43 proteinopathy (WILLIAMS *et al.* 2016).

Two independent case-control studies have shown that *NEK1* LOF mutations contribute to ALS (BRENNER *et al.* 2016; KENNA *et al.* 2016). NEK1 regulates the formation of nonmotile primary cilium in postmitotic cells (SHALOM *et al.* 2008), disruption of which

is known to cause neurological defects and microtubule instability (LEE AND GLEESON 2010; THIEL *et al.* 2011). Since the disruption of the microtubule cytoskeleton has been implicated in ALS pathogenesis, the contribution of *NEK1* variants to the disease are particularly relevant. Moreover, the interaction of NEK1 with two other ALS-associated proteins, ALS2 and VAPB hints at a role in endoplasmic reticulum lipid trafficking, further linking its involvement in ALS (CIRULLI *et al.* 2015).

Recent studies have identified ALS-linked mutations within the glycosyltransferase enzyme, GLT8D1, pointing at a previously uncharacterized pathway in ALS pathophysiology. The precise function of GLT8D1 is unknown, however knockdown and expression of the mutated protein in zebrafish, induces motor defects synonymous with ALS (COOPER-KNOCK *et al.* 2019). Importantly, *GLT8D1* has also been associated with an increased risk of developing schizophrenia, supporting a link between both disorders (SASAYAMA *et al.* 2014; YANG *et al.* 2018).

1.4.6 Genes that confer ALS susceptibility of modify disease

Sporadic ALS is frequently characterized by a disproportionate frequency of rare genetic variants, which have additive effects with regards to ALS risk but alone are not causative of the disease. Some ALS-risk genes also possess disease-modifying properties which may serve as candidate targets in ALS therapy. These include variants in the genes *Unc-13 Homolog A* (*UNC13A*), *myelin associated oligodendrocyte basic protein* (*MOBP*), *sec1 family domain-containing protein 1* (*SCFD1), cilia and flagella associated protein 410* (*CFAP410* ka *C21orf2*), *ataxin2* (*ATXN2*) and *NIPA magnesium transporter 1* (*NIPA1*).

UNC13A, a presynaptic protein that controls release of neurotransmitters at neuromuscular synapses, was identified as a risk factor for ALS (CHIO *et al.* 2009c; VAN ES *et al.* 2009). Independent studies also revealed that UNC13A is associated with a shorter survival in ALS patients, especially in patients with *C9orf72* repeat expansions (VAN BLITTERSWIJK *et al.* 2014). It is hypothesized that disruption of UNC13A function results in abnormal neurotransmitter release, consequently leading to motor neuron death (VAROQUEAUX *et al.* 2005).

A combination of GWAS data and data from an independent replication cohort revealed the genes *SCFD1*, *MOBP* and *C21orf2* as risk loci associated with ALS (VAN RHEENEN *et al.* 2016). *MOBP* mutations have been previously reported in cases of progressive supranuclear palsy (PSP) (HOGLINGER *et al.* 2011) and were shown to modify survival in FTD (IRWIN *et al.* 2014). As a major component of myelin, specifically oligodendrocytes, MOBP plays a role in myelin stabilization in conditions of oxidative stress (MONTAGUE *et al.* 2006). SCFD1 belongs to the Sec/Munc18 (SM) family of proteins that participate in membrane fusion events, which are essential for intracellular vesicular trafficking. In addition, SCFD1 interacts with SNAP-receptor (SNARE) proteins to mediate ER-Golgi transport (HOU *et al.* 2017). A large association study in a Chinese cohort found that *SCFD1* may modulate age at ALS onset, and thus the gene may be a potential target for ALS therapy (CHEN *et al.* 2018). The genome-wide significant association of the *C21orf2* locus was subsequently replicated in a large-scale sequencing study (NICOLAS *et al.* 2018). The precise function of C21orf2 is largely unexplored, however it is known to interact with NEK1 to form a functional complex that is involved in microtubule assembly, mitochondrial function and DNA repair; three common pathways that are implicated in ALS (FANG *et al.* 2015; WATANABE *et al.* 2020).

ATNX2 is involved in multiple aspects of RNA metabolism, including regulation of mRNA stability, polyadenylation and translational activation (AUBURGER *et al.* 2017; CARMO-SILVA *et al.* 2017; LEE *et al.* 2018). ATXN2 predominantly localizes to the cytoplasm and displaces into stress granules upon stress (RALSER *et al.* 2005; NONHOFF *et al.* 2007). Normally, *ATXN2* contains a (CAG)n repeat that encodes a polyglutamine (polyQ) tract in the ATXN2 protein, with ~22-N-terminal repeats. An expansion of more than 34 polyQ repeats is associated with spinocerebellar ataxia type 2 (SCA2) (IMBERT *et al.* 1996), whereas an intermediate polyQ tract (27-33 repeats) were identified as a significant ALS risk factor (ELDEN *et al.* 2010; ROSS *et al.* 2011; VAN DAMME *et al.* 2011). ATXN2 was shown to interact with both TDP-43 and FUS, and upregulation of ATXN2 exacerbates mutant toxicity of both RNA-binding proteins in several animal models (ELDEN *et al.* 2010; FARG *et al.* 2013; BECKER *et al.* 2017).

Similar to *C9orf72* and *ATXN2*, *NIPA1* is reported to contain an expanded genomic repeat motif associated with an increased risk for ALS (BLAUW *et al.* 2012; TAZELAAR *et al.* 2019). *NIPA1* mutations were primarily implicated in hereditary spastic paraplegia type 6 (HSP6) (RAINIER *et al.* 2003). Subsequently, a genome-wide screen of a large international cohort linked rare deletions of *NIPA1* to ALS and additional genetic analyses revealed that expanded polyalanine repeats in the 5'-end of *NIPA1* confer increased disease susceptibility. Furthermore, long *NIPA1* expansions modify survival and are associated with a younger age at disease onset (BLAUW *et al.* 2010; BLAUW *et al.* 2012). Loss-of-function *NIPA1* mutations or abnormal polyalanine expansions are likely to cause defects in vesicular trafficking required for synaptic function and axon development (WANG *et al.* 2007; ZHAO *et al.* 2008; TSANG *et al.* 2009).

The precise disease mechanism of these genes within the context of other established genes requires further elucidation to improve our knowledge of ALS pathophysiology, which seems to involve a number of overlapping biological processes (**Table 3, Figure 1.5**) (GIBSON *et al.* 2017). In addition, it is possible that ALS arises as a consequence of a conflicting interplay between genetic, environmental and other factors, such as ageing, that also need to be taken into account to comprehend the complexity of each ALS case.

Table 3 Basic characteristics of ALS-associated genes.

Gene	Locus	Inheritance	Encoded Protein	Protein Function	Proportion of fALS (%)	Proportion of sALS (%)	Clinical Phenotype
ALS2	2q33.2	AR	Alsin	Vesicle trafficking	<1	<1	ALS; PLS
ANG	14q11.2	AD	Angiogenin	Angiogenesis	1-2	<1	ALS; ALS-FTD, PD
ANXA11	10q22.3	AD	Annexin A11	Proteostasis	1	1.7	ALS; ALS-FTD
ATXN2	12q24.12	AD,RF	Ataxin-2	Ribostasis, endocytosis	1-2	<1	ALS; ALS-FTD; PMA
C21orf2	21q22.3	AD,RF	C21orf2	Cytoskeletal organization	<1	<1	ALS
C9orf72	9p21.2	AD	C9orf72	Autophagy, intracellular & endosomal trafficking, proeostasis	35	5-7	ALS; ALS-FTD; FTD
CAPN14	2p23.1	RF	Calpain 14	Apoptosis, cytoskeletal dynamics	<1	<1	ALS
CCNF	16p13.3	AD	Cyclin-F	Proteostasis	2	1	ALS; ALS-FTD; FTD
CHCHD10	22q11.23	AD, AR	Coiled-coil-helix-coiled-coil-helix domain-containing protein 10	Oxidative phosphorylation	2	<1	ALS; ALS-FTD (rare); FTD (rare)
CHMP2B	3p11.2	AD	Charged multivesicular body protein 2b	Vesicle trafficking	<1	<1	ALS; PMA; FTD
CYLD	16q12.1	AD	CYLD Lysine-63 Ubiquitinase	Deubiquitinase activity	<1	<1	ALS-FTD
DAO	12q24.11	AD	D-amino-acid oxidase	Oxidative deamination	<1	<1	ALS
DCTN1	2p13.1	AD	Dynactin subunit 1	Vesicle trafficking, proteostasis	1	<1	ALS; ALS-FTD
DDX20	1p13.2	RF	DEAD-Box Helicase 20	Ribostasis	<1	<1	ALS; LMN
DNAJC7	17q21.2	AD	DnaJ homolog subfamily C member 7	Proteostasis	<1	<1	ALS
ELP3	8p21.1	RF	Elongator complex protein 3	Ribostasis	<1	<1	ALS
ERBB4	2q34	AD	Receptor tyrosine-protein kinase erbB4	Cell signaling	<1	<1	ALS
EWSR1	22q12.2	AD	EWS RNA-binding protein 1	Ribostasis	<1	<1	ALS
FIG4	6q21	AD	Polyphosphoinositide phosphatase	Vesicle trafficking	<1	<1	ALS; PLS; CMT
FUS	16p11.2	AD	Fused In Sarcoma	Ribostasis	4-5	1	ALS; ALS-FTD; FTD
GGNBP2	17q12	RF	Gametogenetin Binding Protein 2	Cell signaling	<1	<1	ALS
GLE1	9q34.11	AR	GLE1 RNA Export Mediator	Ribostasis	<1	<1	ALS
GLT8D1	3p21.1	AD	Glycosyltransferase 8 domain-containing protein 1	Proteostasis	<1	<1	ALS
GPX3	5q33.1	RF	Glutathione Peroxidase 3	Oxidative stress	<1	<1	ALS
GRN	17q21.31	AD	Granulin precursor	Cell growth	<1	<1	ALS; FTD
HNRNPA1	12q13.13	AD	Heterogenous Nuclear Ribonucleoprotein A1	Ribostasis	1-2	1	ALS; ALS-FTD; FTD (rare)
HNRNPA2B1	7p15.2	AD	Heterogenous Nuclear Ribonucleoprotein A2B1	Ribostasis	<1	<1	ALS-FTD (rare); FTD (rare)
KIF5A	12q13.3	AD	Kinesin heavy chain isoform 5A	Axonal transport, vesicle trafficking	<1	<1	ALS; ALS-FTD; CMT; HSP
KIFAP3	1q24.2	NA	Kinesin-associated protein 3	Axonal transport	<!	<!	ALS
MAPT	17q21.31	AD	Microtubule Associated Protein Tau	Cytoskeletal organization	<1	<1	ALS; FTD
MATR3	5q31.2	AD	Matrin 3	Ribostasis	1-2	1	ALS; ALS-FTD (rare)
MOBP	3p22.1	RF	Myelin Associated Oligodendrocyte Basic Protein	Myelin formation	<1	<1	ALS; PSP
NEFH	22q12.2	AD	Neurofilament Heavy Chain	Axonal transport	<1	<1	ALS
NEK1	4q33	AD	Serine/threonine-protein kinase NEK1	DNA damage repair	1-2	<1	ALS
NIPA1	15q11.2	RF	Non-imprinted in Prader-Willi/Angelman syndrome region protein 1	Vesicle trafficking	<1	<1	ALS; HSP
OPTN	10p13	AD, AR	Optineurin	Autophagy	2-3	<1	ALS; ALS-FTD
PFN1	17p13.2	AD	Profilin-1	Cytoskeleton	1-2	<1	ALS
PRPH	12q13.12	AD	Peripherin	Cytoskeleton	<1	<1	ALS
SARM1	17q11.2	RF	Sterile alpha and TIR motif-containing protein1	Cell signaling	<1	<1	ALS; ALS-FTD
SCFD1	14q12	RF	Sec1 family domain-containing protein 1	Vesicle trafficking	<1	<1	ALS
SETX	9q34.13	AD	Senataxin	Ribostasis	<1	<1	ALS
SIGMAR1	9p13.3	AR	Sigma non-opioid intracellular receptor 1	Cell signaling	<1	<1	ALS; ALS-FTD; FTD
SMN1/2	5q13.2	RF	Survival of motor neuron 1/2	Ribostasis	<1	<1	ALS; LMN
SOD1	21q22.11	AD,AR	Cu-Zn superoxide dismutase	Proteostasis, oxidative stress	12-20	2-7	ALS; PMA; PBP
SPAST	2p22.3	AD	Spastin	Cytoskeletal organization	<1	<1	ALS; HSP
SPG11	15q21.1	AR	Spatacsin	Axonal maintenance, vesicle trafficking	1	<1	ALS; HSP
SQSTM1	5q35.3	AD	Sequestosome 1	Autophagy	1	<1	ALS; ALS-FTD; FTD
SS18L1	20q13.33	AD	Calcium-responsive transactivator (CREST)	Ribostasis	<1	<1	ALS
TAF15	17q12	AD, AR	TATA-binding protein-associated factor 2N	Ribostasis	<1	<1	ALS
TARDBP	1p36.22	AD	TDP-43	Ribostasis	4-5	1	ALS; ALS-FTD; FTD
TBK1	12q14.2	AD	Serine/threonine-protein kinase TBK1	Autophagy	3	<1	ALS; ALS-FTD
TIA1	2p13.3	AD	T-cell-restricted intracellular antigen 1	Ribostasis	2.2	<1	ALS; ALS-FTD
TNIP1	5q33.1	RF	TNFAIP3 Interacting Protein 1	Inflammation	<1	<1	ALS
TUBA4A	2q35	AD	Tubulin α-4a chain	Cytoskeletal organization	1	<1	ALS; ALS-FTD
UBQLN1	Xp11.21	XD	Ubiquilin 2	Proteostasis	<1	<1	ALS; ALS-FTD; FTD
UNC13A	19p13.11	RF	Unc-13 Homolog A	Neurotransmitter release	<1	<1	ALS; ALS-FTD
VAPB	20q13.33	AD	VAMP (vesicle-associated membrane protein)-associated protein B/C	Proteostasis	<1	<1	ALS; PLS; PMA
VCP	9p13	AD	Valosin-containing protein	Proteostasis	1-2	<1	ALS; ALS-FTD; FTD

AD, autosomal-dominant; **AR**, autosomal-recessive; **XD,** X-linked-dominant; **RF,** recombinant frequency; **ALS**, amyotrophic lateral sclerosis; **FTD**, frontotemporal dementia; **PLS**, primary lateral sclerosis; **PD**, Parkinson's disease; **PMA**, progressive muscular atrophy; **LMN**, lower motor neuron disease; **CMT**, Charcot-Marie-Tooth disease; **HSP**, hereditary spastic paraplegia; **PSP**, progressive supranuclear palsy; **PBP**, progressive bulbar palsy. Data extracted from the National Center for Biotechnology Information (NCBI) online database and the Online Mendelian Inheritance in Man (OMIM) database.

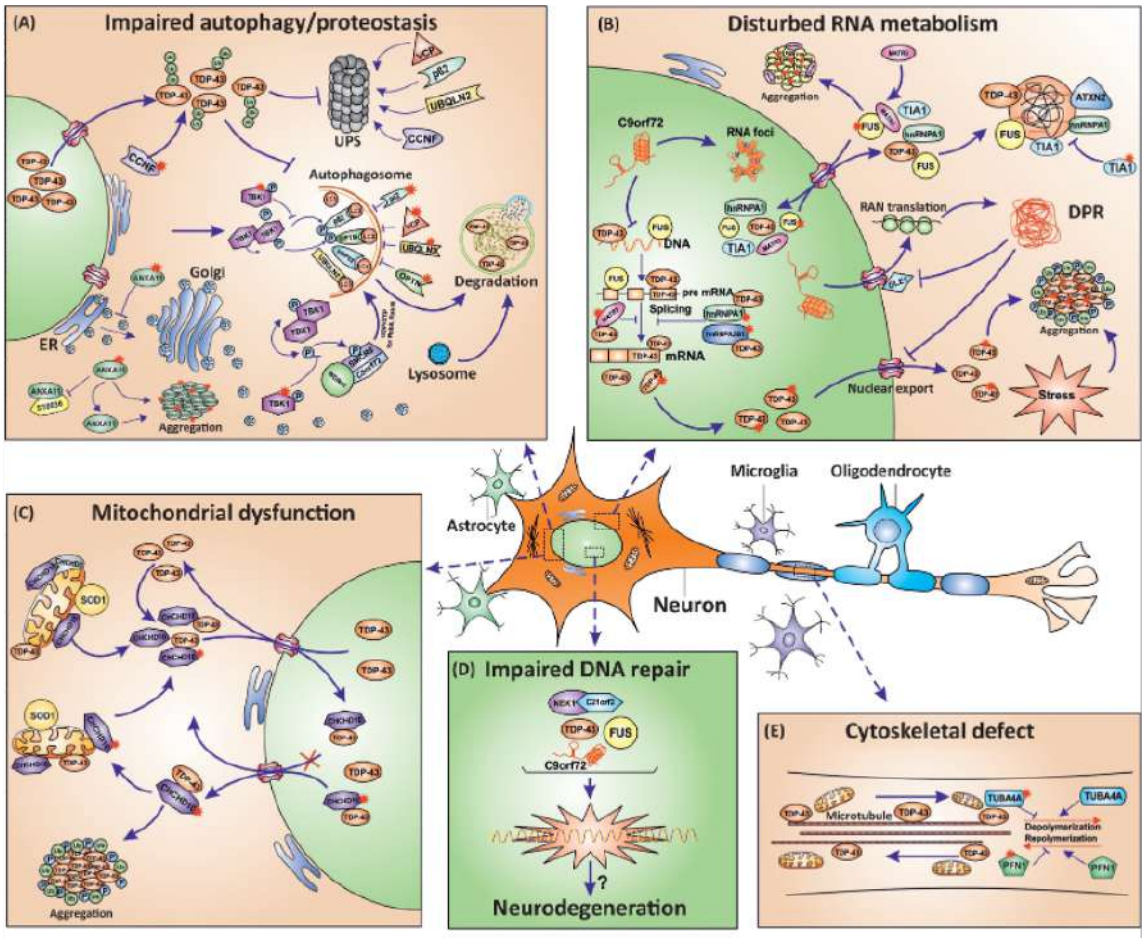

Figure 1.5 Key molecular mechanisms in ALS pathology. (A) Impaired proteostasis as a result of impaired protein degradation by obstruction of UPS and autophagy pathways. This may lead to TDP-43 accumulation in the cytoplasm. (**B**) Altered RNA metabolism may occur due to cytoplasmic mislocalisation of RNA-binding proteins such as TDP-43 or FUS, resulting in transcription and splicing defects. Altered stress granule dynamics may contribute to pathogenesis. (**C**) Mitochondrial dysfunction due to defects in ALS genes that interact with mitochondria results in the increased formation of reactive oxygen species. (**D**) Impaired DNA repair due to defects in ALS-linked genes including *FUS*, *TARDBP*, *NEK1*, *C21orf2* and *C9orf72* that are involved in DNA damage response contribute to ALS pathogenesis. (**E**) Altered cytoskeleton dynamics influences microtubule integrity and axonal transport that may lead to neurofilament accumulation. As a result defects in these pathways may contribute to ALS subsequent to neuroinflammation due to activated microglia that may secrete inflammatory proteins, leading to neurotoxic activity in astrocytes, as well as excitotoxicity, that occurs upon overstimulation of glutamate receptors as a result of increased synaptic glutamate release and reduced glutamate clearance by astrocytes. In addition, oligodendrocyte malfunction may lead to reduced neuronal health. **DPR**, dipeptide repeat aggregates; **ER**, endoplasmic reticulum; **RAN**, repeat-associated non-AUG translation; **UPS**, ubiquitin-proteasome system. Image from (NGUYEN *et al.* 2018).

1.5 PATHOPHYSIOLOGY: NON- GENETIC RISK FACTORS

The past decade has seen a shift in focus in the identification of risk factors associated with ALS, particularly in sporadic cases. Studies became directed at particular life-long exposures that potentially preceded disease onset. Such exposures have included environmental factors as well as exogenous lifestyle factors such as diet or smoking.

1.5.1 Lifestyle risk factors

Evidence-based studies demonstrate that smoking has a possible positive association with ALS (ARMON 2009). Whether the increased ALS risk is caused by oxidative stress, nicotine or other toxic substances such as lead and formaldehyde in tobacco smoke needs to be clarified (ALONSO *et al.* 2010). Analyses of smoking parameters and the risk of ALS in a large European cohort established almost a twofold-increased risk of suffering from ALS in smokers compared to non-smokers. Furthermore, the number of years since smoking cessation was linked with a decreased risk (GALLO *et al.* 2009). A 40% increase of ALS risk was reported in smokers versus never smokers in combined cohorts in the United States. Moreover, initiation of smoking at a younger age among smokers was correlated with an increased risk of ALS (WANG *et al.* 2011b).

Several studies have concluded that increased alcohol consumption is not associated with ALS risk and may even serve as a protective factor in disease, hypothetically due to the antioxidant component in alcohol (DE JONG *et al.* 2012; JI *et al.* 2016; MENG *et al.* 2016). Despite this, the relationship between alcohol consumption and ALS remains unclear as separate studies demonstrated that heavy drinkers had a higher risk of developing ALS compared to non-drinkers, especially in combination with cigarette smoking (KAMEL *et al.* 1999; OKAMOTO *et al.* 2009; LIAN *et al.* 2019). Further investigations, including the effect of different alcohol types, are required to elucidate the role of alcohol in ALS.

The most significant association with regards to dietary risk factors is that of antioxidants, particularly Vitamin E, with a low risk for developing the disease (ASCHERIO *et al.* 2005). This finding has been corroborated in a number of case-control

and cohort studies (WANG *et al.* 2011a; MICHAL FREEDMAN *et al.* 2013), although smaller independent studies have demonstrated that this is not always the case (IWASAKI *et al.* 1995). Other food groups that have been associated with a reduced risk of ALS include decaffeinated coffee, tea, whole bread, a high intake of raw vegetables and fruits (dietary fibre), as well as vegetable fats and folate. Conversely, an increased intake of processed meat and proteins in general, together with sodium, zinc and glutamic acid was reported in ALS patients, thus this particular diet is associated with an increased disease risk (PUPILLO *et al.* 2018). Nonetheless, association of dietary factors with ALS risk has been widely inconclusive and controversial mainly due to different alimentary habits in different geographic areas.

1.5.2 Physical activity and body mass

A higher level of physical fitness and a reduced body mass index (BMI) are associated with a higher risk for ALS (INGRE *et al.* 2015). A Swedish case control study established that weight adjusted physical fitness but not muscle strength is a risk factor for neurodegeneration in ALS with a shorter survival rate (MATTSSON *et al.* 2012). Moreover, a reduction in BMI from disease onset correlates with faster progression of motor neuron death and is a prognostic marker for survival in ALS (JAWAID *et al.* 2010). Individuals that practice vigorous physical activity, specifically professional football or soccer players demonstrate an increased risk of ALS (ABEL 2007; HUISMAN *et al.* 2013; HAMIDOU *et al.* 2014; GALLO *et al.* 2016). Some studies have contradicted these findings and have not found a positive association between physical activity and ALS risk, especially when performed with moderation (FANG *et al.* 2016; LIAN *et al.* 2019). A possible rationale supporting motor neuron degeneration among professional athletes is the increased probability of traumatic injury to the head, neck or spine. Repeated head injuries were equally reported to increase the risk of ALS among military veterans who suffered combat-injuries or participated in competitive sports (MCKEE *et al.* 2010).

1.5.3 Occupation-related risk factors

Several studies have portrayed lifetime occupation as a surrogate for an array of environmental exposures that have been linked with an increased ALS risk. The

occurrence of ALS among individuals with blue-collar occupations continues to underscore strenuous physical labour as an occupation-related risk factor associated with disease. An international population-based study that investigated ALS registries from Italy, Ireland and the United Kingdom revealed that a significant number of affected individuals engaged in physically exhausting occupations compared to controls, with farming/gardening as the prevailing occupation among ALS patients (BEGHI *et al.* 2010). A Danish population study revealed a positive association between ALS and agricultural occupations, as well as an increased ALS prevalence in men employed in construction (DICKERSON *et al.* 2018), consistent with a separate study in Massachusetts that showed increased odds of ALS among construction workers (FANG *et al.* 2009). Other working statuses linking increased physical activity and ALS were also described. A case-control study in China demonstrated that the risk of ALS among housewives aged 50-54 years is more than twice as much that of other types of occupations for that age group (LIAN *et al.* 2019).

Professions that have been associated with an increased ALS risk frequently incur work exposures to hazardous elements such as chemicals, pesticides, metals or electromagnetic fields (EMF) (FANG *et al.* 2009; TALBOTT *et al.* 2016). A higher risk of ALS was detected in construction workers and precision metal workers exposed to metals and organic solvents containing neurotoxicants. Of note, exposure to metals especially lead has been vastly researched as a possible risk factor of neurodegeneration. Indeed, several systematic studies presented convincing evidence for a strong association between exposure to lead and ALS, with an effect in more than 1000 cases making it the most significant risk factor among those studied (BELBASIS *et al.* 2016). Several meta-analyses have demonstrated that exposure to pesticides linked to agricultural occupations is associated with ALS risk (KAMEL *et al.* 2012; MALEK *et al.* 2012; KANG *et al.* 2014). Occupational exposure to solvents in painters, carpenters, hairdressers and industrial hygienists is associated with an elevated ALS risk, possibly as a result of peripheral neuropathy or dysfunction of autonomic nervous system activity (CHIO *et al.* 1991; GOBBA *et al.* 1995; MCGUIRE *et al.* 1997; BECK *et al.* 2005; MALEK *et al.* 2015). Finally, a large meta-analysis study evaluating the effects of electromagnetic radiation on ALS risk found a weak positive association with disease susceptibility, and

hypothesized the involvement of oxidative stress and DNA damage as possible underlying mechanisms (ZHOU *et al.* 2012).

1.5.4 Viruses

Exposure to previous viral infections may also be a determinant in ALS aetiology. Specifically, a role of enteroviral infections such as poliomyelitis has been frequently highlighted in ALS cases where the target cells, similar to ALS, are neurons in the anterior horn of the spinal cord (OKUMURA *et al.* 1995). Other viruses implicated in ALS risk include human herpes virus (HHV)-6 with seropositivity increasing risk by a threefold, that is further elevated by HHV-8 seropositivity (CERMELLI *et al.* 2003). Furthermore, retroviruses including human immunodeficiency virus (HIV) and human T-cell lymphocytic virus-1 also identify with motor neuron conditions (ROWLAND 1991; LORENZONI *et al.* 2018).

In contrast with the successful advances in understanding the role of genetic factors and related patho-mechanisms associated with ALS, little progress has been made in identifying non-genetic risk factors and their impact on ALS aetiology is questionable. A more integral approach is crucial to understand the mechanism linking each individual risk factor to ALS. More importantly, deciphering the interaction of non-genetic risk factors with distinct ALS genetic backgrounds is essential to gain insights on the aethiopathogenesis of ALS.

1.6 ALS TREATMENT

1.6.1 Disease-modifying treatments

Despite decades of research, there is no known cure for ALS. Clinicians and carers have mostly relied on palliative care, such as early nutritional intervention *via* gastronomy tube placement or management of respiratory symptoms by non-invasive ventilation or long-term mechanical ventilation (tracheostomy) to improve the quality of life and survival in patients (HOGDEN *et al.* 2017). Presently, two known disease-modifying treatments that can slow down disease progression are available to ALS patients.

Riluzole (Rilutek) is an anti-glutamatergic agent that prolongs survival by approximately 3 months (or 9% gain in the probability of surviving one year) (DHARMADASA AND KIERNAN 2018). Glutamate is the main modulator of excitotoxicity. In ALS, defects in glutamate receptors leads to aberrant glutamate transport that in turn leads to excessive glutamate release (ROSENBLUM AND TROTTI 2017). Riluzole is thought to decrease excitotoxicity by inhibiting presynaptic glutamate release (BENSIMON *et al.* 1994). The effects of riluzole may vary across different stages of disease (RIVIERE *et al.* 1998; ZOING *et al.* 2006; FANG *et al.* 2018).

The recently United States Food and Drug Administration (U.S. FDA) - approved disease-modifying treatment is edaravone (Radicava), an antioxidant agent that presumably reduces oxidative stress by eliminating lipid peroxide and hydroxyl radicals. As a result, it protects neurons and neighbouring glia from degeneration by oxidative injury (ITO *et al.* 2008; ABE *et al.* 2014). The drug was shown to be especially effective in early-stages of disease, as indicated in a multi-center phase III clinical trial (ClinicalTrials.gov: NCT01492686) in Japan (TANAKA *et al.* 2016; YOSHINO 2019). Edaravone, is yet to be approved by the European Medicines Agency (EMA).

1.6.2 Gene therapy

Recent advances in understanding the role of genetic factors and related patho-mechanisms associated with ALS, have enabled the development of increasingly targeted therapies, and their success in clinical trials can lead to efficacious treatment strategies. Aside from targeting non-specific factors such as excitotoxicity or oxidative stress, a distinct therapeutic approach involves targeting genetic mutations known to cause ALS *via* gene therapy.

Gene therapy enables the delivery of genetic components to target cells in order to import functional copies of dysfunctional genes, deliver trophic factors or genes that can modify disease or to silence damaging genes by means of antisense oligonucleotides (ASOs), RNA interference (RNAi), or clustered regularly interspaced short palindromic repeats (CRISPR) gene-editing technology. Delivery to the central nervous system (CNS)

can be achieved with or without the use of vectors, which include adeno-associated virus (AAV) vectors and other chemical systems such as nanoparticles (CAPPELLA *et al.* 2019; AMADO AND DAVIDSON 2021) (**Figure 1.6**). AAVs are attractive candidates for delivery of genetic material due to their ability to transduce terminally differentiated cells without incurring the risk of insertional mutagenesis. Furthermore, the availability of several AAV serotypes allows for selective tropism (MURLIDHARAN *et al.* 2014). Due to their ability to target motor neurons, the naturally occurring AAV9 and AAVrh10 serotypes are the lead vectors employed in ALS clinical trials thus far (DUQUE *et al.* 2009; TANGUY *et al.* 2015).

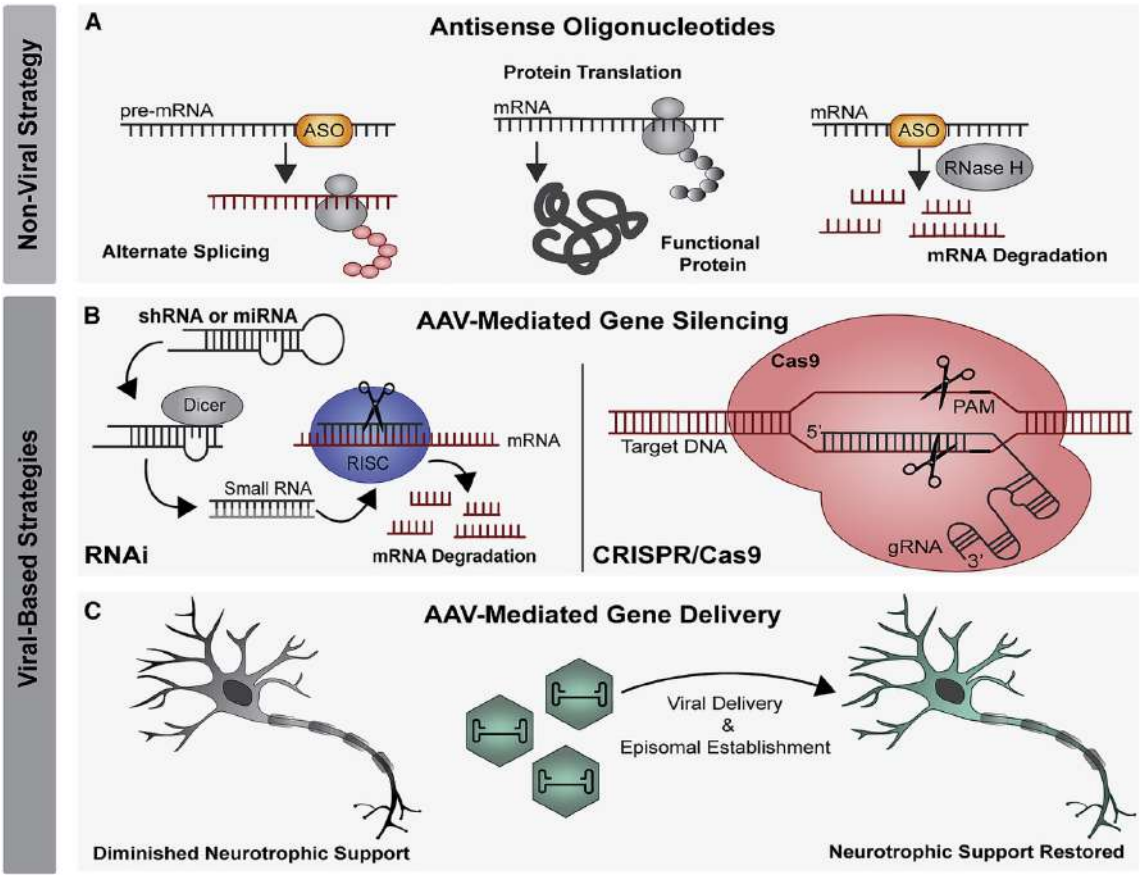

Figure 1.6 Gene therapy strategies. (**A**) Non-viral strategies include ASOs that induce alternate splicing or promote mRNA degradation via recruitment of RNase H enzyme. (**B**, **C**) Viral-based strategies include AAV-mediated gene silencing by RNAi or CRISPR gene-editing technology and AAV-mediated gene delivery of neurotrophic and non-neurotrophic factors. **AAV**, adeno-associated virus; **ASO**, antisense oligonucleotide; **Cas**, CRISPR-associated system; **miRNA**, microRNA; **PAM**, protospacer adjacent motif; **RISC**, RNA-induced silencing complex; **RNAi**, RNA interference; **shRNA**, small hairpin RNA. Image from AMADO AND DAVIDSON 2021.

1.6.2.1 ASOs

ASOs are short, single stranded oligonucleotides that can be designed to complement target mRNAs and promote their cleavage through the recruitment of the RNase H enzyme or to induce alternative splicing of primary transcripts (CERRITELLI AND CROUCH 2009). Over time, several modifications have been employed to increase the stability of ASOs against nuclease degradation, ensuring efficient delivery to target RNA in cells and tissues (BROWN *et al.* 1994; ECKSTEIN 2000). ASOs are unable to cross the blood-brain barrier, but are able to achieve a widespread distribution in the CNS following intrathecal administration (SMITH *et al.* 2006; SCHOCH AND MILLER 2017). The approval of ASOs for the treatment of spinal muscular atrophy (SMA), an inherited lower motor neuron disease by both the EU EMA and U.S. FDA, provides an important proof-of-concept for ALS (CHIRIBOGA *et al.* 2016; FINKEL *et al.* 2017; MENDELL *et al.* 2017).

In a key preclinical study, an ASO targeting *SOD1* reduced *SOD1* mRNA through RNase H activity in the brain and spinal cord of *SOD1*-rats, slowing down disease progression and increasing their mean survival (SMITH *et al.* 2006). This led to the first human phase I clinical trial (ClinicalTrials.gov: NCT01041222) where this approach was tested in patients with *SOD1*-linked ALS. This confirmed tolerability and safety of ASO administration in humans, however it did not reduce SOD1 in the CNS (MILLER *et al.* 2013). A subsequent trial delivered the *SOD1*-ASO, Tofersen, in higher doses. In addition to verifying safety of stronger doses, this led to significant reductions in CNS SOD1 protein, as well as a reduction in the rate of disease progression (MILLER *et al.* 2020). Safety and efficacy are being further evaluated in a phase III clinical trial (ClinicalTrials.gov: NCT02623699).

Similar to *SOD1*, the development of treatments for *C9orf72*-linked ALS using ASO-based strategies have also been explored. The first ASOs developed to reduce toxicity associated with increased *C9orf72* repeat expansions were tested in induced pluripotent stem cells (iPSCs) derived from *C9orf72*-ALS patients (DONNELLY *et al.* 2013; SAREEN *et al.* 2013) and subsequently in mouse models (LAGIER-TOURENNE *et al.* 2013). ASO-mediated reduction of the *C9orf72* transcript *via* RNase H RNA degradation or disruption of G_4C_2-repeat sequestration of RNA binding proteins was shown to reduce

nuclear foci in *C9orf72*-associated ALS. In turn, ASO treatment was able to reverse aberrant gene expression and reduce the risk of excitotoxicity in iPSC-differentiated neurons and improve cognitive deficits in adult mice expressing *C9orf72* expansions (LAGIER-TOURENNE *et al.* 2013; JIANG *et al.* 2016).

Among its diverse functions, ATXN2 is mostly characterized by its role in the formation of stress granules, which is of particular relevance in the development of ASO strategies since aggregation-prone proteins, such as TDP-43, tend to localize to stress granules in response to cellular stress (NONHOFF *et al.* 2007; LIU-YESUCEVITZ *et al.* 2010). Indeed, delivery of ASOs targeting *ATXN2* to TDP-43 ALS mouse models improved motor defects and prolonged survival (BECKER *et al.* 2017). Furthermore, the delivery of *ATXN2*-ASOs to neuronal-differentiated iPSCs from patients with C9orf72 expansions reversed cytoplasmic mislocalisation of nuclear proteins (ZHANG *et al.* 2018). Therefore, aside from patients with *ATXN2*-ALS, this strategy can also benefit a broader ALS population. In virtue of this, a phase I clinical trial (ClinicalTrials.gov: NCT04494256) is currently enrolling patients with *ATXN2* CAG repeat expansions, as well as those without.

1.6.2.2 AAV-mediated gene silencing

A distinct therapeutic approach involves targeting RNA by gene silencing via RNAi, a naturally occurring process which induces homology-dependent degradation of target mRNA. The delivery of small non-coding RNAs, such as small hairpin RNA (shRNA) or artificial microRNA (miRNA) to regulate gene expression, is frequently achieved by AAVs. An alternative strategy to treat gain-of-function disorders is by gene editing. CRISPR-associated (Cas) systems, particularly the RNA-guided Cas9 endonuclease are increasingly adopted to enable targeted genetic modifications (LIU 2017). Additional CRISPR-based systems that have transformative potential and which are small enough for AAV integration have been developed, and their therapeutic application to the ALS field is encouraging (KONERMANN *et al.* 2018).

SOD1 has been the target of several AAV-RNAi-based strategies. The first attempt of this kind involved the delivery of shRNA against *SOD1* by means of AAV9 in *SOD1*-mice of different age groups. This resulted in a 39% increase in survival after a single

administration. This decreased significantly with age and disease progression, and may be possibly linked with preferential glial targeting over neurons with subsequent injections. A substantial increase in survival rate was also observed when treatment was administered after disease onset (FOUST *et al.* 2009; FOUST *et al.* 2013). In a separate study, AVV9-shRNA targeting SOD1 were injected in presymptomatic adult SOD1 rats and authors demonstrated that upper motor neuron *SOD1* suppression alone was sufficient to delay disease onset and increase survival by 20 days (THOMSEN *et al.* 2014). The delivery of artificial miRNA to alter *SOD1* expression using both AAV9 and AAVRh10 vectors also improved survival and extended disease onset in mice. Importantly, it proved successful in silencing *SOD1* as indicated by low SOD1 levels in the motor neurons of monkeys, and the cerebrospinal fluid (CSF) of human ALS patients (BOREL *et al.* 2016; STOICA *et al.* 2016; MUELLER *et al.* 2020). The development of RNAi-based approaches for *C9orf72* has been more complex compared to *SOD1,* due to the challenges of targeting intronic, GC-rich repeats. However, a specialised design allowed for the successful inhibition of G_4C_2 expansions in fibroblast cells derived from ALS patients (PETRI AND MEISTER 2013; HU *et al.* 2015; HU *et al.* 2017).

The first study to evaluate the effects of CRISPR gene editing in ALS employed modified AAV9 to disrupt mutant *SOD1* expression in neonatal *SOD1*-mice. Treated mice exhibited improved motor function, as well as 37% delay in disease onset and an increase in survival by 25% (GAJ *et al.* 2017). A different study confirmed an improvement of motor function and a notable increase in survival, supporting encouraging results for future CRISPR-based strategies (DUAN *et al.* 2020). A recent study of note generated CRISPR-Cas9-mediated deletions in iPSCs derived from patients with *C9orf72* expansion. The expression of the *C9orf72* variant harbouring the repeat expansion was successfully reduced, and in turn improved axonal degeneration (KRISHNAN *et al.* 2020). Another recent study revealed that the overactivated Ku-80-dependent DNA repair pathway contributes to neurodegeneration in a *C9orf72* fly model. In relation to this, partial Ku80 reduction through CRISPR-Cas9 deletion inhibited the activation of a proapoptotic pathway, highlighting additional *in vivo* therapeutic targets in future studies (LOPEZ-GONZALEZ *et al.* 2019).

1.6.2.3 AAV-mediated gene delivery

Despite substantial numbers of clinically tested treatment approaches, the precise pathological mechanisms of ALS are still not clear, thus therapeutic options remain limited. In line of this, investigative efforts have turned to neuroprotective strategies to support degenerating neurons. Neurotrophic factors are essential for neuronal growth and survival. A decline in neurotrophins has been detected in ALS patient and animal models, indicating a potential role in neuronal health (HENRIQUES *et al.* 2010). Nonspecific, brain-derived neurotrophic factors (BDNF), glial cell line derived neurotrophic factor (GDNF), insulin-like growth factor 1 (IGF-1) and vascular endothelial growth factor (VEGF) have been employed to prolong survival in ALS patients. Tissue-specific delivery of neurotrophic factors is achieved using AAVs (WANG *et al.* 2002; KASPAR *et al.* 2003; AZZOUZ *et al.* 2004; DODGE *et al.* 2010). AAV-mediated delivery of non-trophic factors including neuromuscular junction modulators and protein aggregation-focused therapies have also been assessed, and although not curative, provide disease-modifying effects (WANG *et al.* 2017; LEYTON-JAIMES *et al.* 2019).

1.7 STUDY AIMS AND EXPERIMENTAL DESIGN

Owing to the small size and compact genetic pool of the Maltese Islands, it is intriguing to hunt for founder ALS-causing genes or those that influence disease progression among Maltese individuals suffering from motor neuron degeneration. Malta is a southern European island country in the Mediterranean Sea, consisting of an archipelago of three inhabited islands spanning a total area of 316km^2. Malta's population amounted to 514, 564 inhabitants by the end of 2019 according to Malta's National Statistics Office, with highest concentrations in the Northern and Southern harbour regions. Inhabited since prehistoric times, Malta was first colonized by neighbouring Sicilians. The frequencies of Y-chromosome haplogroups reveal that Malta is closest to north western Sicilians within the Central-East Mediterranean cluster that also includes southern Italy, Cyprus and Turkey (CAPELLI *et al.* 2006; CASSAR *et al.* 2008). The national language of Malta that is derived from Siculo-Arabic, is the only Semitic

official language of the European Union, further highlighting the seclusion from other populations in Europe.

In consolidation with the massive leap in sequencing technology, the reduced genetic diversity of an isolated population is considerably favoured in the identification of novel interactors and/or variants associated with disease. A unique Malta ALS/MND Register and BioBank was set up and presently holds biological samples of 38 ALS patients and 45 age-sex-region-matched controls. For this study, analysis of genome and clinical data of 24 patients and 13 controls was performed. Firstly, the incidence and prevalence of ALS in the Maltese Islands, as well as the baseline characteristics of Maltese ALS patients were investigated and compared with those for Maltese control participants. Correlation with environmental and lifestyle factors that might increase ALS risk was also analysed. Maltese ALS patient genomic data was then screened for rare variants in protein-coding regions of all presently known ALS genes and genetic risk loci and compared to data of matched controls. In addition, results were placed into the context of a broader dataset derived from an international biobanking register (PROJECT MINE 2018).

With 4,366 ALS patients and 1,832-matched controls WGS collected so far, the Project MinE initiative has already supported new gene discovery such as the identification of the ALS-causative genes *NEK1* (KENNA et al. 2016) and *KIF5A* (NICOLAS et al. 2018), as well as novel ALS risk variants in *C21orf2* (VAN RHEENEN et al. 2016). Project MinE employs a strategic approach that mainly involves rare-variant burden analyses (rvb) to determine association with ALS risk. The resulting outcome, together with relevant annotations can be accessed on a dedicated databrowser where data can be replicated by other consortia to reproduce comparable ALS genetic data results or to facilitate clinical interpretation of specific ALS patients. The Maltese cohort also forms part of the international collaborative effort with the aim of analysing local data against a broader genetic resource of reliable sample size and ancestral diversity, to allow for accurate identification of effective ALS mutations. Disease association between candidate variants identified in the Maltese cohort and those among the international case-control dataset were investigated to validate their risk effects and to probe for overlapping disease variants among different populations.

A valuable approach to define hotspots within a genome-wide set of genetic variants is to test their impact in a disease model. Coupling human data with animal model genetics can prove beneficial to narrow down gene targets within highlighted genomic regions to reveal those that are significant to the disease process. In view of the remarkable similarity at a genetic and biological level, the fruit fly *Drosophila melanogaster* has been successfully used to model a multitude of neurodegenerative disorders, thereby consolidating molecular understanding of pathogenic mechanisms associated with disease. Several ALS disease models have been generated and include those characterized for TDP-43-associated pathways, disease models expressing large hexanucleotide repeat expansions associated with *C9orf72* mutations, as well as mutant FUS and Ataxin-2 models among others (McGurk *et al.* 2015). Expression of human TDP-43 in the fly generates similar phenotypes to those observed in ALS patients including neuronal degeneration and reduced lifespan as a result of RNA pathway disruption (Li *et al.* 2010; Voigt *et al.* 2010). Comparably, expression of a G_4C_2 repeat in *Drosophila* induces disrupted eye morphology and confers and age-dependent decline in motor function when expressed in fly neurons (Xu *et al.* 2013). Functional characterisation of damaging genes within ALS genetic loci in Maltese ALS patients was carried out to evaluate their effect on fly viability and motor function. This was accomplished through the use of a genetic and biochemical approach.

CHAPTER 2

METHODS

2.1 PARTICIPANT RECRUITMENT

Patient recruitment was carried out within a 2-year period, from 2017 through 2018. Patients were referred by the ALS Malta Foundation, consultant neurologists, general practitioners and neurophysiology units. Alternatively, some patients were independent volunteers. In all cases, ALS diagnosis met the revised El Escorial diagnostic criteria (BROOKS 1994; BROOKS *et al.* 2000). Patients with at least one first-degree relative affected by ALS, were classified as fALS. In total, 24 patients and 13 control participants were enrolled in this study. Controls were matched for age, sex, and geographical region in a 2:1 case-control ratio. Recruitment was accomplished in three main stages that included the completion of a detailed questionnaire (Appendix I), a basic physical examination to test for reflex and motor function, and withdrawal of blood. The final two stages were conducted by the study's medical doctor. Blood sampling was excluded for one sALS case in view of the patient's deteriorating condition. Affected family members for all fALS cases were deceased by the time of recruitment, thus sampling for linkage analysis was not possible. The collection of samples, establishment of the Malta ALS/MND Register and Biobank and experimental design were reviewed and approved by the University Research Ethics Committee (UREC) at the University of Malta. Written informed consent (Appendix II) was sought from all participants including patients, family members and controls.

2.2 CLINICAL DATA

A core clinical dataset was defined for all participants and was stored separately from genetic data. Both datasets can be connected through sample identifiers. The core clinical dataset includes personal information such as age, sex, place of residence and occupation; as well as clinical data including date and site of onset, cognitive status, date of requiring invasive/non-invasive ventilation, ALS Functional Rating Scale-revised (ALSFRS-R) score (CEDARBAUM *et al.* 1999), muscle tone, muscle power according to Medical Research Council (MRC) scale (MEDICAL RESEARCH COUNCIL 1943; DYCK *et al.* 2005) and reflex function status. The core clinical dataset also included information about the creatine kinase (CK) blood levels at recruitment, as a biochemical indicator of skeletal muscle damage.

2.2.1 Physical examination

Examination of the motor system allows for the quantification of motor function impairment and differentiation between central and peripheral lesions. Fundamental elements of the examination included the assessment of muscle tone and appearance, as well as the evaluation of muscle movement and power, and reflexes.

2.2.1.1 Muscle tone

Muscle tone indicates the resistance perceived by the examiner upon passive joint movement within its full range of motion (**Figure 2.1**). During examination, the examiner observed for abnormal findings such as decreased muscle tone (hypotonia) or increased muscle tone (hypertonia). Hypotonia is commonly associated with muscle wasting, weakness and hyporeflexia. This typically occurs in lower motor neuron lesions and is frequently associated with cerebellar disease (BODRANGHIEN *et al.* 2016). Hypertonia is often perceived as spasticity or rigidity. Spasticity is described as resistance to passive quick movements and is a typical feature of an upper motor neuron lesion (BURKE *et al.* 1972; MUKHERJEE AND CHAKRAVARTY 2010). Conversely, rigidity is characterized by a sustained resistance throughout the range of movement (SHERRINGTON 1898). Spasticity is often accompanied by clonus, a rhythmic sequence of contractions, which when sustained is associated with motor neuron damage (ZIMMERMAN AND HUBBARD 2019). Muscle tone was assessed for both upper and lower limbs. The appearance of fasciculations, abnormal posture and asymmetrical movement was also noted.

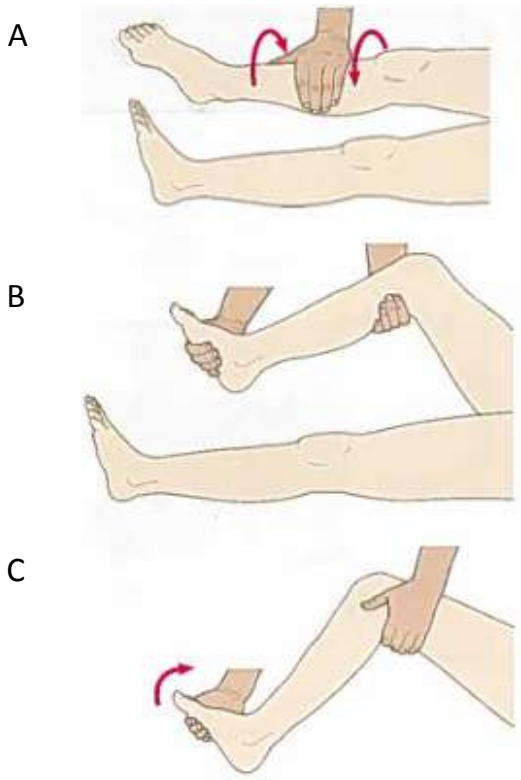

Figure 2.1 Assessment of muscle tone. The examination sequence begins by rotation of the leg from side to side (**A**) and is followed by a brisk full range movement of the knee into a flexed position (**B**). The ankle is tested for clonus by briskly flexing and partially everting the foot, sustaining the pressure (**C**). Upper limb examination is performed in a similar way by holding patient's hand with one hand and supporting elbow with the other (DOUGLAS 2009).

2.2.1.2 Muscle Power

Muscle strength was rated according to the MRC scale for muscle power (MEDICAL RESEARCH COUNCIL 1943). Key muscles from the upper and lower extremities were assessed against the examiner's resistance (**Table 4**) and patient strength was graded accordingly [**0** no muscle contraction visible; **1** muscle contraction visible but there is no movement of the joint; **2** active joint movement is possible with gravity eliminated; **3** movement can overcome gravity but not resistance from the examiner; **4** the muscle group can overcome gravity and move against some resistance from the examiner; **5** full and normal power against resistance] (NAQVI AND SHERMAN 2018). The assessment of neck muscle power was achieved by evaluating neck flexion and extension. Examination of the upper limb muscle group included bilateral abductors of shoulders and elbow flexors and extensors as representatives of the proximal upper extremity muscles; as

well as extensors and flexors of the wrist and bilateral abductors of the thumb as representatives of distal upper extremity muscles. Muscle strength was also tested in bilateral flexors of the hip, knee extensors and flexors as representatives of the proximal lower extremity muscles, as well as in ankle dorsiflexion and plantar flexion muscles as representatives of the distal lower extremity muscles.

Table 4 Assessment of movement and power of different muscle groups.

Movement		Examination Sequence	
NECK	Flexion	Movement of chin to chest. A decreased range is recorded as chin-chest distance.	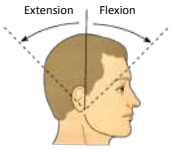
	Extension	Movement of chin away from chest, as far back as possible.	
SHOULDER	Abduction	Lifting of arm away from the side of the body, whilst facing forward.	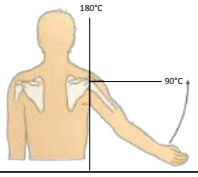
ELBOW	Flexion	Bending of arms to touch shoulders.	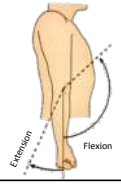
	Extension	Straightening of elbow, as far as possible.	
WRIST	Flexion	Bending of wrist, as far back as possible.	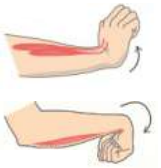
	Extension	Bending of wrist towards pulse.	
THUMB	Abduction	Vertical upward movement of thumb from palm against resistance.	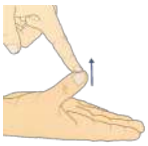
HIP	Flexion	Movement of thigh towards chest from hip joint.	
KNEE	Flexion	Bending of knee to bring foot toward the posterior thigh.	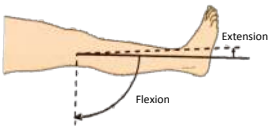
	Extension	Straightening of leg so that the femur and tibia are in longitudinal alignment.	
ANKLE	Dorsiflexion	Backward movement of toes towards shins.	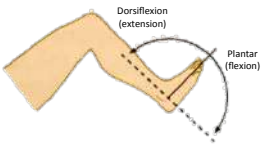
	Plantar Flexion	Pointing of toes away from leg.	

2.2.1.3 Reflexes

Reflex function was assessed using a tendon hammer to elicit deep tendon or muscle stretch reflexes on a fully relaxed joint (**Table 5**). In a normal person, the muscle contracts immediately upon brisk tapping of a particular muscle tendon, a reflex action corresponding to the spinal or brainstem segment innervating the muscle. A diminished or hyperactive response suggests abnormality. Reflex function was graded accordingly [**4+** very brisk, hyper-reflexive, with clonus (rhythmic oscillations between flexion and extension); **3+** brisker than average, possibly but not necessarily indicative of disease; **2+** a brisk response, normal; **1+** somewhat diminished response, low normal; **0** no response] (WALKER 1990; ZIMMERMAN AND HUBBARD 2021).

Five primary deep tendon reflexes including bicep, triceps, brachioradialis, patellar and Achilles reflexes were examined. In addition, the Hoffman's reflex was assessed to test the integrity of the corticospinal tract. This involves the downward forceful flicking of the fingernails. A positive response, indicated by excess thumb flexion and adduction, indicates the presence of upper motor neuron lesions (TANAKA 1986). Although not a deep tendon reflex, the plantar reflex (or Babinski's sign test) is often considered as the lower limb equivalent of the Hoffman's reflex. The plantar reflex test evaluates the response elicited by stroking the plantar surface of the foot. Normally this triggers flexion of both the foot and toes, whereas dorsiflexion of the toes, or a positive Babinski sign, indicates disease in the corticospinal tract (MORROW AND REILLY 2011).

Table 5 Assessment of deep tendon reflexes.

Reflex	Examination Sequence	
BICEPS	Striking bicep tendon of a relaxed arm with a reflex hammer.	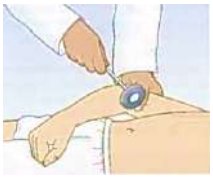
TRICEPS	Striking tricep tendon of a relaxed arm with a reflex hammer.	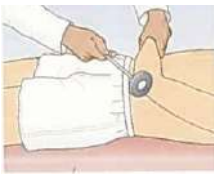
SUPPINATOR	Striking brachioradialis tendon of a relaxed arm with a reflex hammer.	
KNEE	Striking of patellar tendon with a reflex hammer, just below the patella.	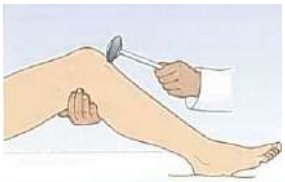
ANKLE	Striking the Achilles tendon with a reflex hammer, whilst foot is dorsiflexed	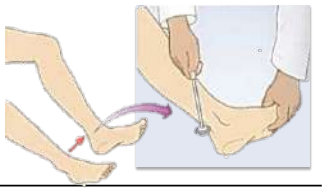
HOFFMANN'S	Flicking of finger downwards. Excess thumb flexion suggests hypertonia.	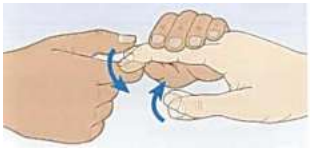
PLANTAR	Running a blunt object along the lateral border of the sole of the foot towards the little toe. A normal response is flexion of all toes.	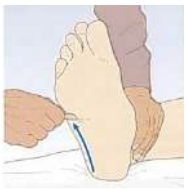

2.2.2 Assessment of physical ability

The ALS Functional Rating Scale (ALSFRS) is a standard measure to evaluate activities of daily living and global physical function. The ALSFRS is independent from strength testing and has been used in both clinical practice and clinical trials to measure disease status and to monitor the progression of disability in ALS patients (STAMBLER *et al.* 1998; MANDRIOLI *et al.* 2015; PINTO *et al.* 2019). Levels of self-sufficiency in functional categories such as feeding, grooming, ambulation and communication were assessed by means of a validated questionnaire-based scale which incorporates four different domains of motor ability that encompass bulbar function, fine motor tasks, gross motor tasks and respiratory function (**Table 6**) (CEDARBAUM AND STAMBLER 1997). Initially, the components of the scale were not equally weighted, therefore the scale was later revised (ALSFRS-R) to incorporate additional questions to better evaluate the progression of respiratory dysfunction in ALS (CEDARBAUM *et al.* 1999). Each function was scored from 4 (normal ability) to 0 (no ability) for a maximum score of 48 points. Hence, a low score was indicative of advanced disease.

Table 6 The ALS Functional Rating Scale – Revised (ALSFRS-R).

DOMAIN		FEATURE
Bulbar function		○ Speech ○ Swallowing ○ Salivation
Motor function	Fine Motor	○ Writing ○ Feeding ○ Dressing
	Gross Motor	○ Turning ○ Walking ○ Climbing stairs
Respiratory function		○ Dyspnoea - difficulty breathing ○ Orthopnoea - shortness of breath in a recumbent position ○ Respiratory insufficiency - use of non-invasive/invasive ventilation

2.2.3 Creatine Kinase

Creatine kinase (CK) catalyses phosphorylation of creatine using adenosine triphosphate (ATP), a reaction which can be reversed to serve as an energy reservoir for tissues or cells that consume ATP rapidly. CK exists as different isoenzymes with highest activity in muscle (CK-MM), heart (CK-MB) and brain (CK-BB), distribution of which varies between tissues (WALLIMANN *et al.* 1992). The dimeric enzyme can be detected in serum, plasma and urine and is commonly elevated upon muscle injury (MOGHADAM-KIA *et al.* 2016).

Elevated CK levels in ALS patients is associated with loss or denervation of motor neurons, as well as muscular atrophy (FELICE AND NORTH 1998; LIMA *et al.* 2003; TAI *et al.* 2018). Increased levels of CK have also been interpreted as a compensatory mechanism for the upregulation of muscular metabolic pathways following motor neuron damage in ALS patients (RAFIQ *et al.* 2016; CECCANTI *et al.* 2020). Nevertheless, CK plasma half-life is relatively short and levels can return to normal following cessation of acute muscle damage and thus results can be conflicting (BAIRD *et al.* 2012; GIBSON *et al.* 2015). A single biochemical assay to test for serum CK levels was performed for all patients at the time of recruitment.

2.3 WHOLE GENOME SEQUENCING

Genomic DNA from peripheral blood was isolated using the QIAamp®DNA Mini QIAcube Kit (QIAGEN – Hilden, Germany) and DNA integrity was measured using the Quantus™ fluorometer (Promega Corporation – Madison, USA). Whole-genome sequencing was performed by the BGISEQ-500 sequencing platform (BGIHong Kong, China) to generate 100-bp paired-end reads that covered target regions to an average depth of 30X. Reads were aligned to the GRCh37 (hg19) reference genome using Burrows-Wheeler Aligner software. Aligned reads were delivered in binary sequence alignment/map format (BAM) together with variant call format (VCF) files that were generated for each individual. VCF files were used to call for single nucleotide variants (SNVs), insertions and deletions (indels), and larger structural variants (SVs) following quality filtering using the Genome Analysis Toolkit (GATK).

Sequence reads were used to estimate genetic ancestry. Specifically, genotypes at shared markers of each study individual and ancestry reference panel members were merged by the LASER (Locating Ancestry from SEquence Reads) software which then applies principal component analysis (PCA) to the merged dataset. This is then placed on a multidimensional space to compute the principal components of each study individual in relation to the selected reference population. The LASER server was used to map Maltese ALS and control samples to reference PCA coordinates for samples from the Human Genome Diversity Panel (HGDP), a worldwide panel including 938 individuals from 53 populations, to estimate continental ancestry (LI *et al.* 2008; TALIUN *et al.* 2017). Results were plotted using the LASER server plot facility which is accessible at http://laser.sph.umich.edu/.

2.4 VARIANT ANALYSIS

The sequencing data of the Maltese ALS patient and control cohort was mined for rare protein-coding and splice-site altering variants in 58 established ALS causative or risk genes (*ALS2*, *ANG*, *ANXA*1, *ATXN2*, *C21ORF2*, *C9ORF72*, *CAPN14*, *CCNF*, *CHCHD10*, *CHMP2B*, *CYLD*, *DAO*, *DCTN1*, *DDX20*, *DNAJC7*, *ELP3*, E*RBB4*, *EWSR1*, *FIG4*, *FUS*, *GGNBP2*, *GLE1*, *GLT8D1*, *GPX3*, *GRN*, *HNRNPA1*, *HNRNPA2B1*, *KIF5A*, *MAPT*, *MATR3*, *MOBP*, *NEFH*, *NEK1*, *NIPA1*, *OPTN*, *PFN1*, *PRPH*, *SARM1*, *SCFD1*, *SETX*, *SIGMAR1*, *SMN1*, *SMN2*, *SOD1*, S*PAST*, *SPG11*, *SS18L1*, *SQSTM1*, *TAF15*, *TARDBP*, *TBK1*, *TIA1*, *TNIP1*, *TUBA4A*, *UBQLN2*, *UNC13*A, *VAPB*, and *VCP*). Analysis was restricted to variants with European minor allele frequency (MAF) of ≤0.02 as estimated by the Genome Aggregation Database (gnomAD). The Allele frequencies for ALS cases and controls within the Project MinE dataset were extracted from the Project MinE databrowser (VAN DER SPEK *et al.* 2019).

Variant pathogenicity was determined by the meta-analytic support vector machine (Meta-SVM) ensemble-based prediction algorithm. This method integrates multiple scoring systems to increase accuracy in variant prediction (DONG *et al.* 2015). Specifically, the Meta-SVM model predicts how amino acid substitutions affect protein function. Unlike other SVM models, this model is designed to accommodate multiple omics data that allows for detection of common and study specific genetic effects across

all studies (KIM *et al.* 2017). Indels and splice-site acceptor/donor variants were automatically classified as deleterious.

Variant clinical significance was also classified according to the American College of Medical Genetics and Genomics (ACMG) – Association for Molecular Pathology (AMP) recommendations. These recommendations constitute a five-tier terminology system that classify sequence variants as "pathogenic", "likely pathogenic", "uncertain significance", "likely benign", and "benign" based on expert, consensus-based available evidence observed for the variant. Principally, two sets of criteria are provided to classify either pathogenic or likely pathogenic variants or benign or likely benign variants. A variant was considered of uncertain significance if it does not fulfill criteria using these guidelines or if the evidence for benign and pathogenic is conflicting. Variant data was gathered from peer-reviewed published data or through public resources such as population or disease databases (RICHARDS *et al.* 2015).

Combined Annotation-Dependent Depletion (CADD) is extensively being used for the effective enrichment of deleterious alleles. CADD ranks genetic variants by integrating a myriad of genomic features including gene model annotations, evolutionary constraint, epigenetic measurements and functional predictions into a single score *via* a machine learning model. The immediate output or "raw" scores is indicative of whether the variant is likely to have derived from a benign "neutral" (negative values) class or a deleterious (positive values) class. Higher values indicate that a variant is more likely to have derived from the phenotypically influential variant set rather that the neutral class and is therefore more likely to have deleterious effects (RENTZSCH *et al.* 2019). Raw CADD scores for rare ALS variants were used to interpret variant deleteriousness in order to support their role in ALS pathogenesis.

Expansion sizes of short tandem repeats (STRs) in *C9orf72* (NM_001256054.2:c.-45+163GGGGCC), *ATXN2* (NM_002973.3:c.496_498CAG) and *NIPA1* (NM_144599.4:c.24_26GGC) were analysed by means of the ExpansionHunter tool. This algorithm is able to identify reads that are of the exact size of the repeat and thus fully span the repeat (spanning reads); reads that include the flanking sequence on one side of the repeat when repeat length is close to the read length (flanking reads) and reads

that are fully contained in the repeat (in-repeat reads). The latter is used when repeat length is longer than the read length. For repeats shorter than the read length of the sequence data, repeat length is quantified via both spanning and flanking reads (DOLZHENKO *et al.* 2017; DOLZHENKO *et al.* 2019; DOLZHENKO *et al.* 2020)

2.5 VERIFICATION OF DAMAGING ALLELES

The identification of heterozygous damaging alleles *DCTN1* c.1864A>T and *SCFD1* c.209T>C was verified by Sanger sequencing. The DNA of patients harbouring these mutations as well as that of controls was amplified from DNA extracts derived from plasma samples. Amplification of DNA was achieved by using the HOT FIREPol Blend master mix (Solis Biodyne - Tartu, Estonia) using primers specific to *DCTN1* (forward: 5'-ATTCCCCACCCAGGTAAGAG-3'; reverse: 5'-GTACACCAGTCCAGCAGCAA-3') and *SCFD1* (forward: TTGGCCAAGATATCTCTCCTC-3'; reverse: 5'CCAAATCTAAGGAAAAGCCACA-3') following manufacturer's instructions. PCR products were then separated by electrophoresis on a 1.5% agarose gel containing ethidium bromide and bands were visualised under ultraviolet light. When suitable bands were obtained, the Invitrogen PureLink Quick Gel extraction kit (Life Technologies - Thermo Fischer Scientific, US) was used to purify DNA fragments from agarose gel. Relevant gel sections were excised and dissolved in solubilization buffer. DNA fragments were then purified and eluted by centrifugation. Purified DNA fragments were then submitted to Eurofins Genomics (Luxembourg, Germany) for light-speed sequencing using their LightRun Tube service. Interpretation of sequencing chromatograms was achieved using the 4Peaks software (A. Griekspoor and Tom Groothuis, Nuclobytes B. V., nucleobytes.com).

2.6 FUNCTIONAL GENETICS

2.6.1 Fly Stocks and Culture

Flies were cultured on standard molasses/maizemeal and agar medium in 50 ml plastic vials and stored in temperature-controlled rooms or incubators. General stock keeping was done at 18°C, whereas specialized assays were performed in conventional

temperatures of 25/29°C. For the purpose of handling and inspection, flies were immobilized by non-toxic levels of carbon dioxide (CO_2) gas dispensed from a needle connected to a CO_2 tank. The pipeline also branches to a CO_2-dispensing porous pad, where flies could be transferred for inspection under the light microscope.

For the majority of genetic mating schemes, virgin females were crossed to males in a fresh vial and transferred to desired incubation temperatures. Following fertilization and embryogenesis, the fertilized egg is deposited into the food, with the first instar larva hatching after approximately 24 hours. The larva continues to feed until it reaches third instar larva, 5 days after deposition and towards the end of this stage prepares for pupation. Metamorphosis occurs during the following 4 days in the pupal case from which adults emerge or eclose approximately 10 days into the cycle (STOCKER AND GALLANT 2008).

2.6.2 *Drosophila* transgenic constructs and expression

Expression of inducible transgenes was performed *via* the GAL4/*upstream activation sequence* (*UAS*) system (CAUCHI AND VAN DEN HEUVEL 2006). This bipartite approach keeps the yeast transcription factor GAL4 and the UAS promotor (which holds the transgene) on different parental strains. When the two strains are mated, the progeny expresses the transgene in specific tissues defined by the GAL4 driver gene (**Figure 2.2**). The expression of the GAL4 gene in several tissue-specific patterns is achieved as a result of multiple 'enhancer-trap' lines that were generated by inserting the GAL4 gene at random positions in the *Drosophila* genome. Such enhancer-trap lines allow for expression of GAL4 under the control of genomic enhancers, so that GAL4 is only expressed in cells where the driver gene has been activated, that is, where the UAS transgenes has been introduced (ST JOHNSTON 2002). The *UAS* transgenes included RNAi constructs that express RNAs containing inverted repeats (IR) derived from the target gene of interest, for ubiquitous or tissue-specific knockdown.

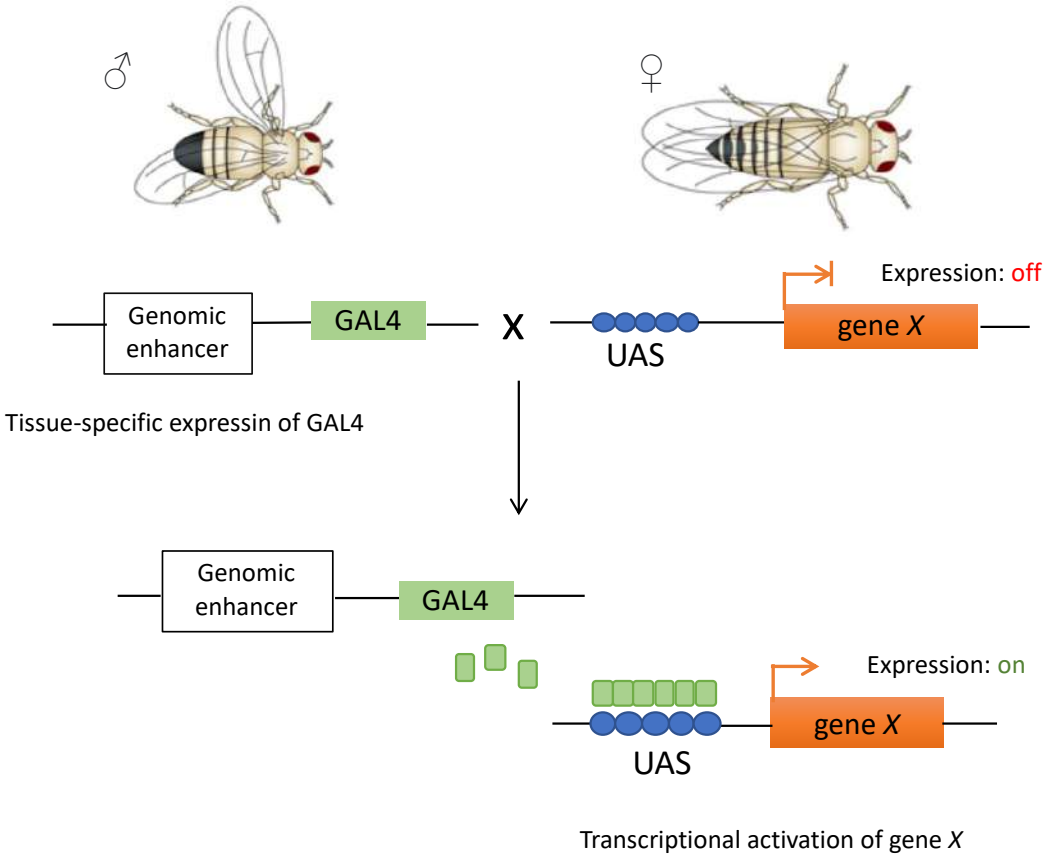

Figure 2.2 The *UAS*-GAL4 system for transgene expression. Tissue-specific expression of GAL4 can be controlled *via* genomic enhancers and is activated upon the introduction of the UAS transgene which is then expressed by the progeny. Adapted from ST JOHNSTON 2002.

Knockdown by RNAi constructs is induced when the gene-specific IR produces hairpin-loop double-stranded RNA (dsRNA) molecules, which are then cleaved by the RNase III endonuclease Dicer, to form small interfering RNAs (siRNAs). Dicer is, in turn, complexed with RNA-binding proteins which are responsible to convey siRNAs to the RNA-induced silencing complex (RISC). At this stage, siRNAs that are loaded onto the RISC are cleaved by Argonaute (Ago) family member, Ago-2, that possesses and active catalytic domain for cleavage activity. The passenger (sense) strand of the siRNA duplex is discarded, and the remaining (antisense) strand serves as a guide to direct RISC to target mRNA by intermolecular base pairing, which is then subject to endonucleolytic cleavage and degradation by the activated complex (**Figure 2.3**) (KIM AND ROSSI 2008).

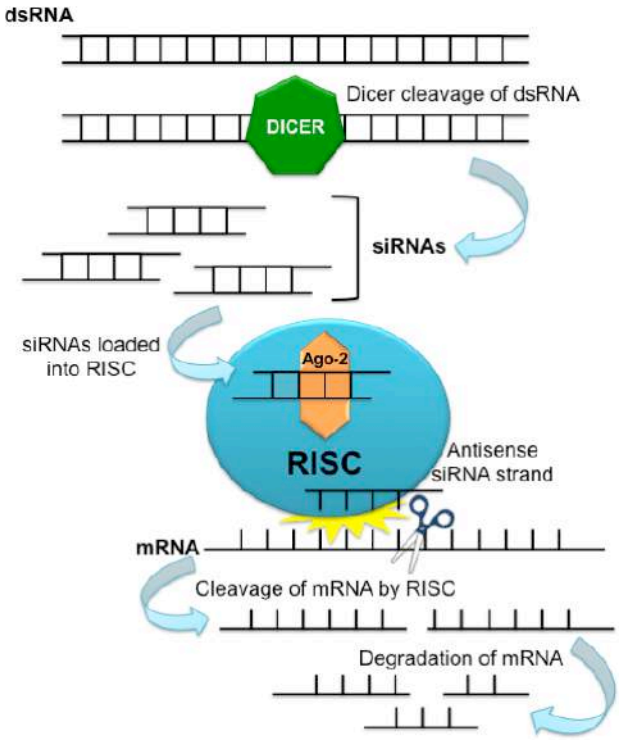

Figure 2.3 RNAi gene knockdown. Cleavage of long dsRNAs by Dicer, produces siRNAs that are associated with the RISC**.** Here they are further cleaved by Ago-2 leading to the unwinding of the double-stranded siRNA. Whilst the sense strand is discarded, the antisense strand acts as a guide strand and directs the RISC complex to cognate mRNA. The homologous mRNA is cleaved by the RISC and degraded. Abbreviations: dsRNA, double-stranded RNA; siRNA, small interfering RNA; RISC, RNA-induced silencing complex, Ago-2, argonaute family member 2. Modified from KIM AND ROSSI 2008.

The *UAS* transgenes used included RNAi constructs, *UAS.Slh*-RNAi [*ME-2*] (ID: 51840), *UAS.Slh*-RNAi (*ME-3*) (ID: 105669) and *UAS.Slh*-RNAi [*ME-4*] (ID: 108778) for knockdown of the *SCFD1 Drosophila* orthologue, *Slh*. RNAi constructs for *DCTN1* Drosophila orthologues included, *UAS.CG9279*-RNAi [*ME-9*] (ID: 45052), *UAS.CG9270*-RNAi [*ME-10*] (ID: 105109) and *UAS.DCTN1-p150*-RNAi [*ME-18*] (ID: 3785). *RNAi* transgenic constructs were all obtained from the Vienna *Drosophila* Resource Centre (VDRC) (Appedix III) (Dietzl *et al.* 2007) and have not been previously described (**Table 7**). The wild-type strain was w^{1118}. The GAL4 lines used to drive expression of *UAS*-linked transgenes are summarized in **Table 8 and described in Appendix IV**. Combination of alleles and transgenes was carried out according to standard genetic crossing schemes. Incubation temperature for viability and functional assays was 25°C. Where, indicated, the temperature was raised to 29°C to enhance expression level of

transgenes (Brand *et al.* 1994). In addition, RNAi-mediated gene silencing was also amplified by enhancing the Dicer-2 expression which promotes more dicer-dependent cleavage of dsRNA and therefore enhances knockdown (Mikuma *et al.* 2004).

Table 7 List of *UAS*-RNAi constructs.

Transgene	VDRC ID	Lab Name	Location	RNAi type	Reference
UAS.Slh-RNAi	51840	ME-2	Chromosome 2	P-element	(DIETZL et al. 2007)
UAS.Slh-RNAi	105669	ME-3	Chromosome 2	phiC31	(Keleman 2009)
UAS.Slh-RNAi	108778	ME-4	Chromosome 2	phiC31	(Keleman 2009)
UAS.CG9279-RNAi	45052	ME-9	Chromosome 3	P-element	(TEGEDER et al. 2019)
UAS.CG9279-RNAi	105109	ME-10	Chromosome 2	phiC31	(SCHNORRER et al. 2010)
UAS.DCTN1 p-150-RNAi	3785	ME-18	Chromosome 2	P-element	(DIETZL et al. 2007)

VDRC: Vienna *Drosophila* Resource Centre

Table 8 GAL4 drivers and their expression patterns.

	DRIVER	EXPRESSION PATTERN	SOURCE
Ubiquitous	*Act5C*-GAL4	Ubiquitous expression with an early onset	BDSC BL/4414
	da-GAL4	Ubiquitous expression	BDSC BL/8641
	tubP-GAL4	Ubiquitous expression	BDSC BL/5138
Muscle	*C57*-GAL4	Expression in mid-first to third stage larval muscles, two sensory cell bodies in body wall and gut	Gift from Vivian Budnik, University of Massachusetts, USA
	G7-GAL4	Expression in embryonic/larval somatic muscle	Gift from A. DiAntonio, Washington University, St. Louis, Missouri, USA
	C179-GAL4	Expression in larval muscle and mesoderm	BDSC BL/6450
	how-GAL4	Expression in mesoderm and larval muscles	BDSC BL/1767
	MHC-GAL4	Pan-muscular expression	Gift from Frank Schnorrer, University of Marseille, France
	Mef2-GAL4	Expression in embryonic cardioblasts, somatic cells and larval muscles	Gift from Barry Dickson, Research Institute of Molecular Pathology, Vienna, Austria
	Mef2-GAL4>Dicer-2	Enhanced muscular dicer expression	BDSC BL/25750
	G14-GAL4	Expression in embryonic hypodermal muscle and larval somatic muscle	Gift from Brian McCabe Columbia University, NY, USA
Brain & Neurons	*1407*-GAL4	Expresses GAL4 in all nerves	BDSC BL/8751
	Nrv-GAL4	Pan-neuronal driver	Gift from Paul Salvaterra, City of Hope National Medical Center, Duarte, California, USA
	D42-GAL4	Motor neuron-specific expression, together with expression in the peripheral nervous system including body wall and sensory neurons	BDSC BL/8816
	OK6-GAL4	Expression in all motor neurons, ventral nerve cord and brain lobes	Gift from Cahir O'Kane, University of Cambridge, UK
	OK6-GAL4>Dicer-2	Enhanced motor neuron dicer expression	Gift from Cahir O'Kane, University of Cambridge, UK
	elav-GAL4	Early onset expression in all postmitotic neurons	BDSC BL/458
	elav-GAL4>Dicer-2	Enhanced pan-neuronal dicer expression	BDSC BL/2575
	nSyb-GAL4	Pan-neuronal expression	Gift from Brian McCabe Columbia University, NY, USA
	Cha-GAL4	Expression in cholinergic neurons	BDSC BL/6793
Other	*GMR*-GAL4	Glass multiple reporter elements are specific to the developing eye, but are thought to have a broader expression profile, affecting also brain, leg discs, trachea and wings.	BDSC BL/9146

BDSC BL: Bloomington *Drosophila* Stock Centre, Indiana University, Bloomington

2.6.3 Analysis of mRNA expression *via* quantitative RT-PCR

RNA was extracted from 12-15 third instar larvae of the desired genotype using the QIAGEN RNeasy Plus Mini kit (QIAGEN – Hilden, Germany). Following selection, larvae were homogenized and lysed. Tissue lysates were then spun through genomic DNA (gDNA) Eliminator spin columns to remove genomic DNA and RNeasy Mini spin columns were subsequently used to purify total RNA. Quantification of *Drosophila SCFD1* or *DCTN1* expression levels was achieved by amplifying corresponding cDNA using MyGo Green 1-Step Low ROX (IT-IS Life Science Ltd. – Dublin, Ireland) or SOLIScript 1-step SolisGeen (Solis Biodyne - Tartu, Estonia) probe-based quantitative polymerase chain reaction (qPCR) reagents.

Equal concentrations of RNA were reverse transcribed into cDNA using M-MuLV or SOLIScript Reverse Transcriptase following manufacturer's instructions. mRNA transcripts were amplified using primers specific to *CG9279* (forward: 5'-CACGGCAGCATTTACTTCAA-3'; reverse: 5'-GAGTCGCCAAAAATTTTCCA-3'), *DCTN1-p150* (forward: 5'-CGCACCAAGGAGAAGCTTAG-3'; reverse: 5'-GGTCGCGATCATAGATGGTT-3'), *Slh* (forward: 5'-TCAGAAGGACGGGCTAAAGA-3') and the reference gene *RPL32* (forward: 5'-TACAGGCCCAAGATCGTGAA-3'; reverse: 5'-GACAATCTCCTTGCGCTTCT-3'). Data was acquired on the SYBR Green channel using optimal cycling conditions. qPCR analysis was performed using the MyGo Mini real-time PCR platform (IT-IS Life Science Ltd. – Dublin, Ireland) and data processing was performed using MyGo Pro software (v3.5.21).

The threshold crossing value for each transcript was recorded and normalized to the reference gene. The relative quantitation of each mRNA was then performed using the comparative cycle threshold (Ct) or double delta Ct (ΔΔCt) method (**Table 9**). Expression levels were calculated as the expression fold change. For each analysis, triplicate qPCR Ct values were obtained for control and experimental conditions of the gene of interest, as well as control and experimental conditions of the housekeeping or reference gene. The average Ct value for each condition was estimated to give four final values [gene being tested experimental (TE), gene being tested control (TC), housekeeping gene experimental (HE) and housekeeping gene control (HC)]. The

difference between experimental values (TE-HE=ΔCtE) and control values (TC-HC=ΔCtC), were calculated to obtain ΔCt values for both conditions and finally, the difference between the ΔCt values for both experimental and control conditions (ΔCtE - ΔCtC) was calculated to obtain the double delta Ct value. Since all calculation are in logarithm base 2, the expression fold is then obtained by calculating the value of 2^-ΔΔCt. A fold change of 1 indicates that the gene expression in the test condition is 100% as much as in the control condition, that is, there is no change between test and control groups. A fold-change value above 1 shows upregulation of the gene of interest relative to the control, whereas values below 1 demonstrates gene downregulation compared to the control (LIVAK AND SCHMITTGEN 2001).

Table 9 Double delta Ct analysis for interpretation of qPCR results.

Average Experimental Ct value		Average Control Ct value		ΔCt value (Experimental)	ΔCt value (Control)	ΔΔCt	Expression Fold Change
Gene of interest	Housekeeping gene	Gene of interest	Housekeeping gene	(TE-HE)	(TC-HC)	ΔCtE-ΔCtC	2^-ΔΔCt
TE	HE	TC	HC	Δ CtE	ΔCtC	ΔΔCt	% Expression

2.6.4 Assessment of viability and survival

Drosophila adult viability assays were performed to determine the effect of knockdown on development of flies from embryo to adult stage. Viability analyses were accomplished by crossing GAL4 driver stocks to *RNAi* transgenes and culturing first at 25°C and subsequently at 29°C to amplify GAL4 activity (Fortier and Belote 2000). Following eclosion, adult flies were screened and counted at regular intervals up to 10 days post eclosion. Viability was calculated as the percentage of the number of adult flies with the appropriate genotype divided by the expected number for the cross. For each temperature point, the assay was performed twice and the average viability was calculated for both vials.

Survival analyses measure the percentage number of adult flies in a population that remain alive with time. Test and control adult male flies were maintained at 25°C at a density of 15-20 flies per vial and survival was assessed for 4 time points. Four vials per

time-point (day 5, 15, 25 and 35 post-eclosion) were assessed. The percentage number of flies alive at each evaluated time point was determined by dividing the number of flies that remain alive by the initial number of flies assessed and multiplying the value by 100.

2.6.5 Assessment of flight performance

The effect of tissue-specific knockdown of the selected target genes on adult *Drosophila* flight performance was assessed in a series of flight assays. RNAi-mediated knockdown was activated by crossing the appropriate GAL4 driver with the RNAi transgene of interest. Cultures were incubated at 25°C and male flies of the desired genotype were subjected to flight assays. Flying ability was measured in the Droso-Drome, a simple in-house device consisting of a 1L glass bottle divided into four, 5cm segments, adding up to a total of 20cm in height. The internal walls of the Droso-Drome were coated with a sticky alcohol-based solution and test and control flies were introduced into the top of the device through a funnel. The number of flies in each sector was counted, divided by the total number of flies investigated and multiplied by 100 to generate a percentage number of flies in each sector. The flight capability of transgenic or control flies influences the height at which flies stick in the Droso-Drome. This means that flies that have normal flight ability are likely to stick to the walls of the upper sectors, whereas, flightless flies drop to the lowest sector. For each genotype, the flight assay was performed at 4 time points: 5, 15, 25 and 35 days post-eclosion to determine whether aging also affects flight performance. The number of tested adult flies in each vial ranged from 15 to 30 males.

2.6.6 Assessment of locomotor ability

2.6.6.1 Adult Climbing Assays

The climbing ability of adult flies was evaluated by two methods: the time-for-first-fly assay and the negative geotaxis assay (**Figure 2.4**). Both assays were performed by using two empty 25mm-diameter polystyrene vials taped vertically at each opening. A vertical distance of 8cm from the bottom surface was marked across the diameter.

Following acclimatisation to the new vial (~1 minute), a group of 10-15 male flies were gently tapped down to the bottom of the vial. The time for the first fly within the group to cross the 8cm mark was recorded by means of a digital timer. Subsequently, the number of flies to climb above the 8cm mark in 10 seconds post tap (negative geotaxis) was recorded as the percentage success rate. Scores documented were the mean number of flies that do not surpass the 8cm mark (n_{bottom}) and the total number of flies assessed (n_{total}). The climbing success rate was then calculated as: (n_{total}-n_{bottom})/n_{total}*100. Both assay measurements were based on an average of four climbing trials for each group. Four groups were assayed for each genotype and both assays were performed at 4 different time points, 5, 15, 25 and 35 days post-eclosion to determine whether aging, influences climbing ability.

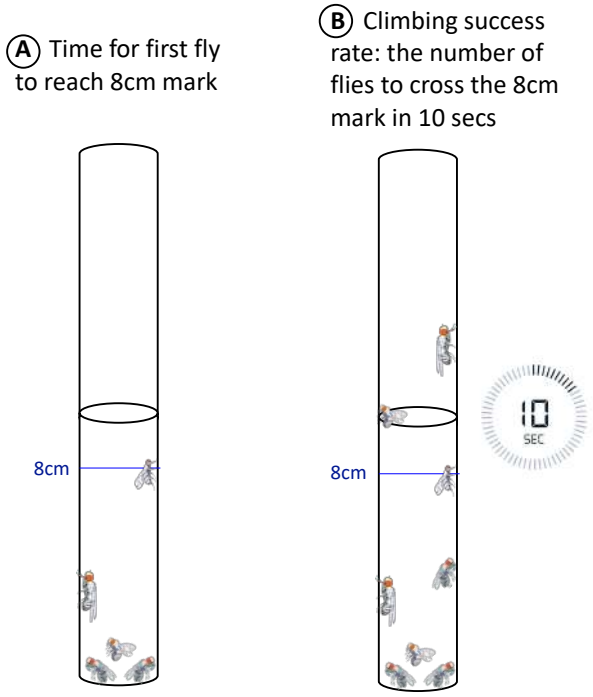

Figure 2.4 Climbing performance assays. (**A**) The time for the first fly to reach an 8cm mark was recorded. (**B**) The climbing success rate for each genotype was determined by recording the number of flies within a population to surpass the 8cm mark in 10 seconds. Both assays were repeated 4 times each to generate an average which was then compared to those obtained by a control genotype to determine the effect of knockdown of a target gene on locomotor ability.

2.6.6.2 Larval Mobility Assays

To determine whether tissue-specific knockdown of a target gene gives rise to locomotor defects before adult stage, third instar larvae bearing RNAi transgenes were subjected to larval mobility assays. Initially, parental male and female flies were allowed to prime in a regular vial for 24 hours to stimulate mating. These were then transferred to a cage consisting of grape juice and 1.5% agar with yeast and incubated at 25^{o}C. The following day, adult flies were removed and laid eggs were allowed to develop up to third instar stage. Third instar larvae were transferred and allowed to acclimatise to a 0.7% plain agar plate. Subsequently, the number of forward body wall contractions exhibited by each organism in 30 seconds were counted. Each larva was assessed three times before an average was taken. This was then compared to that obtained by control larvae for the accurate identification of locomotor defects.

2.6.6.3 Puparial Axial Ratios

Following locomotor assays, larvae were transferred to fresh grape juice cages containing yeast and were allowed to pupate. A representative number of pupal cases were then frozen to halt metamorphosis and were then imaged under the stereomicroscope using an Optika Vision camera (OPTIKA – Bergamo, Italy). Using the Optika Vision Lite, (v. 2.1) software, the length and width of puparia were measured from still images. Calculation of puparial axial ratio was then calculated by dividing the length by the width of the puparia. An increased puparial ratio as a result of elongated and slender puparia suggests inadequate muscle contractions prior to pupariation.

2.6.7 Analysis of larval muscles and neuromuscular junctions

2.6.7.1 Larval dissections and immunohistochemistry

To investigate whether neuromuscular defects are a consequence of structural defects, larval muscle and neuromuscular junction (NMJ) morphology was assessed. Body wall muscles of third instar larvae were dissected in phosphate buffered saline (PBS). This was achieved by pinning the larvae to a dissection plate from the head and between the

posterior spiracles. When the organism was adequately stretched, a horizontal incision was made on the dorsal side of the larva. All internal organs and other debris were removed leaving the body wall intact. The body wall was then stretched by pinning the resulting flaps on each side in a clockwise order to expose the body wall muscles (**Figure 2.5**) (Brent *et al.* 2009).

Muscle tissues were fixed in 4% paraformaldehyde in PBS and washed in 5% Triton X-100. This step is essential to permeabilise the intact cell membranes for optimal penetration of antibodies. Tissues were then unpinned and washed with PBS + 0.1% Triton X-100 (PBT). Following this, muscle tissues were stained with mouse anti-Discs large (anti-Dlg) antibody (Developmental Studies Hybridoma Bank, University of Iowa, Iowa, IA, USA) overnight at room temperature. This binds to Dlg post-synaptic proteins which allows visualization of NMJs. The following day, the primary antibody was removed by subsequent washes in PBT and muscle tissues were stained with anti-mouse Alexa Fluor 488-conjugated secondary goat antibody and Alexa Fluor 546-conjugated Phalloidin at room temperature overnight. The latter has a high affinity to actin filaments (F-actin) and facilitates visualisation of muscles in the red channel of the epifluorescence microscope. The former allows visualisation of NMJs in the green channel. Samples were mounted in 90% glycerol with anti-fade following a final wash in PBT.

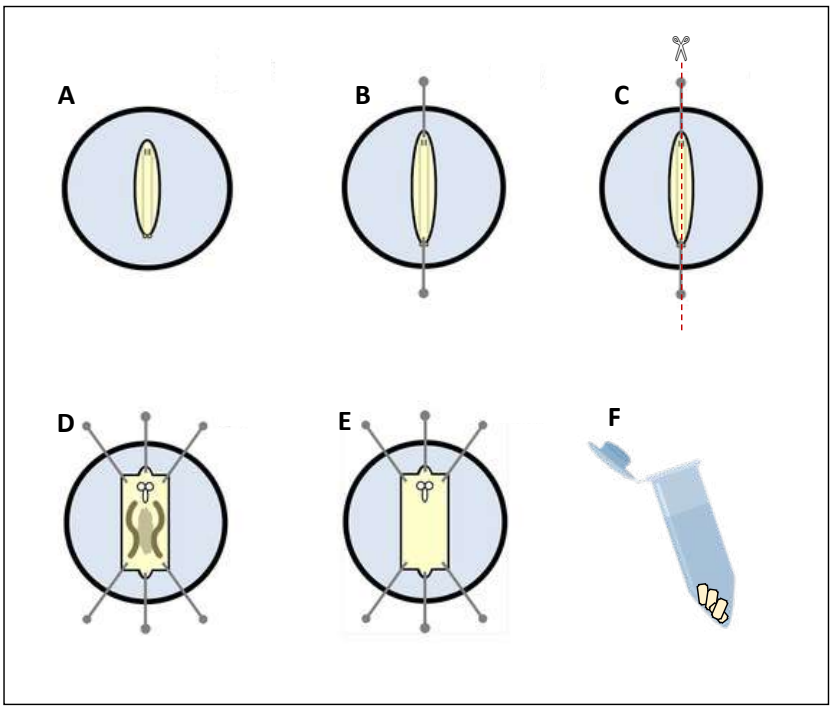

Figure 2.5 Dissection of larval muscle tissues. Third instar larvae were transferred to a dissection plate containing PBS (**A**) and were pinned to the plate from the head, close to the mouth hooks, and between the posterior spiracles (**B**). A horizontal incision was made on the dorsal side of the larva (**C**) and all internal organs were removed. The body wall was then stretched by pinning the resulting flaps on each side in a clockwise order, removing additional debris (**D**) to expose the body wall muscles (**E**). The larval brain can be left attached or removed. Muscle tissues are then fixed with paraformaldehyde and unpinned, to be stained with appropriate antibodies (**F**). Image modified from WANG *et al.* 2015 .

2.6.7.2 Fluorescence microscopy

Analysis and imaging of muscles and NMJs was performed using the Optika B-600TiFL microscope (OPTIKA – Bergamo, Italy). The dissected tissues were scanned for intact abdominal segments in the red channel (**Figure 2.6**). NMJ branches in the ventral longitudinal muscle fibres 6 and 7 within segment A1 were then visualised in the green channel. NMJs within this region are the most commonly studied, partly due to their favourable position at the front of the dissected larvae. Apart from being easy to view, it is less likely that these muscles are damaged since they are situated in the middle segment of the larval body wall. Muscles and corresponding NMJs were imaged accordingly (20x or 40x objectives). ImageJ software (NIH) was then used to quantify both muscle (fibres 6 and 7) and NMJ area. The software allows for superimposition of

muscle and NMJ images to record the relative area of each component which is then used to calculate the NMJ-to-muscle ratio. In addition, branch and bouton number was determined by counting the number of arborisations and boutons within a single NMJ respectively.

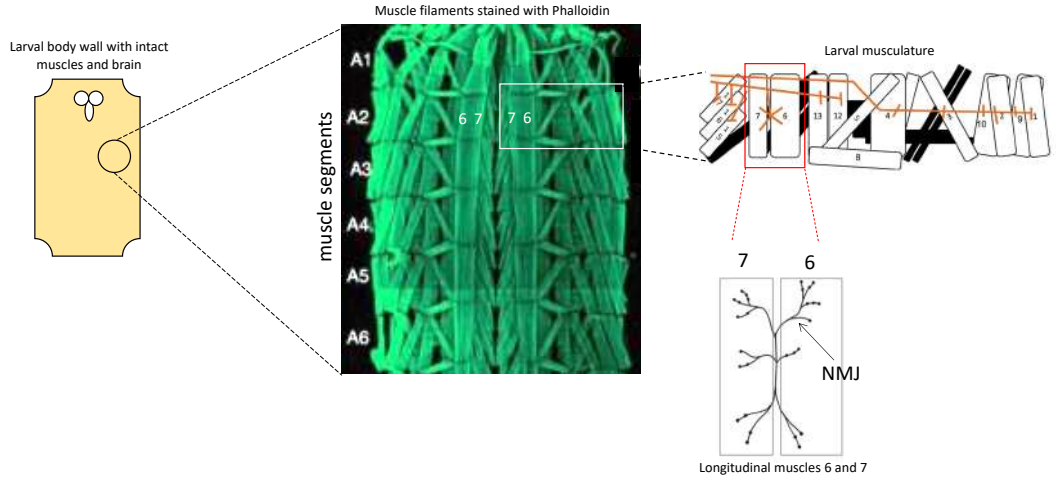

Figure 2.6 Muscle and NMJ imaging. The fluorescence microscope was used to visualize stained muscle tissues. Ventral longitudinal muscles 6 and 7 from abdominal segments and the corresponding postsynaptic region were imaged using the attached camera. Muscles in abdominal segment A1 was used as these are less likely to be damaged by the dissection process. Images were used to measure the NMJ-to-muscle ratio. Branch number was determined by counting the number of arborisations containing at least two boutons within a single NMJ. Bouton number was determined by counting all boutons within a single NMJ.

2.7 STATISTICS

Data were processed with GraphPad Prism v8.4.3 (471) software. Differences between means were determined by the unpaired *t*-test or Two-Way ANOVA followed by Bonferroni's *post hoc* tests for multiple comparisons. All results were expressed as the standard error of mean (S.E.M.) unless specified otherwise. A *p*-value <0.05 was considered significant.

CHAPTER 3

RESULTS

3.1 INCIDENCE AND PREVALENCE RATES

Between the years 2017 and 2018, the annual incidence rate for ALS on the Maltese islands was 2.48/100,000 person-years (95% CI 1.59-3.68), which is shown to increase with age up to 79 years. Within this period, the incidence rate was higher for men (3.25, 95% CI 1.86-5.28) than for women (1.68, 95% CI 0.72-3.31), resulting in a male-to-female incidence ratio of 1.93:1. This trend held across all age groups over 49 years. Incidence rate varied significantly with age among sexes, with peaks occurring in the 50-59 age group among men and in the 70-79 age group among women (**Figure 3.1**). With a total of 17 surviving patients (male=12, female=5) the prevalence of ALS cases by the end of 2018 was 3.44/100,000 (95% CI 2.01-5.52). The male-to-female prevalence ratio was 3.11:1. Hence, prevalence in males (5.16, 95% CI 2.74-8.83) was higher than that in females (1.66, 95% CI 0.45-4.24). The mean age of onset and site of onset did not influence the difference between incidence and prevalence rates.

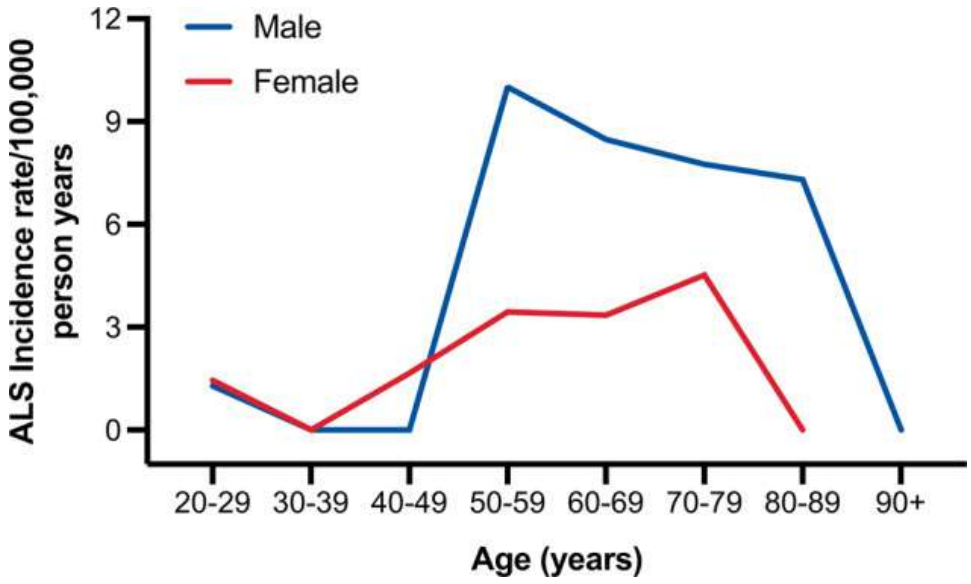

Figure 3.1 Incidence rate of ALS in Malta increases with age. Incidence rate increases with age and is higher for men than for women across all age groups over 49 years. Peak incidence in men occurs between 50-59 years and that in women occurs in the 70-79 age group.

3.2 BASELINE CHARACTERISTICS AND DEMOGRAPHICS OF ALS PATIENTS AND CONTROL SUBJECTS

The majority of patient participants were found to concentrate in the southern and central regions of the Maltese islands. Although an increased exposure to pollution in these areas (NOLLE 2005) might have played a role in triggering ALS, this finding is probably correlated with a higher population density in these regions when compared to the North (NATIONAL STATISTICS OFFICE 2014). The geographical distribution of age and sex-matched controls is similar to that of ALS patients (**Figure 3.2**).

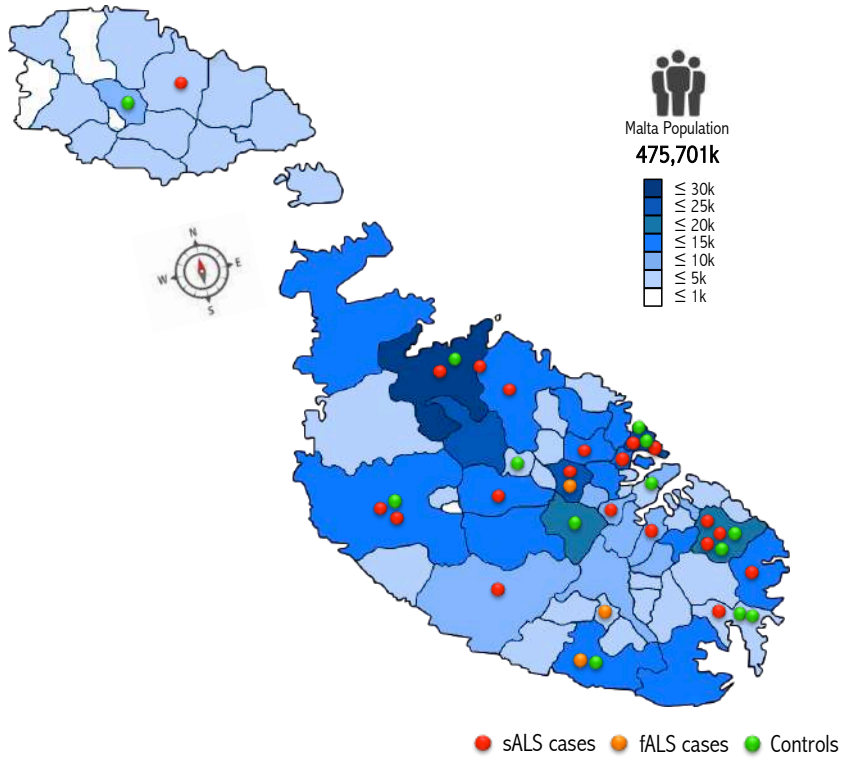

Figure 3.2 Geographical distribution of Maltese ALS patients and their matched controls. The majority of recruited individuals concentrate in the central and southern regions of Malta, where population density is the highest. Control subjects have a similar geographical distribution to that of ALS patients. The population density for each regional unit is based on NSO data in 2017.

The majority of ALS cases were male with a predominant spinal onset of symptoms (**Table 10**). A higher proportion of women presented with bulbar onset ALS (37.5%) when compared to men (18.75%). One female presented with simultaneous bulbar and spinal onset. Median age at onset was marginally lower in females (59.5 years) compared to males (64 years). Only two patients developed ALS symptoms at a young age (<45 years). Early ALS (≤55 years) was more frequently associated with spinal onset (spinal/bulbar ratio = 9:1) and with a longer disease duration (early onset/late onset disease duration = 2:1 years). Familial ALS (fALS) was recorded for a minority of cases and fALS cases had a lower survival rate compared to sALS cases (fALS: 3 ± 1 SD years; sALS: 6.3 ± 5.6 SD years). The proportion of fALS increases to 37.5% with the inclusion of patients with a family history of dementia and other neuropsychiatric disorders, such as schizophrenia and depression, in view of the familial aggregation of both disorders (BYRNE *et al.* 2013; LONGINETTI *et al.* 2017). The mean disease duration was 5.9 ± 5.3 SD years, with males having a faster progression (4.2 ± 3.2 SD years) compared to females (9 ± 7.4 SD years). Spinal onset ALS was associated with longer survival (spinal onset: 6.6 ± 6.1 SD years; bulbar onset = 4.5 ± 2.1 SD years).

Strenuous activity associated with occupation emerged as a common risk factor within the ALS cohort, with more than 50% of patients experiencing increased levels of physical exertion throughout their lifetime. Furthermore, one-third of the ALS patients recruited had a history of cigarette smoking. Heavy alcohol consumption was minimal. Mean CK levels in the patient cohort were only slightly beyond the normal range in males. However, it is relevant to note that in a few cases a number of years have elapsed from onset up to recruitment, when the CK test was performed. Breathing and heart rates were within the normal range. Patient ALSFRS-R scores range from 12 to 44, reflecting a wide variation in phenotypic expression, with an average nearly half that recorded for control subjects (**Table 11**).

Table 10 Baseline characteristics of ALS patients and control subjects.

	ALS PATIENTS	CONTROLS
n	24	13
Sex		
Male, % (n)	66.7 (16)	46.2 (6)
Female, % (n)	33.3 (8)	53.8 (7)
Age at onset, mean year ± SD (range)	59.3 ± 13.2 (27-80)	-
Age at recruitment, mean year ± SD (range)	63.5 ± 11.6 (30-82)	71.2 ± 10.9 (52-90)
Type of ALS		
Familial, % (n)	12.5 (3)	-
Sporadic, % (n)	87.5 (21)	-
Site of onset		
Bulbar, % (n)	25 (6)	-
Spinal, % (n)	70.8 (17)	-
Both, % (n)	4.2 (1)	-
ALSFRS-R score at recruitment, mean ± SD, (range)	25.6 ± 11.1 (11.5-44)	47.9 ± 0.3 (47-48)
Cognitive Status		
Normal (%)	87.5 (21)	100 (13)
Impaired (%)	12.5 (3)	0 (0)
Environmental Factors		
Cigarette smoking, % (n)	37.5 (9)	30.8 (4)
Strenuous activity, % (n)	54.2 (13)	23.1 (3)
Excessive alcohol use, % (n)	8.3 (2)	7.8 (1)
Creatine Kinase (CK) at recruitment, U/l [1]		
♂ Mean* ± SD (range)	311.2 ± 259.7 (15-878)	-
♀ Mean* ± SD (range)	180.8 ± 117.5 (38-336)	-
Breathing rate[2], mean breaths/min ± SD (range)	19.9 ± 6.5 (12-36)	16.3 ± 0.7 (16-18)
Hearth rate[3], mean beats/min ± SD (range)	80.9 ± 14.6 (52-104)	78.5 ± 6.6 (64-88)
Survival		
Total, mean years ± SD (range)	5.9 ± 5.3 (2-21)	-
Deceased, mean years ± SD (range)	4.3 ± 4.4 (2-19)	-
Alive, mean years ± SD (range)	9.1 ± 5.8 (4-21)	-
Deceased, % (n)	66.7 (16)	-

[1] *Normal Range* - **CK:** ♂ 39-308 U/l, ♀ 26-192 U/l; [2] **Breathing Rate:** adults 12-18 breaths/min, elderly ≥ 65 years old 12-28 breaths/min, elderly ≥ 80 years old 10-30 breaths/min; [3] **Heart Rate:** adults & elderly 60-100 beats/min.

Control participants were chosen on the basis of their health status, age, sex and residency in correlation with patient participants. The ratio of male to female control participants of approximately 1:1 does not mirror our patient cohort due to increased difficulty in recruiting healthy male individuals within a certain age group. The average age of the selected controls is 71.2 years (range: 52-90). As expected, high ALSFRS-R scores (47.9 $\pm$ 0.3) in the control cohort indicate a healthy status and normal motor function (KOLLEWE *et al.* 2008). The percentage of cigarette smokers is comparable to that observed in the patient group, however, the percentage of control individuals that experienced heightened levels of physical activity throughout their lifetime is significantly lower compared to ALS patients (**Table 10 - 11**).

Table 11 Summary of control participant data including family pedigree structures.

Subject (Code)	Sex	Age	Family History of ALS and/or neurological disorders	Cigarette Smoking	Alcohol/ Drug Abuse	Strenuous Labour	Family Pedigree
CTRL1	♂	79	Parkinson's Disease	No	No	No	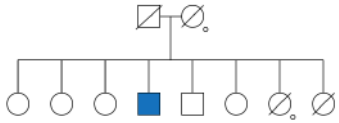
CTRL2	♀	80	None	No	No	No	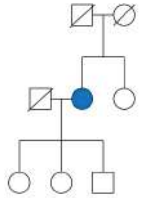
CTRL3	♀	86	None	No	No	No	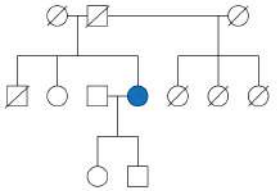
CTRL4	♀	71	None	No	No	No	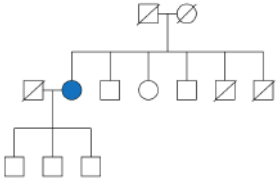

Subject (Code)	Sex	Age	Family History of ALS and/or neurological disorders	Cigarette Smoking	Alcohol/ Drug Abuse	Strenuous Labour	Family Pedigree
CTRL5	♀	61	None	No	No	No	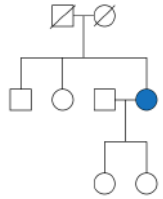
CTRL6	♂	60	Dementia	Former smoker	No	No	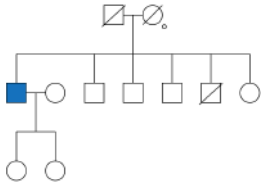
CTRL7	♂	71	Dementia	No	No	No	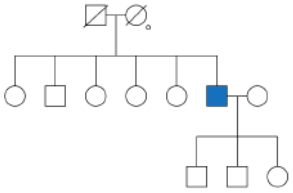
CTRL8	♀	72	ALS*	Former smoker	No	No	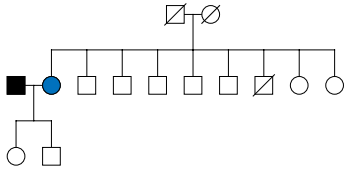

Subject (Code)	Sex	Age	Family History of ALS and/or neurological disorders	Cigarette Smoking	Alcohol/ Drug Abuse	Strenuous Labour	Family Pedigree
CTRL9	♂	52	None	Former smoker	No	No	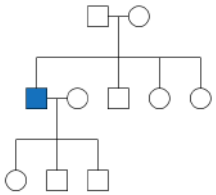
CTRL10	♀	60	None	Former smoker	No	Yes	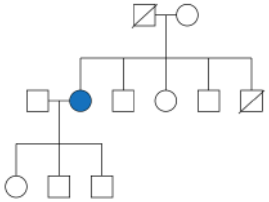
CTRL11	♀	90	None	No	No	No	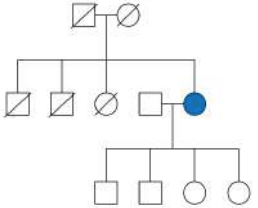
CTRL13	♂	72	None	No	No	No	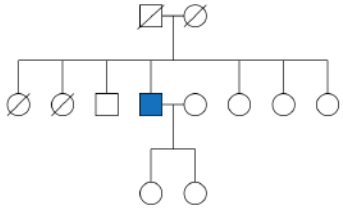

Code	Sex	Age	Family History of ALS and/or neurological disorders	Cigarette Smoking	Alcohol/ Drug Abuse	Strenuous Labour	Family Pedigree
CTRL14	♂	71	None	No	Former alcoholic	Yes	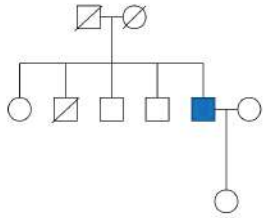

KEY: ■ ● CONTROL; ／ DECEASED; ■ ● AFFECTED ALS; □ ○ AFFECTED ALS-RELATED DISORDER; □ ○ UNAFFECTED

*Spouse had ALS.

3.3 PATIENT PHENOTYPIC DATA

ALS typically presents as a combination of upper and lower motor neuron defects. However, as reflected in the phenotypic data accumulated from our patient cohort, various ALS subtypes can be identified. It is relevant to note the wide array of possible clinical presentations of the disease to reduce delays in patient diagnosis and management. In the majority of cases, disease progression was rapid with average disease duration of 4.3 years from symptom onset. The Hoffmann's sign was absent in all patients, indicating the absence of upper motor neuron (UMN) lesions. The lower equivalent of this test is the Babinski's sign or the plantar reflex test, which if positive also indicates UMN involvement. A normal reflex response for this test was also observed in all cases. Nonetheless, UMN signs are difficult to distinguish and are often not clearly increased in the presence of additional neurogenic weakness as a result of lower motor neuron (LMN) involvement. Furthermore, very severe UMN damage is required to affect the recruitment pattern of muscles required to elicit a plantar response, which may occur at a later stage of the disease (SWASH 2012). Cases were numbered in order of the date of interview.

3.3.1 sALS case presentations

Patient MND01

The patient is a 30-year-old male, who developed bilateral lower limb weakness at the age of 27 (2014). This quickly progressed with further wasting of leg muscles as well as atrophy and weakness of the upper extremities, particularly the left upper limb. The patient was diagnosed with progressive muscular atrophy and ultimately became wheelchair-bound. No dysarthria or dysphagia has been observed, despite early eating difficulties (occasional choking). In recent stages of the disease the patient developed breathing difficulties, especially with movement, as well as orthopnoea. The patient makes use of continuous non-invasive ventilation (BiPAP), however, he recently (September 2018) submitted to tracheostomy mechanical ventilation (TMV). Upon examination (May 2017), hypotonia in both upper and lower limbs was observed

with decreased overall muscle power (MRC scores: 0-2) except for the neck muscles (MRC score: 5). This correlates with a marked increase in creatine kinase (CK) muscle enzyme (878 U/l; normal range 39-308 U/l) post-symptom onset, indicating acute skeletal muscle damage. Reflex function was greatly diminished, however, neurological investigations including Hoffman's sign and plantar reflex examinations were normal. A slightly elevated breathing rate (36 breaths/min, normal adult range: 12-20 breaths/min) was recorded, whilst heart rate (104 breaths/min) marginally exceeded the upper limit of the normal range (60-100 breaths/min). The patient has no family history of ALS/MND (**Figure 3.3**); however, a family history of schizophrenia was recorded. Early studies have previously corroborated a pathophysiological relationship between the two conditions (HOWLAND 1990) and this link has been further supported by recent findings that show a significant genetic correlation (MCLAUGHLIN *et al.* 2017). It is also noteworthy that the subject was involved in moderate sport activities, and is on Riluzole medication, a drug that attempts to delay MND symptoms and progression (BENSIMON *et al.* 1994; LACOMBLEZ *et al.* 1996). The patient still remains alive, 7 years from symptom onset (August 2021).

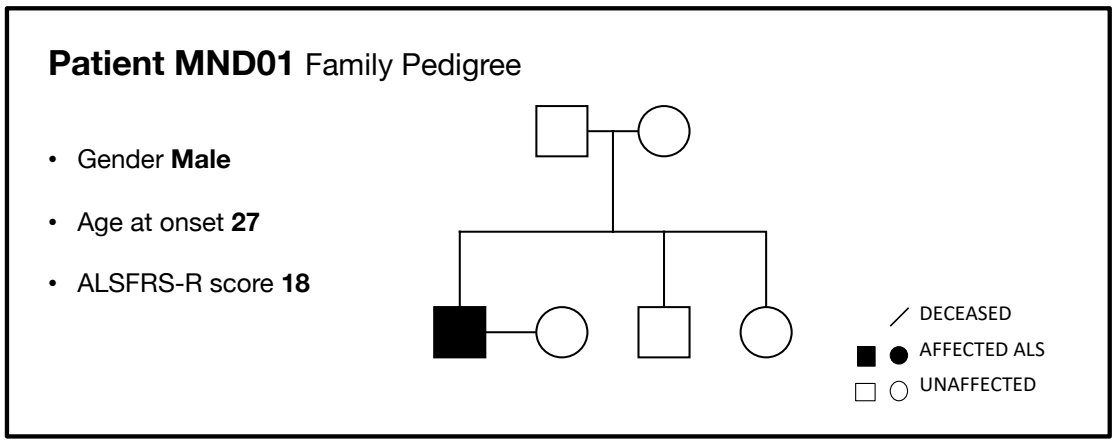

Figure 3.3 Pedigree structure of patient MND01. Squares represent male pedigree members, circles represent female pedigree members, solid symbols represent members with MND/ALS, oblique lines represent deceased members and open symbols represent unaffected members.

Patient MND02

A male patient initially developed muscle weakness in his lower limbs at the age of 73 (2015). Symptoms started to progress slowly at first but a year following initial onset of symptoms, the patient's walking abilities started to decline extensively. Increased weakness of the upper limbs led to the diagnosis of suspected ALS. Consequently, the patient lost all lower limb movement abilities and became wheelchair bound. No dysarthria, dysphagia, dyspnoea or orthopnoea were detected upon examination (May 2017). Muscle tone was normal with increased rigidity in the left lower limb, and whilst upper limb muscle groups overcame gravity (with or without resistance), no visible contraction was observed upon examination of lower limb muscles. A decreased ALSFRS-R score (24/48) was recorded at recruitment. Serum CK levels were within normal range (65 U/l; normal range 39-308 U/l). Reflex function was clearly diminished and neurological investigations were normal, as were breathing rate and heart rate. No family history of MND was disclosed (**Figure 3.4**). The patient was possibly exposed to pesticides and endured strenuous labour through his former occupation (farming). No smoking habits, alcohol or drug abuse were recorded. At the age of 75 the patient suffered from sudden respiratory difficulties and died of respiratory arrest (December 2017). The total duration of the disease was 2 years.

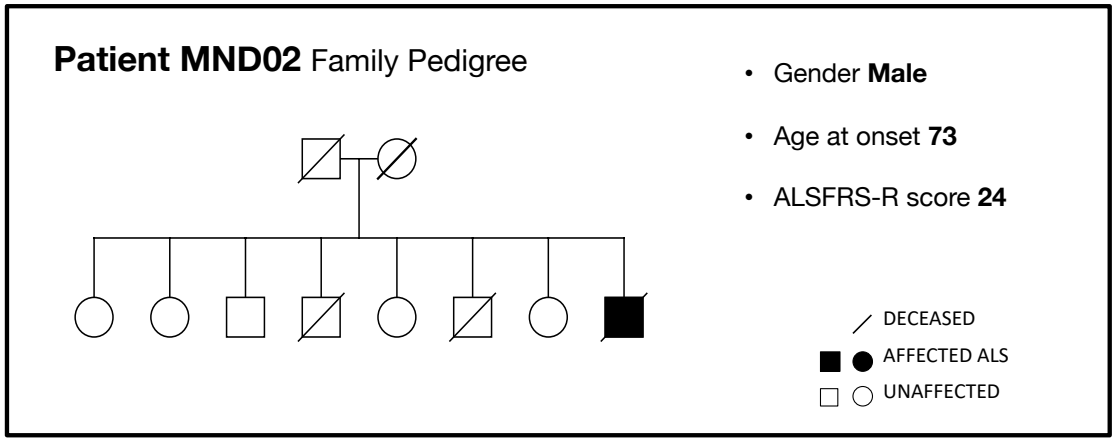

Figure 3.4 Pedigree structure of patient MND02. Squares represent male pedigree members, circles represent female pedigree members, solid symbols represent members with MND/ALS, oblique lines represent deceased members and open symbols represent unaffected members.

Patient MND03

This case involved a 57-year-old male, who started to experience poor balance and loss of coordination at the age of 55 (2015). This slowly progressed to minor weakness in the upper and lower extremities. Despite this, the patient was able to perform normal daily activities independently with some effort and/or decreased efficiency. Upon examination (May 2017), the patient presented with normal muscle tone in both upper and lower limbs with overall normal muscle power against resistance although this was slightly diminished (MRC score: 4) in the left lower limb, This observation suggests that muscle damage was thus far minimal as confirmed by normal blood CK levels (116 U/l; normal range 39-308 U/l). Normal reflex function was observed, with Hoffman's and Babinski's signs being absent. Breathing and heart rate were normal. The patient has a family history of neurological disorders (**Figure 3.5**) including bipolar disorder, borderline personality disorder and schizophrenia. Although the latter are common within the general population, ALS kindreds were shown to have an increased risk for manifesting psychiatric disturbances such as depression and neurotic disorders both before and after their relative's diagnosis (BYRNE *et al.* 2013; O'BRIEN *et al.* 2017). This was especially evident in children of ALS individuals (LONGINETTI *et al.* 2017). The patient's former occupation (carpentry) required strenuous manual labour and might have increased his exposure to toxic chemicals. The patient was a cigarette smoker (cigarette packs/day: 1) for 37 years. No excessive alcohol consumption or drug abuse was recorded. Cerebellar degeneration was recently recorded. The patient remains alive, 6 years from symptom onset (August 2021).

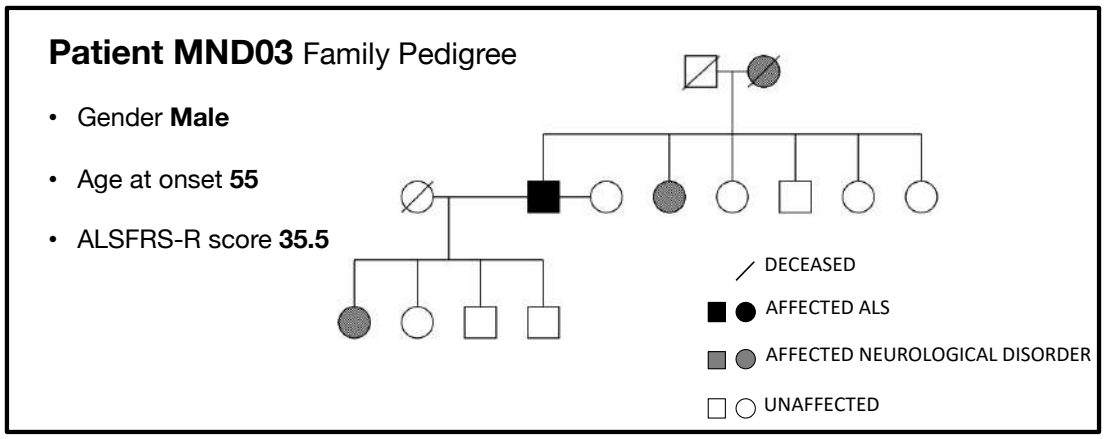

Figure 3.5 Pedigree structure of patient MND03. Squares represent male pedigree members, circles represent female pedigree members, solid symbols represent members with MND/ALS, patterned symbols represent members with a neurological disorder associated with MND/ALS, oblique lines represent deceased members and open symbols represent unaffected members

Patient MND04

A 53-year-old male became aware of hypoesthesia in his left hand at the age of 52 (2016). This steadily advanced to muscle wasting and weakness in the upper limbs, followed by degeneration of lower limb muscles. Eventually the patient became wheelchair-bound and started to experience dysarthria. Collectively, these symptoms together with a series of medical tests led to the diagnosis of probable ALS. In the following months, the patient's dysarthria worsened and the patient experienced close to complete loss of useful speech. Eating habits were normal, and no dyspnoea or orthopnoea were detected. At the time of examination (June 2017), blood CK levels were slightly increased (334 U/l; normal range 39-308 U/l), which may have been attributed to the hypotonia detected in the upper limb muscles. Lower limb muscles had normal tone. Neck, elbow and knee muscle groups displayed normal power; however, wrist, hip and ankle muscle groups showed no muscle contraction. Normal reflex function was observed, except for knee and ankle reflexes, which were somewhat diminished. Neurological investigations were regular and Hoffman's and Babinski signs were absent. Breathing and heart rate were within normal range. The patient had no family history of MND including ALS, but two immediate family members had experienced episodes of epileptic seizures (**Figure 3.6**). Interestingly, ALS and

epilepsy were shown to share a similar metabolic pathophysiology, in that both disorders lead to defects in glucose uptake majorly due to reduced tricarboxylic acid (TCA) cycling (TEFERA AND BORGES 2016; TEFERA *et al.* 2017). Furthermore, knockdown of the recently-identified ALS-associated gene *KIF5A (NICOLAS et al. 2018)* in mice was found to cause severe epilepsy (NAKAJIMA *et al.* 2012). The individual was regularly exposed to chemical compounds, particularly styrene vapours in relation to his occupation (boat construction using fibreglass) that was physically intensive. No smoking habits, alcohol or drug abuse were recorded. The patient died a few months following recruitment (January 2018) after a total disease duration of 2 years.

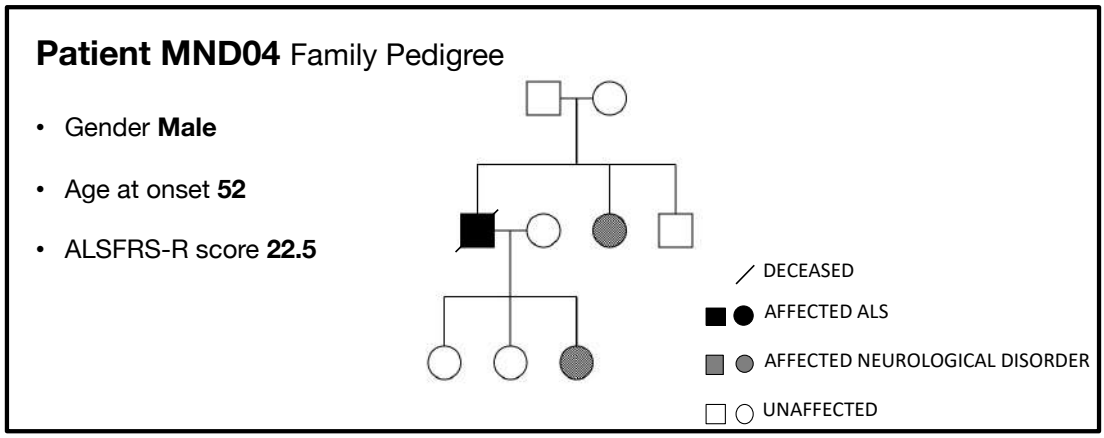

Figure 3.6 Pedigree structure of patient MND04. Squares represent male pedigree members, circles represent female pedigree members, solid symbols represent members with MND/ALS, patterned symbols represent members with a neurological disorder associated with MND/ALS, oblique lines represent deceased members and open symbols represent unaffected members.

Patient MND05

A female patient aged 67 started to experience slurred and slow speech at the age of 63 (2013). This was followed by the development of bilateral upper and lower limb weakness, leading to a spastic gait and hindrance of normal daily activities. Complete loss of useful speech and progression of muscle weakness constrained the patient's mobility drastically, culminating in a bedridden state. No signs of dyspnoea or orthopnoea were observed. The patient became totally dependent, and followed a liquid-only diet. The patient presented with

hypertonia in both upper and lower limbs upon examination (June 2017). Despite this, increased levels of the CK muscle enzyme were detected in the patient's blood (320 U/l; normal range 26-192 U/l). The acute muscle damage indicated by the CK test may have not yet been perceivable by the examiner. In addition, muscle tone assessment was challenging as a result of increased rigidity due to the patient's lack of physical activity. The patient was unable to perform motor tests and showed no response to reflex function tests apart from normal reflex function in the knees. A low ALSFRS-R score (12/48) at recruitment highlights decreased mobility and muscle function. Neurological investigations including Hoffman's and Babinski signs were absent. Breathing and heart rate were within an acceptable range. No family history of MND including ALS was reported (**Figure 3.7**). The patient suffered from clinical depression following her diagnosis. An increased risk of developing mental illnesses such as depression within a year from diagnosis is frequent in patients with ALS when compared to ALS-free individuals, which may be partially due to the emotional burden of disease diagnosis and symptoms (Roos *et al.* 2016). The patient never made use of cigarettes, alcohol or abusive drugs. The patient's physical status continued to regress until she passed away after 7 years from disease onset (January 2020).

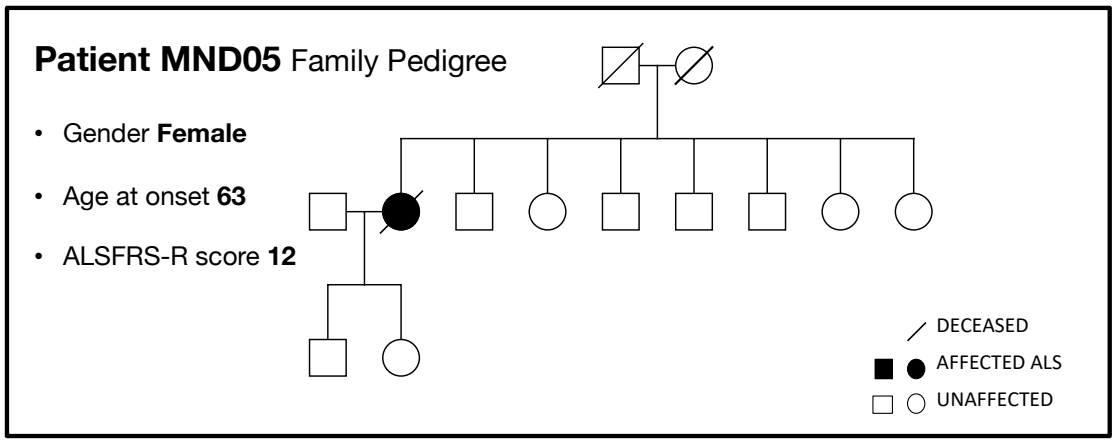

Figure 3.7 Pedigree structure of patient MND05. Squares represent male pedigree members, circles represent female pedigree members, solid symbols represent members with MND/ALS, oblique lines represent deceased members and open symbols represent unaffected members.

Patient MND06

The sixth patient participant was a 76-year-old female, who first noticed muscle weakness in the right leg after she started limping, at the age of 74 (2015). After a few months, the patient started to experience hoarseness and tongue weakness that led to dysarthria. The symptoms started to progress quickly and she was diagnosed with the ALS subtype, bulbar palsy. The disease advanced with bilateral leg weakness and the patient consequently became wheelchair-bound. Despite this, the subject retained complete functionality of her upper limbs. No signs of dyspnoea or orthopnoea were detected and the patient had normal eating habits with some dietary consistency changes. Upon examination (June 2017), the patient presented with hypertonia in both lower limbs and normal muscle tone in the upper limbs. Normal blood CK levels (58 U/l; normal range 26-192 U/l) support the absence of acute muscle damage at that stage of the disease. Muscle strength in the upper limbs was normal but greatly diminished in the lower limbs (MRC scores: 0-2). Reflex function was normal. Hoffman's and Babinski's signs were absent. Breathing rate and heart rate were normal. The patient had no family history of MND including ALS (**Figure 3.8**). The patient was a heavy cigarette smoker (cigarette packets/day: 1.25). No excessive alcohol consumption or drug abuse was noted. At 77 years of age the patient died after 2 years from symptom onset (December 2017).

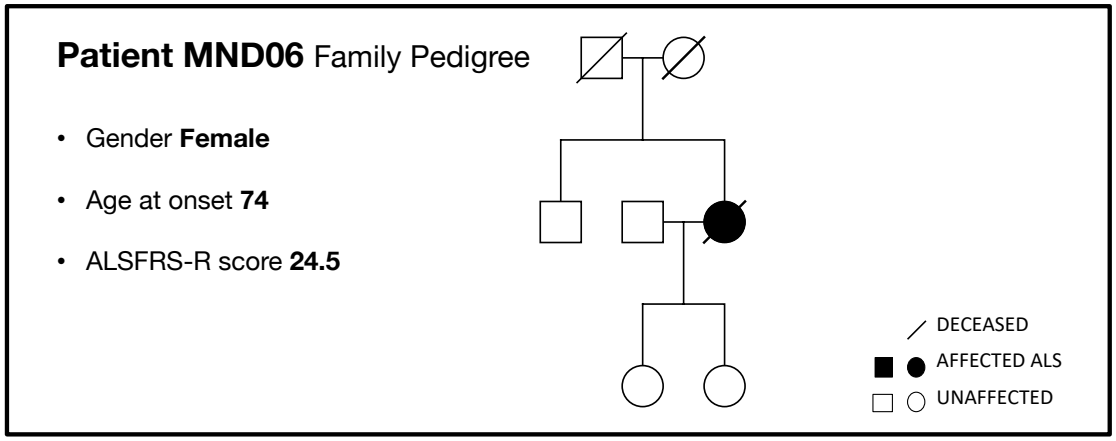

Figure 3.8 Pedigree structure of patient MND06. Squares represent male pedigree members, circles represent female pedigree members, solid symbols represent members with MND/ALS, oblique lines represent deceased members and open symbols represent unaffected members.

Patient MND07

The subject was a 69-year-old male patient who started to experience difficulties in articulating clear speech at the age of 67 (2015). Following this, he developed muscle weakness in the upper extremities. His dysarthria worsened and consequently this led to complete loss of useful speech, which led to a diagnosis of suspected ALS. In the next months, the disease progressed with bilateral leg weakness and his physical abilities severely declined leaving him wheelchair bound. The patient started to have early eating problems with occasional choking but no indications of respiratory disturbances were identified. The subject displayed hypertonia in all muscles except the left lower limb, which had a normal muscle tone (July 2017). A CK blood test showed levels that were within a normal range (69 U/l; normal range 39-308 U/l). Muscle strength was normal in the neck but diminished in all other muscle groups especially in the lower limbs (MRC scores: 0-3). The patient had normal reflex function, absence of Hoffmann's sign and a normal plantar reflex response. Breathing and heart rate were normal. The subject had no family history of MND including ALS (**Figure 3.9**). The patient's former occupation (carpentry) involved strenuous manual labour with the possibility of chemical vapour exposure. The patient was a cigarette smoker (cigarette packets/day: 1.5) for 53 years. No excessive alcohol consumption or drug abuse was recorded. The patient died after 4 years from disease onset due to respiratory complications (June 2019).

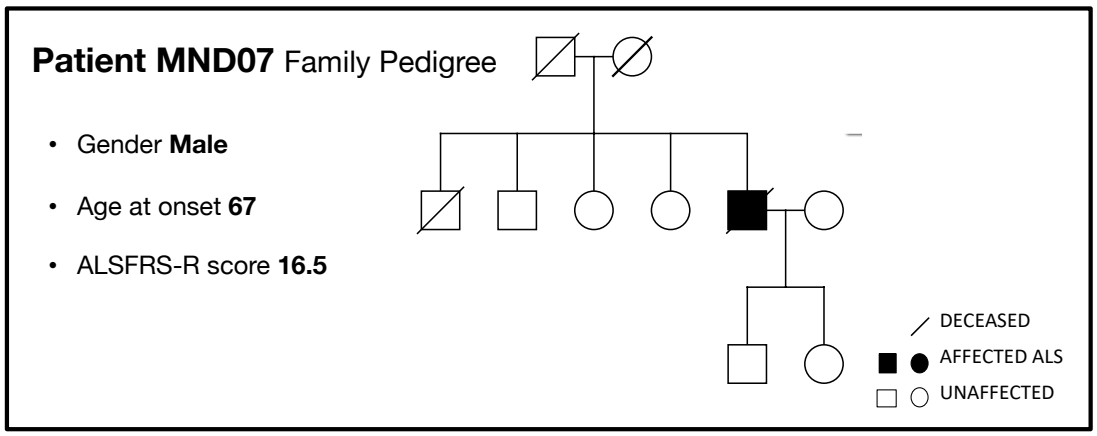

Figure 3.9 Pedigree structure of patient MND07. Squares represent male pedigree members, circles represent female pedigree members, solid symbols represent

members with MND/ALS, oblique lines represent deceased members and open symbols represent unaffected members.

Patient MND09

A 52-year-old male patient started to notice regular fasciculations in his arms at the age of 50 (2015). This advanced to weakness in the upper extremities and discomfort in the neck. After a few months, muscle deterioration and weakness developed in the lower limbs and the patient started to encounter walking difficulties. The early neck discomfort developed to hoarseness and subsequently dysarthria. The patient eventually became wheelchair-bound and was able to interact with limited speech combined with non-vocal communication. No signs of dyspnoea were detected, but the patient needed to be slightly elevated to facilitate respiration during night-time and was on a liquid-only diet. Upon examination (June 2017), the patient presented with hypotonia in the upper limbs and hypertonia in the lower limbs. Muscle power in the neck and lower limb muscle groups was decreased but close to normal, however, muscle strength in the upper limbs was greatly diminished (MRC scores: 0-2). A normal CK blood test (111 U/l; normal range 39-308 U/l) suggests that muscle degeneration was not significant enough to influence this tissue damage marker at the time of examination. Reflex function was normal and no involvement of upper motor neurons was detected. Breathing and heart rate were normal. The patient had no family history of MND including ALS (**Figure 3.10**). At the age of 40, the patient suffered grievous injuries in an accident and overdosed four times on painkillers. His occupation (electrician) involved strenuous physical activity and possible exposure to electromagnetic fields (EMF). A slight but significant increase in ALS risk has been identified among those exposed to EMF and other variables associated with electrical occupations (ZHOU *et al.* 2012). Furthermore, the patient was a heavy smoker (cigarette packets/day: 1) up to his diagnosis. Following two years from symptom onset, the subject suffered a severe decline in health and succumbed to the disease (December 2017).

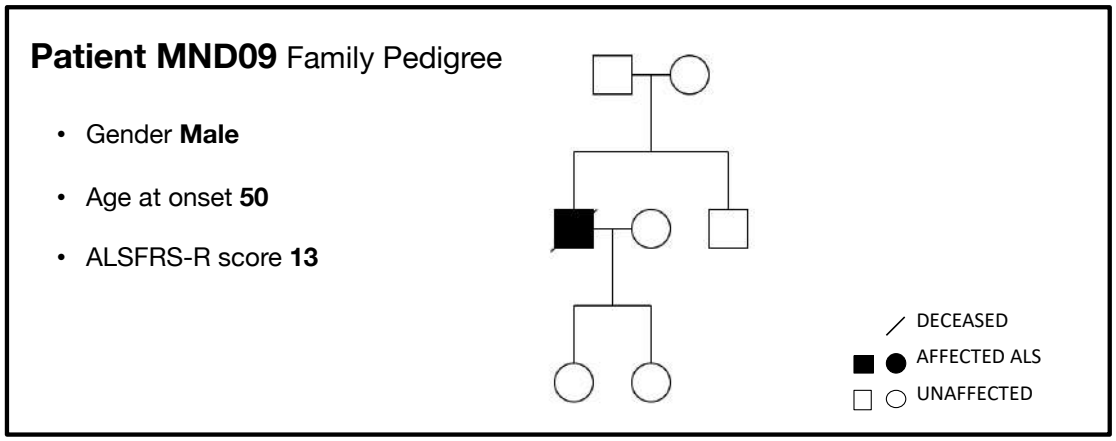

Figure 3.10 Pedigree structure of patient MND09. Squares represent male pedigree members, circles represent female pedigree members, solid symbols represent members with MND/ALS, oblique lines represent deceased members and open symbols represent unaffected members.

Patient MND10

A 66-year-old female patient participant first noticed gait abnormality in the form of a foot drop at the age of 59 (2010). The disease then advanced to the left hand with the patient eventually experiencing bilateral lower limb weakness. As a result, her neurologist diagnosed her with suspected ALS. A few years into the disorder, the abnormal gait worsened, muscles deteriorated further and the patient became wheelchair-bound. The patient then started to experience significant respiratory difficulties and consequently started to make use of continuous non-invasive ventilation. No signs of dysphagia were observed and dietary requirements were normal. Physical examination (June 2017) revealed normal muscle tone in accordance with a normal CK blood test (38 U/l; normal range 26-192 U/l). Good muscle strength was observed in the neck, whilst power was diminished in the upper limbs (MRC scores: 2-4) and no muscle contractions were displayed in the lower limbs. Reflex function was normal overall, but was diminished in the knee and ankle. Hoffman's and Babinski's signs were absent. Breathing rate was higher (36 breaths/min) than the normal range (12-18 breaths/min) but heart rate was normal. No family history of ALS or any other MND was identified (**Figure 3.11**). No smoking habits, alcohol or drug-dependence was recorded. No occupational risk factors that could potentially

associate with motor degeneration were documented. A protracted survival rate was observed in this case, which spanned over a total of 9 years, following the death of the patient at age 68 (June 2019).

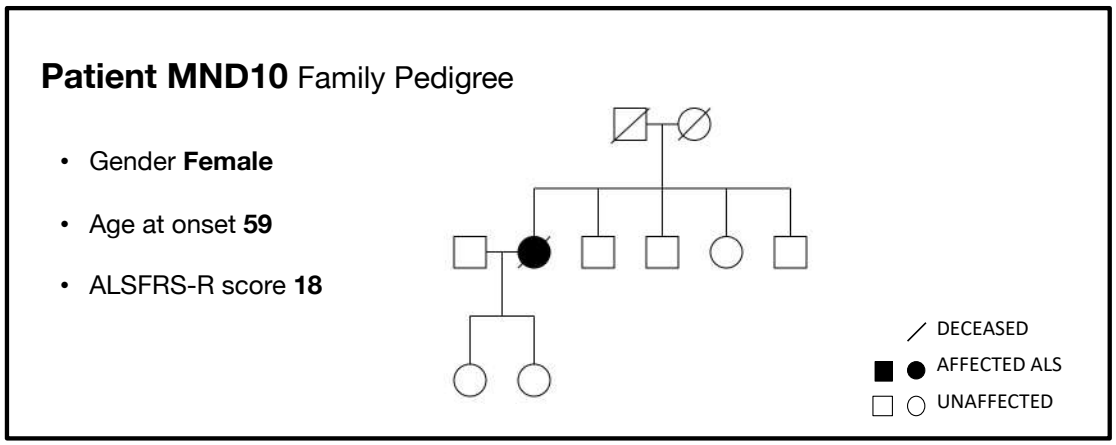

Figure 3.11 Pedigree structure of patient MND10. Squares represent male pedigree members, circles represent female pedigree members, solid symbols represent members with MND/ALS, oblique lines represent deceased members and open symbols represent unaffected members.

Patient MND11

This case involved a 51-year-old female patient who became aware of a choking sensation in her throat, together with excessive salivation at the age of 49 (2015). The disease commenced with hoarseness and discomfort in the throat that quickly progressed to dysarthria and loss of useful speech. Marked weight loss and upper limb weakness partly supported a diagnosis of possible ALS. Symptoms of atrophy and weakness of both upper limbs were also identified. The patient started to experience dyspnoea, particularly with movement, as well as orthopnoea, which together with asthmatic symptoms made respiration very challenging. No swallowing difficulties were displayed and the patient had normal eating habits with some dietary consistency changes. Upon examination (June 2017) the patient presented with normal lower limb muscle tone but reduced muscle tone in the upper limbs. Muscle power was normal in the neck and lower limb muscle groups but reduced (MRC scores: 0-2) in upper limb muscles. Increased CK levels (275 U/l; normal range 26-192 U/l) indicated marked muscle damage. Normal reflex function was observed. Neurological

investigations including Hoffman's sign and plantar reflex examination portrayed normal reactions. The breathing rate was slightly higher (24 breaths/min) than the normal range (12-18 breaths/min), whereas heart rate was normal. No family history of MND or ALS has been detected. However, a family history of dementia (**Figure 3.12**) is highly relevant. The association between ALS and dementia, especially FTD, is highly established and familial aggregation of both disorders is frequently observed. Indeed, several studies have reported as much as a two-fold increase of dementia in relatives of ALS patients when compared to controls (MAJOOR-KRAKAUER *et al.* 1994; FALLIS AND HARDIMAN 2009; BYRNE *et al.* 2013). The total duration of the disease was three years, following her demise as a result of respiratory failure (May 2018).

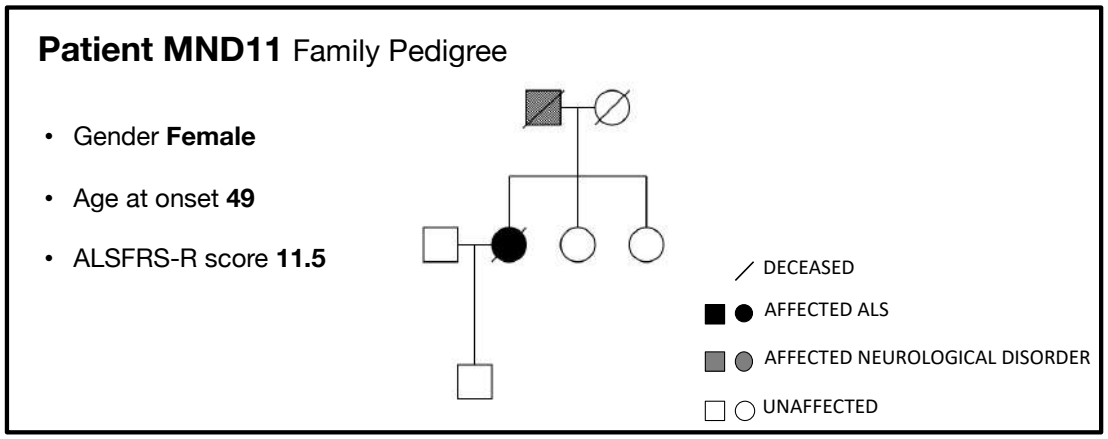

Figure 3.12 Pedigree structure of patient MND11. Squares represent male pedigree members, circles represent female pedigree members, solid symbols represent members with MND/ALS, patterned symbols represent member with ALS/MND – associated neurological disorder, oblique lines represent deceased members and open symbols represent unaffected members.

Patient MND13

A 44-year-old female patient first noticed muscle weakness in both her legs following the birth of her twins, at the age of 27 (2000). This progressed slowly with an unsteady gait and development of bilateral arm weakness. Along the years the patient started to experience hoarseness, leading to dysarthria, which in combination with the initial symptoms supported a diagnosis of probable ALS. Muscle weakness and atrophy of the extremities progressed gradually but

steadily and the patient eventually became wheelchair-bound. Her dysarthria worsened to the point of complete loss of useful speech and the use of an eye-tracking device serves as a communication aid. This indicates normal muscle function of the eye. No signs of dyspnoea but very slight orthopnoea have been noted during the course of the disease. In recent years, the patient started to experience slight dysphagia but has close to normal eating habits with some dietary consistency changes. Upon examination (June 2017), muscle tone was normal with increased rigidity of the left and right upper limbs. Clonus was elicited in both upper and lower limbs. The patient showed decreased muscle power in upper limbs (MRC scores: 0-1) and ankles (MRC score: 1.5), as well as overall average reflex function. Neurological investigations including Babinski's and Hoffman's sign were absent. Serum CK levels were within the normal range (156 U/l; normal range 26-192 U/l). Breathing and heart rate were regular. No history of MND or ALS has been detected within first-degree family members (**Figure 3.13**). However, second-degree relatives were diagnosed with dementia. The patient was possibly exposed to pesticides and her former occupation involved strenuous labour (farming). No smoking habits, alcohol or drug abuse were reported. Since ALS is fairly uncommon at reproductive age, it is possible that pregnancy may affect ALS onset or clinical expression. In this case, hormonal modifications, mainly an increased progestin activity, may increase susceptibility to ALS or expose an already existing but clinically undistinguished disease. Furthermore, increased neuro-inflammation and cytokine activity during pregnancy may have a toxic effect on motor-neurons that may contribute to an increased susceptibility to ALS (MARSLI *et al.* 2020). Due to the rarity of such cases, data about the association between ALS and pregnancy is scarce and is yet to be defined (CHIO *et al.* 2003). Permanent nerve damage as a complication of spinal or epidural injections during birth may also be considered. Nonetheless, this is very rare and has never been directly associated with MND (COOK *et al.* 2009; WIGGANS 2016). The patient still remains alive, 21 years from symptom onset (August 2021).

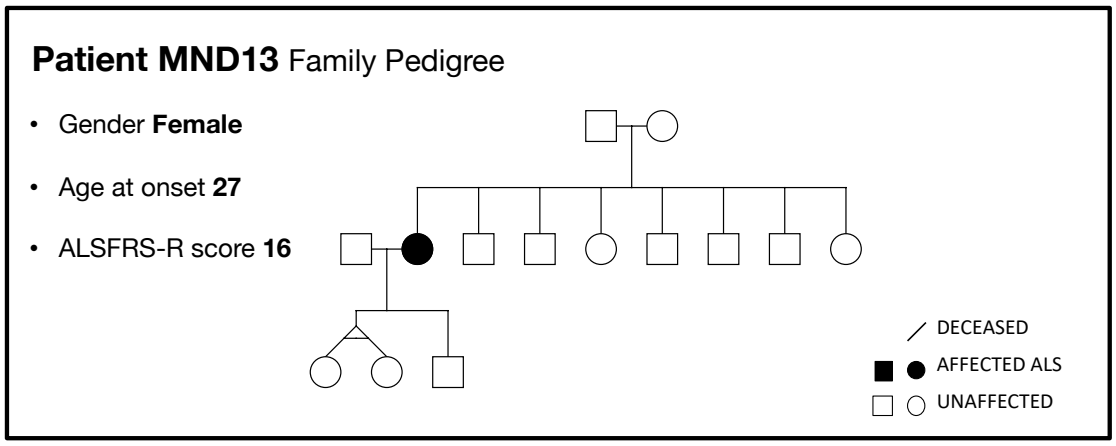

Figure 3.13 Pedigree structure of patient MND13. Squares represent male pedigree members, circles represent female pedigree members, solid symbols represent members with MND/ALS, oblique lines represent deceased members and open symbols represent unaffected members.

Patient MND14

The patient was a 73-year-old male who developed a slowly progressing motor neuron syndrome at the age of 70 (2014). Initially, the patient became aware of facial muscle and tongue weakness following the sudden death of his wife. In the consecutive months, the indicated discomfort advanced to dysarthria where the patient started to experience detectable speech disturbances. Following this, the development of a minor hip flexion weakness led to early ambulation difficulties. As a result, the patient was able to walk independently but at a slow pace. No signs of dysphagia were noted by the patient, bar occasional choking on water. Signs of dyspnoea and orthopnoea were not present. The patient had normal muscle tone in all limbs upon physical examination (November 2017) and very good muscle strength overall, with the exception of a slight decrease in bilateral hip flexion power (MRC score: 4.5). This correlated with normal blood CK levels (235 U/l; normal range 39-308 U/l). Reflex function, including the plantar reflex, was normal and Hoffman's sign was absent. The patient had a normal breathing and heart rate. No family history of ALS or any other MND was detected (**Figure 3.14**). The patient had a physically challenging occupation (construction worker) and was never a smoker or substance abuser. Stressful life events that lead to psychological trauma have been proposed as predisposing factors for a number of neurodegenerative disorders, including multiple sclerosis (SAUL *et al.* 2017),

dementia including Alzheimer's disease (JOHANSSON *et al.* 2010) and Parkinson's disease (SUGAMA *et al.* 2016). However, a recent study has shown that psychological stress stemming from such events, that range in severity from death of a spouse (as in this case) to minor law violations is not likely to play a role in ALS pathogenesis (PARKIN KULLMANN *et al.* 2018). The patient still remains alive, 7 years from symptom onset (August 2021).

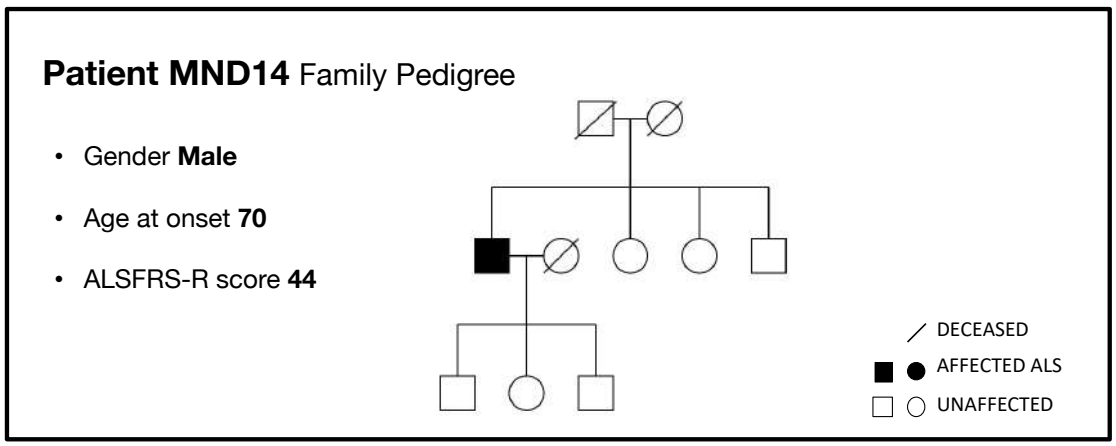

Figure 3.14 Pedigree structure of patient MND14. Squares represent male pedigree members, circles represent female pedigree members, solid symbols represent members with MND/ALS, oblique lines represent deceased members and open symbols represent unaffected members.

Patient MND16

A 65-year-old male acknowledged muscle weakness in both his lower limbs which affected his walking ability at the age of 54 (2006). Muscle weakness progressed slowly and extended to his upper limbs which resulted in a loss of gripping strength. The patient continued to suffer from general muscle atrophy and became wheelchair-bound. In recent years, the patient started to experience signs of dysarthria and gradually lost the ability to speak clearly. Hypersalivation and early eating difficulties were noted at recruitment (February 2018). The patient showed no signs of dyspnoea; however, intermediate orthopnoea was suggested. Muscle tone was increased in all limbs with rigidity especially pronounced in the upper limbs. The patient had average muscle strength upon examination except in the thumb and knee muscles, where it was notably diminished (MRC scores: 0-3). Normal reflex function was reported. Withdrawal

of blood from this patient was not possible, therefore CK results and sequencing data are not available. The patient's occupations (painting and maintenance, baker) required intense physical exertion and may have involved the exposure to hazardous components such as metallic pigments and volatile organic compounds, which are shown to contribute to the disruption of motor function in ALS (RATNER *et al.* 2018; ASH *et al.* 2019). In addition, the patient was a heavy smoker (cigarette packets/day: 3) up to his diagnosis. No immediate family members previously suffered from MND including ALS (**Figure 3.15**). The patient still remains alive, 15 years from symptom onset (August 2021).

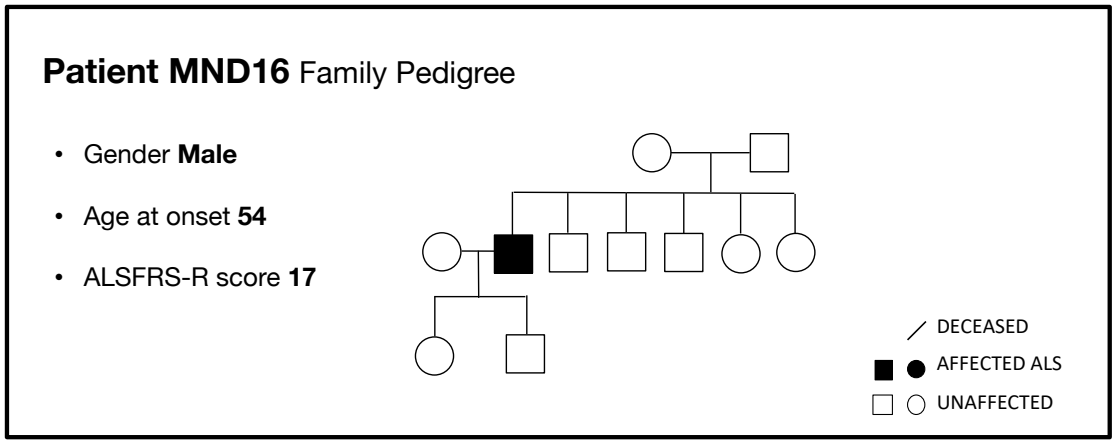

Figure 3.15 Pedigree structure of patient MND16. Squares represent male pedigree members, circles represent female pedigree members, solid symbols represent members with MND/ALS, oblique lines represent deceased members and open symbols represent unaffected members.

Patient MND17

The patient was a 69-year-old female, who suffered from a gait abnormality as a result of foot drop at the age of 52 (2000). After a number of years, she suffered from multiple slipped discs in her lower back that further hindered her ability to move around with ease. Due to several complications, diagnosis was delayed and following substantial recovery, persistent weakness in the lower limbs together with shortness of breath supported a diagnosis of probable ALS. The disease progressed with slight weakness in the patient's grip. Despite this, the subject was able to perform day-to-day tasks in a restricted manner. The patient had no speech defects, had normal eating habits with occasional choking on water and

used a walking aid to facilitate movement. Intermittent dyspnoea was reported, which worsened by frequent asthma attacks. The patient notably suffered from shortness of breath when lying down and made use of non-invasive ventilation, particularly during night-time. Physical examination (March 2018) revealed normal muscle tone in the upper limbs but increased muscle tone in the lower limbs. Conversely, acute muscle damage was evident, as marked by an increase in CK blood levels (336 U/l; normal range 26-192 U/l). Motor unit tests were normal but diminished (MRC scores: 0-4) in the lower limbs. No response upon triceps and ankle reflex examination was observed. Hoffmann's and Babinski's reflex responses were negative. Both respiratory rate and heart rate were normal at time of examination. The patient had a family history of Parkinson's disease (PD) (**Figure 3.16**). Interestingly, the ALS-associated angiogenic gene *ANG* was also demonstrated to confer an increased risk to PD (VAN ES *et al.* 2011). In addition, epidemiological studies have indicated that kindreds of ALS patients are at an increased risk of developing PD (MAJOOR-KRAKAUER *et al.* 1994; LOGROSCINO *et al.* 2008). The patient's former occupation (chambermaid) was physically challenging. No smoking habits, alcohol or drug abuse were recorded. The patient died from respiratory complications, 19 years after symptom onset (April 2019).

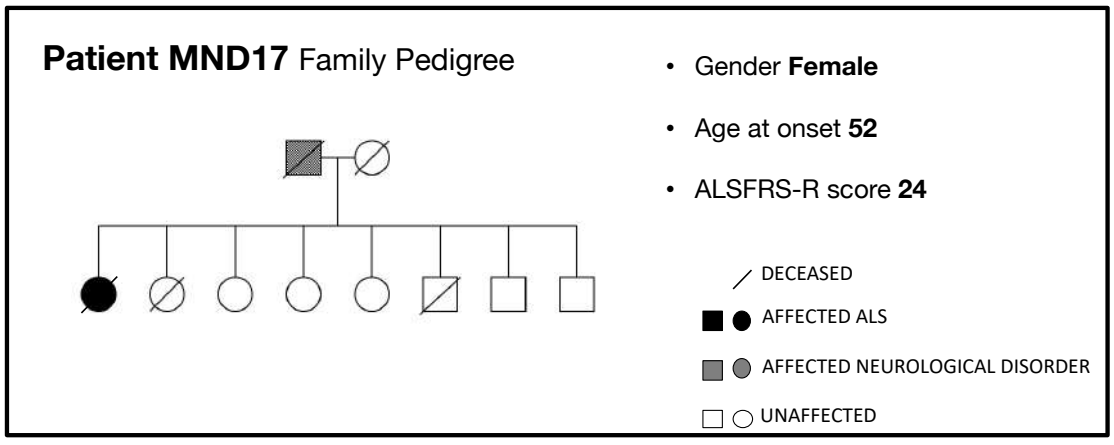

Figure 3.16 Pedigree structure of patient MND17. Squares represent male pedigree members, circles represent female pedigree members, solid symbols represent members with MND/ALS, patterned symbols represent members affected by ALS-associated neurological disorders, oblique lines represent deceased members and open symbols represent unaffected members.

Patient MND18

A 71-year-old male first started to experience loss of balance at the age of 69 (2016). Subsequently he noticed wasting and weakness in the lower limbs, especially in the right leg. The disease progressed with marked atrophy in the lower limbs and the patient became wheelchair-bound supporting a diagnosis of spinal onset suspected ALS. Despite this, the patient could still control his upper limbs and had no signs of speech disturbances or respiratory discomfort. In addition, the patient had normal eating habits with a regular dietary consistency. Normal muscle tone was detected upon examination in March 2018. Muscle strength was normal in the neck and upper limbs and somewhat diminished (MRC scores: 3-4) in muscles that control shoulder movement. On the other hand, a marked decrease (MRC scores: 0-2) in muscle strength was observed in the lower limbs, particularly in the right leg. Despite this, the patient's ALSFRS-R score was higher than the average patient ALSFRS-R score (32/48). Normal reflex function was observed. Breathing and heart rate, as well as CK levels (114 U/l; normal range 39-308 U/l), were normal. The patient was a very physically active individual and participated in vigorous sports. Furthermore, he was a cigarette smoker (cigarette packets/day: 0.5) for around 30 years, during which he also consumed alcohol on a regular basis. No family history of ALS or any other MND was associated with this case (**Figure 3.17**). The patient succumbed to the degenerative symptoms of the disease after a total duration of 2 years (July 2018).

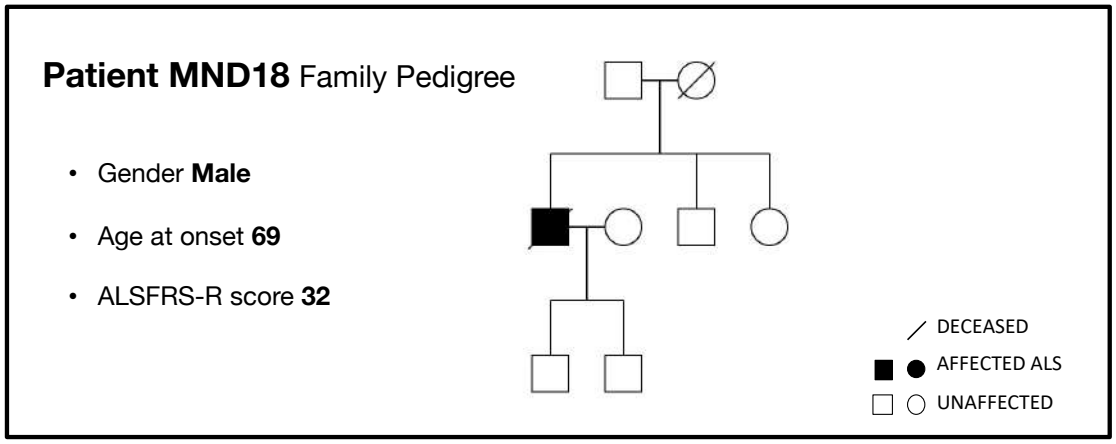

Figure 3.17 Pedigree structure of patient MND18. Squares represent male pedigree members, circles represent female pedigree members, solid symbols represent

members with MND/ALS, oblique lines represent deceased members and open symbols represent unaffected members.

Patient MND19

A 71-year-old female started to experience muscle weakness in her right shoulder at the age of 70 (2017). Muscle weakness extended to the upper extremities and the patient lost the ability of normal upper limb function including the ability to clench her fists. No weakness in the lower limbs were identified, and the individual was able to walk normally up to the date of recruitment. In addition, no signs of speech disturbances or dietary issues were noted. However, the patient still required intermittent assistance due to upper limb impairment. Signs of dyspnoea or orthopnoea were absent. Hypotonia together with diminished muscle strength (MRC scores: 0-4) was clearly exhibited in both upper limbs upon examination (April 2018). Muscle tone and power in the lower limbs was normal. CK blood levels were normal (91 U/l; normal range 26-192 U/l), indicating no significant muscle tissue damage at the time of recruitment. ALSFRS-R score was higher than the average ALS patient score (30.5/48). No reflex response was elicited upon upper limb reflex examination. Reflex function in the lower limbs was normal, and Hoffman's and Babinski's signs were absent. Non-genetic risk factors that might have contributed to the patient's diagnosis include the endurance of strenuous labour linked to her previous occupation (house cleaner), together with harmful substances associated with tobacco smoke. The subject used to be a heavy smoker (cigarette packets/day: 1) for over 50 years. The patient had no family history of ALS/MND or related disorders (**Figure 3.18**). The disease duration for this patient was 3 years, following her death at the age of 73 (July 2020).

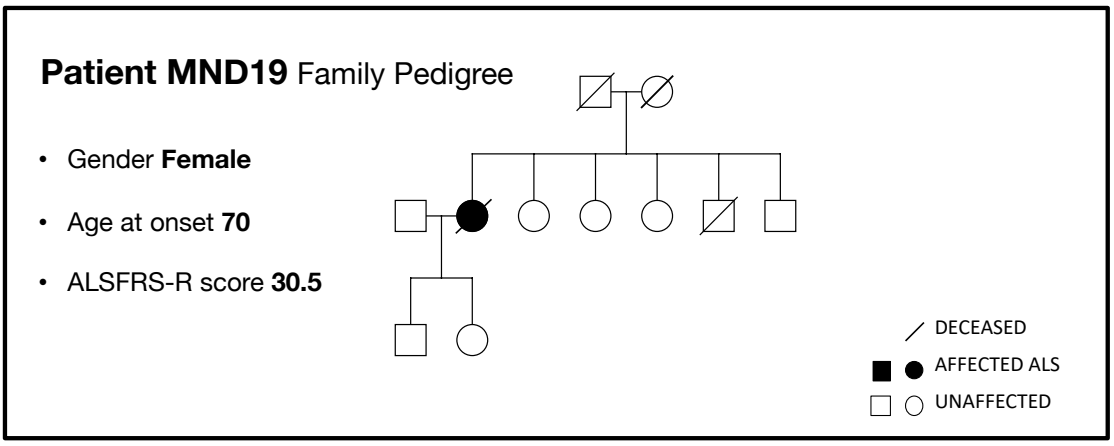

Figure 3.18 Pedigree structure of patient MND19. Squares represent male pedigree members, circles represent female pedigree members, solid symbols represent members with MND/ALS, oblique lines represent deceased members and open symbols represent unaffected members.

Patient MND20

A 72-year-old male first complained of loss of balance at the age of 70 (2016). The disease progressed slowly with mild weakness in the lower limbs, particularly on the left side. These findings partially led to a diagnosis of MND. Subsequently, the patient started to experience ambulatory difficulties and required walking assistance. This was followed by gradual signs of muscle weakness in his upper extremities that were repeatedly worse on the left side. The patient had no symptoms associated with dysarthria, dyspnoea or orthopnoea and had normal eating habits. Upon examination (July 2018), the patient's muscle tone was normal. Upper body muscle strength was good with the exception of a slight weakness (MRC score: 4) in the left thumb muscles. A decline in muscle power could be observed in the left lower limb (MRC score: 3). Increased CK levels (539 U/l; normal range 39-308 U/l) suggested acute muscle damage. Reflex function and neurological investigations were normal. Breathing rate and heart rate were regular. The patient had no history of ALS or any other MND (**Figure 3.19**). In the past, the subject suffered from heart conditions, underwent coronary bypass surgery and made use of a cardiac pacemaker. His former occupation (hairdressing) involved long standing hours. The patient was a cigarette smoker (cigarette packets/day: 1) for 30 years, starting at the age of

13 years. No excessive alcohol consumption or drug abuse was recorded. The patient is still alive, 5 years after symptom onset (August 2021).

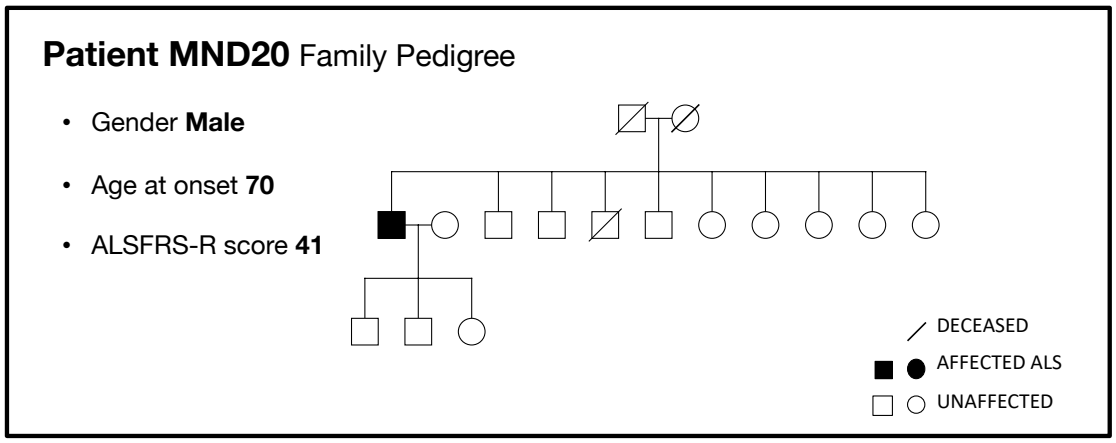

Figure 3.19 Pedigree structure of patient MND20. Squares represent male pedigree members, circles represent female pedigree members, solid symbols represent members with MND/ALS, oblique lines represent deceased members and open symbols represent unaffected members.

Patient MND21

The subject is a 59-year-old male who noticed a gait abnormality at the age of 54 (2013). He was shortly diagnosed with foot drop in his right leg. Lower limb weakness progressed slowly and as the patient continued to experience ambulatory difficulties, he made use of a splint support as a walking aide. In recent years, the patient started to notice weakness in the upper extremities, although this did not hinder day-to-day activities to a large extent. No signs of bulbar involvement, dyspnoea or orthopnoea were observed. The patient had normal eating habits. Both upper and lower limbs displayed normal muscle tone upon examination (July 2018). The patient was unable to perform ankle plantar flexion indicating no muscle contraction. Muscle strength was normal in the other muscle groups. Increased CK levels (452 U/l; normal range 39-308 U/l) demonstrate significant muscle damage at the time of recruitment. No response to reflex function tests was observed, demonstrating poor sensory and motor pathway function. No upper motor neuron involvement was detected as confirmed by absent Hoffmann's and Babinski's signs. Heart and breathing rate were within the normal range. No family history of ALS or any other MND was

detected (**Figure 3.20**). The patient suffered from a slipped disk at the age of 42, which initially made the diagnosis challenging. No smoking habits, alcohol or drug abuse was recorded. The patient remains alive, 8 years from symptom onset (August 2021).

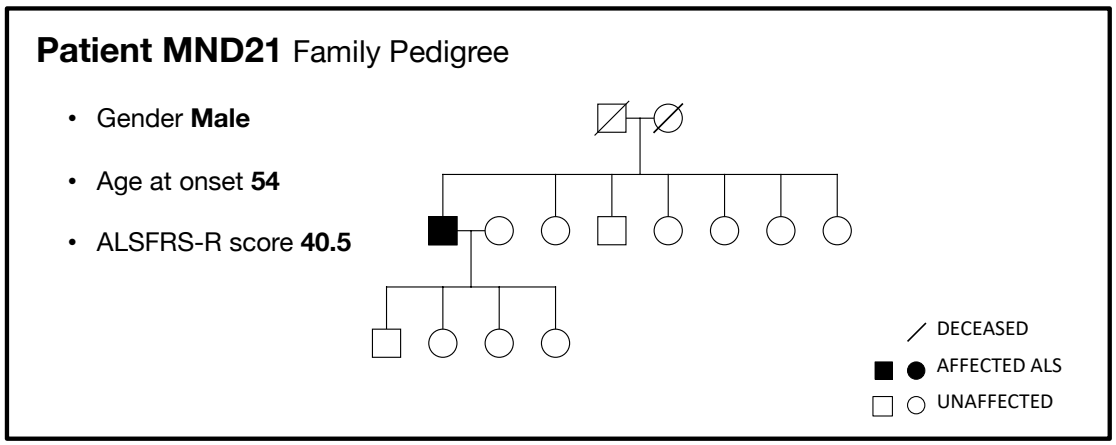

Figure 3.20 Pedigree structure of patient MND21. Squares represent male pedigree members, circles represent female pedigree members, solid symbols represent members with MND/ALS, oblique lines represent deceased members and open symbols represent unaffected members.

Patient MND22

An 82-year-old patient started to suffer from sharp pain and weakness in his right shoulder when he was 80 years old (March 2016). He was initially diagnosed with severe arthritis, and the discomfort later extended to his left shoulder. The symptoms advanced with fasciculations in both the upper limbs, together with the development of bilateral lower limb muscle wasting and weakness. The patient lost complete function of his upper limbs and started to experience ambulatory disturbances. Ultimately, he became wheelchair-bound. The patient noted that he experienced dysphagia before muscle weakness became apparent. This worsened and was accompanied by further tongue atrophy and weakness. Subsequently this led to dysarthria with close to complete loss of useful speech. Finally, the patient developed breathing difficulties and started oxygen therapy (nasal cannula) at a flow rate of 2L per minute. The patient's health status continued to decline steadily and he became bedridden. Upon examination (September 2018), hypotonia of both right and left

upper limbs was observed whereas lower limbs displayed a normal muscle tone. No muscle contraction was elicited in both upper limbs and diminished muscle strength (MRC scores: 3-4) could be observed in the lower limbs. Mild muscle contractures that are reminiscent of an infantile polio infection were observed in the left foot. Normal power was observed in neck muscles. Reflex function was distinctly diminished with poor reflexes throughout. No Babinski's or Hoffmann's signs were recorded. The patient's serum CK levels were low (15 U/l) when compared to the normal range for males (39-308 U/l). Low CK activity has been previously associated with rheumatic diseases mainly brought about by a high inflammatory response and which can be linked to muscle weakness (SANMARTI *et al.* 1996; STUCKI *et al.* 1996). The patient's previous history of arthritis could play a role in the resultant subnormal CK activity. Breathing and heart rate were normal at time of examination. Following recruitment, increased respiratory difficulties constrained the patient to make use of continuous non-invasive ventilation (BiPAP). The individual suffered several ventilatory complications secondary to viral infections and his health status declined severely, leading to his passing (January 2019) after three years from symptom onset The patient's former occupation (farming) required strenuous manual labour with the possible exposure to chemicals. No family history of ALS/MND was reported (**Figure 3.21**); the patient did not smoke or consume abnormal levels of alcohol.

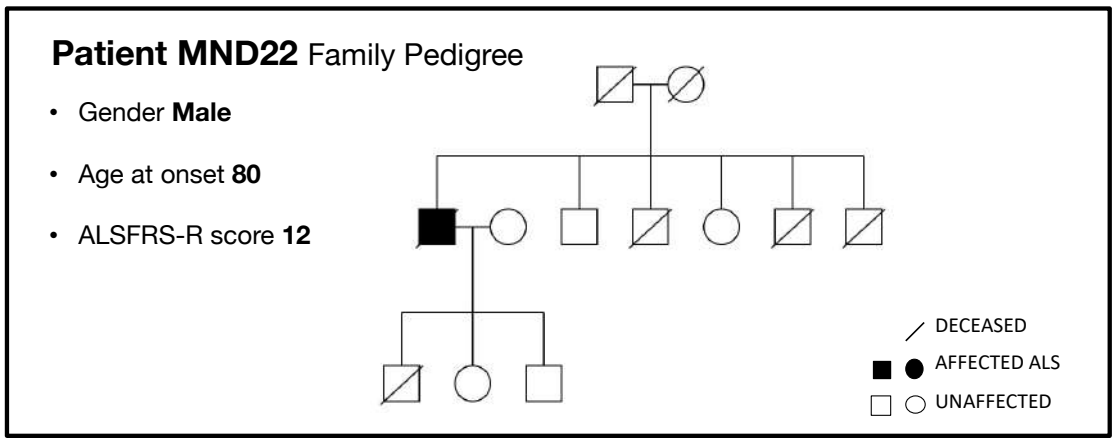

Figure 3.21 Pedigree structure of patient MND22. Squares represent male pedigree members, circles represent female pedigree members, solid symbols represent

members with MND/ALS, oblique lines represent deceased members and open symbols represent unaffected members.

Patient MND23

The patient is a 71-year-old male who started to experience weakness in his right shoulder following surgery to repair a muscle tear (2017). A few months into recovery, the weakness persisted and extended to his left shoulder, subsequently inhibiting the patient's mobility. He then started to lose strength in his lower arms that manifested with a weak hand-grip. The patient was ultimately diagnosed with suspected ALS after excluding the possibility of related conditions via several tests and an electromyography. No detectable speech disturbances or respiratory difficulties were observed and the individual had not been constrained to make any dietary consistency changes till the date of recruitment (October 2018). Despite a fairly normal walking ability, early ambulatory difficulties were noted and the patient occasionally made use of a walking aid. Physical examination revealed a normal muscle tone in both upper and lower limbs. Muscle strength was generally healthy except for that of both shoulders and elbows, which exhibited reduced power (MRC scores: 0-2) that was particularly prominent on the right side. Reflex examinations revealed normal reflex function overall, however once again the effect of upper limb weakness could be reflected in the absence of reflex reactions in these regions. A marked increase in serum CK at the time of recruitment suggested acute muscle damage (714 U/l; normal range 39-308 U/l). The patient has no family history of ALS, however, his mother suffered from dementia (**Figure 3.22**), which may be suggestive of pathological overlap between the two disorders. No exposure to genetic-independent risk factors seems to have preceded the disorder bar strenuous labour (store keeping) endured during his working years. The patient remains alive, 4 years from symptom onset (August 2021).

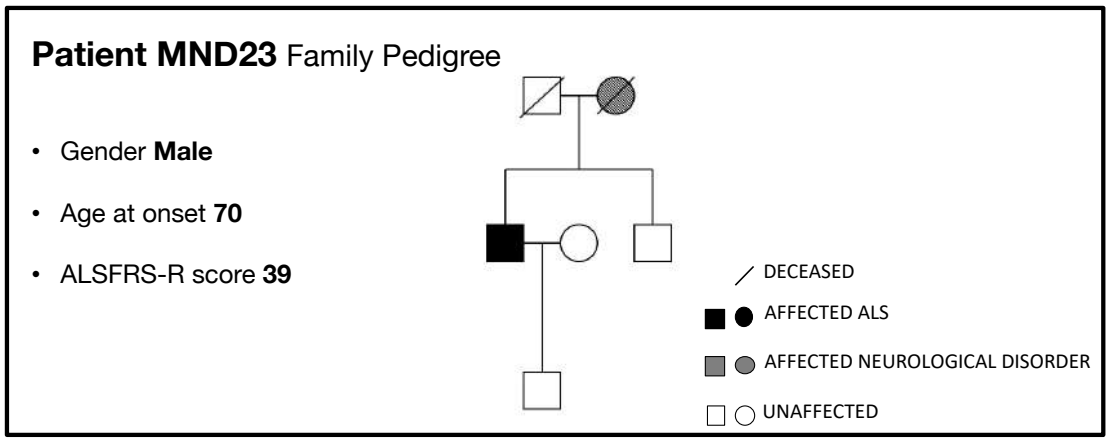

Figure 3.22 Pedigree structure of patient MND23. Squares represent male pedigree members, circles represent female pedigree members, solid symbols represent members with MND/ALS, patterned symbols represent members affected by ALS-associated neurological disorders, oblique lines represent deceased members and open symbols represent unaffected members.

Patient MND25

The patient was a 63-year-old male with bulbar-onset ALS. Initially, the patient's relatives started to notice early symptoms of depression including confusion and debilitating mood swings (2017). Consequently, a cranial CT-scan revealed brain atrophy and the patient was diagnosed with mild cognitive impairment. After a few months he started to experience slurred and slow speech as a result of tongue and facial muscle weakness. The patient continued to note a decline in articulation and also had to make dietary consistency changes, requiring supplemental tube feeding. Symptoms later progressed with a flicker sensation in his upper limbs and mild hand-grip weakness. Nonetheless, he retained the ability to perform day-to-day activities with increased effort and some assistance. Consequently, the ALS-FRS score at the time of recruitment (December 2018) was higher than the average score obtained by patients (37/48). Re-evaluation of symptoms led to a shift in diagnosis pointing to an MND scenario with cognitive decline. The individual exhibited good or slightly diminished (MRC scores: 4-5) power in all muscle groups. On the other hand, deep tendon reflex examinations revealed a decline in reflex function. Hoffmann's sign was absent and the patient had a normal response to plantar reflex examination. Serum CK levels were within the normal range for males

(155 U/l; normal range 39-308 U/l). A family history of dementia in more than one second-degree family member is clinically relevant (**Figure 3.23**). The patient was exposed to a number of potential harmful risk factors associated with his former occupations (power station construction, tile laying) including strenuous labour, high levels of combustion products and particulates (asbestos). A number of case-control studies have reported that occupational exposure to toxic particles and hydrocarbon fuels especially silica and diesel exhaust may underlie particular occupations that are associated with ALS (PAMPHLETT AND RIKARD-BELL 2013; VISSER *et al.* 2019). Furthermore, the subject used to be a heavy tobacco smoker (cigarette packets/day: 1) but ceased more than a decade ago. The patient died due to MND-associated complications after 2 years from disease onset at age 64 (April 2019).

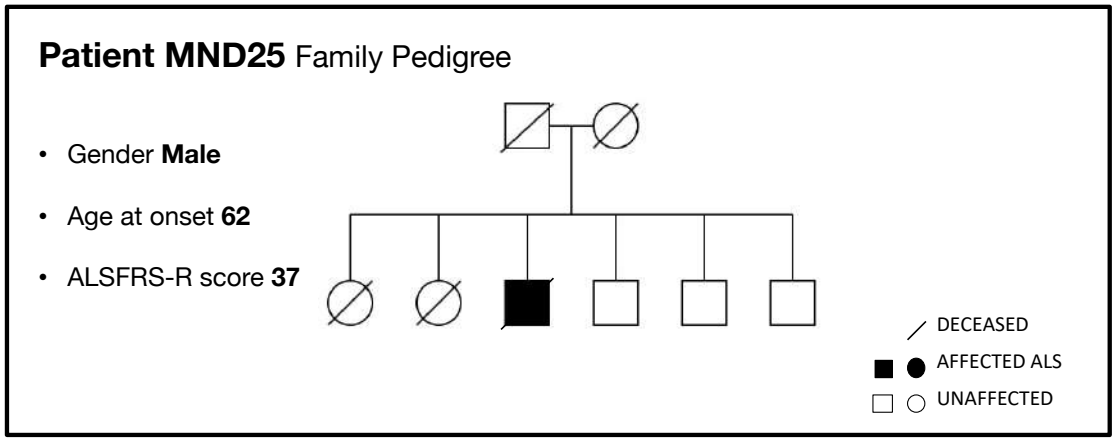

Figure 3.23 Pedigree structure of patient MND25. Squares represent male pedigree members, circles represent female pedigree members, solid symbols represent members with MND/ALS, oblique lines represent deceased members and open symbols represent unaffected members.

3.3.2 fALS case presentations

Patient MND08

A 55-year-old male patient first complained of muscle weakness in his left leg at the age of 54 (2016) This developed with a spastic gait and the need for walking assistance. Following a series of medical tests, he was diagnosed with probable ALS. The likelihood of genetic involvement in this case is substantial since at

least two immediate family members were also affected with MND (**Figure 3.24**). Initially, the progression of the disease was rather slow and the patient was able to carry out the majority of normal daily activities independently with some assistance or decreased efficiency. Physical examination (June 2017) revealed normal muscle tone and good muscle strength with the exception of the left lower limb that displayed decreased strength (MRC score: 0). Overall reflex function was normal and Babinski's and Hoffmann's signs were not present. Serum CK levels were moderately increased (397 U/l; normal range 39-308 U/l). Breathing and heart rate were normal. Throughout the succeeding months, the patient's health deteriorated steadily with bilateral leg weakness causing mobility defects as well as extension of muscle deterioration in both upper limbs. The subject also started to experience signs of dyspnoea and made use of intermittent respiratory assistance. At the time of examination, the ALSFRS-R score was only slightly abnormal (42/48) but it is highly likely that a decrease occurred in subsequent months. No signs of dysarthria or orthopnoea have been reported. The duration of disease was that of 2 years, following the death of the patient at age 57 (September 2019). This case forms part of the minor group of familial ALS cases in this cohort, where previous family history of the disease has been documented. The patient was a heavy smoker (cigarette packets/day: 2) and used to consume a relatively high amount of alcohol. No significant occupational risk factors were communicated on recruitment.

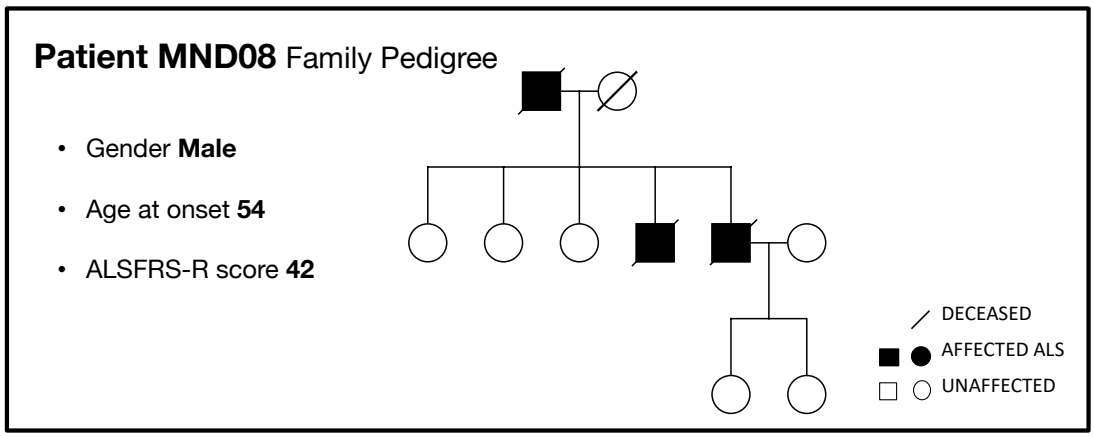

Figure 3.24 Pedigree structure of patient MND08. Squares represent male pedigree members, circles represent female pedigree members, solid symbols represent members with MND/ALS, patterned symbols represent members affected by ALS-

associated neurological disorders, oblique lines represent deceased members and open symbols represent unaffected members.

Patient MND12

The patient was a 64-year-old female, who first started to experience slurred speech and tongue weakness at the age of 60 (2013). An ALS diagnosis was suspected after the patient complained of weakness in both her upper limbs, which prompted relevant medical investigations. Her relatives also began to notice some early symptoms of cognitive impairment. Subsequently, the patient's dysarthria progressed steadily and the patient displayed loss of useful speech, followed by bilateral upper limb wasting and weakness. The patient began to experience walking difficulties and the strength in her arms deteriorated further. Signs of dysphagia began to emerge and the patient required significant dietary consistency changes and experienced slight shortness of breath when lying down. Physical examination (July 2017) revealed normal muscle tone in both upper and lower limbs. Muscle power was mostly diminished (MRC scores: 0-3) in the upper limbs, especially the left side whilst that of the neck and lower limbs was close to normal (MRC scores: 4-5). Reflex function was somewhat diminished to low. Babinski's and Hoffmann's signs were absent. Regular serum levels of CK were detected (172 U/l; normal range 26-192 U/l). Breathing rate during examination was slightly elevated (24 breaths/min, normal adult range: 12-20 breaths/min) and heart rate was also normal. Three members of the patient's family, her mother and two sisters, had been previously diagnosed with MND, classifying this case as familial ALS (**Figure 3.25**). The patient was a smoker (cigarette packs/day: 0.5) for a brief period of time and did not consume harmful amounts of alcohol or any drugs. The patient succumbed to the illness following disease complications marking 4 years from symptom onset (August 2017).

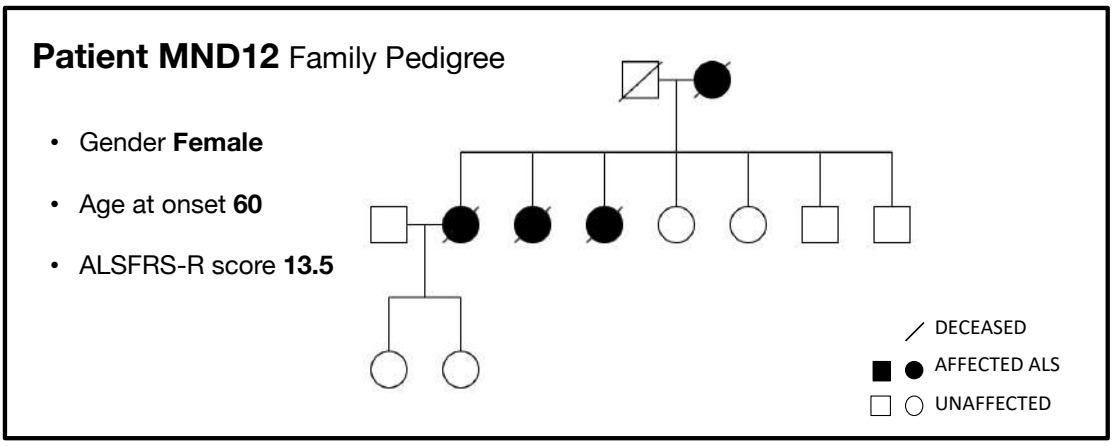

Figure 3.25 Pedigree structure of patient MND12. Squares represent male pedigree members, circles represent female pedigree members, solid symbols represent members with MND/ALS, patterned symbols represent members affected by ALS-associated neurological disorders, oblique lines represent deceased members and open symbols represent unaffected members.

Patient MND24

This is a familial case of ALS that involved a 69-year-old male patient. A female family member was also previously diagnosed with the disorder and died a few years post-diagnosis. Furthermore, the patient's mother suffered from Alzheimer's disease, which may be suggestive of an overlapping genetic background (**Figure 3.26**). At the age of 67, the subject started to experience an intermittent walking instability that frequently constrained him to stumble unexpectedly (2017). Lower limb weakness progressed steadily and the patient started to rely on a mobility aid for walking assistance. The disease developed with weakness of throat muscles that led to unclear articulation that is however intelligible with repeating. In addition, poor oral and facial muscle control also contributed to hyper-salivation. Despite this, eating habits were normal with occasional choking. Close to the date of visit (December 2018), the patient also noticed early signs of muscle weakness in his upper limbs that manifested as decreased grip strength. This was confirmed upon muscle power examinations, as the patient found it challenging to fully extend and flex both wrists, which was specifically pronounced in the left hand (MRC scores: 0-2). Shoulder muscle strength was also slightly diminished (MRC score: 4). Lower limb examination revealed an overall slight decrease in muscle power where the patient was able

to achieve full range of motion against some resistance (MRC scores: 3-5). Once again, the patient required more effort to perform movement of the left lower limb. Reflex function appeared to be normal as certified by normal deep tendon reflex examinations. Muscle tone was normal in both upper and lower limbs and no signs of respiratory defects were detectable. Increased levels of CK in the blood (474 U/l; normal range 39-308 U/l) indicate potential acute muscle damage. Following recruitment, the disease progressed with behaviours associated with dementia including confusion and memory loss, which continues to highlight a scenario of MND with cognitive involvement and thus a disease overlap. In addition, dysarthria progressed rapidly with complete loss of useful speech. The overall physical status of the patient continued to deteriorate steadily leading to his death (July 2019), 2 years from symptom onset. The patient never smoked cigarettes or consumed excessive levels of alcohol or drugs. No-occupational risk can be associated with ALS symptoms. It is relevant to note that the patient's daughter developed symptoms of psychosis well before he received his MND diagnosis.

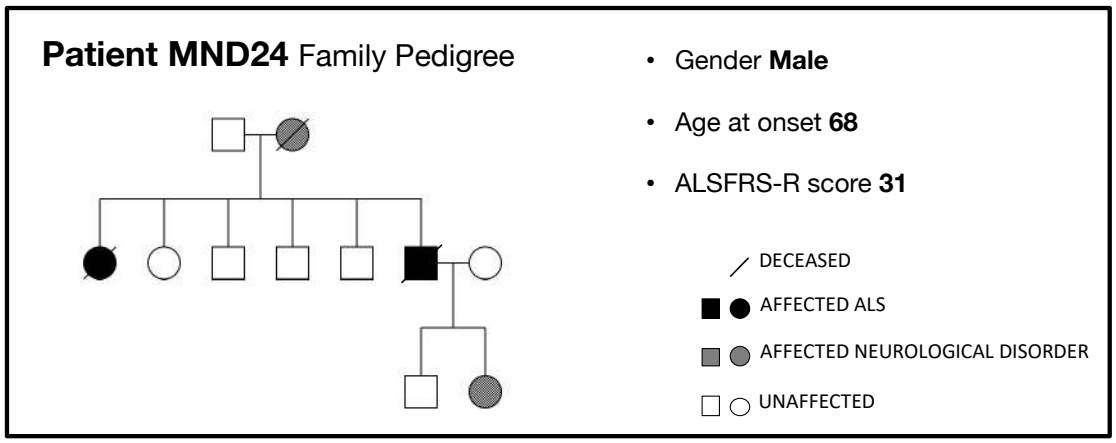

Figure 3.26 Pedigree structure of patient MND24. Squares represent male pedigree members, circles represent female pedigree members, solid symbols represent members with MND/ALS, patterned symbols represent members affected by ALS-associated neurological disorders, oblique lines represent deceased members and open symbols represent unaffected members.

3.4 MUSCLE POWER AND REFLEX FUNCTION

Muscle strength was scored on the MRC scale (six points, range: 0-5) to identify neurological deficits. Muscle examination was carried out on several muscle groups to collectively test for neck, upper limb and lower limb function. The average total muscle power for patients was 3.5 ± 1.2 SD; whilst that of controls was 5 ± 0 SD, the highest grade achievable. Neck flexion and extension were examined as representatives of neck muscle power. The average MRC scale grade for this muscle group in patients was similar to that achieved by controls (**Figure 3.27A**). Examination of the upper limb muscle group included bilateral abductors of shoulders and elbow flexors and extensors as representatives of the proximal upper extremity muscles; as well as extensors and flexors of the wrist and bilateral abductors of the thumb as representatives of distal upper extremity muscles. Upper limb muscle power in patients averaged at a grade of 2.8 (± 1.9 SD, range: 0.5-4.9), close to half that obtained by controls (5 ± 0 SD) (**Figure 3.27B**). Muscle strength was also tested in bilateral flexors of the hip, knee extensors and flexors as representatives of the proximal lower extremity muscles, as well as in ankle dorsiflexion and plantar flexion muscles as representatives of the distal lower extremity muscles. The average MRC scale grade obtained for the lower limb muscle group in patients was similar to that obtained for the upper limbs (2.9 ± 1.8 SD, range: 0-4.9) (**Figure 3.27C**). The median grade was highest in neck muscle groups and lowest for upper limb muscle groups, whereas the range in scores was comparable for each muscle group (**Figure 3.27D**).

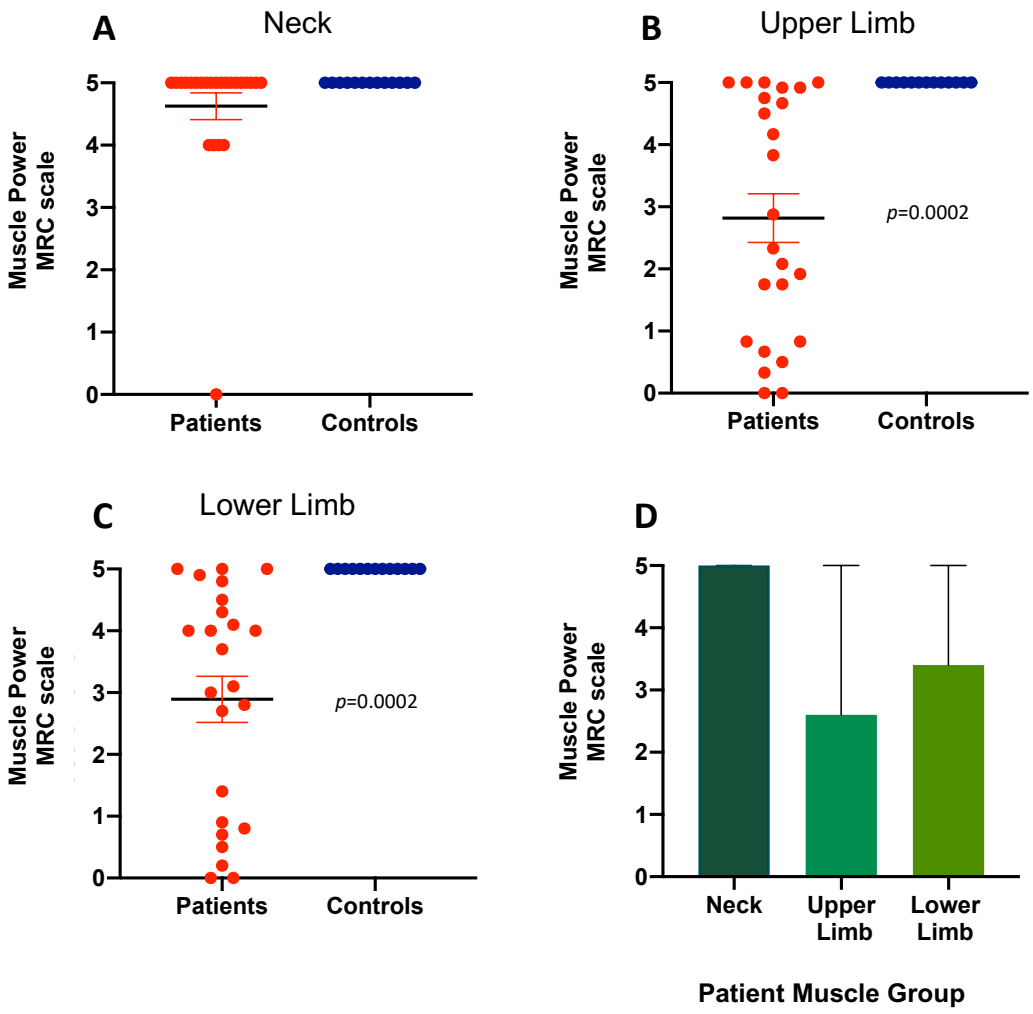

Figure 3.27 MRC scale grading for muscle power in different muscle groups. (**A**) The average muscle power for the neck muscle group in patients is similar to that for controls. (**B, C**) In the upper and lower extremity muscle groups, the average MRC score grade obtained by patients was close to half that obtained by controls. (**D**) The median grade was highest in neck muscle groups and lowest for upper limb muscle groups, whereas the range in grades was comparable for each muscle group. Data presented in **A-C** are mean ± S.E.M and significance was tested by the unpaired *t*-test as indicated by the exact *p*-value, dots represent the mean MRC score for individual muscles representing each muscle group. Data presented in **D** are the median and range.

The recruited patients were divided into four categories according to their MRC score (≤2, 3, 4 & 5) for the average muscle power in three muscle groups (neck, upper limb and lower limb) to investigate whether an association exists between muscle power and ALSFRS-R score or disease duration. As expected, a high MRC scale score correlates with a superior ALSFRS-R score across all muscle groups,

confirming that increased muscle strength results in a better physical function (**Figure 3.28A**). Conversely, MRC scale score is not associated with disease duration since a high MRC scale indicating good muscle power, did not appear to increase survival (**Figure 3.28B**). Furthermore, duration of disease is not affected by any particular muscle group. The average disease duration with regards to overall muscle power (5.9 ± 0.8 SD, years) is similar to the average disease duration for neck and upper limb muscle power average (neck: 5.4 ± 4.1 SD, years; upper limb: 5.4 ± 2.6 SD, years) but slightly lower than that for lower limb muscle power (7.4 ± 6.8 SD, years). The average disease duration for the latter muscle group was increased mostly as a result of an increased disease duration (17.7 ± 4.9 SD, years) for patients that scored in the second category (score 3) of the MRC scale for lower limbs. No patient had an MRC scale score of 3 upon examination of the neck muscle group, hence, ALSFRS-R score and disease duration drop to 0 (**Figure 3.28A, B**).

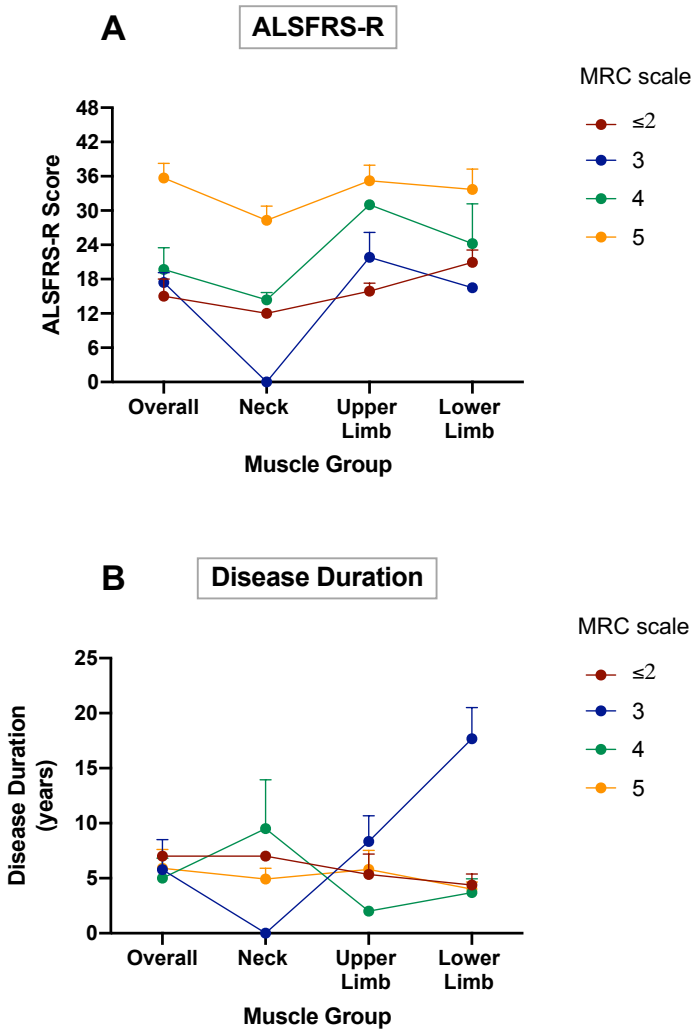

Figure 3.28 The effect of MRC scale score on ALSFRS-R score and disease duration. (**A**) A high MRC scale score is associated with a better ALSFRS-R score across all muscle groups. (B) Disease duration is not affected by MRC scale score for any muscle category except the lower limbs, where patients with an MRC scale score of 3 had higher survival. No patient scored a MRC scale score of 3 upon examination of the neck muscle group, hence, ALSFRS-R and disease duration could not be investigated for this category. Data presented are mean ± S.E.M.

Reflex function was determined by examining five primary deep tendon reflexes including bicep, triceps, brachioradialis, patellar and ankle, to evaluate the integrity of the nerve (motor system) associated with their corresponding muscle. A decrease or loss of reflex indicates involvement of lower motor neurons, whereas an increased reflex indicates involvement of the upper motor

neurons (RODRIGUEZ-BEATO AND DE JESUS 2021). A normal reflex action marked with 2+ of the reflex scale, occurred in more than half of the patients (54.6%) and nearly all of the controls (99.2%) (**Table 12**). The involvement of lower motor neurons is evidently marked in patients, where a diminished or absent response occurred in a substantial number of patients compared to controls (**Table 12**). In one instance, a control recruit elicited no response upon examination of the right patellar tendon, likely due to unilateral total knee replacement surgery. Minor involvement of the upper motor neurons (reflex scale 3+/4+) was observed in a low number of patients compared to none in controls.

Table 12 Reflex function in patients and controls.

Reflex Scale	Reflex Action	Deep Tendon Reflex	**PATIENTS** reflex occurrence % (frequency)	**CONTROLS** reflex occurrence % (frequency)
0	No response	**Overall**	32.5 (78)	0.77 (1)
		Bicep	25 (12)	0 (0)
		Tricep	39.6 (19)	0 (0)
		Suppinator	37.5 (18)	0 (0)
		Knee	14.6 (7)	3.8 (1)*
		Ankle	45.8 (22)	0 (0)
1+	Somewhat diminished	**Overall**	11.25 (27)	0 (0)
		Bicep	14.6 (7)	0 (0)
		Tricep	4.2 (2)	0 (0)
		Suppinator	6.3 (3)	0 (0)
		Knee	25 (12)	0 (0)
		Ankle	6.25 (3)	0 (0)
2+	Normal	**Overall**	54.58 (131)	99.23 (129)
		Bicep	52.1 (25)	100 (26)
		Tricep	56.3 (27)	100 (26)
		Suppinator	56.3 (27)	100 (26)
		Knee	60.4 (29)	96.2 (25)
		Ankle	47.9 (23)	100 (26)
3+	Brisker than average	**Overall**	1.67 (4)	0 (0)
		Bicep	8.3 (4)	0 (0)
		Tricep	0 (0)	0 (0)
		Suppinator	0 (0)	0 (0)
		Knee	0 (0)	0 (0)
		Ankle	0 (0)	0 (0)
4+	Very brisk, hyper-reflexive	**Overall**	0 (0)	0 (0)
		Bicep	0 (0)	0 (0)
		Tricep	0 (0)	0 (0)
		Suppinator	0 (0)	0 (0)
		Knee	0 (0)	0 (0)
		Ankle	0 (0)	0 (0)

* No response likely due to total knee replacement of the right lower limb.

3.5 GENETIC ANCESTRY

To control for population stratification, PCA was employed to estimate the genetic ancestry of the Maltese cohort. Cases and control were within 3 standard deviations of the mean for the combined samples along principal components (PC) 1-4, which are used to separate major continental groups in the Human Genome Diversity Panel (HGDP) reference panel (WANG *et al.* 2014). This certifies adequate matching of cases and controls. Mapping the ancestry coordinates of Maltese ALS patients and control samples to HGDP reference PCA coordinates of the first two principal components, shows overlap with the Middle-Eastern cluster, neighbouring the European cluster (**Figure 3.29**). A genetic affinity with Middle Eastern populations is also apparent in southern Italian regions as with other Mediterranean populations (DI GAETANO *et al.* 2012).

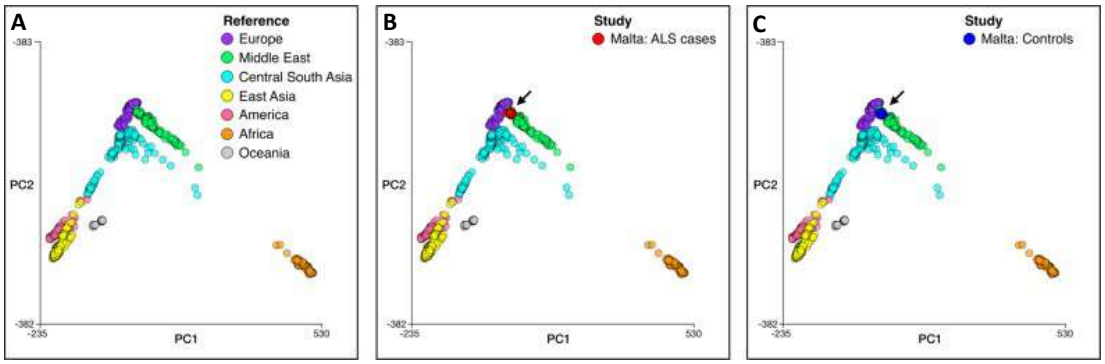

Figure 3.29 Genetic ancestry of Maltese cases and controls against HGDP reference panel. (**A**) Reference PCA coordinates for HGDP reference panel samples; (**B**) Maltese ALS cases mapped to reference PCA coordinates; (**C**) Maltese controls mapped to reference PCA coordinates.

3.6 GENOMIC ANALYSES OF MALTESE ALS PATIENTS

3.6.1 Mining for the major ALS-causative genes

No rare SNVs in the most prevailing ALS genes (*C9orf72*, *SOD1*, *TARDBP* or *FUS*) were identified in any familial or sporadic cases. Screening for all variants in these loci mostly revealed silent mutations with a high allelic frequency (**Table**

13). Eight *C9orf72* missense mutations were identified, which were expressed at an allele frequency of ~ 0.1, and are not likely to cause disease. Evaluation of indels, specifically *C9orf72* repeat expansions, indicates that expansions within this region do no exceed the 24-expansion repeat threshold associated with ALS (IACOANGELI *et al.* 2019) (**Figure 3.30**), and are therefore not pathogenic. The expansion repeat size ranged from 2 to 13 in ALS patients and from 2 to 10 in controls. As in previous studies, a repeat length of 2 was the most predominant in either group (52.2% in ALS cases and 42.3% in controls) (RENTON *et al.* 2011; SMITH *et al.* 2013).

Table 13 SNVs identified within the four most common ALS genes.

Gene	dbSNP ID	European gnomAD MAF	Function	MetaSVM Prediction	Number of Variants	Number of Patients	Number of Controls
C90rf72	rs10122902	0.2067	SILENT	-	11	6	4
	rs17769294	0.1396	MISSENSE	-1.0828(T)	8	3	4
SOD1	rs143100990	0	SILENT	-	1	-	1
TARDBP	rs61730366	0.0015	SILENT	-	1	1	-
FUS	rs1052352	0.5083	SILENT	-	32	19	13
	rs741810	0.3337	SILENT	-	8	6	2

dbSNP, Single Nucleotide Polymorphism Database; **gnomAD**, Genomes Aggregation Database; **T**, Tolerated.

In addition to *C9orf72*, trinucleotide repeat expansions were identified in the genes *ATXN2* (CAG) and *NIPA1* (GCG), which have also been shown to increase the risk of ALS (ELDEN *et al.* 2010; BLAUW *et al.* 2012). The longest *ATXN2* trinucleotide repeat expansion (28 repeats) was identified in the homozygous state and is linked to a male patient, who developed spinal onset fALS (MND24) No DNA samples of affected relatives associated with this case were available for the study. An *ATXN2* repeat expansion of 25 repeats was encountered in one healthy control in the heterozygous state. Repeat lengths in the remaining ALS patients and controls did not exceed 23 repeats. As suggested in previous studies, *ATXN2* alleles most commonly have repeat lengths of 22 (VAN DAMME *et al.* 2011; GELLERA *et al.* 2012). Similarly, the *ATXN2* CAG-repeat size in the cohort studied was 22 triplets in 84.8% of the alleles in ALS patients and in 88.5% of the

alleles in controls. Several studies have reported that the most frequent alleles for *NIPA1* consist of 7 or 8 polymorphic repeats (BLAUW *et al.* 2012; CORRADO *et al.* 2019; TAZELAAR *et al.* 2019). This also applied to this study, with allele frequency for 7 repeats estimated at 26.1% in ALS patients and 7.7% in controls, and that for 8 repeats being 67.4% in patients and 73.1% in controls. Three ALS patients in our cohort had *NIPA1* alleles that exceeded 8 GCG repeats (13.04%, range: 12-21), with one male patient having a heterozygous expansion of 21 repeats (**Figure 3.30**). The patient concerned (MND02) developed sporadic ALS with spinal onset at the age of 73. Survival was shorter (<2.5 years) compared with the median survival (3.5 years) in our ALS cohort. However, no clear indications on the effect of repeat-length differences on survival have been yet established (BLAUW *et al.* 2012; TAZELAAR *et al.* 2019). For controls, expanded alleles within this region did not exceed 13 repeats (range: 5-13).

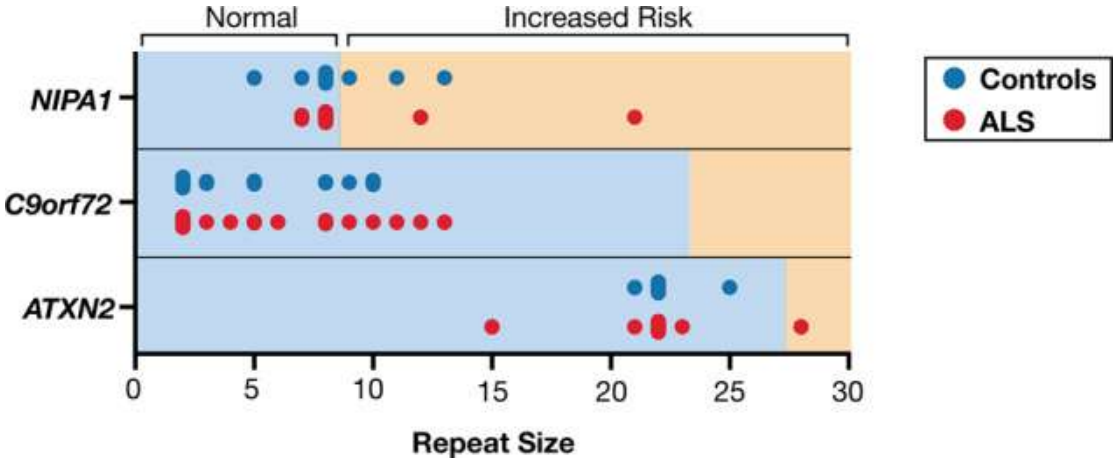

Figure 3.30 Expansion repeat size for *NIPA1, C9orf72* and *ATXN1* genes in ALS cases and controls. Scatter plot showing length and frequency of expansion repeats, indicated by circles.

3.6.2 Genetic variants in known ALS-linked genes

The sequencing data of the Maltese ALS patient and control cohort was mined for rare (European MAF ≤0.02) SNVs in 58 ALS-associated genes. As a result, 35 rare coding variants that were present in Maltese ALS patients but were absent in controls were identified (**Table 14**). Considering their absence in the dbSNP (v155) database (August 2021), two novel SNVs were identified in the genes

DDX20, and *EWSR1*. No allele frequency on the dbSNP[155] database has been reported for the *GLE1* variant, NM_001003722.1: c.2078C>T; p.(Ser693Phe), which was submitted to dbSNP as a novel allele as part of this study. This variant was reported in a recent study as a founder mutation in the Maltese population, that plays a role in a severe form of motor neuron disease that results in premature fetal death (SAID *et al.* 2017). As predicted by MetaSVM, 8 variants in the genes *ALS2*, *DAO*, *DCTN1*, *ERBB4*, *SARM1*, *SCFD1*, *SETX* and *SPG11* were considered to be damaging. All damaging variants were detected in sALS cases. The NM_001917.4:c.250G>A; p.(Ala84Thr) *DAO* variant was identified in two patients, who revealed deleterious variants in more than one gene (MND11: *DAO* and *DCTN1;* MND04: *DAO* and *SARM1*). The highest number of variants (8) were found in the gene *SPG11*.

Analysis of indels revealed a rare heterozygous deletion in *SETX* in a patient with sALS. The deletion is predicted to result in a frameshift, consequently producing a truncated protein that is therefore predicted to associate with disease (**Table 14**). Rare SNVs or indels unique to controls were also identified, except for the NM_015046.5:c.3047T>C; p.(Ile1016Thr) variant in the *SETX* gene, the NM_004984.2:c.2927C>T; p.(Thr976Ile) variant in the *KIF5A* gene and the NM_198935.2:c.961G>A; p.(Ala321Thr) variant in the gene *SS18L1*, which were also present in ALS patients (**Table 15**). One SNV in *FIG4* was not found in dbSNP[155]. Not all rare variants in the Maltese cohort could be recovered in the international Project MinE case-control dataset (**Table 16**). Interestingly, three damaging variants in *DAO, ERBB4* and *SPG11* were absent from the database highlighting their relevance within the Maltese cohort. Furthermore, the damaging variants in *ALS2*, *SCFD1* and *SETX* detected in Maltese sALS patients were found to have higher allele frequencies in ALS patients within the Project MinE dataset when compared to controls, thereby underscoring their probable pathogenicity. In some cases, no association with ALS genes or risk loci could be identified, underscoring the requirement for further studies to elucidate novel genes that cause ALS.

Table 14 Rare non-synonymous single-nucleotide variants and indels in Maltese ALS patients.

Gene	cDNA change	Protein change	dbSNP[155] ID	European gnomAD MAF	MetaSVM Prediction	Clinical Significance ACMG-AMP Standards	CADD Raw Scores	No. of patients	Patient Code	ALS type	Zygosity
ALS2	NM_020919.3:c.3206G>A	p.(Gly1069Glu)	rs200706696	0.0003	**Damaging**	VUS	7.109487	1	MND14	sALS	het
ATXN2	NM_002973.3:c.2950A>C	p.(Ile984Leu)	rs1338140819	0.00001	Tolerated	VUS	3.267463	1	MND06	sALS	het
C21orf2	NM_001271441.1:c.661G>A	p.(Ala221Thr)	rs746114248	0	Tolerated	VUS	0.024537	1	MND13	sALS	het
CAPN14	NM_001145122.1:c.1249C>T	p.(Leu417Phe)	rs181906086	0.0080	Tolerated	VUS	-0.488874	1	MND12	fALS	het
DAO	NM_001917.4:c.250G>A	p.(Ala84Thr)	rs781658657	0.00001	**Damaging**	LP	3.097973	2	MND04, MND11	sALS	het
DCTN1	NM_004082.4:c.1484G>A	p.(Arg495Gln)	rs17721059	0.014	Tolerated	VUS	3.136239	1	MND24	sALS	het
DCTN1	NM_004082.4:c.586A>G	p.(Ile196Val)	rs55862001	0.0055	Tolerated	VUS	1.814549	1	MND03	sALS	**hom**
DCTN1	NM_004082.4:c.1864A>T	p.(Ile622Phe)	rs1328116832	0.00001[a]	**Damaging**	LP	4.28153	1	MND11	sALS	het
DDX20	NM_007204.4:c.2237T>C	p.(Leu746Ser)	NA	NA	Tolerated	VUS	-1.270721	1	MND24	fALS	het
DNAJC7	NM_001144766.2:c.2T>C	p.(Met1?)	rs371236469	0.00005	Tolerated	VUS	2.07013	1	MND01	sALS	het
ERBB4	NM_005235.2:c.3814G>A	p.(Gly1272Arg)	rs371332509	0.00001	**Damaging**	LP	3.742097	1	MND10	sALS	het
ERBB4	NM_005235.2:c.1122T>G	p.(His374Gln)	rs76603692	0.0009	Tolerated	VUS	0.116795	1	MND19	sALS	het
ERBB4	NM_005235.2:c.3176T>C	p.(Met1059Thr)	rs373685875	0.00001	Tolerated	VUS	1.427567	1	MND25	sALS	het
EWSR1	NM_013986.3:c.1798G>A	p.(Asp600Asn)	NA	NA	Tolerated	VUS	2.377744	1	MND24	fALS	het
EWSR1	NM_013986.3:c.1408G>A	p.(Gly470Ser)	rs41311143	0.0121	Tolerated	VUS	4.947276	1	MND19	sALS	het
GLE1	NM_001003722.1:c.2078C>T	p.(Ser693Phe)	rs1564162129	NA	Tolerated	VUS	6.182627	1	MND18	sALS	het
MOBP	NM_001278322.1:c.586C>A	p.(Arg196Ser)	rs1188260744	0	Tolerated	VUS	2.807917	1	MND03	sALS	het
NEFH	NM_021076.3:c.2009T>A	p.(Val670Glu)	rs190692435	0.00676	Tolerated	LB	0.356137	2	MND13, MND24	sALS, fALS	het
NEK1	NM_001199397.1:c.107A>G	p.(Asn36Ser)	rs1404362599	NA	Tolerated	VUS	2.461611	1	MND04	sALS	het
SARM1	NM_015077.4:c.1498T>C	p.(Tyr500His)	rs144613221	0.00228	**Damaging**	VUS	3.180344	1	MND04	sALS	het
SCFD1	NM_016106.3:c.209T>C	p.(Ile70Thr)	rs61754480	0.00403	**Damaging**	VUS	4.006022	1	MND13	sALS	het
SCFD1	NM_016106.3:c.1297A>G	p.(Thr433Ala)	rs61754285	0.018024	Tolerated	VUS	1.775176	2	MND09,MND11	sALS	het
SETX	NM_015046.5:c.7640T>C	p.(Ile2547Thr)	rs151117904	0.0032	Tolerated	LB	-0.550969	1	MND18	sALS	het
SETX	NM_015046.5:c.2425A>G	p.(Ile809Val)	rs906452681	0.00003	Tolerated	VUS	-2.23941	1	MND14	sALS	het
SETX	NM_015046.5:c.5308_5311del	p.(Glu1770Ilefs*15)	rs750959420	0	**Damaging**[b]	LP	NA	1	MND23	sALS	het
SPG11	NM_025137.3:c.1618C>T	p.(Arg540Cys)	rs758046989	0.00001	**Damaging**	VUS	7.758618	1	MND17	sALS	het
SPG11	NM_025137.3:c.6759C>G	p.(Asp2253Glu)	rs141818132	0.00003	Tolerated	VUS	-0.322925	1	MND10	sALS	het
SPG11	NM_025137.3:c.1698T>G	p.(Asp566Glu)	rs79708848	0.01798	Tolerated	VUS	1.060442	1	MND19	sALS	het
SPG11	NM_025137.3:c.16G>A	p.(Gly6Arg)	rs200573434	0.00208	Tolerated	VUS	2.483469	1	MND06	sALS	het
SPG11	NM_025137.3:c.3037A>G	p.(Lys1013Glu)	rs111347025	0.01224	Tolerated	VUS	1.687244	1	MND01	sALS	het
SPG11	NM_025137.3:c.3425C>G	p.(Ser1142Cys)	rs201082396	0.0001	Tolerated	VUS	3.265311	1	MND12	fALS	het
SPG11	NM_025137.3:c.2656T>C	p.(Tyr886His)	rs139687202	0.0001	Tolerated	VUS	1.030837	1	MND20	sALS	het
SPG11	NM_025137.3:c.7256A>G	p.(Lys2419Arg)	rs76116949	0.0001	Tolerated	VUS	3.324705	1	MND10	sALS	het
TNIP1	NM_001252390.1:c.437C>T	p.(Ala146Val)	rs2233289	0.0103	Tolerated	VUS	0.306309	1	MND23	sALS	het

dbSNP Single Nucleotide Polymorphism database, **gnomAD** Genomes Aggregation database, **MAF** minor allele frequency, **NA** not available, **VUS** variant of uncertain significance, **LP** likely pathogenic, **LB** likely benign, **CADD** Combined Annotation Dependent Depletion, **het** heterozygote, **hom** homozygote.

[a]Data from Trans-Omics for Precision Medicine (Topmed) database; [b]Indel was automatically considered deleterious.

Table 15 Rare non-synonymous single-nucleotide variants in Maltese controls including those also present in ALS patients.

Gene	cDNA change	Protein Change	dbSNP[155] ID	European gnomAD MAF	MetaSVM Prediction	Clinical Significance ACMG-AMP Standards	CADD Raws Scores	No. of controls	No. of patients	Control/Patient Code	Zygosity
ATXN2	NM_002973.3:c.743G>A	p.(Ser248Asn)	rs7969300	0.0031	Tolerated		2.280725	2	0	CTRL4, CTRL8	het
ATXN2	NM_002973.3:c.1507G>C	p.(Val503Leu)	rs771843383	0.00002	Tolerated		2.512218	1	0	CTRL9	het
CCNF	NM_001761.2:c.2122G>C	p.(Ala708Pro)	rs754766175	NA	Tolerated		2.747088	1	0	CTRL6	het
CCNF	NM_001761.2:c.1188G>T	p.(Glu396Asp)	rs36008785	0.0001	Tolerated		4.186215	1	0	CTRL1	het
CYLD	NM_015247.2:c.665C>A	p.(Thr222Lys)	rs587778225	0.00011	Tolerated		1.563325	2	0	CTRL2, CTRL9	het
ERBB4	NM_005235.2:c.3859G>A	p.(Glu1287Lys)	rs367568427	0.00003	**Damaging**		6.587377	1	0	CTRL11	het
FIG4	NM_014845.5:c.434C>T	p.(Pro145Leu)	NA	NA	Tolerated		7.220484	1	0	CTRL7	het
GLE1	NM_001003722.1:c.5C>G	p.(Pro2Arg)	rs150246404	0.0008	Tolerated		6.025362	1	0	CTRL2	het
KIF5A	NM_004984.2:c.2927C>T	p.(Thr976Ile)	rs139801016	0.0001	Tolerated	VUS	4.095564	1	1	CTRL6/MND08	het
NEFH	NM_021076.3:c.1684C>G	p.(Pro562Ala)	rs530872313	0.00001	Tolerated		-1.539828	1	0	CTRL14	het
NEK1	NM_001199397.1:c.1535C>T	p.(Ala512Val)	rs771824152	0.00006	Tolerated		2.485457	1	0	CTRL3	het
SETX	NM_015046.5:c.3047T>C	p.(Ile1016Thr)	rs200856903	0.00001	**Damaging**	VUS	6.255945	1	1	CTRL13/MND06	het
SPG11	NM_025137.3:c.820G>A	p.(Val274Ile)	rs543316224	0.00001	Tolerated		-0.661108	1	0	CTRL11	het
SS18L1	NM_198935.2:c.961G>A	p.(Ala321Thr)	rs36106901	0.00042	Tolerated	VUS	1.503385	2	2	CTRL14, CTRL8/MND06, MND02	het
TIA1	NM_022173.2:c.1070A>G	p.(Asn357Ser)	rs116621885	0.0125	Tolerated		1.672601	1	0	CTRL6	het
TNIP1	NM_001252390.1:c.1748C>T	p.(Pro583Leu)	rs888695021	0.0000	Tolerated		4.359246	1	0	CTRL1	het
TNIP1	NM_001252390.1:c.1049C>T	p.(Thr350Ile)	rs369725837	0.00002	Tolerated		4.366224	1	0	CTRL7	het

dbSNP Single Nucleotide Polymorphism database, **gnomAD** Genomes Aggregation database, **MAF** minor allele frequency, **NA** not available, **CADD** Combined Annotation Dependent Depletion, **het** heterozygote.

Table 16 Evaluation of Maltese rare SNVs in the Project MinE dataset.

		Project MinE Allele Frequency			Maltese Dataset	
Gene	dbSNP[155] ID	All	ALS cases	Controls	No. of ALS Patients	No. of Controls
ALS2	rs200706696	0.0000807	0.000115	0	1	0
ATXN2	rs1338140819	NA	NA	NA	1	0
ATXN2	rs771843383	NA	NA	NA	0	1
ATXN2	rs7969300	0.00492	0.00492	0.00491	0	1
CAPN14	rs181906086	0.00508	0.00481	0.00573	1	0
CCNF	rs36008785	0.000323	0.000458	0	0	1
CCNF	rs754766175	NA	NA	NA	0	1
DAO	rs781658657	NA	NA	NA	2	0
DCTN1	rs17721059	0.0179	0.0183	0.0169	1	0
DCTN1	rs55862001	0.00581	0.00561	0.00628	1	0
DCTN1	rs1328116832	NA	NA	NA	1	0
DDX20	NA	NA	NA	NA	1	0
DNAJC7	rs371236469	0.0000807	0.000115	0	1	0
ERBB4	rs76603692	0.00153	0.00126	0.00218	1	0
ERBB4	rs373685875	NA	NA	NA	1	0
ERBB4	rs371332509	NA	NA	NA	1	0
ERBB4	rs367568427	NA	NA	NA	0	1
EWSR1	NA	NA	NA	NA	1	0
EWSR1	rs41311143	0.0133	0.0132	0.0137	1	0
FIG4	NA	NA	NA	NA	0	1
GLE1	rs1564162129	NA	NA	NA	1	0
GLE1	rs150246404	0.000565	0.000687	0.000273	0	1
KIF5A	rs139801016	NA	NA	NA	1	1
MOBP	rs1188260744	NA	NA	NA	1	0
NEFH	rs530872313	NA	NA	NA	0	1
NEK1	rs1404362599	NA	NA	NA	1	0
NEK1	rs771824152	NA	NA	NA	0	1
SARM1	rs144613221	0.00363	0.00366	0.00355	1	0
SCFD1	rs61754480	0.00524	0.0055	0.00464	1	0
SCFD1	rs61754285	0.0196	0.0187	0.0218	2	0
SETX	rs906452681	0.0000807	0	0.000273	1	0
SETX	rs151117904	0.00581	0.00653	0.00409	1	0
SETX	rs200856903	NA	NA	NA	1	1
SETX	rs750959420	0.0000807	0.000115	0.00	1	0
SPG11	rs758046989	NA	NA	NA	1	0
SPG11	rs139687202	0.000323	0.000344	0.000273	1	0
SPG11	rs111347025	0.0175	0.0173	0.018	1	0
SPG11	rs200573434	0.00202	0.00218	0.00164	1	0
SPG11	rs76116949	NA	NA	NA	1	0
SPG11	rs141818132	NA	NA	NA	1	0
SPG11	rs201082396	0.0000807	0.000115	0	1	0
SPG11	rs543316224	NA	NA	NA	0	1
SS18L1	rs36106901	0.00105	0.00126	0.000546	2	2
TIA1	rs116621885	0.00766	0.0087	0.00519	1	1
TNIP1	rs2233289	NA	NA	NA	1	0
TNIP1	rs888695021	NA	NA	NA	0	1
TNIP1	rs369725837	0.000161	0	0.000546	1	0

dbSNP Single Nucleotide Polymorphism database, **NA** not available.

3.7 FUNCTIONAL CHARACTERIZATION OF ALS-LINKED GENES

3.7.1 *DCTN1*

3.7.1.1 Location of *DCTN1* rare non-synonymous variants identified in Maltese ALS patients

Three rare non-synonymous variants that were exclusive to ALS patients in the Maltese cohort, were associated with the *DCTN1* gene. The *DCTN1* gene is located on chromosome 2 (2L:74361154-74380355) and produces a transcript that has 32 exons, encoding for a 20kb protein of 1279 amino acids, making it the largest dynactin subunit (**Figure 3.31**). DCTN1 is mainly composed of two central coiled coils. The short coiled-coil contains a CAP-Gly motif and forms the projecting arm of the protein at the N-terminus, whilst the long coiled-coil associates with another dynactin domain, Arp1 at the C-terminal. DCTN1 also provides a platform for the binding of multiple proteins, especially microtubule-binding proteins (SCHROER 2004). The NM_004082.4:c.586A>G; p.(I196V) *DCTN1* variant is located on exon 8 in the FAM76 protein region, whilst the NM_004082.4:c.1484G>A; p.(R495Q) variant is inserted at the CCDC144C coiled-coil region on exon 14. Both these variants are not indicated to have disease causing potential by *in silico* methods. The NM_004082.4:c1864A>T; p.(I622F) *DCTN1* variant, predicted to be damaging, is located on exon 17 within the dynactin dynein associated protein region. Several studies have reported that functional abnormalities of the molecular motor dynein as a result of disturbed interaction with the dynactin complex contribute to a motor neuron disease phenotype that in most cases is linked to impairment of axonal transport (LAMONTE *et al.* 2002; IKENAKA *et al.* 2012). The damaging heterozygous variant *DCTN1* c.1864A>T was verified by Sanger sequencing analysis (**Figure 3.32**). It was identified in a female patient (MND11) who developed bulbar onset ALS at the age of 51, which progressed with marked weight loss and upper limb muscle weakness. The patient died of respiratory arrest, 3 years after symptom onset.

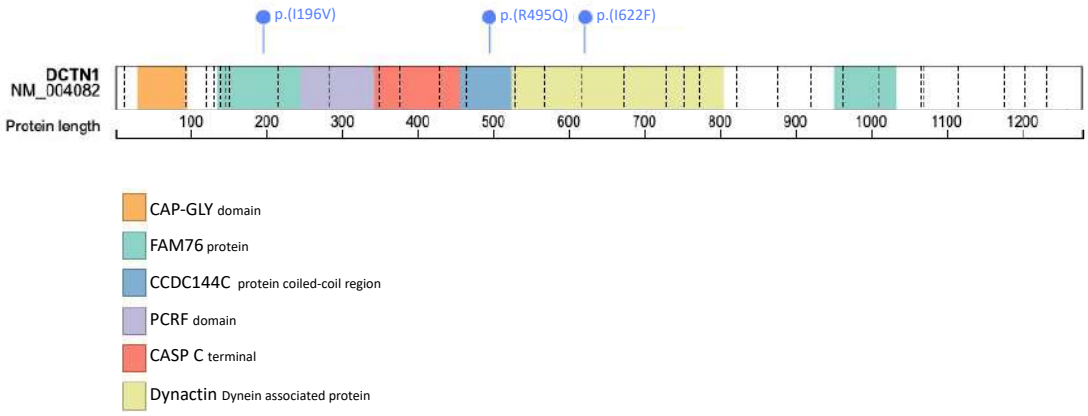

Figure 3.31 Location of *DCTN1* rare variants found in Maltese ALS patients. Rare variants identified in Maltese ALS patients are present in the FAM76 protein region, the CCDC144C coiled-coil region and in the dynein associated protein region of the DCTN1 domain. Visualization of genetic mutations was achieved using the ProteinPaint web application (ZHOU *et al.* 2016).

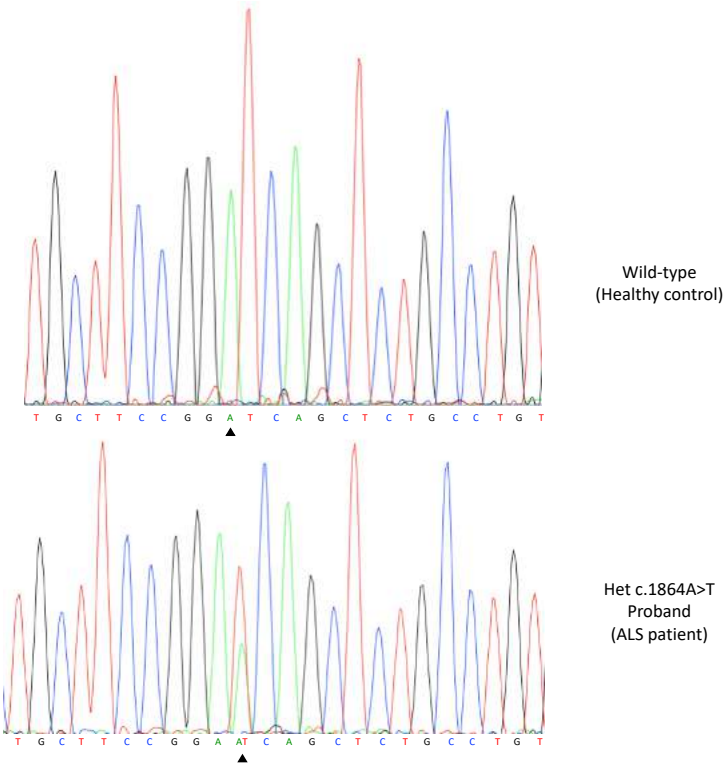

Figure 3.32 Sanger sequencing verification of the damaging heterozygous *DCTN1* c.1864A>T variant. The proband shows a mutation in the 1864th base resulting in adenine substituted into thymine. Interpretation of sequencing chromatograms was achieved using the 4peaks (A. Griekspoor and Tom Groothuis, Nuclobytes B. V., nucleobytes.com) software.

3.7.1.2 *Drosophila* orthologues of *DCTN1*

Drosophila is thought to have 2 orthologues of *DCTN1*, including *DCTN1-p150* (*CG9206*) that shares 32% identity (similarity, 55%) to the human polypeptide sequence (**Figure 3.33**) and *CG9279* that matches the human sequence by 24% (similarity, 41%) (**Figure 3.34**) (DIOPT - https://www.flyrnai.org/diopt). Both *Drosophila* genes are located on chromosome 3 and have 4 exons. *DCTN1-p150* encodes a 141.2 kDa protein of 1265 amino acids and *CG9279* encodes a 152.5 kDa protein of 1399 amino acid residues. A number of *Drosophila*-based studies, particularly those involving the DCTN1-p150, have demonstrated that the role of *DCTN1* in microtubule-dependent cargo trafficking is essential for axonal transport (McGrail *et al.* 1995; Pilling *et al.* 2006; Haghnia *et al.* 2007). In this study both orthologues were characterized to determine the effect of knockdown of either protein on viability and motor function in the fly model, to better understand the functional role of *DCTN1* in relation to motor neuron degeneration in ALS.

3.7.1.3 Global knockdown and expression of *DCTN1-p150* and *CG9279*

Alterations in viability in response to ubiquitous knockdown was assessed by means of the *UAS*-GAL4 system, specifically using ubiquitously expressing drivers combined with RNAi lines. *DCTN1* gene expression was then analyzed by qPCR to confirm knockdown specificity and efficiency. Ubiquitous depletion of CG9279 making use of the *da*-GAL4 or *Act*-GAL4 drivers was achieved by expressing two UAS-*RNAi* transgenes: CG9279-IR^{ME9} that targets exon 3 and *CG9279*-IR^{ME10} that targets exon1, which encodes for the CAP-Gly domain (**Figure 3.35A**). Both transgenes did not appear to induce adult viability defects and an increase in temperature-dependent transgene expression did not alter this effect (**Figure 3.35B**). Quantitative RT-PCR on mRNA obtained from larvae having ubiquitous knockdown through the CG9279-IR^{ME9} RNAi transgene demonstrated an average 29% reduction in CG9279 expression. On the other hand, knockdown by *CG9279*-IR^{ME10} resulted in a mean *CG9279* gene expression of 23.3% relative to the control, thus a reduction of 76.7% (**Figure 3.35C**). The *UAS-RNAi*

transgene *DCTN1-p150-IR^{ME18}*, targeting exon 3 of the *DCTN1-p150* mRNA transcript (**Figure 3.35A**), was activated by the driver *Act*-GAL4 to induce ubiquitous knockdown of *DCTN1-p150*. This severely affected fly viability, resulting in lethality at the larval stage at an incubation temperature of 25^{o}C. This suggests that the *DCTN1-p150* gene is essential for adult fly viability. A strong reduction (80%) of *DCTN1-p150* was achieved by ubiquitous expression of RNAi transgene *DCTN1-p150-IR^{ME18}* (**Figure 3.35C**).

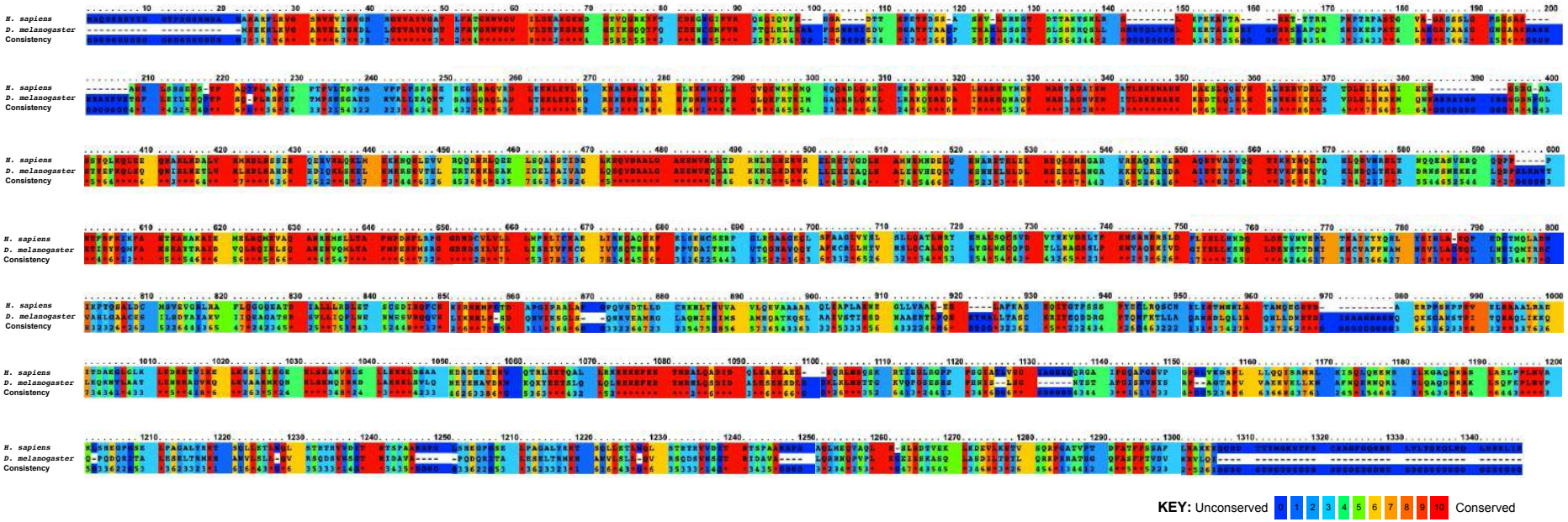

Figure 3.33 Sequence alignment of human DCTN1 and the *Drosophila* DCTN1-p150 orthologue. Alignment was achieved using PRofile ALIgNEment (PRALINE) multiple sequence alignment toolbox that employs a profile-profile multiple alignment approach based on database searching that collects homologues for each sequence in a given set. Conservation levels are displayed by a colour scheme according to the colour key (SIMOSSIS AND HERINGA 2005; SIMOSSIS *et al.* 2005). Consistency among a set of sequences is measured *via* library generation and library extension, increasing alignment accuracy (PEI *et al.* 2003).

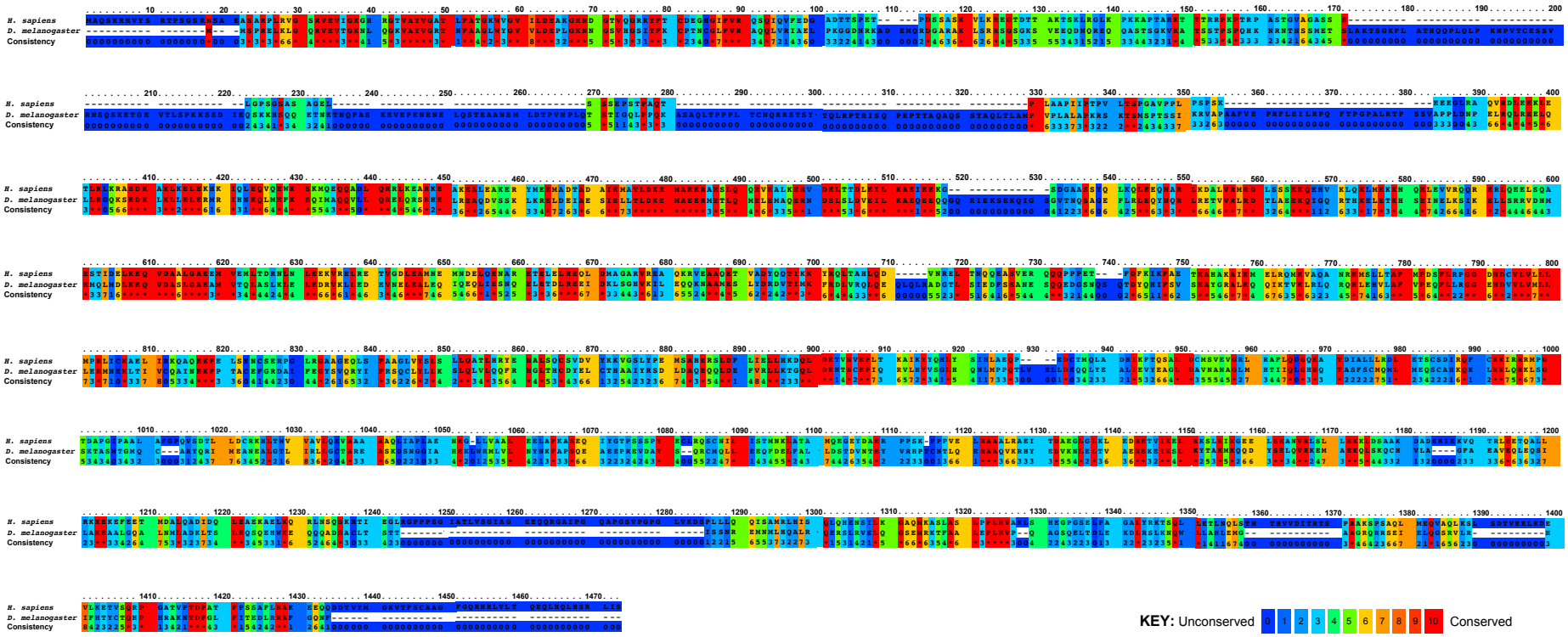

Figure 3.34 Sequence alignment of human DCTN1 and the *Drosophila* CG9279 orthologue. Alignment was achieved using PRofile ALIgNEment (PRALINE) multiple sequence alignment toolbox that employs a profile-profile multiple alignment approach based on database searching that collects homologues for each sequence in a given set. Conservation levels are displayed by a colour scheme according to the colour key (SIMOSSIS AND HERINGA 2005; SIMOSSIS *et al.* 2005). Consistency among a set of sequences is measured *via* library generation and library extension, increasing alignment accuracy (PEI *et al.* 2003).

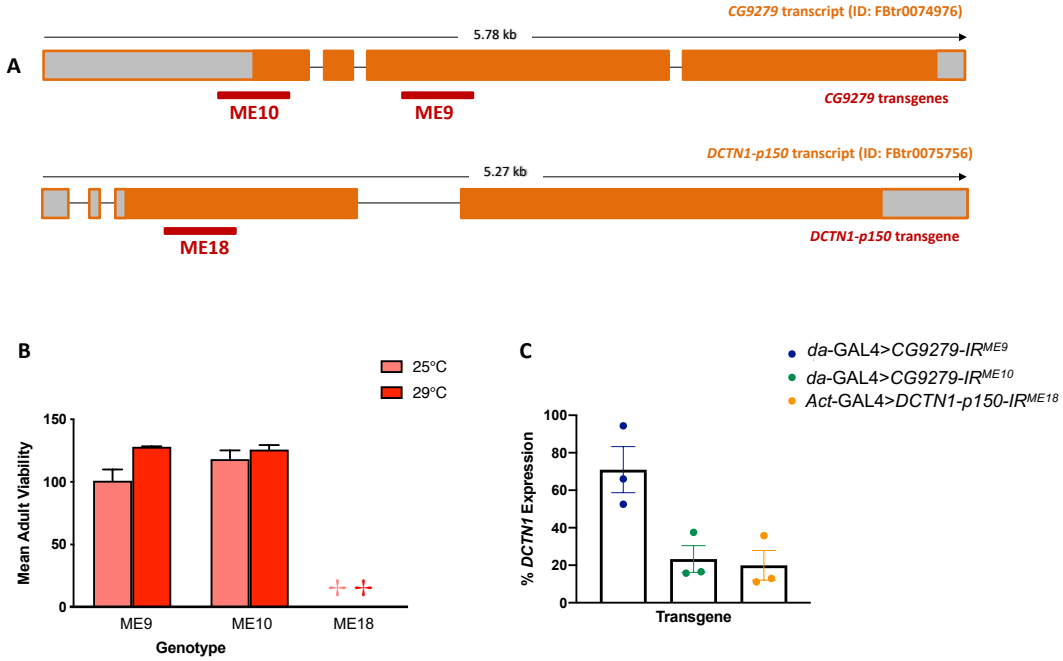

Figure 3.35 Ubiquitous knockdown of *Drosophila DCTN1* orthologues *CG9279* and *DCTN1-p150*. (**A**) Transcript of *Drosophila DCTN1* orthologues, and location of transgenes. Orange boxes are coding sequences, grey boxes are untranslated regions (UTR) (HOWE *et al.* 2021). (**B**) *RNAi*-mediated downregulation of *CG9279* when expressing *DCTN1-IR*^{ME9} and *DCTN1-IR*^{ME10} transgenes in a ubiquitous pattern via *Act*-GAL4 driver does not depress adult viability, whilst knockdown of *DCTN1-p150* when expressing the transgene *DCTN1-IR*^{ME18} was lethal at larval stage. (**C**) Knockdown specificity and efficiency were assessed by quantitative RT-PCR analysis. Data presented in (B) and (C) are the mean ± S.E.M. For (B), statistical significance (p<0.05) was determined for differences between expression at 25°C and 29°C by the *t*-test.

3.7.1.4 Muscle-specific knockdown of *CG9279*

Considering that no repercussions on adult viability were observed upon ubiquitous depletion of CG9279, the effect of knockdown on lifespan and/or motor function was analyzed. Somatic muscular expression was achieved by muscle-specific GAL4 drivers and flies were subjected to flight and climbing assays. Flight performance was assessed by introducing flies at the top of the Droso-Drome apparatus and correlating flight capacity with consequent sector distribution (**Figure 3.36A**). Climbing performance was assessed by determining the time it takes for the first fly within a group to cross a predetermined

threshold. Climbing success was then measured by determining the total number of flies per group that can climb the pre-set mark in 10 seconds. Pan-muscular expression of *CG9279-IR^{ME10} via* the *Mef2*-GAL4 driver induced a subtle yet statistically significant difference in flight performance at late adulthood (day 35 post-eclosion), where a significant percentage of transgenic flies aggregated in the lowest sector of the Droso-Drome apparatus, hence flies were non-fliers. Flight was not impaired upon knockdown by *CG9279-IR^{ME9}* at any time point (**Figure 3.36B**). *CG9279-IR^{ME-10}*-induced knockdown in muscles had no effect on lifespan, as indicated by no significant difference in flies alive compared to controls at all time points, whereas a minor effect on survival was observed upon knockdown by *CG9279-IR^{ME9}* (**Figure 3.36C**).

Depletion of CG9279 in muscles had effects on climbing ability (**Figure 3.37**). On assessment, the first fly within the *Mef2*-GAL4>*CG9279-IR^{ME10}* fly population, took significantly longer to reach a pre-set target compared to controls after day 15 post-eclosion (**Figure 3.37A**). A significant decline in climbing success for the same population compared to controls, was only apparent after day 15 post-eclosion. Hence, an overall effect by genotype could not be detected in this assay (**Figure 3.37B**). Expression of *CG9279-IR^{ME9}* in muscles resulted in a significant difference in time for the first fly to reach a target height when compared to controls at all time points (**Figure 3.37C**). Consequently, a decline in climbing success was observed, particularly in the first two weeks post-eclosion (**Figure 3.37D**). Therefore, an overall highly significant genotype effect on climbing ability in both assays for this fly population was apparent (**Figure 3.37C, D**).

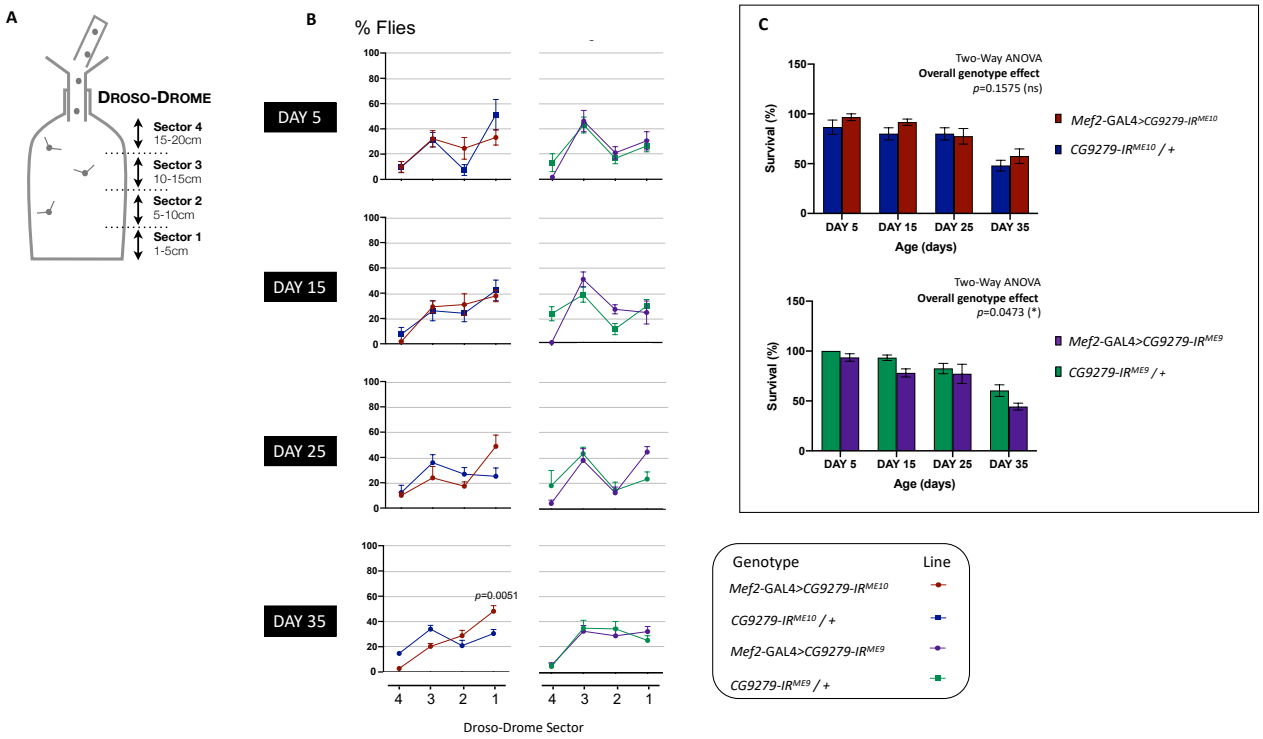

Figure 3.36 Effect of muscle-specific knockdown of *CG9279* on flight behaviour and lifespan. (**A**) Flight performance was assessed using the Droso-Drome apparatus, which quantifies flight defects according to which sector flies land after they are introduced at the top. (**B**) RNAi-mediated knockdown of *CG9279* with the pan-muscular *Mef2*-GAL4 driver does not alter flight ability at any time point except the last (day 35 post-eclosion), upon knockdown by *CG9279-IR*^{ME10} only. (**C**) Muscle-specific knockdown of *CG9279* had a minimal overall effect on survival compared to controls upon knockdown by *CG9279-IR*^{ME9}. Data presented are the mean ± S.E.M. for a minimum of 4 independent experiments, where n≥60 per genotype, per time-point. Significance was tested by the unpaired *t*-test (B) and Two-Way ANOVA, followed by Bonferroni's *post hoc* tests (C). When differences are statistically significant, the exact *p*-value is indicated.

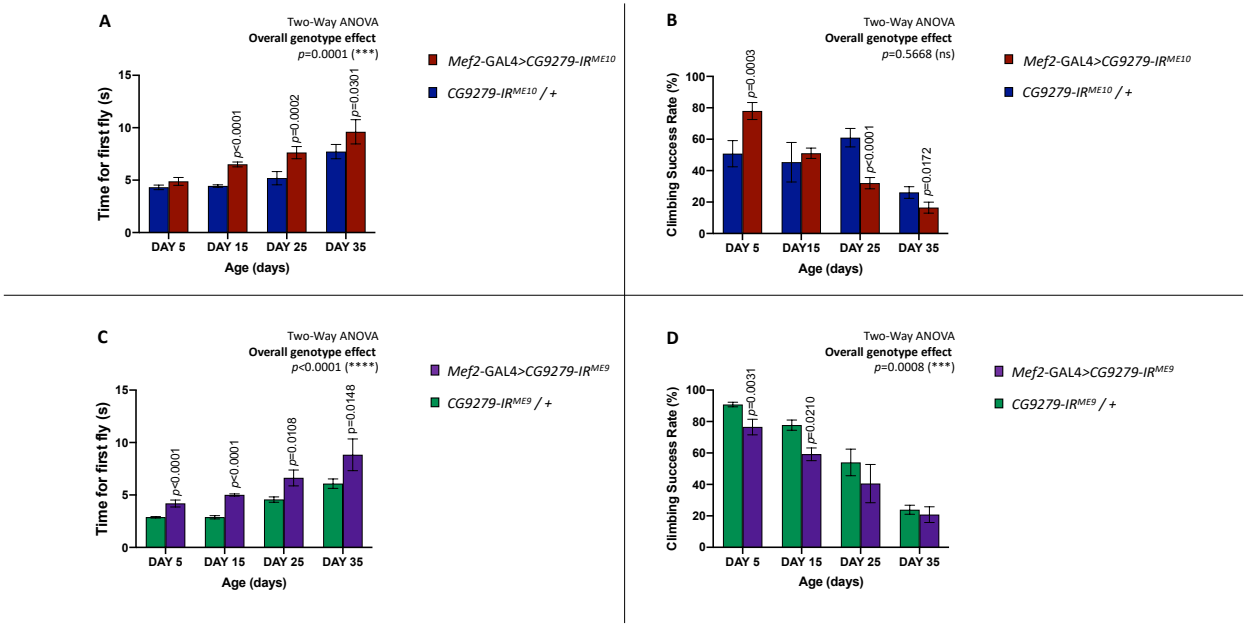

Figure 3.37 Effect of pan-muscular knockdown of *CG9279* on climbing ability. (**A**) Flies took significantly longer to reach a pre-set threshold after day 5 post-eclosion compared to controls, upon pan-muscular knockdown of *CG9279* by *Mef2*-GAL4>*CG9279-IR*^{ME10}. The overall genotype effect on this behaviour was significant. (**B**) A marked decline in climbing success for the same fly population was only observed after day 15 post-eclosion, resulting in a non-significant genotype effect. (**C**) In contrast to the control genotype, *Mef2*-GAL4>*CG9279-IR*^{ME9} flies took significantly longer to surpass a predetermined height across all age groups. (**D**) For the same genotype, a decline in climbing success was especially marked in the first two age groups. For both (C) and (D), a highly significant genotypic effect on both assays was detected. Data presented are the mean ± S.E.M. for a minimum of 4 independent experiments, where n≥60 per genotype, per time-point. Significance was tested by Two-Way ANOVA, followed by Bonferroni's *post hoc* tests. When differences are statistically significant, the exact *p*-value is indicated.

The effect of strong pan-muscular *CG9279* knockdown on mobility and lifespan was assessed *via* the *Mef2*-GAL4 driver in the presence of excess Dicer-2 (Dcr-2) levels, to determine whether enhanced RNAi levels exacerbate viability or locomotion phenotypes. When restricted to muscles, depletion of CG9279 *via* expression of *CG9279-IR^{ME10}* RNAi transgene resulted in severe flight defects as early as day 5 post-eclosion, with the majority of flies landing in sector 1 of the Droso-Drome (**Figure 3.38A**). For the same fly population, the percentage number of flies alive by day 15 post-eclosion was also significantly reduced from the previous time-point, and reductions in survival also occurred on the remaining time points of assessment (day 25 and day 35 post-eclosion. Hence, a significant overall genotype effect on adult survival could be detected (**Figure 3.38B**). When subjected to climbing performance assays, flies took significantly longer to reach a target height at all time points (**Figure 3.38C**), when compared to controls and consequently, no flies were able to surpass the pre-set height in time, resulting in a low percentage climbing success rate at all time points (**Figure 3.38D**). When restricted to muscles, enhanced *CG9279* knockdown *via* the *CG9279-IR^{ME9}* RNAi transgene, resulted in an insufficient number of viable progeny, with percentage viability being 16.7% ± 4.6 S.E.M., therefore, relevant adult functional assays could not be performed for this genotype. Preliminary results nonetheless show that there is a sex-difference in motor ability of 'escapers' with females having reduced flight and climbing capacity and males being apparently normal.

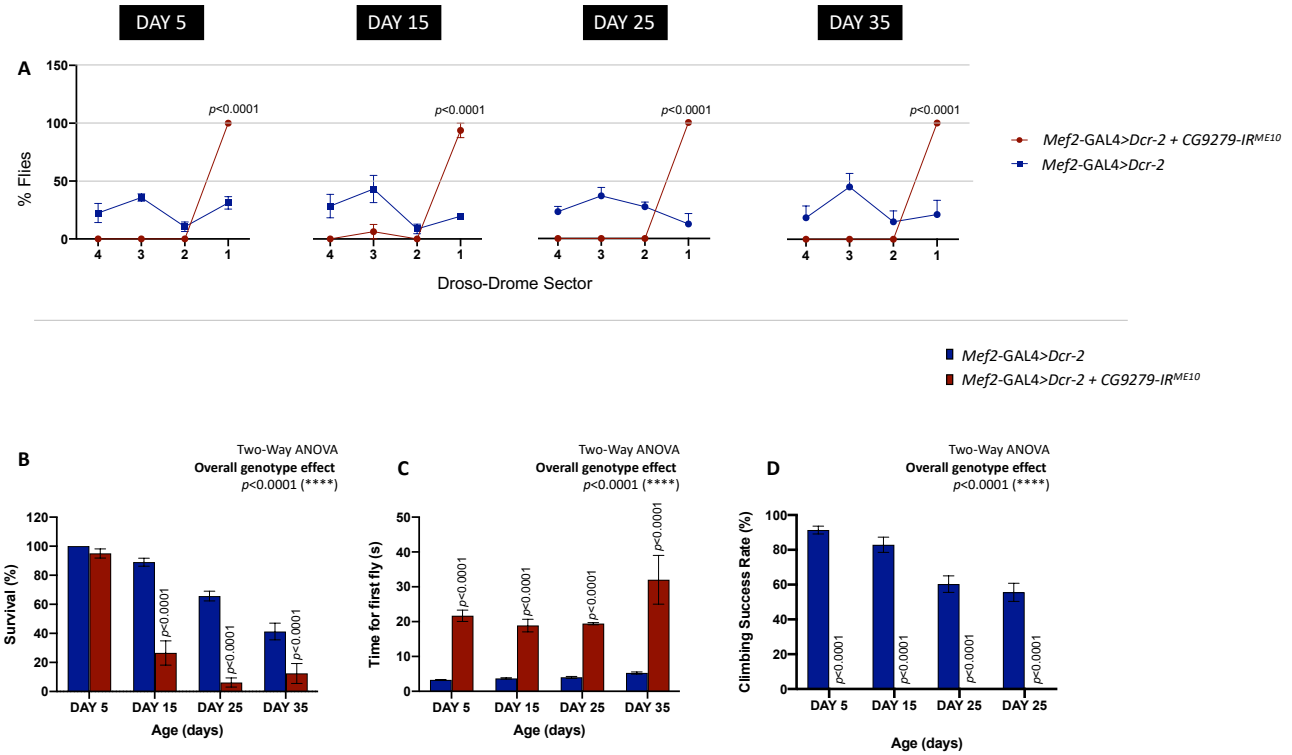

Figure 3.38 Enhanced knockdown of *CG9279* in muscles had a negative effect on flight performance and lifespan. (**A**) Severe flight defects were observed at a very early stage upon muscle-specific enhanced knockdown of *CG9279 via* the *CG9279-IR^{ME10}* RNAi transgene with the highest percentage of flies falling to sector 1 of the flight assay apparatus. This phenotype was also obvious on all the other time points assessed. (**B**) Pan-muscular *CG9279-IR^{ME10}*-induced knockdown also had a negative effect on lifespan, where the number of surviving flies was significantly reduced starting on day 15 post-eclosion, with reductions also experienced on day 25 and day 35 post-eclosion . (**C**-**D**) Compared to control genotypes, the time taken for the first fly to reach a predetermined threshold was significantly increased in early adult stages and in conjunction, climbing success was markedly reduced at all time points assessed, hence, overall genotype effect was statistically significant. Data presented are the mean ± S.E.M. for a minimum of 4 independent experiments, where n≥60 per genotype, per time-point. Significance was tested by the unpaired *t*-test (A) and Two-Way ANOVA, followed by Bonferroni's *post hoc* tests (B-D). When differences are statistically significant, the exact *p*-value is indicated.

3.7.1.5 Brain-selective knockdown of *CG9279*

Pan-neuronal *CG9279* knockdown was achieved *via* the *elav*-GAL4 driver in the presence of enhanced levels of Dicer-2 (Dcr-2) which maximizes RNAi knockdown. Reduced levels of *CG9279* in the brain did not impair the flying ability of flies at any time point for both *elav*-GAL4>*Dcr-2 + CG9279-IR*^{ME10} and *elav*-GAL4>*Dcr-2 + CG9279-IR*^{ME9} fly populations. Indeed, no significant differences were observed between both groups and the corresponding control populations in the number of flies that had no flight ability (sector 1) compared to those that retained the ability to fly (sectors 2-4) (**Figure 3.39A**). In addition, RNAi-mediated knockdown of *CG9279* had no effect on survival since the difference in percentage number of flies alive compared to control and across each time point was not significant (**Figure 3.39B**).

When assessed for climbing ability, flies with enhanced expression of *CG9279-IR*^{ME10} RNAi transgene in the brain took significantly longer to reach a prespecified threshold compared to the control genotype only at day 15 and day 35 post-eclosion, hence overall genotype effect was non-statistically significant. (**Figure 3.40A**). For the same fly population, a decline in climbing success was also observed at day 15 and day 35 post-eclosion compared to controls. Since the difference between genotypes at these timepoints was sizeable, an overall genotype effect was detected. (**Figure 3.40B**). The average time taken for the first fly to reach a pre-set height within the *elav*-GAL4>*Dcr-2 + CG9279-IR*^{ME9} fly population, was significantly longer than that displayed by controls in all age groups (**Figure 3.40C**). Consequently, climbing success rate was drastically reduced compared to controls at all time points (**Figure 3.40D**). As a result, an overall statistically significant genotype effect was observed for both climbing performance assays upon intensified pan-neuronal expression of *CG9279-IR*^{ME9} was significant (**Figure 3.40 C-D**).

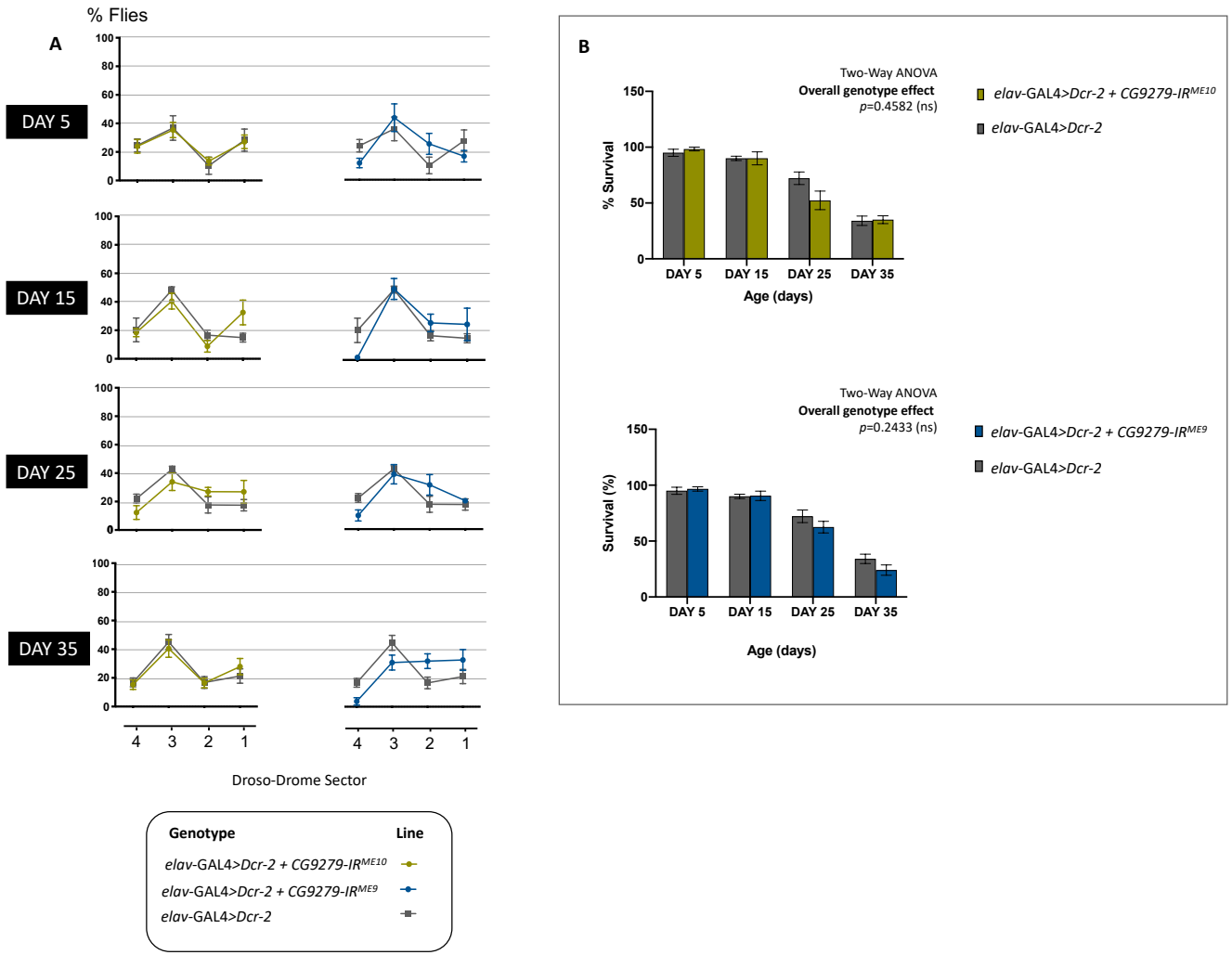

Figure 3.39 Effect of brain-specific knockdown of *CG9279* on flight ability and lifespan. (**A**) Low levels of CG9279 in neurons do not alter flight performance at any time point. (**B**) Survival, as indicated by percentage of living flies at each time point, was also not significantly affected by pan-neuronal knockdown of *CG9279*. Data presented are the mean ± S.E.M. for a minimum of 4 independent experiments, where n≥60 per genotype, per time-point. Significance was tested by the unpaired *t*-test (A) and Two-Way ANOVA, followed by Bonferroni's *post hoc* tests (B). When differences are statistically significant, the exact *p*-value is indicated.

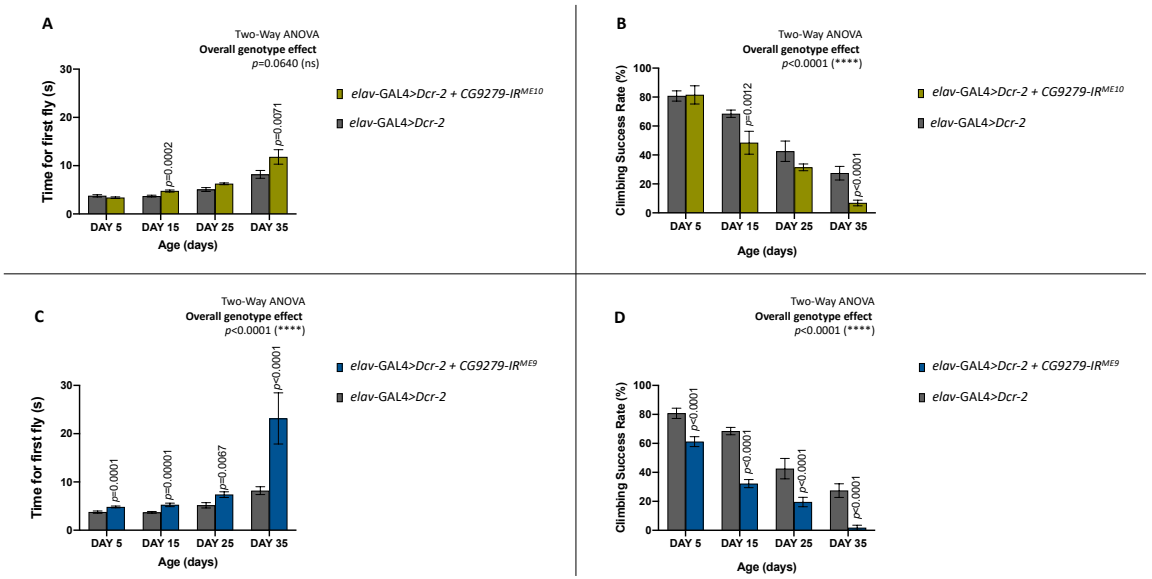

Figure 3.40 Effect of brain-selective CG9279 reduction on climbing ability. (**A**) On day 15 and day 35 post-eclosion, flies took significantly longer to reach a pre-set threshold upon enhanced pan-neuronal knockdown by *CG9279-IR^{ME10}* compared to controls. An overall genotype effect could not be detected. (**B**) For the same population, climbing success rate was drastically reduced in contrast to the control genotype on both day 15 and day 35 of adulthood. A highly statistically significant overall genotype effect was apparent for this assay. (**C**) Neuron-restricted enhanced expression of *CG9279-IR^{ME9}* resulted in flies that took significantly longer to reach a pre-set threshold when compared to controls, at all age groups. A marked overall genotype effect can be detected. (**D**) A significant decrease in the total percentage number of flies that reached the pre-set threshold within a specified timeframe was observed for the same genotype when compared to control flies, across all time points. A significant overall genotype effect was observed. Data presented are the mean ± S.E.M. for a minimum of 4 independent experiments, where n≥60 per genotype, per time-point. Significance was tested by Two-Way ANOVA, followed by Bonferroni's *post hoc* tests. When differences are statistically significant, the exact *p*-value is indicated.

3.7.1.6 Tissue specific knockdown of *DCTN1-p150*

A strong reduction of *DCTN1-p150* in all tissues through *Act*-GAL4-driven RNAi transgenic expression resulted in lethality at the larval stage. To determine whether a requirement for adult viability is due to a function within the neuromuscular system, *DCTN1-p150* knockdown was restricted to muscles or motor neurons and motor function was assessed. Enhanced, muscle-specific knockdown achieved by the *Mef2*-GAL4 driver in the presence of excess Dicer-2, impaired flight as early as day 5 post-eclosion compared to controls, leading to flies that are entirely flightless (**Figure 3.41A**). No significant decline in lifespan occurred in the first two weeks post-eclosion (**Figure 3.41B**). Depletion of DCTN1-p150 in muscles led to climbing defects in adult flies assessed at day 5 and day 15 of adulthood. In effect, climbing assessment determined that flies with low levels of DCTN1-p150 in muscles, took significantly longer to reach a pre-set threshold in contrast to the control genotype (**Figure 3.41C**). Furthermore, a severe decline in climbing success rate was also observed (**Figure 3.41D**). As expected, an overall genotype effect was detected for both climbing assays (**Figure 3.41 C-D**).

Brain-specific DCTN1-p150 depletion *via* the *elav*-GAL4 driver in the presence of excess levels of Dicer-2, did not give rise to the same flight defects observed on muscle-specific depletion (**Figure 3.42**). No significant difference in the percentage number of flies in each sector of the Droso-Drome device was observed, when compared to controls. Conversely, a significant progressive decline in lifespan was observed with age (**Figure 3.42B)**. Moreover, knockdown of *DCTN1-p150* in the neurons induced climbing defects which were absent in controls (**Figure 3.42 C-D**). For each age group, the average time for the first fly to reach a predetermined threshold was significantly longer than that for controls. Climbing defects were also evident upon assessment of climbing success rate. The percentage number of flies which were able to surpass a target height in a specified time frame was significantly lower, in contrast to the control genotype across all age groups. An overall genotype effect could be detected for survival and motor ability (**Figure 3.42 B-D**).

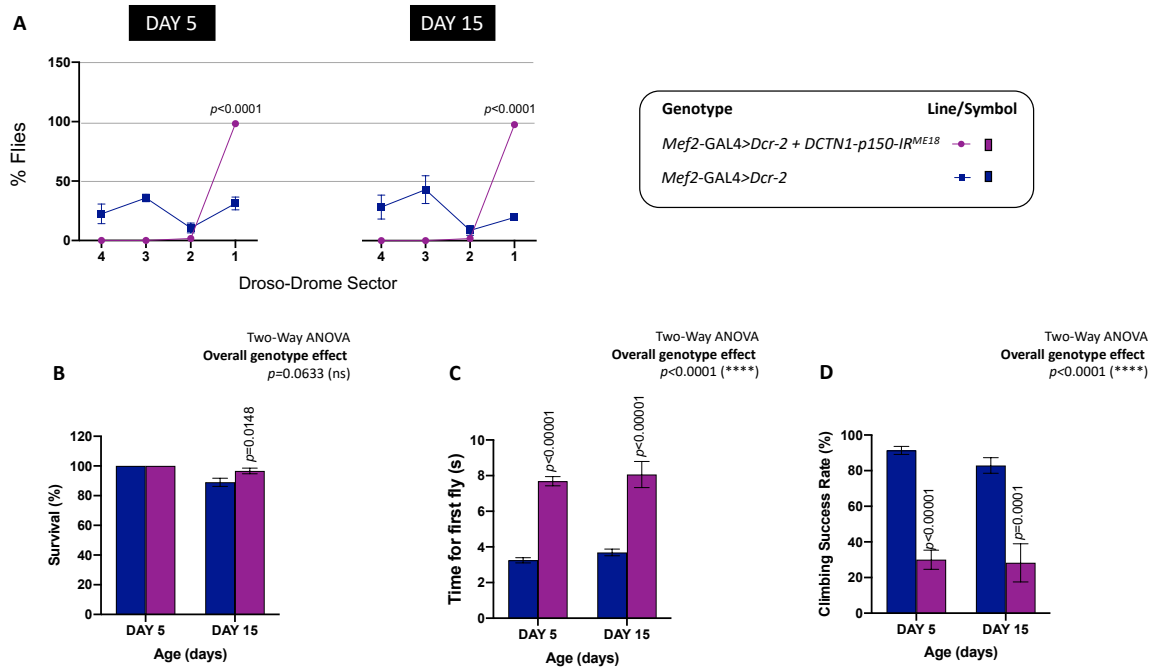

Figure 3.41 Muscle-specific knockdown of *DCTN1-p150* led to severe mobility defects. (**A**) Low levels of DCTN1-p150 in muscles resulted in flightless flies at an early adult stage. (**B**) Survival, as indicated by the percentage of live flies over time, was however, not significantly impaired by pan-muscular depletion of DCTN1-p150. (**C**) When restricted to muscles, *DCTN1-p150* knockdown led to adult flies with climbing disabilities. On assessment, the first fly took significantly longer to reach a target height compared to controls. (**D**) At a population level, climbing success was relevantly reduced. For both (C) and (D) an overall genotype effect on motor ability was detected Data presented are the mean ± S.E.M. for a minimum of 4 independent experiments, where n≥60 per genotype, per time-point. Significance was tested by the unpaired *t*-test (A) and Two-Way ANOVA, followed by Bonferroni's *post hoc* tests (B-D). When differences are statistically significant, the exact *p*-value is indicated.

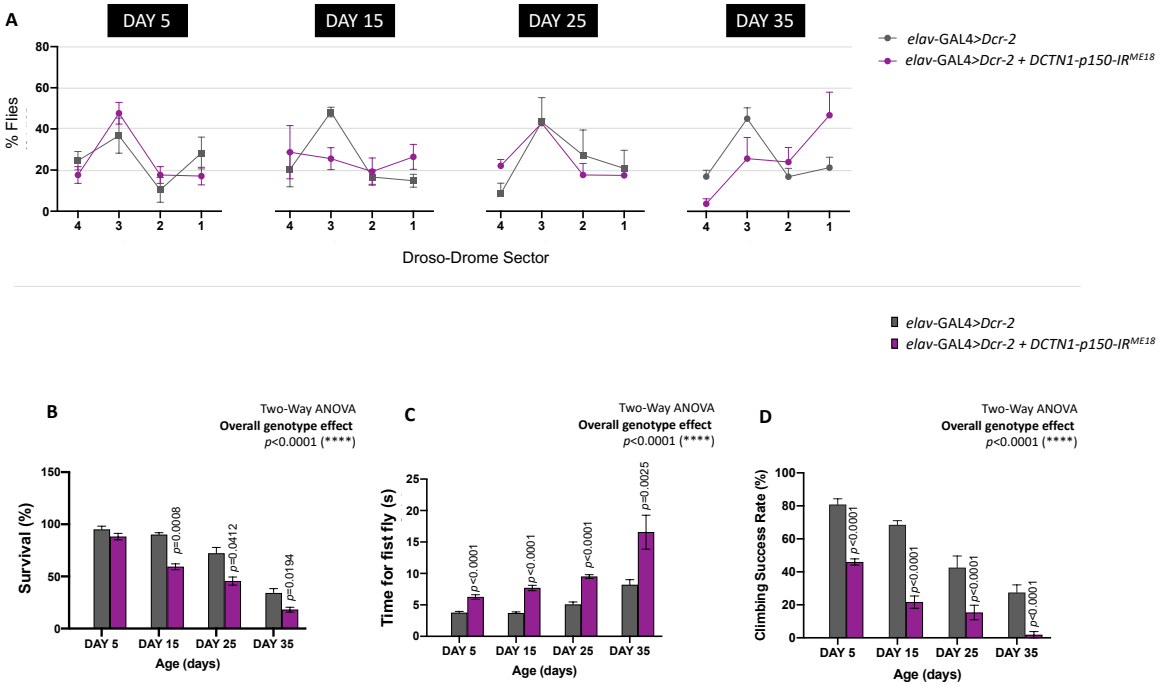

Figure 3.42 Decreased levels of DCTN1-p150 in neurons had a negative effect on lifespan and climbing performance. (A) Neural knockdown of *DCTN1-p150* had no effect on flight performance across all age groups. (**B**) Distinctly, a progressive decline in lifespan was observed (**C**) Assessment of the time taken for the first fly to exceed a specific threshold showed that flies took significantly longer to reach the target in contrast with the control genotype. (**D**) The climbing success rate for the experimental genotype was profoundly reduced when compared to the corresponding controls. (B-D) An overall genotype effect on survival and motor function was detected. Data presented are the mean ± S.E.M. for a minimum of 4 independent experiments, where n≥60 per genotype, per time-point. Significance was tested by the unpaired *t*-test (A) and Two-Way ANOVA, followed by Bonferroni's *post hoc* tests (B-D). When differences are statistically significant, the exact *p*-value is indicated.

3.7.2 *SCFD1*

3.7.2.1 Location of *SCFD1* rare non-synonymous variants identified in Maltese ALS patients

Several genome-wide studies have implicated *SCFD1* as a significant genetic modifier of ALS (VAN RHEENEN *et al.* 2016; CHEN *et al.* 2018). In the Maltese population, two SNPs within this locus were identified in ALS patients only. The human *SCFD1* gene, which is located on chromosome 14 (14L:30622322-30737192), consists of 25 exons and encodes a 72 KDa protein of 639 amino acids. Both variants identified in Maltese ALS patients were found within the Sec1 domain, which is a prominent feature of the Sec1/Mun18 (SM) protein family that includes SCFD1. This family of proteins participates in membrane fusion events by associating with the soluble N-ethlymaleimide-sensitive factor attachment protein receptors (SNAREs) such as syntaxin (CARR AND RIZO 2010). For instance, *SCFD1* associates with Syntaxin 5 to mediate ER to Golgi transport (DASCHER AND BALCH 1996; ROWE *et al.* 1998; YAMAGUCHI *et al.* 2002).

The NM_016106.3:c.1297A>G; p.(T433A) *SCFD1* variant is located on exon 15 whilst the second variant identified, NM_016106.3:c.209T>C; p.(I70A) inserts at exon 3 and is predicted to have disease causing potential by *in-silico* methods (**Figure 3.43**). The latter was identified in a female patient (MND13) who primarily presented with bilateral lower limb weakness at the young age of 27. The patient is presently wheelchair bound and is able to communicate only *via* eye laser technology. The heterozygous c.209T>C mutation was verified by Sanger sequencing analysis. In addition, DNA samples of both the patient's parents, who do not suffer from MND or other linked disorders, were also sequenced to investigate the origin of the damaging variant (**Figure 3.44**). Interestingly, sequencing analysis confirmed that the I70T protein change was inherited from the paternal side, thus the mutation is not a *de novo* variant. Since the variant was also identified in the patient's father, an elderly healthy individual, the patient's genome was analyzed for rare non-synonymous variants and indels that were damaging or deleterious in all genes since these could

contribute to phenotype modification (**Table 17-18**). As a result, rare variant analysis in all the patient's genome revealed a collection of genes with a role in pathways that are associated with neurodegeneration. These include transcription regulation, protein homeostasis, cytoskeletal organization, cell signaling and transport, DNA repair, as well as neural development and maintenance. Furthermore, the implication of some of these loci in other motor neuropathies, which also result in progressive muscle weakness, is suggestive of a disease genetic overlap. These findings hint that neuromuscular dysfunction exhibited by the patient is a result of flaws in a spectrum of molecular mechanisms which might have been absent or not triggered in the patient's father. Nonetheless, absence of variants within these loci in the parental genome needs to be verified in the future.

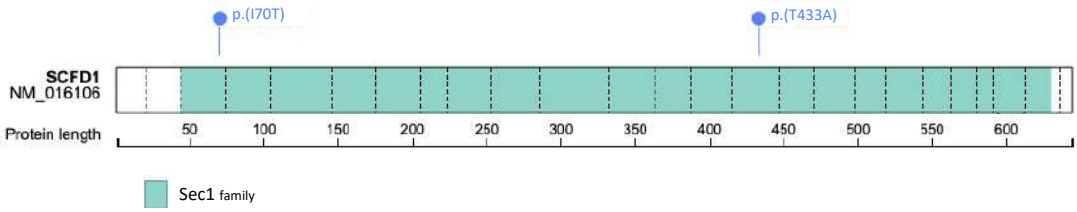

Figure 3.43 *SCFD1* rare variants identified in Maltese ALS patients. The *SCFD1* transcript has 25 exons and encodes a 642 amino acid protein that forms part of the Sec1/Mun18 protein family. A rare SNV identified in the ALS-associated locus does not have disease causing potential and is located on exon 15, whilst a second variant located on exon 3 is likely pathogenic. Visualization of genetic mutations was achieved using ProteinPaint web application (ZHOU *et al.* 2016).

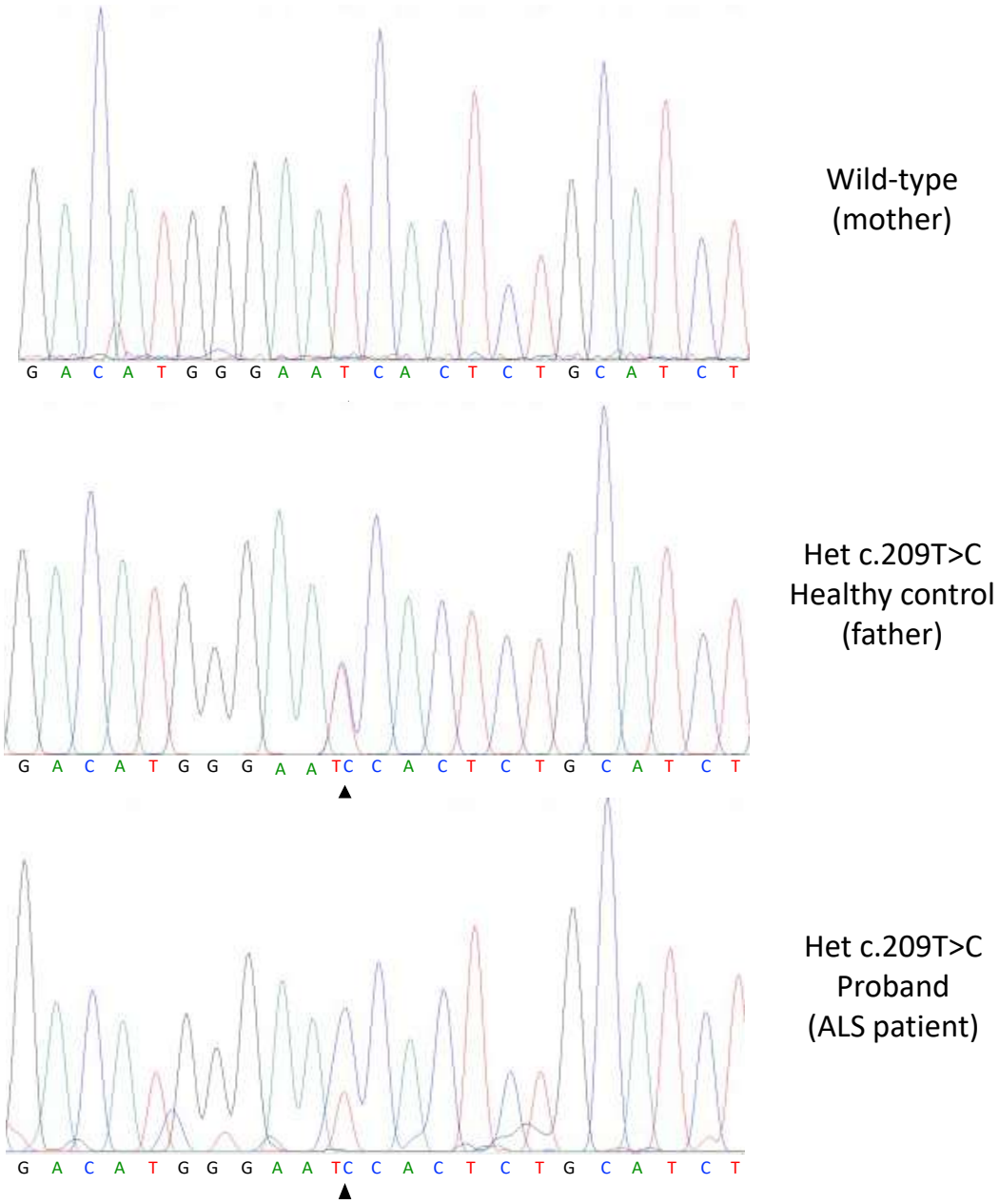

Figure 3.44 Sanger sequencing verification of the damaging heterozygous c.209T>C variant in *SCFD1*. The proband shows a variant in the 209th base resulting in isoleucine substituted into thymine. The same variant is absent in the patient's mother, but present in the father, indicating that the variant was inherited from the paternal side. Both parents are healthy individuals. Interpretation of sequencing chromatograms was achieved using the 4peaks (A. Griekspoor and Tom Groothuis, Nuclobytes B. V., nucleobytes.com) software.

Table 17 Rare, non-synonymous, damaging SNVs in non-ALS-associated genes of a Maltese ALS patient MND13.

Gene	Location	cDNA change	Protein change	dbSNP ID	European MAF	Biological Process	Associated disease
ABCB7	Xq13.3	NM_004299.4:c.13G>C	p.Ala5Pro	rs767573185	0.000006	Transmembrane transport	Spinocerebellar ataxia
ACAD10	12q24.12	NM_001136538.1:c.3248A>C	p.Lys1083Thr	rs746066481	0.000008	Oxidoreductase activity	Type II diabetes
C10orf12	10q24.1	NM_015652.2:c.692C>A	p.Thr231Asn	rs139845028	0	Ribostasis	-
CDKL4	2p22.1	NM_001009565.1:c.158G>A	p.Arg53His	rs35454041	0.0042	Proteostasis	Colorectal cancer
CFAP58	10q25.1	NM_001008723.1:c.1859G>A	p.Arg620His	rs181614354	0.003	Cell motility	Spermatogenic failure
CKAP5	11p11.2	NM_001008938.3:c.5734G>A	p.Val1912Met	rs565252536	0.00005	Cell division; RNA transport	-
COL4A4	2q36.3	NM_000092.4:/c.17T>C	p.Ile6Thr	rs16823264	0.002	Collagen fibril organisation	Alport syndrome (glomerulonephritis)
DNAH3	16p12.3	NM_017539.1:c.8346C>G	p.Ile2782Met	rs76979211	0	ATP binding; microtubule motor activity	Neurodegeneration
DNAH5	5p15.2	NM_001369.2:c.4542T>G	p.Phe1514Leu	rs761704400	0.000015	ATP binding; microtubule motor activity	Neurodegeneration
DSC1	18q12.1	NM_024421.2:c.1720G>A	p.Ala574Thr	rs777889677	0.00003	Cell-cell adhesion	Immune disease
EHMT1	9q34.3	NM_024757.4:c.1181A>C	p.Glu394Ala	rs773281152	0.000015	Chromatin oganisation	Mental retardation
ELMOD3	2p11.2	NM_001135021.1:c.949G>A	p.Glu317Lys	NA	NA	GTPase activator activity	Deafness
EPG5	18q12.3	NM_020964.2:c.4034A>G	p.His1345Arg	rs200456950	0.000141	Autophagy	Vici syndrome (agenesis, seizures, motor development delay)
EVC	4p16.2	NM_153717.2:c.284A>G	p.Asp95Gly	rs41269547	0.006	Smoothened signalling pathway	Skeletal dysplasia
FHAD1	1p36.21	NM_052929.1:c.296C>T	p.Pro99Leu	rs6679905	0	Ribostasis	-
GBE1	3p12.2	NM_000158.3:c.118C>A	p.Pro40Thr	rs35196441	0	Glycogen biosynthesis	Glycogen storage disease
GDF5	20q11.22	NM_000557.4:c.80G>T	p.Gly27Val	rs1167132767	0.000007	Cell signaling	Chondrodysplasia
GEMIN5	5q33.2	NM_015465.4:/c.3046C>T	p.Arg1016Cys	rs61749643	0.005	Ribostasis	Spinal Muscular Atrophy; ALS
IFT46	11q23.3	NM_020153.3:c.232C>T	p.Arg78Trp	rs142901726	0.003	Intrafragellar transport	-
KMT2C	7q36.1	NM_170606.2:c.9245C>T	p.Pro3082Leu	rs61730545	0.001	Ribostasis	Carcinoma
KPTN	19q13.32	NM_007059.3:c.631G>C	p.Gly211Arg	rs182019900	0	Actin filament organization	Mental retardation; Epilepsy
LAMB4	7q31.1	NM_007356.2:c.1054G>A	p.Gly352Ser	rs755316783	0.000024	Cell migration	Diverticulitis
MAGEC1	Xq27.2	NM_005462.4:c.2714C>T	p.Thr905Ile	rs149706249	0	Tumor-specific antigen	Melanoma

Table 17...Continued.

Gene	Location	cDNA change	Protein change	dbSNP ID	European MAF	Biological Process	Associated disease
MTNR1B	11q14.3	NM_005959.3:c.412C>T	p.Arg138Cys	rs61746674	0.004	Melatonin receptor activity	Type II diabetes
MYH15	3q13.3	NM_014981.1:c.3204G>C	p.Glu1068Asp	NA	NA	Cytoskeletal motor activity	ALS
NRN1L	16q22.1	NM_198443.1:c.266A>C	p.Glu89Ala	rs73593844	0.003	Neuron projection extension	-
OR2Z1	19p13.2	NM_001004699.2:c.403C>T	p.Leu135Phe	rs61746164	0	Olfactory transduction	-
OR52L1	11p15.4	NM_001005173.3:c.890G>A	p.Trp297*	rs186343423	0.008	Olfactory transduction	-
OR6C4	12q13.2	NM_001005494.1:c.248T>C	p.Met83Thr	rs11835716	0.002	Olfactory transduction	-
PEAR1	1q23.1	NM_001080471.1:c.813C>A	p.Asn271Lys	rs368846340	0.001	Platelet aggregartion	Cardiovascular disease
SDHD	11q23.1	NM_001276506.1:c.332C>T	p.Ala111Val	rs113458823	0	Mitochondrial electron transport	Paraganglioma
SERINC2	1p35.2	NM_001199038.1:c.353T>C	p.Phe118Ser	rs782415572	0.0001	Lipid metabolic process	Alcoholism; Carcinoma
SETD1B	12q34.21	NM_015048.1:c.2504C>T	p.Pro835Leu	rs764113442	0.00007	Transcription regulation	Neuroevelopmental disorder; Epilepsy; Seizures
SEZ6L2	16p11.2	NM_001243332.1:c.86C>G	p.Pro29Arg	rs1368859612	0.000007	Cell signaing	Cerebellar ataxia
SFRP5	10q24.2	NM_003015.3:c.652C>T	p.Arg218Trp	rs35379499	0	Cell signaing	Cardiovascular disease
SLC36A1	5q33.1	NM_078483.2:c.110C>T	p.Ser37Phe	rs1315258803	0.000004	Transmembrane transport	Spinocerebellar ataxia
SOX8	16p13.3	NM_014587.4:c.929C>A	p.Ala310Asp	rs1439790155	0.00001	Ribostasis; neural development	Cognitive disability in Thalassaemia; Hepatocellular carcinomas
TAF1C	16q24.1	NM_005679.3:c.1165C>T	p.Arg389Cys	rs140327311	0.003	Ribostasis	Pediatric neurodevelopmental disorder
TAS2R8	12p13.2	NM_023918.1:c.142C>T	p.Leu48Phe	rs74611066	0.007	Taste transduction	-
TM7SF3	12p11.23	NM_016551.2:c.536C>G	p.Pro179Arg	rs34735713	0	Proteostasis	Cohen syndrome (developmental delay, muscle hypotonia)
TMEM173	5q31.2	NM_198282.2:c.376C>A	p.Leu126Ile	rs142609349	0	Immune response	-
TNKS	8p23.1	NM_003747.2:c.2356C>T	p.Pro786Ser	rs764611012	0.000007	Cell division, vesicle trafficking	Lung carcinoma
TONSL	8q24.3	NM_013432.4:c.3910C>T	p.Arg1304Trp	rs1032777372	0.000008	DNA damage repair	Skeletal dysplasia
XIRP1	3p22.2	NM_194293.2:c.2576C>T	p.Pro859Leu	rs150942268	0.001	Actin filament organization	Muscular dystrophy
ZEB1	10p11.22	NM_001174096.1:c.1661A>G	p.Lys554Arg	rs35753967	0	Ribostasis; neuron differentiation	-
ZFYVE27	10q24.2	NM_001002261.3:c.79C>G	p.Pro27Ala	rs34979921	0	Vesicle trafficking; neuron projection development	Spastic paraplegia
ZNF362	1p35.1	NM_152493.2:c.157A>T	p.Ile53Phe	rs780102584	0.000008	Ribostasis	Duchenne muscular dystrophy

dbSNP Single Nucleotide Polymorphism database, **MAF** minor allele frequency, **NA** not available.

All damaging alleles identified are heterozygous with respect to the gene.

Table 18 Rare deleterious indels in non-ALS-associated genes of a Maltese ALS patient MND13.

Gene	Location	cDNA change	Protein change	dbSNP ID	European MAF	Biological Process	Associated disease
ADAMTS7	15q25.1	NM_014272.3:c.4069_4070ins	p.Lys1357_Gly1358fs	rs781638345	0.00359	Proteostasis	Coronery artery disease
ASCL4	12q23.3	NM_203436.2:c.510del	p.Glu170fs	rs201513808	0.005	Ribostasis	-
C8orf44	8q13.1	NM_019607.2:c.80del	p.Arg27fs	rs377182380	0.006	-	-
CABS1	4q13.3	NM_033122.3:c.309del	p.Thr103fs	NA	NA	Spermatogenesis	-
CNOT2	12q15	NM_001199302.1:c.1622_1623ins	NA	rs35192504	NA	Ribostasis	Intellectual developmental disorder
FAM209B	20q13.31	NM_001013646.3:c.110_111ins	p.Thr103fs	NA	NA	-	-
*FAM20C**	7p22.3	NM_020223.3:c.952_953ins	p.Asp318_Arg319fs	rs1554254768	0	Odontoblast differentiation	Raine syndrome (stenosis, cerebral calcifications)
GRTP1	13q34	NM_001286732.1:/c.924_925ins	p.Val308_Cys309fs	rs150462856	0.003	Cell transport	-
KLHL35	11q13.4	NM_001039548.2:c.201_226del	p.Arg67fs	rs756778027	0.00645	-	-
KLLN	10q23.31	NM_001126049.1:c.339_340del	p.Thr113fs	rs749052307	0.00259	Apoptosis	Cowden syndrome (hamartomas)
NMNAT1	1p36.22	NM_001297778.1:c.362del	p.Glu121fs	NA	NA	Neuron repair	-
OR6C4	12q13.1	NM_001005494.1:c.575_578del	p.Leu192fs	rs59693527	0	Olfactory transduction	-
SERPINA9	14q32.13	NM_175739.3:c.616del	p.Val206fs	rs74947133	0.002	Endopeptidase activity inhibitor	-
TAS2R46	12p13.2	NM_176887.2:c.259_260ins	p.Val87_Trp88fs	NA	NA	Taste transduction	-
TCN2	22q12.2	NM_000355.3:c.744del	p.Leu248fs	NA	NA	Ion transport	-
UNC5B	10q22.1	NM_170744.4:c.2461_2462ins	p.Ile821_Phe822fs	NA	NA	Axon guidance	Parkinson's disease
ZNF208	19p12	NM_007153.3:c.2731del	p.His911fs	rs752073888	0.000022	Ribostasis	Carcinoma
ZNF302	19q13.11	NM_001289188.1:c.398_428del	p.Ter133fs	NA	NA	Ribostasis	-
ZNF85	19p12	NM_001256171.1:c.1707_1708del	p.Thr569fs	NA	NA	Ribostasis	Thrombocytopenia

dbSNP Single Nucleotide Polymorphism database, **MAF** minor allele frequency, **NA** not available.

All deleterious indels identified except one detected in the gene *FAM20C* (*) are heterozygous with respect to the gene.

3.7.2.2 *Drosophila* orthologue of *SCFD1*

The *Drosophila* Slh polypeptide sequence shares 58% identity and 76% similarity to the human *SCFD1* gene product (DIOPT - https://www.flyrnai.org/diopt) (**Figure 3.45**). The *Drosophila Slh* transcript has 5 exons and encodes a protein of 639 amino acid residues and is located on chromosome 2 (2L:2488197-2492671). Similar to the human gene, *Slh* is predicted to have syntaxin binding activity and localizes to the Golgi-associated vesicle, cis-Golgi network and plasma membrane (LITTLETON 2000; D'AMBROSIO AND VALE 2010). The effect of abnormally low levels of Slh on viability and motor performance was assessed to clarify its functional role in *Drosophila*, in an attempt to study the implication of *SCFD1* on ALS pathophysiology.

3.7.2.3 Ubiquitous knockdown and expression of *Slh*

Target *UAS*-RNAi transgenes were used to determine alterations in viability, lifespan and motor function in response to ubiquitous or tissue-specific knockdown. Specifically, *Slh* RNAi-mediated knockdown was achieved by the expression of *Slh-IR^{ME2}*, *Slh-IR^{ME3}* and *Slh-IR^{ME4} via* the *UAS*-GAL4 system of tissue-specific drivers. The first RNAi transgene targets the second exon, whilst the last two target the 3'-UTR of the *Drosophila SCFD1* orthologue, *Slh* (**Figure 3.46A**). Ubiquitous depletion of Slh, accomplished by *Slh-IR^{ME2}* and *Slh-IR^{ME4} via Act*-GAL4 driver, did not affect adult viability and an increase in temperature-dependent transgene expression did not alter this outcome (**Figure 3.46B**). The expression of *Slh-IR^{ME3}* in all tissues, distinctly resulted in lethality at larval stage. Knockdown efficiency and specificity of *Slh* RNAi transgenes was verified by quantitative RT-PCR. The least efficient transgene, demonstrating a 21% reduction of Slh, was *Slh-IR^{ME4}*. *Slh* retained 45% expression when it was depleted in all tissues by *Slh-IR^{ME2}*, whilst a striking reduction of 97% was achieved by *Slh-IR^{ME3}*-mediated knockdown (**Figure 3.46C**). The powerful knockdown effect, resulting in a weak *Slh* gene expression of 3%, complement the adverse effect on viability seen when *Slh-IR^{ME3}* transgene is expressed globally.

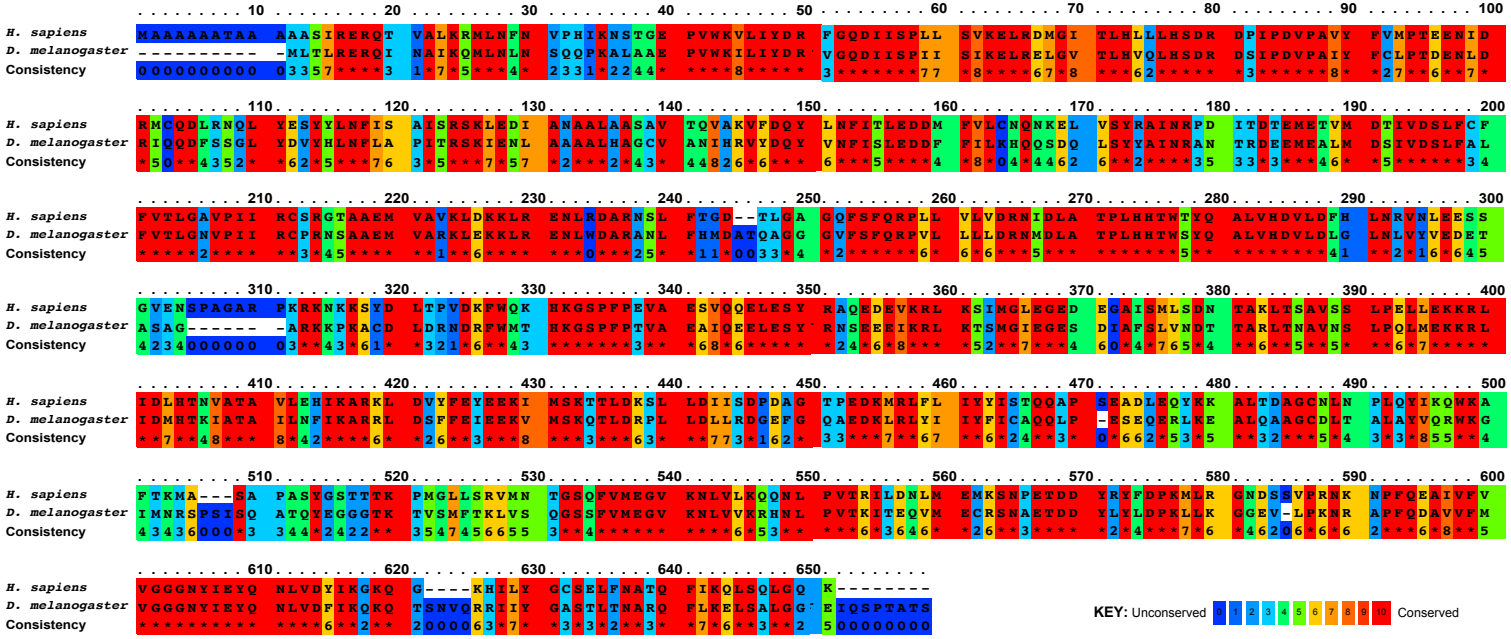

Figure 3.45 Sequence alignment of human SCFD1 and the *Drosophila* Slh orthologue. Alignment was achieved using PRofile ALIgNEment (PRALINE) multiple sequence alignment toolbox that employs a profile-profile multiple alignment approach based on database searching that collects homologues for each sequence in a given set. Conservation levels are displayed by a colour scheme according to the colour key (SIMOSSIS AND HERINGA 2005; SIMOSSIS *et al.* 2005). Homology is present throughout the entire length of the protein. Consistency among a set of sequences is measured *via* library generation and library extension, increasing alignment accuracy (PEI *et al.* 2003).

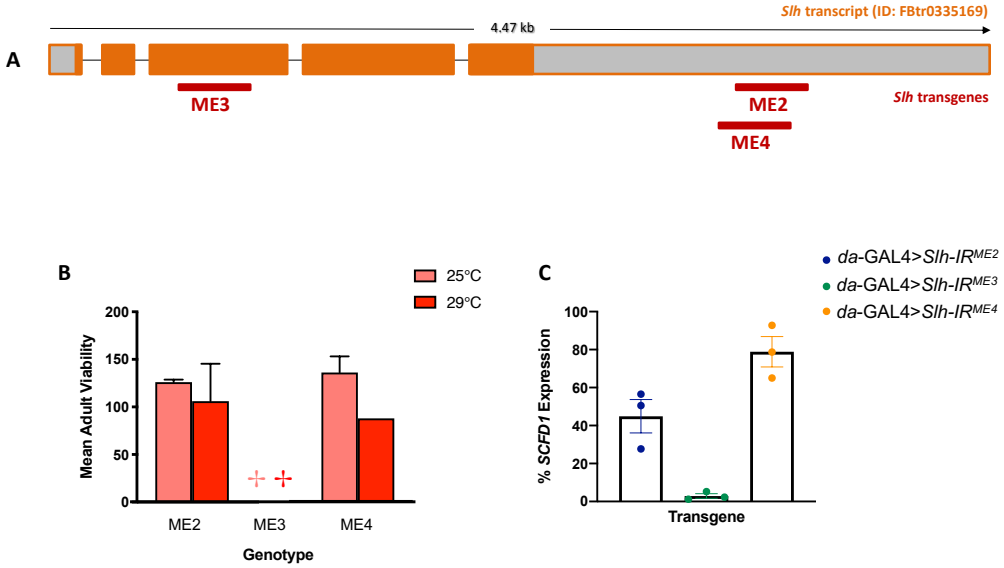

Figure 3.46 Ubiquitous knockdown of *Slh* in *Drosophila*. (**A**) *Slh* gene structure showing location of transgenes. Orange boxes are coding sequences, grey boxes are UTR (HOWE *et al.* 2021). (**B**) Depletion of Slh when *Slh-IR*^{ME2} and *Slh-IR*^{ME4} RNAi transgenes were expressed in a ubiquitous pattern *via Act*-GAL4 driver did not influence adult viability. Knockdown *via Slh-IR*^{ME3}, led to lethality at the larval stage. (**C**) Knockdown efficiency was assessed by quantitative RT-PCR analysis. Data presented are the mean ± S.E.M. Statistical significance was determined for differences between expression at 25°C and 29°C by the *t*-test.

3.7.2.4 Knockdown of *Slh* in muscles

Muscle-specific depletion of Slh was achieved by using the *Mef2*-GAL4 driver in the presence of excess levels of Dicer-2, for enhanced RNAi expression. When *Slh* knockdown was restricted to muscles by expression of *Slh-IR*^{ME2}, a marked decline in flight performance was observed at early adult stages, which advanced to entirely flightless flies by day 35 post-eclosion. In contrast, the difference between the percentage number of flies that fell to sector 1, the lowest sector of the Droso-Drome apparatus, and the other sectors was only significant in late adult stages upon pan-muscular expression of *Slh-IR*^{ME4} (**Figure 3.47A**). Lifespan was not negatively affected by low levels of Slh in muscles. At certain time points, the percentage number of viable flies with low levels of Slh was higher than that of the control genotype (**Figure 3.47B**). Climbing ability in the *Slh* transgenic

populations was significantly impaired. When *Slh* expression was reduced in muscles, flies exhibit an age-progressive decline in climbing ability compared to control populations. A highly statistically significant overall genotype effect on motor function could therefore be observed for flies expressing either *Slh-IR^{ME2}* or those expressing *Slh-IR^{ME4}* (**Figure 3.48 A-D**)

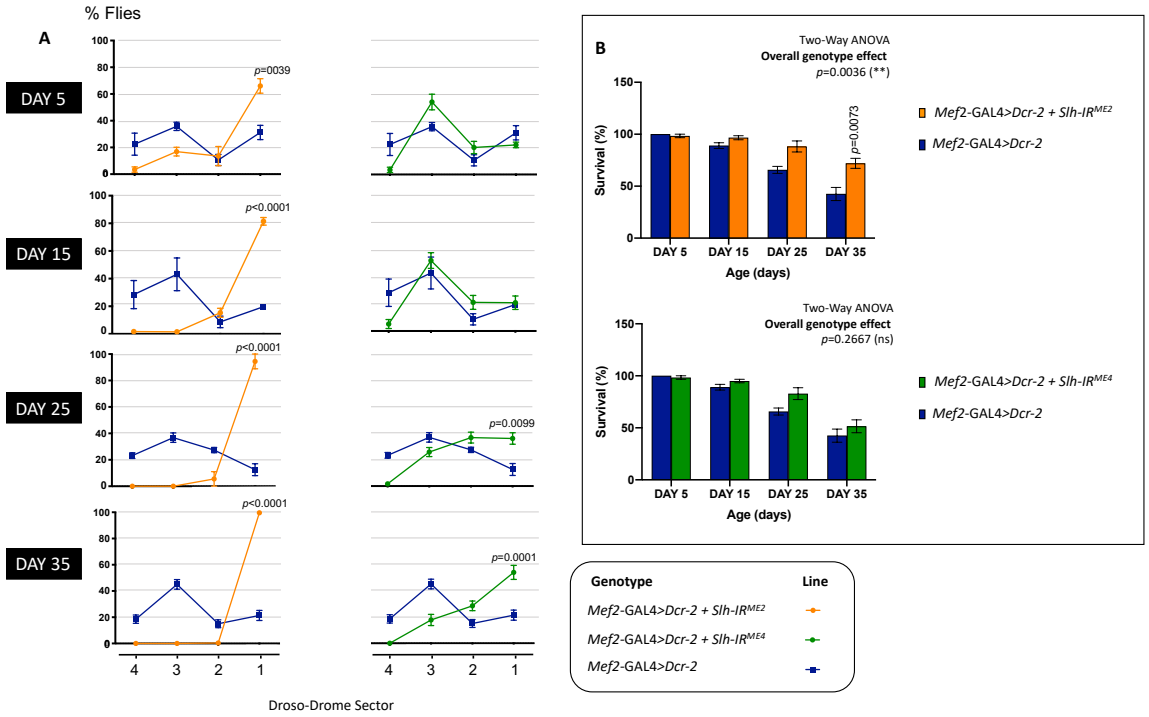

Figure 3.47 Effect of low levels of Slh in muscles on viability and motor behaviour. (**A**) RNAi-mediated knockdown of *Slh* perturbs flight ability at all time points upon muscle-specific knockdown by *Slh-IR^{ME2}*. *Mef2-Gal4>Dcr-2 + Slh-IR^{ME4}* flies exhibited severe flight defects only at late adult stages. (**B**) Slh deficiency in muscles had no significant negative effect on adult viability in relation to controls. Data presented are the mean ± S.E.M. for a minimum of 4 independent experiments, where n≥60 per genotype, per time-point. Significance was tested by the unpaired *t*-test (A) and Two-Way ANOVA, followed by Bonferroni's *post hoc* tests (B). When differences are statistically significant, the exact *p*-value is indicated.

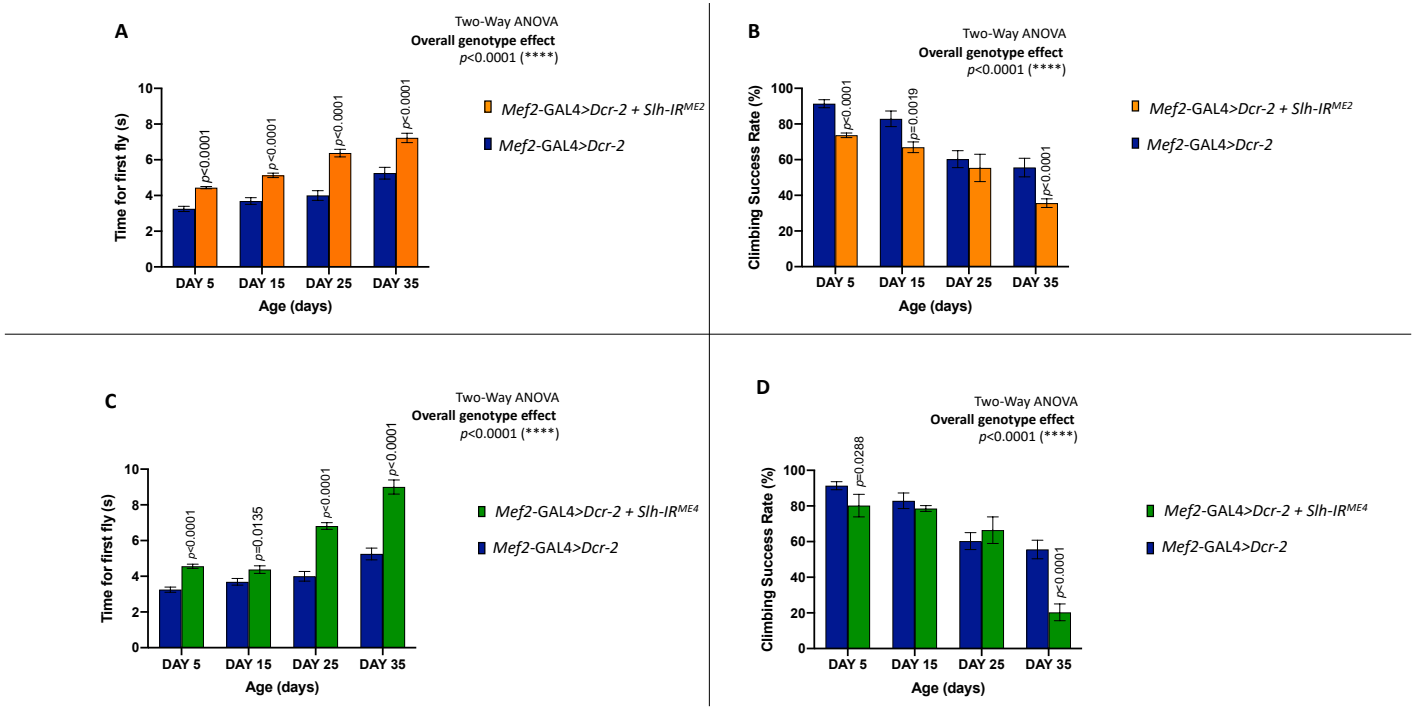

Figure 3.48 Effect of enhanced muscle-specific knockdown of *Slh* on climbing performance. (**A**) Flies with muscle-specific *Slh* knockdown *via* *Slh-IR*^{ME2}, took significantly longer to reach a predetermined threshold compared to control genotypes. (**B**) Climbing success was reduced in an age-progressive manner up to day 35 post-eclosion. (**C**) On RNAi-mediated muscle-specific knockdown of *Slh* by *Slh-IR*^{ME4} the first fly took significantly longer to reach a predetermined threshold compared to control flies at all time points assessed. (**D**) Climbing success for this genotype was affected on day 5 and day 35 post-eclosion. For (A-C), an overall genotype effect that was statistically significant was detected. Data presented are the mean ± S.E.M. for a minimum of 4 independent experiments, where n≥60 per genotype, per time-point. Significance was tested by the unpaired *t*-test (A) and Two-Way ANOVA, followed by Bonferroni's *post hoc* tests (B). When differences are statistically significant, the exact *p*-value is indicated.

3.7.2.5 Knockdown of *Slh* in the nervous system

To evaluate whether brain-specific *Slh* knockdown also leads to motor dysfunction, pan-neuronal expression of *Slh-IR^{ME2}* and *Slh-IR^{ME4}* was activated by the *elav*-GAL4 driver, enhanced by increased level of Dicer-2 for an amplified effect on protein depletion. No decline in flight performance was observed when Slh was reduced in the neuronal compartment of the neuromuscular system throughout all adult stages (**Figure 3.49A**). Furthermore, no significant difference in the percentage number of flies alive was evident, compared to controls indicating normal survival in the experimental genotypes compared to the control genotypes (**Figure 3.49B**). Evaluation of the climbing performance following neuronal restricted *Slh* knockdown, indicated that there was no overall genotype effect on the time it took for the first fly out of a population of flies to reach a target height (**Figure 3.50A, C**). Indeed, at several time points flies either took longer than controls or their performance was not different from that of controls. At a population level, a statistically significant overall genotype effect was observed for *elav-Gal4>Dcr-2 + Slh-IR^{ME2}* flies (**Figure 3.50B**) but not for *elav-Gal4>Dcr-2 + Slh-IR^{ME4}* flies (**Figure 3.50D**) when compared to controls. The most significant decline in climbing ability for flies with neuron-selective expression of *Slh-IR^{ME2}* was observed for day 15 and day 35 post-eclosion (**Figure 3.50B**).

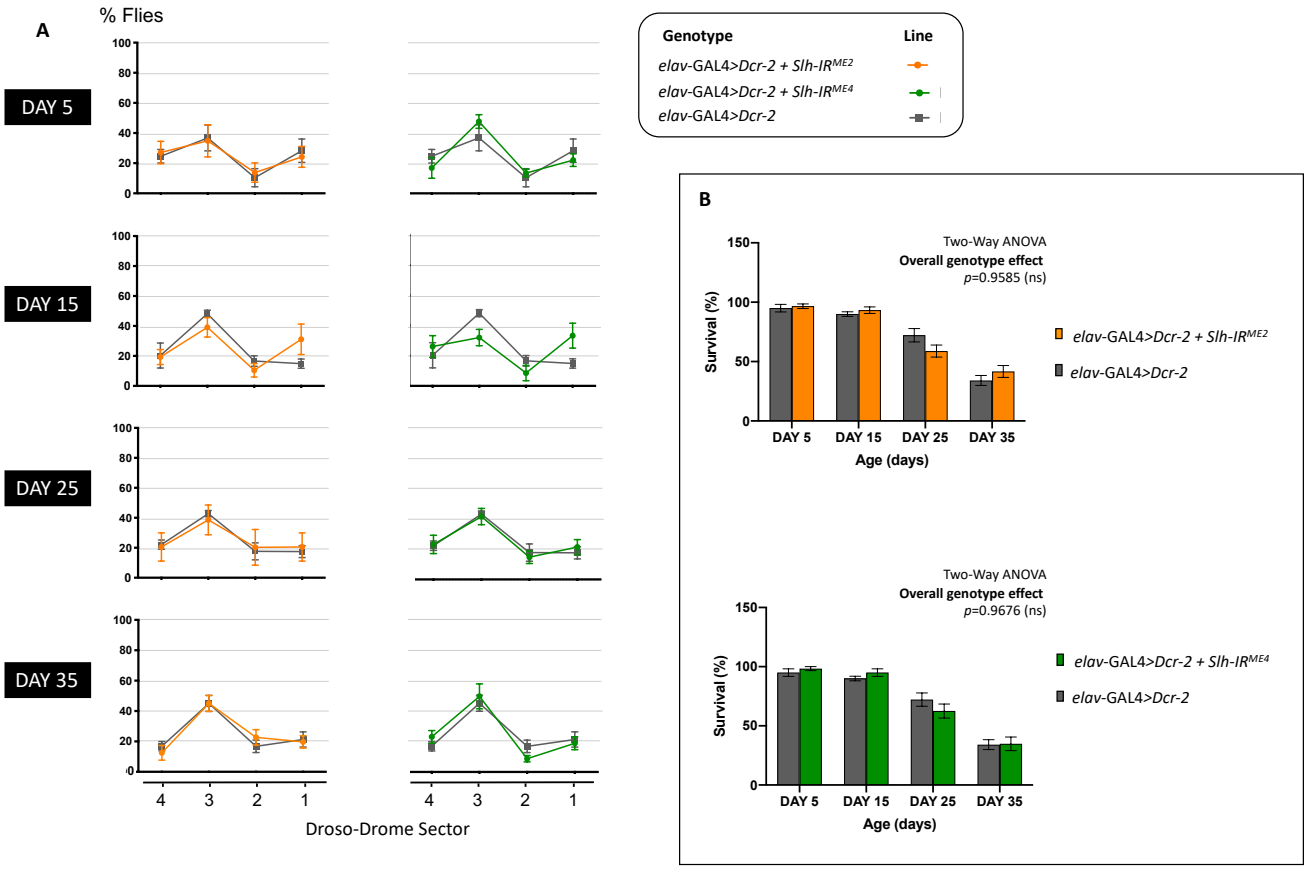

Figure 3.49 Effect of enhanced pan-neuronal *Slh* knockdown on motor behaviour and viability. (**A**) Flight assessment of flies with neuron-restricted depletion of Slh leads to flies that exhibit no significant difference in flight ability when compared to controls. (**B**) *Slh* knockdown in neurons does not impact adult viability. Data presented are the mean ± S.E.M. for a minimum of 4 independent experiments, where n≥60 per genotype, per time-point. Significance was tested by the unpaired *t*-test (A) and Two-Way ANOVA, followed by Bonferroni's *post hoc* tests (B). When differences are statistically significant, the exact *p*-value is indicated.

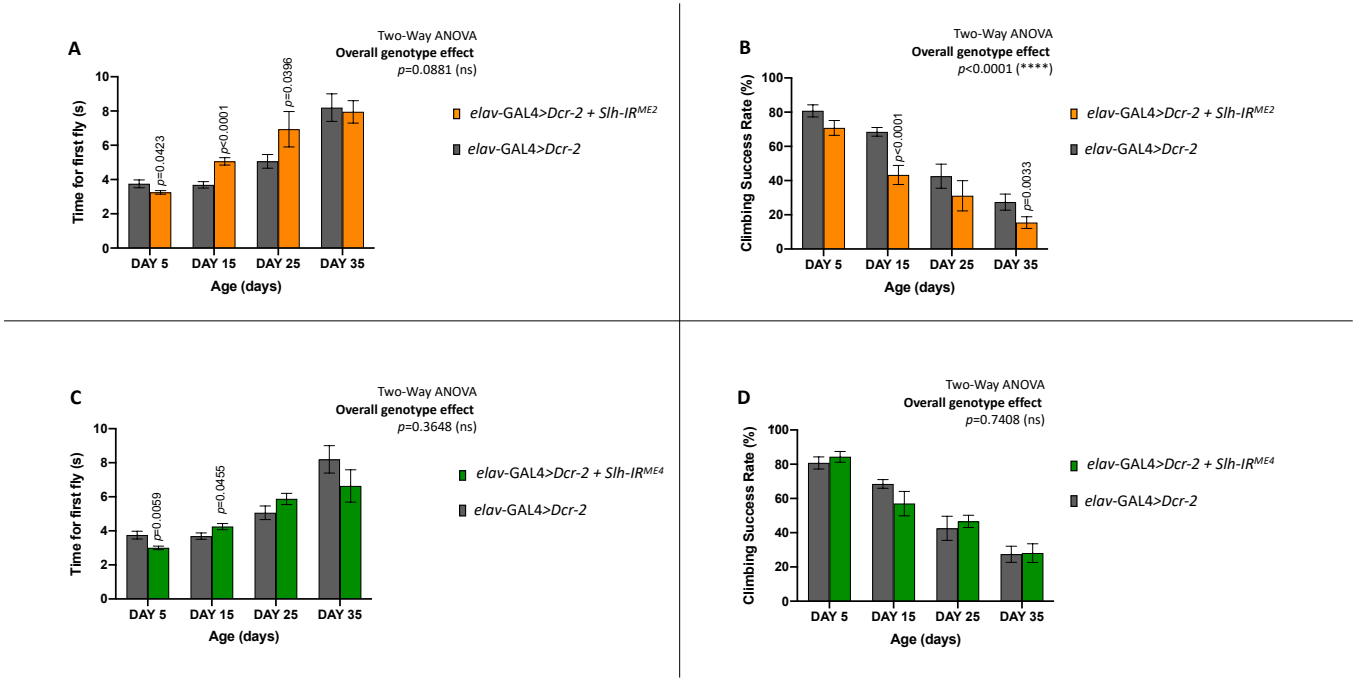

Figure 3.50 Effect of neuron-restricted *Slh* knockdown on climbing performance. (**A**) No consistent trend was observed for flies with a deficiency of *Slh* in neurons, hence, there was no overall genotype effect on motoric ability assayed by this assay. (**B**) Compared to controls, *elav-Gal4>Dcr-2 + Slh-IR^{ME2}* flies exhibited a significant decline in climbing success rate at both day 15 and day 35 post-eclosion, hence, a statistically significant overall genotype effect was obvious. (**C**) *elav-Gal4>Dcr-2 + Slh-IR^{M4}* flies did not exhibit a consistent trend in motor function, hence, there no overall genotype effect was detected. (**D**) Pan-neuronal expression of *Slh-IR^{ME4}* had no effect on the climbing success rate in relation to controls. Data presented are the mean ± S.E.M. for a minimum of 4 independent experiments, where n≥60 per genotype, per time-point. Significance was tested by Two-Way ANOVA, followed by Bonferroni's *post hoc* tests. When differences are statistically significant, the exact *p*-value is indicated.

3.7.2.6 Tissue-specific requirement of *Slh* for adult viability

The lethality phenotype attributed to ubiquitous knockdown of *Slh* by *Slh-IR^{ME3}*, suggests that *Slh* is an essential gene. To verify whether the requirement of *Slh* for adult viability is associated with a function within the neuromuscular system, *Slh-IR^{ME3}*-based knockdown was restricted to muscle tissues or neurons *via* *Mef2*-GAL4 and *elav*-GAL4, respectively (**Figure 3.51**). In the presence of increased Dicer-2 levels, knockdown *via* either of the two GAL4 drivers resulted in lethality before adult stage. *Slh-IR^{ME3}*-mediated knockdown was then activated in additional tissue lineages to probe for potential tissue-specific functions (**Figure 3.51**). Recurring viability defects were prominently linked to knockdown in muscle lineages. Indeed, in addition to *Mef2*-GAL4 and *Mef2*-GAL4 boosted by Dicer-2 levels, reduction of Slh *via* strong pan-muscular GAL4 drivers such as *how*-GAL4, *C179*-GAL4 and *MHC*-GAL4, also led to lethality before the adult stage. In addition, at culture temperatures associated with maximal GAL4 activity (29°C), RNAi driven by the somatic muscle-specific *G14*-GAL4 driver was also lethal. Slh depletion *via* the pan-neuronal *elav*-GAL4 driver or the motor neuron *OK6*-GAL4 driver induced lethality only if maximal transgenic effect was achieved either through culture at 29°C or in the presence of increased Dicer-2 levels. Knockdown *via* the neuronal-specific *1407*-GAL4 driver reduced adult viability at both culture temperatures, with an enhanced effect observed at the elevated temperature of 29°C. At the latter temperature, a reduction in viability was also observed upon *D42*-GAL4-mediated *Slh* knockdown in motor neurons.

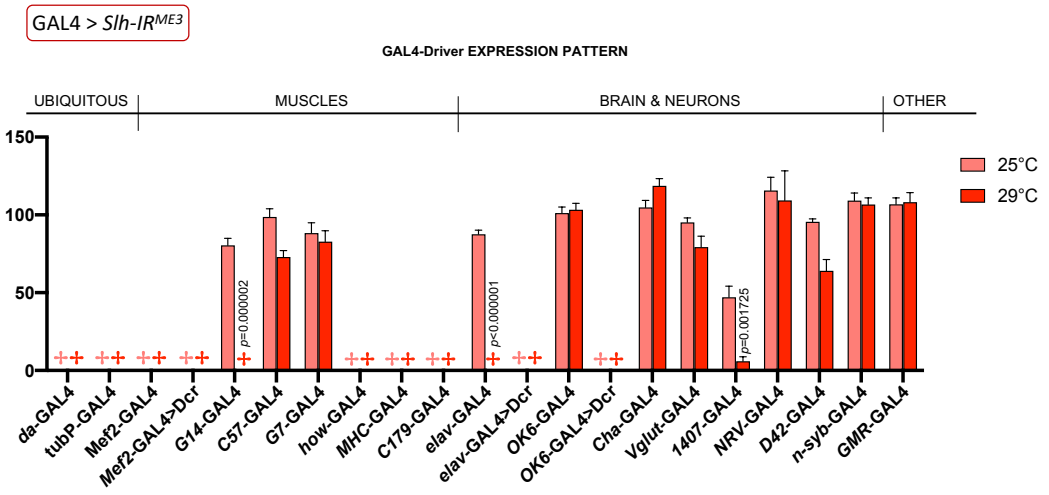

Figure 3.51 *Slh* is required for adult viability in either muscles or neurons. Lethality attributed to global Slh reduction (*da*-GAL4 or *tubP*-GAL4) was recapitulated when knockdown was restricted to muscles *via* strong pan-muscular GAL4-drivers (*Mef2*-GAL4, *Mef2*-GAL4>*Dcr-2*, *how*-GAL4, *MHC*-GAL4 and *C179*-GAL4) or when enhanced RNAi-based knockdown is restricted to the nervous system (*elav*-GAL4>*Dcr-2*, *OK6*-GAL4>*Dcr-2*). Bar charts show the percentage adult fly viability assayed at 25°C and 29°C, on tissue-specific knockdown of *Slh*. Individual bar charts represent the mean viability ± S.E.M. of at least 4 independent experiments. Statistical significance was determined for differences between expression at 25°C and 29°C by multiple *t*-tests. Culture temperatures of 29°C or an enhanced Dicer-2 background are associated with maximal GAL4 activity.

3.7.2.7 Requirement of *Slh* for larval neuromuscular function

Owing to the efficiency of *Slh-IR*^{ME3}, ubiquitous or tissue-specific expression of this RNAi transgene often led to lethality before the adult stage, restricting the investigator from assessing adult motor function. To investigate whether depletion of Slh perturbs neuromuscular function prior to lethality, third instar larvae were assessed for mobility defects. Larval mobility of flies with an enhanced deficiency of *Slh* in muscles or neurons was analyzed by determining the rate of body wall contractions (**Figure 3.52A**). When Slh was strongly reduced in muscles, larvae failed to contract adequately when compared to corresponding controls. The affected larvae formed puparia that had a significantly larger puparial axial ratio when compared to the control genotype (**Figure 3.52B**). A milder depletion of Slh in muscles, in the absence of Dicer-2,

did not impact larval mobility (**Figure 3.52A**). However, for this genotype, a slight difference in puparial axial ratios that is nonetheless significantly different was observed compared to controls (**Figure 3.52B**). When knockdown of *Slh* was restricted to neurons *via elav*-GAL4, in the presence of increased levels of *Dcr-2*, larvae also exhibited less frequent movements when compared to controls (**Figure 3.52A**), however this did not induce a significant difference in puparial axial ratio (**Figure 3.52B**).

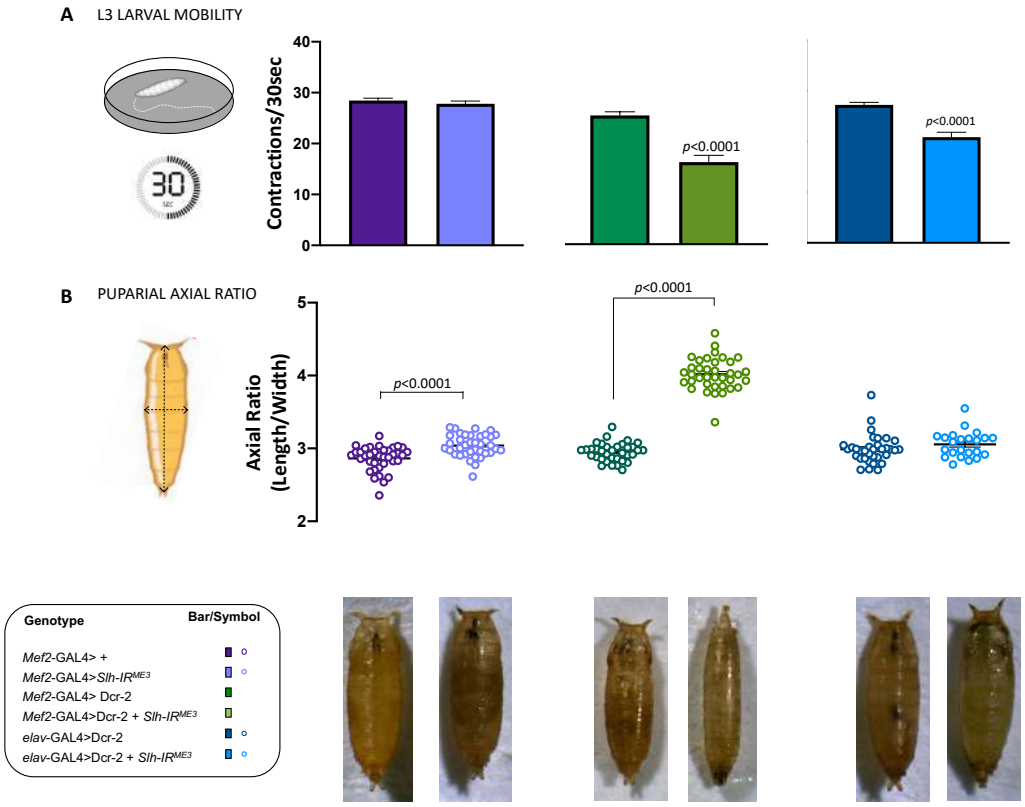

Figure 3.52 Effect of reduced levels of Slh on neuromuscular function in larvae. (**A**) Third instar larvae with muscle specific Slh depletion were slower when compared controls only in the presence excess Dcr-2 levels. Enhanced pan-neuronal *Slh* knockdown also induced a significant decrease in larval mobility compared to controls. (**B**) Puparial formation is hindered when *Slh* knockdown is restricted to muscles but is not affected upon knockdown in neurons, despite lethargic larval behaviour. Data presented are the mean ±S.E.M. of at least 3 independent experiments, and n ≥15 per genotype for mobility and n ≥24 for axial ratios. Significance was tested by the unpaired *t*-test as indicated by the exact *p*-value.

In view of their failure to contract adequately during pupariation, consequent to a decline in muscle power, the neuromuscular junction (NMJ) morphology of *Mef2-GAL4> Dcr-2 + Slh-IR^{ME3}* third instar larvae was assessed. Visual inspection revealed that enhanced muscle-directed knockdown of *Slh* induced NMJ defects, as verified by abnormal NMJ morphology parameters (**Figure 3.53**). In effect, the normalized NMJ area, which is the NMJ area in relation to muscle size, was significantly reduced when compared to that of controls. In addition, the number of terminal branches per NMJ were also considerably reduced. Subsequently, a drastic decrease in the number of synaptic boutons within a single NMJ was observed compared to controls. In conjunction these findings suggest a requirement for *Slh* in muscle tissue for normal NMJ morphology.

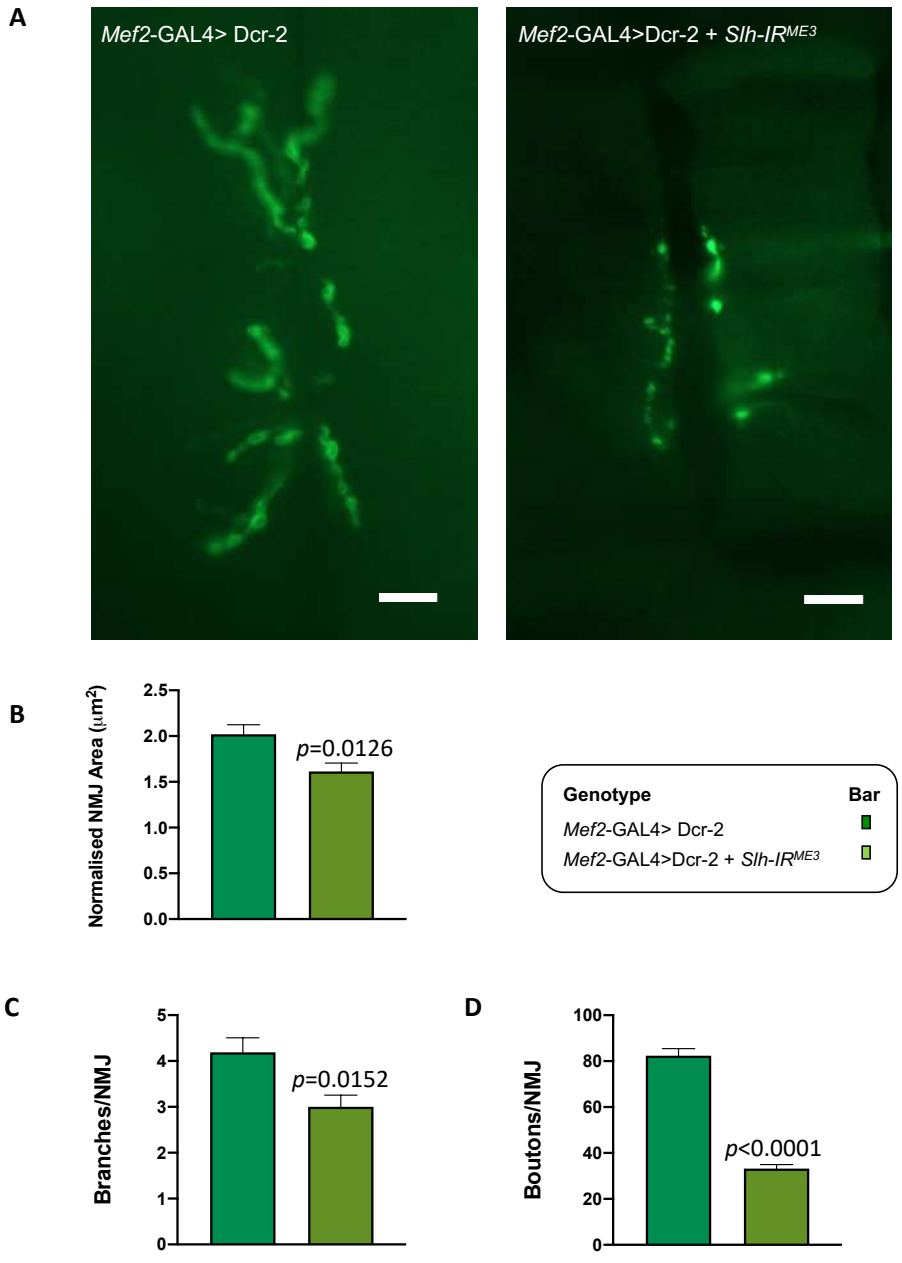

Figure 3.53 Effect of enhanced muscle-specific Slh depletion on NMJ morphology. (**A**) Images represent NMJs innervating ventral longitudinal muscles 6 and 7 in third instar larvae stained with post-synaptic anti-DLG antibody (scale bar = 10μm). Visual inspection revealed that compared to control NMJs, enhanced expression of *Slh-IR*^{ME3} in muscles induced NMJ defects. (**B**) These observations were confirmed upon quantification of normalized NMJ area, which was significantly reduced compared to that of controls, as was the number of branches per NMJ (**C**) and the number of synaptic boutons within a single NMJ (**D**). In (B-D), data presented are the mean ±S.E.M. and n≥10 per genotype. Significance was tested by the unpaired *t*-test, which if statistically significant is indicated by the exact *p* value.

CHAPTER 4
DISCUSSION

In the first whole-genome, population-based study of ALS in the Maltese islands, the characteristics and genetic profile of Maltese ALS patients were investigated. Furthermore, the incidence and prevalence of ALS in the Maltese population were calculated. Interestingly, although several population-specific aspects of the Maltese ALS cohort correlate with those reported for neighbouring European populations, genetic markers were skewed towards the Middle-Eastern gradient. Indeed, rare deleterious variants in the major ALS genes, including *C9orf72, SOD1*, *TARDBP* and *FUS* were absent in Maltese ALS patients analysed in this study. Mutations in these loci are highest in northern European countries such as Belgium and Finland and are associated with fALS. However, disease associated with these genes is recorded with low frequency in the south of Europe such as in Spain and mainland Italy (ZOU *et al.* 2017). Thus, this study continues to emphasize that ethnic diversity and geographical distribution influence the genetics underpinning ALS pathogenesis.

Nevertheless, whole-genome analysis of Maltese ALS patients identified deleterious alleles in 'minor' ALS genes including *ALS2*, *DAO*, *DCTN1, ERBB4, SARM1, SCFD1, SETX* and *SPG11.* Physiological functions linked to these genetic findings highlight vesicular trafficking (HOU *et al.* 2017; BURK AND PASTERKAMP 2019a), cell signalling (TAKAHASHI *et al.* 2013; FIGLEY *et al.* 2021), cytoskeletal organization (CASTELLANOS-MONTIEL *et al.* 2020) and ribostasis (TANNER AND LINDER 2001) as key cellular pathways that might contribute to ALS pathogenesis in Maltese patients. In view of their inheritance pattern and their previous association with ALS, most damaging alleles identified in the Maltese patient cohort are likely disease-causing. On the other hand, for pathogenic mutations in ALS risk loci, such as *SCFD1*, a modifying or additive effect is speculated.

Considering the oligogenic basis and heterogeneity of the disease, it cannot be excluded that the process of motor neuron degeneration in some Maltese ALS patients is multifactorial. In addition, the influence of environmental factors is highly relevant. Indeed, compared to controls, a higher percentage of ALS patients in this study reported an occupation associated with heavy physical exertion, five of which had ALS-associated deleterious mutations. This

occupation-related difference was corroborated in a larger follow-up study of the Maltese case-control cohort, which confirmed that the likelihood of individuals with a blue collar occupation to develop ALS was double that for controls (FARRUGIA WISMAYER *et al.* 2021). Individuals with blue collar jobs have increased exposure to strenuous physical activity. Cigarette smoking, which has also been previously implicated in ALS (PETERS *et al.* 2020), appeared to be more frequently associated with ALS patients compared to controls in the Maltese cohort. However, as sustained by a subsequent study with a larger sample size, this difference was not significant (FARRUGIA WISMAYER *et al.* 2021).

In the second part of the study, animal models of ALS were generated in an attempt to replicate disease phenotypes and better understand the consequent mechanisms. In view of their relevance within the Maltese population, the presence of putative *Drosophila* orthologues and lack of associated functional studies, the ALS-linked genes *DCTN1* and *SCFD1* were characterized in the *Drosophila* animal model. Ubiquitous and tissue-specific knockdown was achieved by targeted RNAi transgenes to determine the effect of DCTN1 or SCFD1 depletion on viability, survival and motor function. Low levels of DCTN1 resulted in severe motoric defects, as identified by a decline in flight performance and climbing ability when knockdown was restricted to either muscles or neurons. In contrast, motor defects associated with depletion of SCFD1 were mostly evident upon knockdown in the muscle compartment of the neuromuscular system. This work establishes that both genes are required for neuromuscular function *in vivo* and, therefore, strengthens their role in ALS pathoaetiology. The genes also flag vesicular trafficking and cargo transport as potential mechanisms underpinning neuromuscular degeneration in *Drosophila*, and, in turn, in ALS patients, fuelling the design of therapeutic targets targeting these pathways.

4.1 PATIENT-POPULATION ASPECTS

Considering the geographic isolation of the Maltese islands, a number of ALS linked patient population aspects overlap those described in other European populations. The incidence of ALS in Malta is higher than some southern-most regions in the Mediterranean (**Table 19**), such as Sicily and Puglia in Italy and Catalonia in Spain (LOGROSCINO *et al.* 2005; RAGONESE *et al.* 2012; PRADAS *et al.* 2013), and is comparable to that in northern Italian regions such as Sardinia and Emilia Romagna as well as other northern European countries such as Scotland and Germany (FORBES *et al.* 2007; PUGLIATTI *et al.* 2013; MANDRIOLI *et al.* 2014; UENAL *et al.* 2014). ALS incidence rates which are higher than that observed in the Maltese study have also been described in other neighboring regions including Limousin in France and Liguria in Italy (BANDETTINI DI POGGIO *et al.* 2013; MARIN *et al.* 2014). Nonetheless, ALS incidence in Malta surpasses the median ALS incidence for all European studies [2.08/100,000 (95% Cl 1.47-2.43)] (CHIO *et al.* 2013) and is one of the highest in the Mediterranean basin. The prevalence of ALS in Malta is generally lower than most other European countries, however the male-to-female prevalence ratio is considerably increased compared to these regions (O'TOOLE *et al.* 2008; CHIO *et al.* 2009b; HUISMAN *et al.* 2011; RAGONESE *et al.* 2012; PUGLIATTI *et al.* 2013).

Table 19 Crude ALS incidence and prevalence rates in European countries.

Subcontinent	Country	Region	Crude Incidence (per 100,000 person-years)	Crude Prevalence (per 100,000 population)	Reference
Northern Europe	Scotland	Countrywide	2.38 (95% CI 2.25-2.52)	-	(FORBES et al. 2007)
	Ireland	Countrywide	2.0 (95% CI 1.9-2.2)	6.2 (95% CI 5.3-7.1)	(O'TOOLE et al. 2008)
Western Europe	Germany	Swabia	2.5 (95% CI 2.3-2.7)	-	(UENAL et al. 2014)
	Netherlands	Countrywide	2.77 (95% CI 2.63-2.91)	10.32 (95% CI 9.78-10.86)	(HUISMAN et al. 2011)
	France	Limousin	3.19 (95% CI 2.81-3.56)	-	(MARIN et al. 2014)
Southern Europe	Italy	Lombardy	2.09 (95% CI 1.17-3.18)	-	(BEGHI et al. 2007)
	Italy	Piemonte	2.90 (95% CI 2.72-3.09)	7.89 (95% CI 7.09- 8.75)	(CHIO et al. 2009)
	Italy	Emilia Romagna	2.63 (95% CI 7.89-7.9)	-	(MANDRIOLI et al. 2014)
	Italy	Liguria	3.22 (95% CI 2.66-3.90)	-	(BANDETTINI DI POGGIO et al. 2013)
	Italy	Puglia	1.6 (95% CI 1.3-1.9)	-	(LOGROSCINO et al. 2005)
	Italy	Sardinia	2.5 (95 % CI 0.1-4.9)	10.8 (95 % CI 8.6-13.1)	(PUGLIATTI et al. 2013)
	Italy	Sicily	1.4 (95% CI 1.33-1.47)	6.0 (95% CI 5.97-6.03)	(RAGONESE et al. 2012)
	Spain	Catalonia	1.4 (95% CI 1.3-1.8)	5.4 (95% CI 2.99-7.01)	(PRADAS et al. 2013)
	Malta	Countrywide	2.48 (95% CI 1.59-3.68),	3.44 (95% CI 2.01-5.52)	(BORG et al. 2021)

Male sex has invariably, except for minor cases, been considered as a risk factor for ALS and in line with several reports (LOGROSCINO *et al.* 2010; INGRE *et al.* 2015; LONGINETTI AND FANG 2019), observed ALS incidence rates in the Maltese population were higher for males compared to females. The mean age at disease onset (59.3 ± 13.2 SD years) was slightly lower compared to previous studies but very close to that observed in a Sicilian study cohort (58.3 ± 14.6 SD years) (LOGROSCINO *et al.* 2010; RAGONESE *et al.* 2012). Although male gender is a strong dominator of ALS cases worldwide, it is noteworthy that in specific populations in the southern gradient of the Mediterranean as well as in Malta, age at disease onset is higher in males than in females (LOGROSCINO *et al.* 2005; RAGONESE *et al.* 2012; DEMETRIOU *et al.* 2017; KACEM *et al.* 2020). However, this is not the case for northern populations in the Mediterranean basin including the regions of Emilia Romagna, Friuli-Venezia Giulia and Liguria in Italy, and Catalonia in Spain (PRADAS *et al.* 2013; MANDRIOLI *et al.* 2014; SCIALO *et al.* 2016; PALESE *et al.* 2019). Numerous population-based studies have reported that ALS incidence typically increases rapidly after the age of 40 and reaches a peak around the 70-year mark, followed by a steep decline (LOGROSCINO *et al.* 2005; BEGHI *et al.* 2007; O'TOOLE *et al.* 2008; LOGROSCINO *et al.* 2010). For both genders, a similar progressive increase between 49 and 79 years of age, with a rapid decrease thereafter was observed in this study. This suggests that motor neuron degeneration is in-part, an age-related clinical condition.

Gender differences in ALS may be explained by unequal exposures to pathogenic agents or different responses to environmental hazards. For instance, occupational exposures and physical activity levels differ among men and women, where males are generally more physically active (GUNNARSSON *et al.* 1991). In the present study, a higher percentage (56.3%) of male ALS patients reported an occupation associated with strenuous activity compared to females (37.5%). In this context, the main occupations associated with ALS in a larger Maltese cohort including recruits from this study, were those associated with craftsmanship and related trades such as carpentry and construction, which are predominantly male occupations (FARRUGIA WISMAYER *et al.* 2021). In addition, cigarette smoking which is also increasingly associated with ALS risk (CALVO *et*

al. 2016; PETERS *et al.* 2019) is more common in men (PAMPEL 2006; ALLEN *et al.* 2016). This is also reflected in the number of male smokers (60%) versus female smokers (37.5%) in this study. Furthermore, differences between the male and female nervous system (ZHOU *et al.* 2000) and the role of gonadal hormones in neuroprotection, particularly oestrogen (SIMPKINS AND SINGH 2008), are other mechanisms that might influence gender differences in ALS.

In accordance with data derived from European population-based registries (LOGROSCINO *et al.* 2010), the majority of ALS patients in Malta presented with spinal onset. However, bulbar onset ALS had a slightly higher occurrence in females (57.2%). In relation to this, gender-based differences in disease incidence may also be associated with differences in site of disease onset. An increased incidence of bulbar onset among female ALS patients in Malta was common across the 49-70 age group, in contrast to findings reported in Italian and Irish populations, that identified a higher bulbar onset among women only in older age groups, particularly in subjects over 70 years of age (O'TOOLE *et al.* 2008; GEORGOULOPOULOU *et al.* 2011; BANDETTINI DI POGGIO *et al.* 2013). Bulbar onset ALS in the Maltese cohort was associated with a worse disease prognosis compared to spinal onset, in agreement with several European registry-based studies (TYSNES *et al.* 1991; LOUWERSE *et al.* 1997; CHIO *et al.* 2002; TESTA *et al.* 2004). This finding may in-part be explained by the increased frequency of bulbar disease in old age. The majority (85.7%) of Maltese patients with bulbar onset ALS were older than 60 years.

The correlation between decreased survival time and increasing age in symptom onset observed in a significant number of studies makes age the most consistent factor related to ALS prognosis. This might be related to the motor neuron loss that often accompanies aging (NORRIS *et al.* 1993; LEE *et al.* 1995; TRAYNOR *et al.* 2000; FORBES *et al.* 2004). Age was also considered a prognostic factor in the present study, where patients presenting with an old age at onset (>55 years) had a shorter average disease duration (3.9 ± 2.3 SD, years) than patients presenting with onset at a younger age (8.4 ± 7.3 SD, years). Interestingly, two patients with an onset age <40 years remain alive. This may be explained by a

better compensation of declining motor function in younger people, especially for the respiratory system which is naturally compromised at older age (DANNESKIOLD-SAMSOE *et al.* 1984; BROOKS 1999; ARMON *et al.* 2000).

Compared to the incidence of fALS in Sicily (0%) (RAGONESE *et al.* 2012) and northern Italian populations of Piemonte (5.8%) (CHIO *et al.* 2009b) and Liguria (10%) (BANDETTINI DI POGGIO *et al.* 2013), a higher percentage (12.5%) of fALS cases was reported in Malta, which is however nearly half that reported for the island of Sardinia (26.7%) (PUGLIATTI *et al.* 2013). Nonetheless, the lack of a definitive definition for fALS often masks the true rate of familial disease. Since ALS is increasingly associated with a wide spectrum of neurodegenerative disorders including dementia and other neuropsychiatric conditions, the recognition of family history in related diseases such as FTD is likely to influence the ALS percentage withing this group. This is supported by the identification of familial clusters of FTD and MND, as well as recent findings demonstrating a pronounced overlap between ALS, FTD and other psychiatric illnesses in family members of ALS patients (BURRELL *et al.* 2011; BYRNE *et al.* 2013; LONGINETTI *et al.* 2017). Consequently. the inclusion of neurological conditions in kindreds that have a genetic overlap with ALS, increases the percentage of fALS in Malta by threefold (37.5%). Similar to previous studies (LOUWERSE *et al.* 1997; CHIO *et al.* 2002), no difference in disease prognosis was observed between patients with fALS and sALS in the present study. However, it is accepted that different gene mutations can have different effects on age at onset and progression of disease. Moreover, large intrafamilial variations in age at onset or clinical phenotypes occur in the presence of the same mutations, suggesting the presence of additional genetic or environmental factors contributing to these differences (CUDKOWICZ *et al.* 1997; AGGARWAL AND NICHOLSON 2005; ANDERSEN 2006). Two out of three patients in the Maltese cohort that had a family history of ALS developed cognitive impairment. Although patients with ALS-FTD were found to have a shorter survival compared to those with normal behavioural function, no population-based studies correlating disease outcome and cognition in ALS have been performed (ARMON AND BRANDSTATER 1999; CHIO *et al.* 2009a). With regards to this study, the average survival for patients who developed ALS with cognitive

impairment was close to half that for patients that did not (mean survival: 2.7 ± 1.2, SD years).

4.2 CLINICAL PRESENTATION AND DISEASE PROGRESSION

A wide variability of clinical symptoms that potentially influence activities of daily living (ADL) and prognosis was observed in the Maltese ALS cohort. Previous studies demonstrate that neck muscles, specifically the sternocleidomastoid or neck flexor muscle, is the only muscle with the potential to independently predict survival in ALS patients following examination of muscle power (PINTO AND DE CARVALHO 2008; NAKAMURA *et al.* 2013; VASTA *et al.* 2021). Neck flexors muscle weakness is essentially interpreted as weakness of the diaphragm, and thus respiratory impairment, in view of shared spinal segments of the motor neuron column. Indeed, a recent study showed that the risk of developing respiratory impairment is almost doubled in the presence of neck flexors weakness at diagnosis (VASTA *et al.* 2021). Considering that respiratory insufficiency is the main cause of death in ALS patients, the correlation between neck flexors weakness and decreased survival time is likely. Muscle power in the neck was not affected in Maltese ALS patients, who displayed an average MRC score close to that achieved by controls upon neck flexor and extensor examination and, therefore, neck muscle weakness could not be correlated with disease prognosis in the ALS cohort investigated in the present study. However, it was observed that in most cases, patients were able to flex or extend neck muscles with increased effort. Head drop, which is associated with neck extensor muscle weakness (UEMURA *et al.* 2013) was also observed in a few Maltese ALS patients. The average upper and lower limb scores for muscle power were close to half those reported for controls, indicating increased muscle weakness within these regions for patients, although repeatedly this did not affect survival. A high variability of ALSFRS-R scores was observed among ALS patients in the Maltese cohort. As expected, and as shown in previous studies (MAGNUS *et al.* 2002; PFOHL *et al.* 2018), normal muscle power as interpreted by high MRC scores correlates with higher ALSFRS-R scores, and, therefore, a superior physical function.

Elevated CK levels in ALS patients is associated with loss or denervation of motor neurons, as well as muscular atrophy (FELICE AND NORTH 1998; LIMA *et al.* 2003; TAI *et al.* 2018). Increased levels of CK have also been interpreted as a compensatory mechanism for the upregulation of muscular metabolic pathways following motor neuron damage in ALS patients (RAFIQ *et al.* 2016; CECCANTI *et al.* 2020). Nevertheless, CK plasma half-life is relatively short and levels can return to normal following cessation of acute muscle damage, thus results can be conflicting (BAIRD *et al.* 2012; GIBSON *et al.* 2015). This may explain the presence of normal CK levels in some patients despite muscle weakness. Several studies have shown higher serum CK levels in male ALS patients compared to females (RAFIQ *et al.* 2016; TAI *et al.* 2017), which is not consistent with findings in this study. However, others have highlighted that this could be explained by differences in muscle mass (GIBSON *et al.* 2015). In the Maltese cohort, elevated CK levels were more frequent in patients with spinal onset ALS compared to those with bulbar onset of disease supporting the hypothesis that muscle damage influences CK mechanism. This was also confirmed in previous studies (ILZECKA AND STELMASIAK 2003; RAFIQ *et al.* 2016; TAI *et al.* 2017). The repercussions of serum CK on survival outcome in ALS patients has been controversial. Whilst some studies found a positive correlation between CK levels and survival (GIBSON *et al.* 2015; CECCANTI *et al.* 2020), others did not (CHIO *et al.* 2014; TAI *et al.* 2017). Similar to the latter, no independent correlation between CK levels and duration of illness in ALS patients was evident in this study.

4.3 PHENOTYPE-GENOTYPE CORRELATION

In light of the large number of causative and disease-modifying genes that have been implicated in ALS, the detection of specific mutations or risk variants that contribute to disease pathogenesis in different patients is a challenging feat. This is enhanced by the clinical heterogeneity exhibited in ALS patients carrying specific mutations or variants. To this end, unravelling genotype-phenotype correlations is important to provide further insight on genetic factors, improving

the understanding of disease aetiology. Screening for genes on the basis of their phenotypic expression may also contribute to gain insight on novel variants which may serve as therapeutic targets for a specific population. Moreover, this type of genetic characterization does not only assist in diagnosis but may also advise on the clinical management and prognosis of patients.

A genetic predisposition can be found in 60-80% of patients with familial history of ALS, which is most frequently associated with highly penetrant causal variants in *C9orf72*, *SOD1, TARDP* or *FUS* (ZOU *et al.* 2017; PERRONE AND CONFORTI 2020). Genetic heritability of sALS is less understood. The Maltese ALS patient cohort was found to be negative for deleterious variants in the four major ALS genes. Nonetheless, deleterious alleles were detected in 'minor' ALS genes, including *ALS2*, *DAO*, *DCTN1*, *ERBB4*, *SARM1*, *SETX*, *SCFD1* and *SPG11*, genetically determining up to 40% of apparent sALS cases within the Maltese cohort. In addition, ALS-linked repeat expansions were identified in *ATXN2* and *NIPA1*.

Age of disease onset is an important factor for genetic correlations and can be divided into juvenile and adult onset. *ALS2* and *SPG11* have been associated with juvenile-onset ALS under a recessive disease model (ORLACCHIO *et al.* 2010; SIDDIQI *et al.* 2014). Both have been implicated in the upper motor neuron disease, hereditary spastic paraplegia (HSP), suggesting disease overlap (EYMARD-PIERRE *et al.* 2002; PAISAN-RUIZ *et al.* 2008). In the typical adult onset, mutations in *ALS2* and *SPG11* are rare (HAND *et al.* 2003; ORLACCHIO *et al.* 2010). Although rare variants in *ALS2* and *SPG11* had some of the highest CADD scores observed in the cohort, supporting a deleterious effect, Maltese ALS patients (MND14 and MND17 respectively) carried these variants solely in heterozygous configurations and had adult-onset ALS. Therefore, it is likely that these alleles were not disease causing. However, the possibility of a modifying or additive contribution within an oligogenic model of disease cannot be excluded. Consistently, the exposure to occupation-related strenuous activity reported for both patients is highly relevant. Considering that juvenile onset ALS is frequently associated with a slower progression of disease (TESTA *et al.* 2004), it is expected that variants within these loci also correlate with a longer disease duration.

Indeed, a 20-year disease duration for patient MND17 was reported, whereas patient MND14 remains alive, 7 years from disease onset.

Variants in *SETX* have initially been described in a rare autosomal dominant form of juvenile-onset ALS, characterized with delayed muscle weakness and atrophy. Frequently, disease associated with mutations in *SETX* manifests with upper motor neuron symptoms but without bulbar or respiratory involvement. (CHEN *et al.* 2004; HIRANO *et al.* 2011). Additional studies have since described *SETX* damaging alleles in patients with adult-onset ALS (KENNA *et al.* 2013; TRIPOLSZKI *et al.* 2017). With regards to this study, a heterozygous damaging deletion in *SETX* was linked to a male patient (MND23) who presented with bilateral upper arm weakness at the age of 70. Muscle weakness eventually extended to the lower arms and spread to his legs within a year, leading to ambulatory difficulties. Bulbar and respiratory muscles were not affected, and the patient remains alive, four years from disease onset. Considering the autosomal dominant mode of inheritance of *SETX*, the deleterious allele in this gene is likely disease-causing. A "likely pathogenic" clinical significance for this variant as classified according to ACMG-AMP guidelines supports this hypothesis.

A *de novo* mutation in *ERBB4* has been recently associated with an autosomal-dominant, late-onset form of sALS, characterised by the involvement of a combination of both upper and lower motor neurons, with a relatively slow progression (TAKAHASHI *et al.* 2013). A similar variant in *ERBB4* was reported in this study and was classified as "likely pathogenic" according to ACMG-AMP criteria. The patient carrying this deleterious allele (MND10) developed bilateral limb weakness at the age of 59. Upper motor neuron involvement was not detected at time of recruitment, however upper motor neuron symptoms could have developed at a later stage of the disease, in view of the protracted disease duration of 9 years.

The co-occurrence of multiple gene variants in a single patient is highly suggestive of an oligogenic model of disease, where one variant alone could be tolerated but when combined with a second damaging variant would increase

the susceptibility to neurodegeneration (CADY *et al.* 2015; SCARLINO *et al.* 2020). The co-occurrence of deleterious alleles in the genes *DAO* and *SARM1* (MND04) and the genes *DAO* and *DCTN1* (MND11) in two Maltese patients supports the hypothesis of a multistep model of disease. Variants in the gene *DAO* have been associated with classical onset fALS (MITCHELL *et al.* 2010a). Disease-associated *DCTN1* alleles were first identified in a family with an autosomal dominant form of lower motor neuron disease with slow progression (PULS *et al.* 2003). However, *DCTN1* mutations have also been implicated in Perry syndrome, Parkinson's disease and progressive supranuclear palsy (PSP), highlighting the phenotypic variability of variants within this locus (FARRER *et al.* 2009; ARAKI *et al.* 2014; CAROPPO *et al.* 2014). The Maltese ALS patient MND04 was a male individual who initially developed upper limb and lower limb muscle weakness, whereas patient MND11 was a female participant who presented with bulbar onset ALS. Despite the positive correlation of female bulbar onset and survival, disease duration for patient MND04 (1.5 years) was half that shown for patient MND11 (3 years). Considering that both patients have damaging variants in *DAO*, this difference in disease duration may either be attributed to a higher rare variant burden of *SARM1* compared to *DCTN1*, or to the interaction of non-genetic factors. In view of similar CADD scores for these variants, the contribution of environmental factors is more likely. In effect, MND04 reported an exposure to styrene vapours related to his occupation, which was also physically intensive.

SCFD1 has only been recently identified as an ALS risk locus (VAN RHEENEN *et al.* 2016), thus a modifying or additive effect is suspected for the damaging variant reported in this gene. This variant was identified in an ALS patient (MND13) with a young age at onset (27 years) whose disease progression is remarkably slow. The patient initially presented with spinal onset but has developed bulbar symptoms along the years. The identification of the same damaging variant in the patient's father, a healthy individual, corroborates the implication of *SCFD1* as a disease-modifying gene, whereby the consequent ALS pathogenesis is influenced by the presence of other genes and/or environmental factors.

Despite the increased ALS risk associated with long repeat expansions in *ATXN2* (ELDEN *et al.* 2010; VAN DAMME *et al.* 2011) and *NIPA1* (BLAUW et al. 2012), their effect on disease phenotype has not been widely studied and no correlation between age at onset or survival has been reported. Abnormal *ATXN2* repeat expansions have also been linked to motor neuron degeneration in spinocerebellar ataxia type 2 (SCA2) which may contribute to motor neuron involvement in ALS (IMBERT *et al.* 1996; INFANTE *et al.* 2004; NANETTI *et al.* 2009). The longest *ATXN2* ALS-associated trinucleotide expansion identified in the Maltese case-control cohort was detected in a fALS patient, however its clinical significance based on ACMG-AMP guidelines is uncertain. The concerned patient (MND24) developed late-stage spinal onset ALS that progressed rapidly with some extent of cognitive impairment. The genetic cause of the other two-thirds of Maltese fALS cases remain unexplained. An expanded *NIPA1* GCG repeat motif in the heterozygous state was identified in one male patient with sALS (MND02). The patient presented with bilateral weakness in the lower limbs that subsequently spread to the upper limbs and culminated with respiratory insufficiency and death after 2.5 years from symptom onset.

4.4 EFFECTS OF *DCTN1* KNOCKDOWN IN *DROSOPHILA*

The dynactin complex is composed of 11 different subunits (**Figure 4.1A**) that form two main structural domains, the actin-related protein, Arp1 rod and a sidearm containing microtubule-binding sites. DCTN1 (also known as $p150^{Glued}$) is the largest subunit of the dynactin complex and together with the subunits p50 dynamitin (DCTN2) and p24/22 (DCTN3) forms the dynactin arm. The cytoskeleton-associated protein glycine-rich (CAP-Gly) domain of DCTN1 forms the projecting portion of the arm at the extreme N-terminus of the subunit and mediates microtubule binding. Beyond the CAP-Gly domain, the N-terminal third of DCTN1 is predicted to fold into the first coiled-coil domain (CC1) followed by an inter-coiled-coil domain (ICD) region. Dynein binding is predicted to occur along this region. The DCTN1 C-terminal contains the second coiled-coil (CC2) domain. Compared to the N-terminal, the function of this region is less well-defined but it has been shown to promote a variety of protein-protein

interactions. The CC2, in particular contains an actin-binding motif that directly binds Arp1(**Figure 4.1B**) (SCHROER 2004).

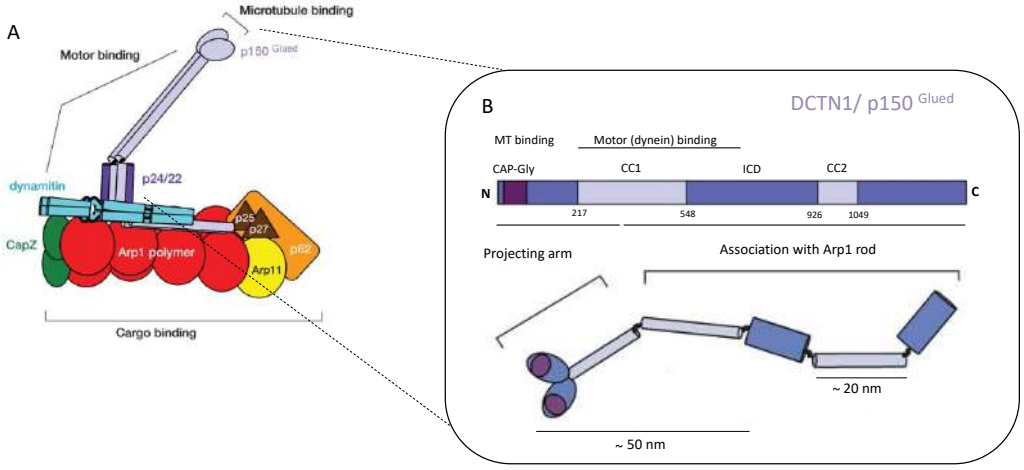

Figure 4.1 Structure of the dynactin complex. (**A**) Structural features and location of dynactin subunits, including the Arp1 filament rod and dynactin sidearm consisting of p150, p22/24 and p50. (**B**) Domain organization and proposed functions of DCTN1 dynactin domain. Arp1, actin-related protein 1; CapZ, actin-capping protein; CAP-Gly, cytoskeleton-associated protein glycine-rich; CC1, coiled-coil domain 1; ICD, inter-coiled-coil domain; CC2, coiled-coil domain 2; MT, microtubule; Arp1, actin-related protein1. Adapted from SCHROER 2004.

The damaging I622F *DCTN1* variant identified in a Maltese ALS patient is located within the dynein-dynactin binding region of the dynactin arm that serves as a link between both complexes for retrograde transport of vesicles and organelles along microtubules (**Figure 4.2**). The I622F *DCTN1* variant is hypothesised to result in *DCTN1* haploinsufficiency. In support, gene expression profiles have revealed that *DCTN1* expression in spinal motor neurons of sALS patients was markedly reduced, confirming that *DCTN1* loss of function can underpin the pathophysiology of ALS (KUZMA-KOZAKIEWICZ *et al.* 2013). In an attempt to mimic DCTN1 downregulation or loss of function, for this work, *DCTN1*-ALS *Drosophila* models were generated. Findings through these models show a requirement of *DCTN1* for motor function *in vivo*.

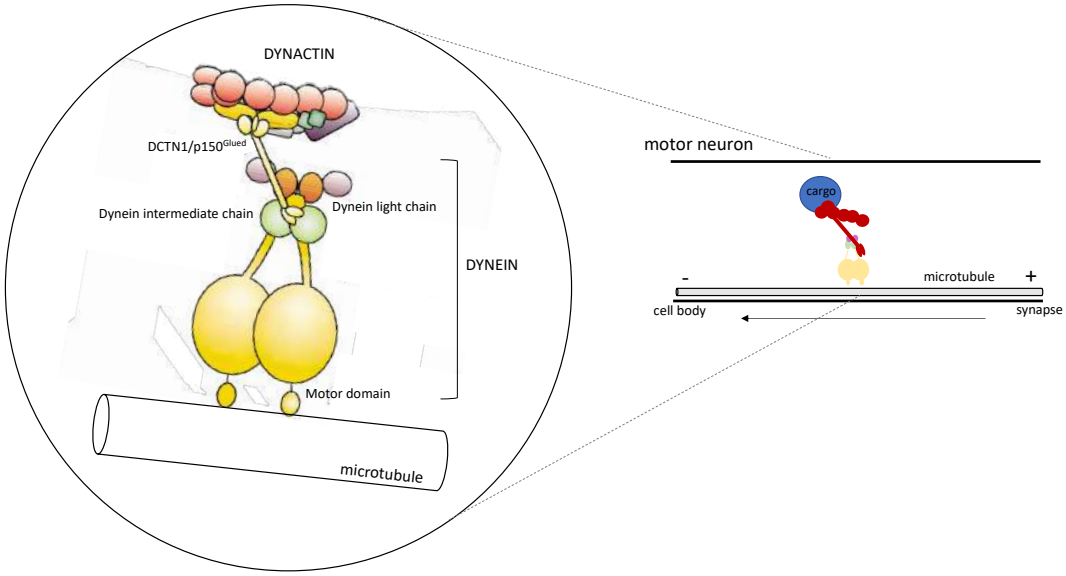

Figure 4.2 Dynactin-dynein complex. Dynein associates with dynactin via interaction between its intermediate chain and the dynactin DCTN1 subunit. This interaction is crucial for the transport of cargo such as neurofilaments, degraded/misfolded proteins and neurotrophins along the axon. Image adapted from KARCHER *et al.* 2002 and LEVY AND HOLZBAUR 2006.

Two *Drosophila* genes are predicted to be homologous to *DCTN1*. Although *DCTN1-p150* (*CG9206*) is thought to be the bona fide homologue (also suggested by its name), this work also characterised the relatively unknown function of *CG9279*, a gene with high levels of homology to human *DCTN1*. Two RNAi transgenes were utilised to knockdown *CG9279*, generating a *in vivo* situation where the gene is reduced to about 71% (moderately low expression, *CG9279-IR^{ME9}*) and 23.3% (low expression, *CG9279-IR^{ME10}*). Ubiquitous RNAi-mediated knockdown *via* both RNAi transgenes demonstrated that the *CG9279* gene is not essential for *Drosophila* viability. One RNAi transgene (*DCTN1-p150-IR^{ME18}*) was utilised to knockdown *DCTN1-p150*, resulting in an *in vivo* situation where *DCTN1-p150* is expressed at around 20%. Low levels of *DCTN1-p150* led to lethality at an early developmental stage.

Flight and climbing defects were observed as early as day 5 of adulthood when CG9279 was targeted in muscles via the most effective RNAi transgene (*CG9279-IR^{ME10}*) in the presence of enhanced Dcr-2 levels. Survival was also negatively impacted. Climbing but not flight or survival deficits were observed in the

absence of enhanced Dcr-2 levels. Flies in which CG9279 was targeted in muscle by the less effective RNAi transgene (*CG9279-IR^{ME9}*) did not have major flight defects thought climbing defects were obvious. In the presence of excess Dcr-2 levels, survival of flies to adulthood was however severely affected. The low number of 'escapers' prevented the investigator from doing extensive motor behaviour assays.

Brain-specific depletion of CG9279 *via* either RNAi transgene in the presence of excess levels of Dcr-2 did not alter the survival of adult flies which, in addition, did not appear to have flight defects at any time point. Nonetheless, flies had significant climbing defects. The difference in climbing success rates between control and test populations was equally significant for brain-specific knockdown using both *CG9279* RNAi transgenes. However, that for time-for-first-fly assay was not significant for CG9279 knockdown via *CG9279-IR^{ME0}*. Whilst the climbing success rate measures the climbing ability of the fly population in question, the time-for-first-fly assay indirectly measures the knockdown efficiency within the entire population. If knockdown is effective throughout, all flies will be slow and the fastest fly will take longer to reach the predetermined threshold. If knockdown is not entirely effective, the time for a potentially unaffected fly to reach the threshold may be comparable to that for controls, hence leading to a normal time for first fly, even if climbing success rate for that population is diminished. Considering that the *CG9279-IR^{ME10}* RNAi transgene induces a greater knockdown when ubiquitously expressed compared to the *CG9279-IR^{ME9}* RNAi transgene, the possibility exists that the latter transgene has a genetic background that is influencing the result.

Flies with enhanced muscle-specific knockdown of *DCTN1-p150* were flightless as early as day 5 post-eclosion. In addition, a significant decline in locomotor function was evident as a consequence of severe climbing defects. Low levels of DCTN1-p150 in the brain led to a decreased lifespan. Although no flight defects were detectable, neural knockdown of *DCTN1-p150* led to a dramatic decline in climbing ability. Overall, these results suggest that in *Drosophila* both *CG9279* or

DCTN1-p150 are required in muscle and to a lesser extent in neurons for normal motor behaviour.

Several studies have reported that functional abnormalities of the molecular motor dynein, as a result of disturbed interaction with the dynactin complex, contribute to a motor neuron disease phenotype that in most cases is linked to impairment of axonal transport (LAMONTE *et al.* 2002; IKENAKA *et al.* 2013). However, other potential consequences of disrupted dynein/dynactin function in ALS pathology may also include disruption of intracellular autophagosome trafficking, altered synaptic processes of motor neurons and dysregulation of kinesin bidirectional transport (LEVY *et al.* 2006). However, the precise relationship between disrupted dynein/dynactin function and the pathological features in ALS patients is unclear and whether *DCTN1* variants contribute to disease onset through loss or gain of function is not known.

A plethora of animal models with mutated or ablated *DCTN1* have been generated to unravel the precise mechanisms leading to motor neuron degeneration. Depletion of *DCTN1* in a zebrafish model led to neuromuscular junction instability and locomotion defects as a result of electrophysiological dysfunction that is independent of changes in axonal transport dynamics or cytoskeletal modulation underlining a role in synapse stability (BERCIER *et al.* 2019). The first *DCTN1* missense mutation, G59S, was identified in a family with an autosomal dominant form of lower motor neuron disease and is located in the N-terminal CAP-Gly DCTN1 domain. Overexpression of this mutant in mice model of motor neuron disease induced severe muscle weakness as a result of the decrease affinity of the mutant to microtubules (CHEVALIER-LARSEN *et al.* 2008; LAIRD *et al.* 2008). Consistently, expression of the corresponding mutant in *Drosophila* larval NMJs results in synapse instability and impaired neurotransmitter release in a proposed loss-of-function or dominant-negative mechanism. In addition, transgenic adult flies exhibit a dramatic decline in locomotor activity and a markedly reduced lifespan (LLOYD *et al.* 2012). Toxic gain-of-function mechanisms have also been implicated in motor neuron disease. Although expression of the G59S substitution in motor neuron cell lines

decreases microtubule binding and affected the overall efficiency of retrograde axonal transport in a proposed loss-of-function mechanism, it also led to the formation of dynein-dynactin aggregates leading to motor neuron cell death as a result of gain of toxic function (LEVY *et al.* 2006). Knockdown of the *C. elegans DCTN1* homolog *dnc-1* caused adult onset motor deficits with axonal degeneration. In addition, this model displays the accumulation of autophagosomes in the degenerated neurons, as a result of impaired axonal transport. Consequent locomotor dysfunction and neuronal degeneration were correlated with the autophagosome aggregation (IKENAKA *et al.* 2013).

In this study, three *Drosophila* models were generated to mimic the down-regulation of DCTN1 hypothesised in ALS patients carrying a damaging copy of *DCTN1*. In particular, a Maltese female patient MND11 who developed adult-onset bulbar ALS was found to carry a "likely pathogenic" (ACMG-AMP assertion criteria), deleterious *DCTN1* variant (as indicated by *in situ* prediction methods) located in the dynein associated protein region. Therefore, it is hypothesised that half of the DCTN1 protein produced might not function correctly, with this having a negative impact on the interaction and, therefore, function of the dynein-dynactin complex. In addition, considering that the patient also harboured additional ALS-related damaging alleles, motor neuron degeneration related to *DCTN1* depletion could be influenced by an oligogenic disease aetiology, hence contributing to a modifying effect. The clinical features observed in patient MND11 are similar to those observed in this study in flies subjected to reduced levels of either *CG9279* or *DCTN1-p150* including loss of muscle power and a shortened lifespan. The *Drosophila* models described in this work provide *in vivo* evidence that *DCTN1* loss of function can lead to neuromuscular deficits.

4.5 EFFECTS OF *SCFD1* KNOCKDOWN IN *DROSOPHILA*

SCFD1 (also known as *SLY1*) is a member of the SecI/Mun18 (SM) family of proteins that participate in membrane fusion events by associating with the soluble N-ethlymaleimide-sensitive factor attachment protein receptors (SNAREs) (CARR AND RIZO 2010). Membrane fusion is the final stage of

intracellular vesicular trafficking and is required for a wide range of functions from cell growth to neurotransmitter secretion (WICKNER AND SCHEKMAN 2008). The process is tightly regulated so as to ensure precise cargo delivery to destination compartments, which is in part controlled by *SCFD1* as implicated in yeast models (LOBINGIER *et al.* 2014). Moreover, in conjunction with syntaxin 5, *SCFD1* has a role in ER to Golgi transport where it assists membrane fusion and vesicle transport from one compartment to another. As shown in mammalian cells, it is also involved in the assembly of pre-Golgi intermediates through interactions with syntaxin 17 and 18 (DASCHER AND BALCH 1996; ROWE *et al.* 1998; YAMAGUCHI *et al.* 2002) and its interaction with the oligomeric Golgi complex subunit 4 (COG4) suggests a role in intra-Golgi-retrograde transport (NOGUEIRA *et al.* 2014; HOU *et al.* 2017). SCFD1 was also shown to exert anti-apoptotic effects in response to oxidative stress, preventing cell death by contributing to protein trafficking and the suppression of stress-associated morphological changes associated with ER (BANDO *et al.* 2005). Pathological modifications of the Golgi apparatus have been widely implicated in many neurodegenerative diseases including ALS (HAASE AND RABOUILLE 2015), hence the increased susceptibility to neurodegeneration linked with *SCFD1* polymorphisms is merely surprising. Nevertheless, an association between *SCFD1* and neuromuscular dysfunction in an *in vivo* model system is still lacking.

In this study, RNAi transgenes targeting the *Drosophila SCFD1* orthologue, *Slh*, were used to determine whether low levels of the ALS-risk gene alone are enough to induce defects that mimic those observed in ALS patient MND13. In addition, tissue-specific knockdown was performed to gain insights on where Slh function is required in *Drosophila*, in an attempt to understand the mechanisms through which disrupted SCFD1 function may influence ALS pathogenesis. Quantification of RNA following ubiquitous knockdown of *Slh*, demonstrated that the *Slh-IR^{ME3}*, *Slh-IR^{ME2}* and *Slh-IR^{ME4}* transgenes reduced gene expression levels by 97%, 55% and 21%, respectively. Therefore, the *in vivo* consequences of different *Slh* expression levels including extremely low, low or moderately low, could be investigated *in vivo*.

Extremely low levels of Slh (generated by ubiquitous expression of RNAi transgene *Slh-IR^{ME3}*) led to lethality at the larval stage. Flies expressing moderately low levels of Slh in muscles (*via* RNAi transgene *Slh-IR^{ME4}*) had severe flight defects in late adulthood. Flight defects were enhanced in flies expressing low levels of Slh, brought about by an increase in knockdown efficiency (via RNAi transgene *Slh-IR^{ME2}*). In this regard, a high percentage of flies were already flightless in early adulthood. Further motor deficits were revealed by a dramatic decline in climbing ability, a phenotype which was similar in flies with either moderately low or low levels of Slh in muscles. Conversely, pan-neuronal *Slh* knockdown did not induce the same motor dysfunctions. Indeed, flies with Slh-deficient neurons displayed normal flight performance, comparable to that observed for corresponding controls. However, low levels of Slh in neurons (*via* the RNAi transgene *Slh-IR^{ME2}*) induced defects in climbing performance (a decreased climbing success rate). Similarly, as implied by a decline in motoric ability extremely low levels of Slh were consequential when restricted to either muscles or neurons. In the former, severe NMJ morphology defects could also be uncovered. All these findings suggest that Slh is required in both muscles and neurons for normal motor behaviour.

A mechanism through which *SCFD1* loss of function leads to neuromuscular dysfunction *in vivo* still needs to be established. A combined effect incorporating oxidative stress, protein dysfunction, and disturbances of vesicle transport and membrane fusion events is speculated. The implication of these SCFD1-associated putative mechanisms in other neurodegenerative diseases such as Parkinson's disease, support this hypothesis (BANDO *et al.* 2005). Knockdown of *Slh* in *Drosophila* S2 cells induced growth defects as a result of aberrant mitochondrial quality control influenced by disrupted vesicle trafficking at the Golgi apparatus (GERARDS *et al.* 2018). Furthermore, depletion of SCFD1/Sly1 in HeLa cells resulted in an increase in autophagosome-associated-microtubule-associated proteins, suggestive of increased autophagosome biogenesis and impaired degradation of autophagic substrates, hence exerting a dual effect on the autophagy pathway (RENNA *et al.* 2011). The preponderance of flaws in

processes that are regulated by ER to Golgi transport, sheds light on the pathways that may lead to ALS-associated motor defects when hindered.

The *SCFD1* variant (T433A) recovered in the Maltese ALS cohort belonged to a female patient who developed spinal onset ALS at a young age, and whose disease progression is exceptionally slow. A non-coding variant with a high allelic frequency in the *SCFD1* gene identified in a large Chinese population was not associated with ALS risk but was shown to modulate age of onset, where age of onset in patients carrying the minor allele within the Chinese Han population was 4 years earlier that that observed in other populations. However, the variant did not correlate with differences in mean survival time, suggesting that *SCFD1* may not influence the remaining process of neuron loss post disease onset (CHEN *et al.* 2018). Although the effect of this variant is expected to be very different from the variant identified in the present study, a similar scenario is speculated in relation to the protracted survival of Maltese ALS case, considering the contrasting lifespan-affecting phenotypes observed in the *SCFD1/Slh* fly models generated and described here. Nonetheless, the phenotypic variability brought about by the *SCFD1*-knockdown fly models in this study may potentially mimic the situation observed in ALS patients. Hence, although one model had severe motor deficits and lethality at an early stage as a result of extremely low levels of SCFD1/Slh, the phenotypic features observed in the affected ALS patient resemble the milder phenotypes observed in fly models with low or moderately low SCFD1/Slh levels, where, here, motor function was affected but lifespan was not. One can speculate that ALS fly models with low or moderately low levels of SCFD1/Slh mirror the situation of ALS patient MND13, where it is hypothesised (based on *in situ* prediction methods) that the T433A *SCFD1* variant is disrupting the function of one of the two *SCFD1* gene copies, leading to half of the expression levels of SCFD1 normally expected. However, one cannot exclude the possibility that other factors either genetic or environmental or both are interacting with this variant to induce disease. With regards to the former, patient MND13 was found to carry a large number of rare deleterious variants.

4.6 FUTURE PROSPECTS

Despite the important implications demonstrated by findings in this study, limitations are unavoidable and further investigations are warranted. Limitations of this study include a low sample size. A sample size which is not representative of the whole population can make it difficult to determine if a particular outcome is a true finding. An increase in patient and more importantly, control recruitment should ensure accuracy by preventing bias or under coverage, thereby decreasing the margin of error. However, a low sample size is expected considering the rare frequency of ALS and the relatively low number of Maltese inhabitants. Considering that a high proportion of sALS patients in the Maltese cohort are probably genetically determined, whole genome sequencing of ALS patient relatives may inform on the nature, mode of inheritance and phenotypic outcome of the variant in question. This will, in turn, consolidate genotype-phenotype correlations, thus improving associations between damaging alleles and disease.

Another study limitation is the lack of periodical patient follow-ups. Despite being laborious and extremely time-consuming, the introduction of a follow-up system will enable better monitoring of disease progression. This will also favour genotype-phenotype correlations in relation to factors such as disease duration and functional ability. Included patients can simply be followed up by intermittent telephone surveys or by re-evaluating neurological examinations every few months. Other improvements to detect phenotypic changes in disease progression could include the use of a spirometer to monitor respiratory involvement which might be more accurate in detecting respiratory impairment than measuring the breathing rate. This small device works by measuring lung airflow, that is, the amount of air breathed in and out in one forced breath. Recording phenotypic changes related to type of onset can also be beneficial. For instance, voice recordings can be used to monitor speech defects and visible phenotypic changes such as weight loss and features synonymous with muscle wasting such as limb and tongue fasciculations can be photographed.

Further *Drosophila*-related research is required to better understand disease mechanisms underlying consequential ALS genes identified in the Maltese population. Preceding this, isogenisation of fly stocks will help eliminate the effects of genetic background of transgenic lines which may influence phenotypic traits, leading to results that are not entirely linked to the gene of interest. An isogenic background can be achieved by backcrossing, whereby a genetic trait or characteristic is introgressed from a donor parent into the genomic background of a recurrent parent. This involves crossing the transgene of interest with flies having a wild-type background. The progeny is then selected for the characteristic of interest, often facilitated by the use of visible markers (for instance, eye colour) and are subsequently backcrossed to the recurrent parent. As backcrossed generations increase, the proportion of the genome of the donor parent tends to zero, bar the segment containing the characteristic of interest. Thus resulting genomes are almost identical, ensuring that no recessive damaging allele is present in the background and resulting phenotypes are attributes solely to the transgene effect (EVANGELOU *et al.* 2019).

In view of their numerous functions, the sub-cellular localisation of *DCTN1* and *SCFD1* could provide insights on the exclusive pathways that are being perturbed in the studied *Drosophila* ALS models. This can be achieved by tagging the desired gene with a fluorescent protein tag such as GFP, and obtaining larval muscle and brain dissections, which are then stained with specific antibodies that permit visualisation under the fluorescence microscope. Immunofluorescence can also be used to investigate genetic interactions and their effect on the neuromuscular system by tagging transgenes with different epitope tags and evaluating whether the localisation of both proteins overlap *in vivo*. Furthermore, to determine whether the effect of *DCTN1* or *SCFD1* transgenes can be modified by other genetic factors, the consequence of combined transgenes on viability and motor function can be analysed. The presence of a modified effect can be a potential target for modified ALS therapy.

Protein-protein interactions may also be investigated *via* co-immunoprecipitation (co-IP) interaction profiles. Advanced peptide-based mass

spectroscopy (MS) enables the isolation of binding partners by using the target protein itself as an affinity reagent. The process involves the immunoprecipitation of the desired protein with a specific antibody to form an immune complex. The affinity-tagged 'bait' protein attracts interacting proteins, whilst those that are not part of the multi-component complex are washed away. The protein complex is then eluted and purified so that the proteins can be separated and visualized on sodium dodecyl sulfate-polyacrylamide gel electrophoresis (SDS-PAGE) followed by western blotting. Co-IP coupled with MS analysis is able to identify previously unknown protein-protein interactors and is used to identify both direct and indirect protein-protein interactions (FREE *et al.* 2009; LIN AND LAI 2017). In this way, co-IP can be applied to extracts derived from *Drosophila* S2 cells and/or transgenic flies to unravel common pathways implicated in ALS.

RNA-Seq transcriptome profiling uses deep-sequencing technologies to quantify changing expression levels of a complete set of transcripts in a cell for a specific developmental stage under different physiological conditions. Principally, a population of RNA is converted to cDNA fragments with adaptors attached to either one or two ends. Each molecule is then sequenced in a high-throughput manner to obtain single-end or pair-end sequences. This is followed by the alignment of resulting reads to a reference genome or reference transcripts or *de novo* assembly in the absence of the genomic sequence to produce a genome-scale transcription map consisting of the expression level for each gene (WANG *et al.* 2009). In this context, RNA derived from *Drosophila* brain or muscle derived from the ALS models developed in this work can be used to precisely compare transcript expression levels of transgenic versus control flies, hence, defining pathways that are affected on loss of function of the gene under consideration.

Lastly, the effect of environmental modifiers may be analysed by exposing ALS fly models to different stressors which may include sensitivity to sedative effects of ethanol, starvation, heat and increased physical activity. The differences in lifespan between "stressed" and "unstressed" flies as well as those of controls can be compared to measure levels of modification by environmental stressors.

In addition, this could shed light on which ALS-associated genes are more susceptible to environmental modifiers which may also serve as potential therapeutic targets.

4.7 CONCLUSION

This study has highlighted important implications about ALS in the Maltese population. Although some patient population aspects, including incidence of ALS in Malta, are similar to those of neighbouring countries, conflicting findings were also identified, especially with regards to the genetic architecture. This emphasizes genetic isolation imposed by geographical distribution. The effects of *DCTN1* and *SCFD1* knockdown in *Drosophila* underscore a requirement of both genes for viability and normal neuromuscular function, which in part mimic the phenotypes observed in select Maltese ALS patients. Although one can speculate that consequent defects are associated with the disruption of vesicular trafficking and/or axonal transport, work on defining the precise pathophysiologic pathways is warranted. The genetic diversity observed in the Maltese ALS population, accentuates the need for personalised medicine therapy. Therefore, further elucidation is necessary to strengthen the molecular understanding of pathogenic mechanisms associated with disease aiming at singling out potential therapeutic targets.

CHAPTER 5

REFERENCES

Abe, K., Y. Itoyama, G. Sobue, S. Tsuji, M. Aoki *et al.*, 2014 Confirmatory double-blind, parallel-group, placebo-controlled study of efficacy and safety of edaravone (MCI-186) in amyotrophic lateral sclerosis patients. Amyotroph Lateral Scler Frontotemporal Degener 15**:** 610-617.

Abel, E. L., 2007 Football increases the risk for Lou Gehrig's disease, amyotrophic lateral sclerosis. Percept Mot Skills 104**:** 1251-1254.

Aggarwal, A., and G. Nicholson, 2005 Age dependent penetrance of three different superoxide dismutase 1 (sod 1) mutations. Int J Neurosci 115**:** 1119-1130.

Al-Chalabi, A., O. Hardiman, M. C. Kiernan, A. Chio, B. Rix-Brooks *et al.*, 2016 Amyotrophic lateral sclerosis: moving towards a new classification system. Lancet Neurol 15**:** 1182-1194.

Al-Saif, A., F. Al-Mohanna and S. Bohlega, 2011 A mutation in sigma-1 receptor causes juvenile amyotrophic lateral sclerosis. Ann Neurol 70**:** 913-919.

Alarcon, C. R., H. Goodarzi, H. Lee, X. Liu, S. Tavazoie *et al.*, 2015 HNRNPA2B1 Is a Mediator of m(6)A-Dependent Nuclear RNA Processing Events. Cell 162**:** 1299-1308.

Allen, A. M., T. S. Scheuermann, N. Nollen, D. Hatsukami and J. S. Ahluwalia, 2016 Gender Differences in Smoking Behavior and Dependence Motives Among Daily and Nondaily Smokers. Nicotine Tob Res 18**:** 1408-1413.

Alonso, A., G. Logroscino and M. A. Hernan, 2010 Smoking and the risk of amyotrophic lateral sclerosis: a systematic review and meta-analysis. J Neurol Neurosurg Psychiatry 81**:** 1249-1252.

Amado, D. A., and B. L. Davidson, 2021 Gene therapy for ALS: A review. Mol Ther.

Andersen, P. M., 2006 Amyotrophic lateral sclerosis associated with mutations in the CuZn superoxide dismutase gene. Curr Neurol Neurosci Rep 6**:** 37-46.

Aparicio-Erriu, I. M., and J. H. Prehn, 2012 Molecular Mechanisms in Amyotrophic Lateral Sclerosis: The Role of Angiogenin, a Secreted RNase. Front Neurosci 6**:** 167.

Araki, E., Y. Tsuboi, J. Daechsel, A. Milnerwood, C. Vilarino-Guell *et al.*, 2014 A novel DCTN1 mutation with late-onset parkinsonism and frontotemporal atrophy. Mov Disord 29**:** 1201-1204.

Armon, C., 2009 Smoking may be considered an established risk factor for sporadic ALS. Neurology 73**:** 1693-1698.

Armon, C., and M. E. Brandstater, 1999 Motor unit number estimate-based rates of progression of ALS predict patient survival. Muscle Nerve 22**:** 1571-1575.

Armon, C., M. C. Graves, D. Moses, D. K. Forte, L. Sepulveda *et al.*, 2000 Linear estimates of disease progression predict survival in patients with amyotrophic lateral sclerosis. Muscle Nerve 23**:** 874-882.

Arnold, E. S., S. C. Ling, S. C. Huelga, C. Lagier-Tourenne, M. Polymenidou *et al.*, 2013 ALS-linked TDP-43 mutations produce aberrant RNA splicing and adult-onset motor neuron disease without aggregation or loss of nuclear TDP-43. Proc Natl Acad Sci U S A 110**:** E736-745.

Ascherio, A., M. G. Weisskopf, J. O'Reilly E, E. J. Jacobs, M. L. McCullough *et al.*, 2005 Vitamin E intake and risk of amyotrophic lateral sclerosis. Ann Neurol 57**:** 104-110.

Ash, P. E. A., U. Dhawan, S. Boudeau, S. Lei, Y. Carlomagno *et al.*, 2019 Heavy Metal Neurotoxicants Induce ALS-Linked TDP-43 Pathology. Toxicol Sci 167**:** 105-115.

Auburger, G., N. E. Sen, D. Meierhofer, A. N. Basak and A. D. Gitler, 2017 Efficient Prevention of Neurodegenerative Diseases by Depletion of Starvation Response Factor Ataxin-2. Trends Neurosci 40**:** 507-516.

Azzouz, M., G. S. Ralph, E. Storkebaum, L. E. Walmsley, K. A. Mitrophanous *et al.*, 2004 VEGF delivery with retrogradely transported lentivector prolongs survival in a mouse ALS model. Nature 429**:** 413-417.

Baird, M. F., S. M. Graham, J. S. Baker and G. F. Bickerstaff, 2012 Creatine-kinase-and exercise-related muscle damage implications for muscle performance and recovery. J Nutr Metab 2012**:** 960363.

Bandettini di Poggio, M., M. P. Sormani, R. Truffelli, P. Mandich, P. Origone *et al.*, 2013 Clinical epidemiology of ALS in Liguria, Italy. Amyotroph Lateral Scler Frontotemporal Degener 14**:** 52-57.

Bando, Y., T. Katayama, M. Taniguchi, T. Ishibashi, N. Matsuo *et al.*, 2005 RA410/Sly1 suppresses MPP+ and 6-hydroxydopamine-induced cell death in SH-SY5Y cells. Neurobiol Dis 18**:** 143-151.

Barman, B., 2010 Clinical Sign Revisted: Hoffman's Sign. Indian Journal of Medical Specialities 1**:** 44-45.

Bartolome, F., H. C. Wu, V. S. Burchell, E. Preza, S. Wray *et al.*, 2013 Pathogenic VCP mutations induce mitochondrial uncoupling and reduced ATP levels. Neuron 78**:** 57-64.

Beaulieu, J. M., H. Jacomy and J. P. Julien, 2000 Formation of intermediate filament protein aggregates with disparate effects in two transgenic mouse models lacking the neurofilament light subunit. J Neurosci 20**:** 5321-5328.

Beck, M., P. Flachenecker, T. Magnus, R. Giess, K. Reiners *et al.*, 2005 Autonomic dysfunction in ALS: a preliminary study on the effects of intrathecal BDNF. Amyotroph Lateral Scler Other Motor Neuron Disord 6**:** 100-103.

Becker, L. A., B. Huang, G. Bieri, R. Ma, D. A. Knowles *et al.*, 2017 Therapeutic reduction of ataxin-2 extends lifespan and reduces pathology in TDP-43 mice. Nature 544**:** 367-371.

Beghi, E., G. Logroscino, A. Chio, O. Hardiman, A. Millul *et al.*, 2010 Amyotrophic lateral sclerosis, physical exercise, trauma and sports: results of a population-based pilot case-control study. Amyotroph Lateral Scler 11**:** 289-292.

Beghi, E., A. Millul, A. Micheli, E. Vitelli, G. Logroscino *et al.*, 2007 Incidence of ALS in Lombardy, Italy. Neurology 68**:** 141-145.

Belbasis, L., V. Bellou and E. Evangelou, 2016 Environmental Risk Factors and Amyotrophic Lateral Sclerosis: An Umbrella Review and Critical Assessment of Current Evidence from Systematic Reviews and Meta-Analyses of Observational Studies. Neuroepidemiology 46**:** 96-105.

Bendotti, C., M. Marino, C. Cheroni, E. Fontana, V. Crippa *et al.*, 2012 Dysfunction of constitutive and inducible ubiquitin-proteasome system in amyotrophic lateral sclerosis: implication for protein aggregation and immune response. Prog Neurobiol 97**:** 101-126.

Benjaminsen, E., K. B. Alstadhaug, M. Gulsvik, F. K. Baloch and F. Odeh, 2018 Amyotrophic lateral sclerosis in Nordland county, Norway, 2000-2015: prevalence, incidence, and clinical features. Amyotroph Lateral Scler Frontotemporal Degener 19**:** 522-527.

Bennett, C. L., S. G. Dastidar, S. C. Ling, B. Malik, T. Ashe *et al.*, 2018 Senataxin mutations elicit motor neuron degeneration phenotypes and yield TDP-43 mislocalization in ALS4 mice and human patients. Acta Neuropathol 136**:** 425-443.

Bensimon, G., L. Lacomblez and V. Meininger, 1994 A controlled trial of riluzole in amyotrophic lateral sclerosis. ALS/Riluzole Study Group. N Engl J Med 330**:** 585-591.

Bercier, V., J. M. Hubbard, K. Fidelin, K. Duroure, T. O. Auer *et al.*, 2019 Dynactin1 depletion leads to neuromuscular synapse instability and functional abnormalities. Mol Neurodegener 14**:** 27.

Bergeron, C., K. Beric-Maskarel, S. Muntasser, L. Weyer, M. J. Somerville *et al.*, 1994 Neurofilament light and polyadenylated mRNA levels are decreased in amyotrophic lateral sclerosis motor neurons. J Neuropathol Exp Neurol 53**:** 221-230.

Bjorkoy, G., T. Lamark and T. Johansen, 2006 p62/SQSTM1: a missing link between protein aggregates and the autophagy machinery. Autophagy 2**:** 138-139.

Blauw, H. M., A. Al-Chalabi, P. M. Andersen, P. W. van Vught, F. P. Diekstra *et al.*, 2010 A large genome scan for rare CNVs in amyotrophic lateral sclerosis. Hum Mol Genet 19**:** 4091-4099.

Blauw, H. M., W. van Rheenen, M. Koppers, P. Van Damme, S. Waibel *et al.*, 2012 NIPA1 polyalanine repeat expansions are associated with amyotrophic lateral sclerosis. Hum Mol Genet 21**:** 2497-2502.

Bodranghien, F., A. Bastian, C. Casali, M. Hallett, E. D. Louis *et al.*, 2016 Consensus Paper: Revisiting the Symptoms and Signs of Cerebellar Syndrome. Cerebellum 15**:** 369-391.

Boehringer, A., K. Garcia-Mansfield, G. Singh, N. Bakkar, P. Pirrotte *et al.*, 2017 ALS Associated Mutations in Matrin 3 Alter Protein-Protein Interactions and Impede mRNA Nuclear Export. Sci Rep 7**:** 14529.

Borel, F., G. Gernoux, B. Cardozo, J. P. Metterville, G. C. Toro Cabrera *et al.*, 2016 Therapeutic rAAVrh10 Mediated SOD1 Silencing in Adult SOD1(G93A) Mice and Nonhuman Primates. Hum Gene Ther 27**:** 19-31.

Borg, R., M. Farrugia Wismayer, K. Bonavia, A. Farrugia Wismayer, M. Vella *et al.*, 2021 Genetic analysis of ALS cases in the isolated island population of Malta. Eur J Hum Genet 29**:** 604-614.

Bradshaw, W. J., S. Rehman, T. T. Pham, N. Thiyagarajan, R. L. Lee *et al.*, 2017 Structural insights into human angiogenin variants implicated in Parkinson's disease and Amyotrophic Lateral Sclerosis. Sci Rep 7**:** 41996.

Brenner, D., K. Muller, T. Wieland, P. Weydt, S. Bohm *et al.*, 2016 NEK1 mutations in familial amyotrophic lateral sclerosis. Brain 139**:** e28.

Brenner, D., R. Yilmaz, K. Muller, T. Grehl, S. Petri *et al.*, 2018 Hot-spot KIF5A mutations cause familial ALS. Brain.

Brooks, B. R., 1994 El Escorial World Federation of Neurology criteria for the diagnosis of amyotrophic lateral sclerosis. Subcommittee on Motor Neuron Diseases/Amyotrophic Lateral Sclerosis of the World Federation of Neurology Research Group on Neuromuscular Diseases and the El Escorial "Clinical limits of amyotrophic lateral sclerosis" workshop contributors. J Neurol Sci 124 Suppl**:** 96-107.

Brooks, B. R., 1999 What are the implications of early diagnosis? Maintaining optimal health as long as possible. Neurology 53**:** S43-45; discussion S55-47.

Brooks, B. R., R. G. Miller, M. Swash, T. L. Munsat and D. World Federation of Neurology Research Group on Motor Neuron, 2000 El Escorial revisited: revised criteria for the diagnosis of amyotrophic lateral sclerosis. Amyotroph Lateral Scler Other Motor Neuron Disord 1**:** 293-299.

Brown, D. A., S. H. Kang, S. M. Gryaznov, L. DeDionisio, O. Heidenreich *et al.*, 1994 Effect of phosphorothioate modification of oligodeoxynucleotides on specific protein binding. J Biol Chem 269**:** 26801-26805.

Brown, R. H., Jr., and A. Al-Chalabi, 2017 Amyotrophic Lateral Sclerosis. N Engl J Med 377**:** 1602.

Bruijn, L. I., M. W. Becher, M. K. Lee, K. L. Anderson, N. A. Jenkins *et al.*, 1997 ALS-linked SOD1 mutant G85R mediates damage to astrocytes and promotes rapidly progressive disease with SOD1-containing inclusions. Neuron 18**:** 327-338.

Bruijn, L. I., M. K. Houseweart, S. Kato, K. L. Anderson, S. D. Anderson *et al.*, 1998 Aggregation and motor neuron toxicity of an ALS-linked SOD1 mutant independent from wild-type SOD1. Science 281**:** 1851-1854.

Burk, K., and R. J. Pasterkamp, 2019a Disrupted neuronal trafficking in amyotrophic lateral sclerosis. Acta Neuropathol 137**:** 859-877.

Burk, K., and R. J. Pasterkamp, 2019b Disrupted neuronal trafficking in amyotrophic lateral sclerosis. Acta Neuropathol.

Burke, D., L. Knowles, C. Andrews and P. Ashby, 1972 Spasticity, decerebrate rigidity and the clasp-knife phenomenon: an experimental study in the cat. Brain 95**:** 31-48.

Burrell, J. R., M. C. Kiernan, S. Vucic and J. R. Hodges, 2011 Motor neuron dysfunction in frontotemporal dementia. Brain 134**:** 2582-2594.

Byrne, S., M. Heverin, M. Elamin, P. Bede, C. Lynch *et al.*, 2013 Aggregation of neurologic and neuropsychiatric disease in amyotrophic lateral sclerosis kindreds: a population-based case-control cohort study of familial and sporadic amyotrophic lateral sclerosis. Ann Neurol 74**:** 699-708.

Cady, J., P. Allred, T. Bali, A. Pestronk, A. Goate *et al.*, 2015 Amyotrophic lateral sclerosis onset is influenced by the burden of rare variants in known amyotrophic lateral sclerosis genes. Ann Neurol 77**:** 100-113.

Calvo, A., A. Canosa, D. Bertuzzo, P. Cugnasco, L. Solero *et al.*, 2016 Influence of cigarette smoking on ALS outcome: a population-based study. J Neurol Neurosurg Psychiatry 87**:** 1229-1233.

Capelli, C., N. Redhead, V. Romano, F. Cali, G. Lefranc *et al.*, 2006 Population structure in the Mediterranean basin: a Y chromosome perspective. Ann Hum Genet 70**:** 207-225.

Cappella, M., C. Ciotti, M. Cohen-Tannoudji and M. G. Biferi, 2019 Gene Therapy for ALS-A Perspective. Int J Mol Sci 20.

Carmo-Silva, S., C. Nobrega, L. Pereira de Almeida and C. Cavadas, 2017 Unraveling the Role of Ataxin-2 in Metabolism. Trends Endocrinol Metab 28**:** 309-318.

Caroppo, P., I. Le Ber, F. Clot, S. Rivaud-Pechoux, A. Camuzat *et al.*, 2014 DCTN1 mutation analysis in families with progressive supranuclear palsy-like phenotypes. JAMA Neurol 71**:** 208-215.

Carr, C. M., and J. Rizo, 2010 At the junction of SNARE and SM protein function. Curr Opin Cell Biol 22**:** 488-495.

Cassar, M., C. Farrugia and C. Vidal, 2008 Allele frequencies of 14 STR loci in the population of Malta. Leg Med (Tokyo) 10**:** 153-156.

Castellanos-Montiel, M. J., M. Chaineau and T. M. Durcan, 2020 The Neglected Genes of ALS: Cytoskeletal Dynamics Impact Synaptic Degeneration in ALS. Front Cell Neurosci 14**:** 594975.

Cauchi, R. J., and M. van den Heuvel, 2006 The fly as a model for neurodegenerative diseases: is it worth the jump? Neurodegener Dis 3**:** 338-356.

Ceccanti, M., V. Pozzilli, C. Cambieri, L. Libonati, E. Onesti *et al.*, 2020 Creatine Kinase and Progression Rate in Amyotrophic Lateral Sclerosis. Cells 9.

Cedarbaum, J. M., and N. Stambler, 1997 Performance of the Amyotrophic Lateral Sclerosis Functional Rating Scale (ALSFRS) in multicenter clinical trials. J Neurol Sci 152 Suppl 1**:** S1-9.

Cedarbaum, J. M., N. Stambler, E. Malta, C. Fuller, D. Hilt *et al.*, 1999 The ALSFRS-R: a revised ALS functional rating scale that incorporates assessments of respiratory function. BDNF ALS Study Group (Phase III). J Neurol Sci 169**:** 13-21.

Cerero Lapiedra, R., L. A. Moreno Lopez and G. C. Esparza Gomez, 2002 Progressive bulbar palsy: a case report diagnosed by lingual symptoms. J Oral Pathol Med 31**:** 277-279.

Cermelli, C., M. Vinceti, F. Beretti, V. Pietrini, G. Nacci *et al.*, 2003 Risk of sporadic amyotrophic lateral sclerosis associated with seropositivity for herpesviruses and echovirus-7. Eur J Epidemiol 18**:** 123-127.

Cerritelli, S. M., and R. J. Crouch, 2009 Ribonuclease H: the enzymes in eukaryotes. FEBS J 276**:** 1494-1505.

Chen, S., P. Sayana, X. Zhang and W. Le, 2013 Genetics of amyotrophic lateral sclerosis: an update. Mol Neurodegener 8**:** 28.

Chen, S., X. Zhang, L. Song and W. Le, 2012 Autophagy dysregulation in amyotrophic lateral sclerosis. Brain Pathol 22**:** 110-116.

Chen, Y., Q. Zhou, X. Gu, Q. Wei, B. Cao *et al.*, 2018 An association study between SCFD1 rs10139154 variant and amyotrophic lateral sclerosis in a Chinese cohort. Amyotroph Lateral Scler Frontotemporal Degener 19**:** 413-418.

Chen, Y. Z., C. L. Bennett, H. M. Huynh, I. P. Blair, I. Puls *et al.*, 2004 DNA/RNA helicase gene mutations in a form of juvenile amyotrophic lateral sclerosis (ALS4). Am J Hum Genet 74**:** 1128-1135.

Chen, Y. Z., S. H. Hashemi, S. K. Anderson, Y. Huang, M. C. Moreira *et al.*, 2006 Senataxin, the yeast Sen1p orthologue: characterization of a unique protein in which recessive mutations cause ataxia and dominant mutations cause motor neuron disease. Neurobiol Dis 23**:** 97-108.

Chevalier-Larsen, E. S., K. E. Wallace, C. R. Pennise and E. L. Holzbaur, 2008 Lysosomal proliferation and distal degeneration in motor neurons expressing the G59S mutation in the p150Glued subunit of dynactin. Hum Mol Genet 17**:** 1946-1955.

Chia, R., A. Chio and B. J. Traynor, 2018 Novel genes associated with amyotrophic lateral sclerosis: diagnostic and clinical implications. Lancet Neurol 17**:** 94-102.

Chio, A., A. Calvo, G. Bovio, A. Canosa, D. Bertuzzo *et al.*, 2014 Amyotrophic lateral sclerosis outcome measures and the role of albumin and creatinine: a population-based study. JAMA Neurol 71**:** 1134-1142.

Chio, A., A. Calvo, N. Di Vito, M. Vercellino, P. Ghiglione *et al.*, 2003 Amyotrophic lateral sclerosis associated with pregnancy: report of four new cases and review of the literature. Amyotroph Lateral Scler Other Motor Neuron Disord 4**:** 45-48.

Chio, A., G. Logroscino, O. Hardiman, R. Swingler, D. Mitchell *et al.*, 2009a Prognostic factors in ALS: A critical review. Amyotroph Lateral Scler 10**:** 310-323.

Chio, A., G. Logroscino, B. J. Traynor, J. Collins, J. C. Simeone *et al.*, 2013 Global epidemiology of amyotrophic lateral sclerosis: a systematic review of the published literature. Neuroepidemiology 41**:** 118-130.

Chio, A., P. Meineri, A. Tribolo and D. Schiffer, 1991 Risk factors in motor neuron disease: a case-control study. Neuroepidemiology 10**:** 174-184.

Chio, A., G. Mora, A. Calvo, L. Mazzini, E. Bottacchi *et al.*, 2009b Epidemiology of ALS in Italy: a 10-year prospective population-based study. Neurology 72**:** 725-731.

Chio, A., G. Mora, M. Leone, L. Mazzini, D. Cocito *et al.*, 2002 Early symptom progression rate is related to ALS outcome: a prospective population-based study. Neurology 59**:** 99-103.

Chio, A., J. C. Schymick, G. Restagno, S. W. Scholz, F. Lombardo *et al.*, 2009c A two-stage genome-wide association study of sporadic amyotrophic lateral sclerosis. Hum Mol Genet 18**:** 1524-1532.

Chiriboga, C. A., K. J. Swoboda, B. T. Darras, S. T. Iannaccone, J. Montes *et al.*, 2016 Results from a phase 1 study of nusinersen (ISIS-SMN(Rx)) in children with spinal muscular atrophy. Neurology 86**:** 890-897.

Chow, C. Y., J. E. Landers, S. K. Bergren, P. C. Sapp, A. E. Grant *et al.*, 2009 Deleterious variants of FIG4, a phosphoinositide phosphatase, in patients with ALS. Am J Hum Genet 84**:** 85-88.

Chow, C. Y., Y. Zhang, J. J. Dowling, N. Jin, M. Adamska *et al.*, 2007 Mutation of FIG4 causes neurodegeneration in the pale tremor mouse and patients with CMT4J. Nature 448**:** 68-72.

Cirulli, E. T., B. N. Lasseigne, S. Petrovski, P. C. Sapp, P. A. Dion *et al.*, 2015 Exome sequencing in amyotrophic lateral sclerosis identifies risk genes and pathways. Science 347**:** 1436-1441.

Colombrita, C., E. Zennaro, C. Fallini, M. Weber, A. Sommacal *et al.*, 2009 TDP-43 is recruited to stress granules in conditions of oxidative insult. J Neurochem 111**:** 1051-1061.

Cook, T. M., D. Counsell, J. A. Wildsmith and P. Royal College of Anaesthetists Third National Audit, 2009 Major complications of central neuraxial block: report on the Third National Audit Project of the Royal College of Anaesthetists. Br J Anaesth 102**:** 179-190.

Cooper-Knock, J., T. Moll, T. Ramesh, L. Castelli, A. Beer *et al.*, 2019 Mutations in the Glycosyltransferase Domain of GLT8D1 Are Associated with Familial Amyotrophic Lateral Sclerosis. Cell Rep 26**:** 2298-2306 e2295.

Corrado, L., M. Brunetti, A. Di Pierro, M. Barberis, R. Croce *et al.*, 2019 Analysis of the GCG repeat length in NIPA1 gene in C9orf72-mediated ALS in a large Italian ALS cohort. Neurol Sci 40**:** 2537-2540.

Cote, F., J. F. Collard and J. P. Julien, 1993 Progressive neuronopathy in transgenic mice expressing the human neurofilament heavy gene: a mouse model of amyotrophic lateral sclerosis. Cell 73**:** 35-46.

Cox, L. E., L. Ferraiuolo, E. F. Goodall, P. R. Heath, A. Higginbottom *et al.*, 2010 Mutations in CHMP2B in lower motor neuron predominant amyotrophic lateral sclerosis (ALS). PLoS One 5**:** e9872.

Cudkowicz, M. E., D. McKenna-Yasek, P. E. Sapp, W. Chin, B. Geller *et al.*, 1997 Epidemiology of mutations in superoxide dismutase in amyotrophic lateral sclerosis. Ann Neurol 41**:** 210-221.

D'Ambrosio, M. V., and R. D. Vale, 2010 A whole genome RNAi screen of Drosophila S2 cell spreading performed using automated computational image analysis. J Cell Biol 191**:** 471-478.

D'Angiolella, V., V. Donato, S. Vijayakumar, A. Saraf, L. Florens *et al.*, 2010 SCF(Cyclin F) controls centrosome homeostasis and mitotic fidelity through CP110 degradation. Nature 466**:** 138-142.

Danneskiold-Samsoe, B., V. Kofod, J. Munter, G. Grimby, P. Schnohr *et al.*, 1984 Muscle strength and functional capacity in 78-81-year-old men and women. Eur J Appl Physiol Occup Physiol 52**:** 310-314.

Dascher, C., and W. E. Balch, 1996 Mammalian Sly1 regulates syntaxin 5 function in endoplasmic reticulum to Golgi transport. J Biol Chem 271**:** 15866-15869.

Datar, K. V., G. Dreyfuss and M. S. Swanson, 1993 The human hnRNP M proteins: identification of a methionine/arginine-rich repeat motif in ribonucleoproteins. Nucleic Acids Res 21**:** 439-446.

De Conti, L., M. V. Akinyi, R. Mendoza-Maldonado, M. Romano, M. Baralle *et al.*, 2015 TDP-43 affects splicing profiles and isoform production of genes involved in the apoptotic and mitotic cellular pathways. Nucleic Acids Res 43**:** 8990-9005.

de Jong, S. W., M. H. Huisman, N. A. Sutedja, A. J. van der Kooi, M. de Visser *et al.*, 2012 Smoking, alcohol consumption, and the risk of amyotrophic lateral sclerosis: a population-based study. Am J Epidemiol 176**:** 233-239.

De Marchi, F., M. F. Sarnelli, V. Solara, E. Bersano, R. Cantello *et al.*, 2019 Depression and risk of cognitive dysfunctions in amyotrophic lateral sclerosis. Acta Neurol Scand 139**:** 438-445.

DeJesus-Hernandez, M., I. R. Mackenzie, B. F. Boeve, A. L. Boxer, M. Baker *et al.*, 2011 Expanded GGGGCC hexanucleotide repeat in noncoding region of C9ORF72 causes chromosome 9p-linked FTD and ALS. Neuron 72**:** 245-256.

Demetriou, C. A., P. M. Hadjivasiliou, K. A. Kleopa, Y. P. Christou, E. Leonidou *et al.*, 2017 Epidemiology of Amyotrophic Lateral Sclerosis in the Republic of Cyprus: A 25-Year Retrospective Study. Neuroepidemiology 48**:** 79-85.

Deng, H., K. Gao and J. Jankovic, 2014 The role of FUS gene variants in neurodegenerative diseases. Nat Rev Neurol 10**:** 337-348.

Deng, H. X., W. Chen, S. T. Hong, K. M. Boycott, G. H. Gorrie *et al.*, 2011 Mutations in UBQLN2 cause dominant X-linked juvenile and adult-onset ALS and ALS/dementia. Nature 477**:** 211-215.

Dewey, C. M., B. Cenik, C. F. Sephton, D. R. Dries, P. Mayer, 3rd *et al.*, 2011 TDP-43 is directed to stress granules by sorbitol, a novel physiological osmotic and oxidative stressor. Mol Cell Biol 31**:** 1098-1108.

Dharmadasa, T., and M. C. Kiernan, 2018 Riluzole, disease stage and survival in ALS. Lancet Neurol 17**:** 385-386.

Di Gaetano, C., F. Voglino, S. Guarrera, G. Fiorito, F. Rosa *et al.*, 2012 An overview of the genetic structure within the Italian population from genome-wide data. PLoS One 7**:** e43759.

Dickerson, A. S., J. Hansen, M. A. Kioumourtzoglou, A. J. Specht, O. Gredal *et al.*, 2018 Study of occupation and amyotrophic lateral sclerosis in a Danish cohort. Occup Environ Med 75**:** 630-638.

Dodge, J. C., C. M. Treleaven, J. A. Fidler, M. Hester, A. Haidet *et al.*, 2010 AAV4-mediated expression of IGF-1 and VEGF within cellular components of the ventricular system improves survival outcome in familial ALS mice. Mol Ther 18**:** 2075-2084.

Dolzhenko, E., M. F. Bennett, P. A. Richmond, B. Trost, S. Chen *et al.*, 2020 ExpansionHunter Denovo: a computational method for locating known and novel repeat expansions in short-read sequencing data. Genome Biol 21**:** 102.

Dolzhenko, E., V. Deshpande, F. Schlesinger, P. Krusche, R. Petrovski *et al.*, 2019 ExpansionHunter: a sequence-graph-based tool to analyze variation in short tandem repeat regions. Bioinformatics 35**:** 4754-4756.

Dolzhenko, E., J. van Vugt, R. J. Shaw, M. A. Bekritsky, M. van Blitterswijk *et al.*, 2017 Detection of long repeat expansions from PCR-free whole-genome sequence data. Genome Res 27**:** 1895-1903.

Dong, C., P. Wei, X. Jian, R. Gibbs, E. Boerwinkle *et al.*, 2015 Comparison and integration of deleteriousness prediction methods for nonsynonymous SNVs in whole exome sequencing studies. Hum Mol Genet 24**:** 2125-2137.

Donnelly, C. J., P. W. Zhang, J. T. Pham, A. R. Haeusler, N. A. Mistry *et al.*, 2013 RNA toxicity from the ALS/FTD C9ORF72 expansion is mitigated by antisense intervention. Neuron 80**:** 415-428.

Dormann, D., and C. Haass, 2011 TDP-43 and FUS: a nuclear affair. Trends Neurosci 34**:** 339-348.

Dormann, D., R. Rodde, D. Edbauer, E. Bentmann, I. Fischer *et al.*, 2010 ALS-associated fused in sarcoma (FUS) mutations disrupt Transportin-mediated nuclear import. EMBO J 29**:** 2841-2857.

Dorst, J., L. Chen, A. Rosenbohm, J. Dreyhaupt, A. Hubers *et al.*, 2019 Prognostic factors in ALS: a comparison between Germany and China. J Neurol 266**:** 1516-1525.

Douglas, G. N., F.; Robertson, C., 2009 *Macleod's Clinical Examination*. CHURCHILL LIVINGSTONE Elsevier.

Dreyfuss, G., M. J. Matunis, S. Pinol-Roma and C. G. Burd, 1993 hnRNP proteins and the biogenesis of mRNA. Annu Rev Biochem 62**:** 289-321.

Duan, W., M. Guo, L. Yi, Y. Liu, Z. Li *et al.*, 2020 The deletion of mutant SOD1 via CRISPR/Cas9/sgRNA prolongs survival in an amyotrophic lateral sclerosis mouse model. Gene Ther 27**:** 157-169.

Duis, J., S. Dean, C. Applegate, A. Harper, R. Xiao *et al.*, 2016 KIF5A mutations cause an infantile onset phenotype including severe myoclonus with evidence of mitochondrial dysfunction. Ann Neurol 80**:** 633-637.

Duque, S., B. Joussemet, C. Riviere, T. Marais, L. Dubreil *et al.*, 2009 Intravenous administration of self-complementary AAV9 enables transgene delivery to adult motor neurons. Mol Ther 17**:** 1187-1196.

Dyck, P. J., C. J. Boes, D. Mulder, C. Millikan, A. J. Windebank *et al.*, 2005 History of standard scoring, notation, and summation of neuromuscular signs. A current survey and recommendation. J Peripher Nerv Syst 10**:** 158-173.

Eckstein, F., 2000 Phosphorothioate oligodeoxynucleotides: what is their origin and what is unique about them? Antisense Nucleic Acid Drug Dev 10**:** 117-121.

Elden, A. C., H. J. Kim, M. P. Hart, A. S. Chen-Plotkin, B. S. Johnson *et al.*, 2010 Ataxin-2 intermediate-length polyglutamine expansions are associated with increased risk for ALS. Nature 466**:** 1069-1075.

Evangelou, A., A. Ignatiou, C. Antoniou, S. Kalanidou, S. Chatzimatthaiou *et al.*, 2019 Unpredictable Effects of the Genetic Background of Transgenic Lines in Physiological Quantitative Traits. G3 (Bethesda) 9**:** 3877-3890.

Eymard-Pierre, E., G. Lesca, S. Dollet, F. M. Santorelli, M. di Capua *et al.*, 2002 Infantile-onset ascending hereditary spastic paralysis is associated with mutations in the alsin gene. Am J Hum Genet 71**:** 518-527.

Fallis, B. A., and O. Hardiman, 2009 Aggregation of neurodegenerative disease in ALS kindreds. Amyotroph Lateral Scler 10**:** 95-98.

Fang, F., U. Hallmarker, S. James, C. Ingre, K. Michaelsson *et al.*, 2016 Amyotrophic lateral sclerosis among cross-country skiers in Sweden. Eur J Epidemiol 31**:** 247-253.

Fang, F., P. Quinlan, W. Ye, M. K. Barber, D. M. Umbach *et al.*, 2009 Workplace exposures and the risk of amyotrophic lateral sclerosis. Environ Health Perspect 117**:** 1387-1392.

Fang, T., A. Al Khleifat, J. H. Meurgey, A. Jones, P. N. Leigh *et al.*, 2018 Stage at which riluzole treatment prolongs survival in patients with amyotrophic lateral sclerosis: a retrospective analysis of data from a dose-ranging study. Lancet Neurol 17**:** 416-422.

Fang, X., H. Lin, X. Wang, Q. Zuo, J. Qin *et al.*, 2015 The NEK1 interactor, C21ORF2, is required for efficient DNA damage repair. Acta Biochim Biophys Sin (Shanghai) 47**:** 834-841.

Farg, M. A., K. Y. Soo, S. T. Warraich, V. Sundaramoorthy, I. P. Blair *et al.*, 2013 Ataxin-2 interacts with FUS and intermediate-length polyglutamine expansions enhance FUS-related pathology in amyotrophic lateral sclerosis. Hum Mol Genet 22**:** 717-728.

Farg, M. A., V. Sundaramoorthy, J. M. Sultana, S. Yang, R. A. Atkinson *et al.*, 2014 C9ORF72, implicated in amytrophic lateral sclerosis and frontotemporal dementia, regulates endosomal trafficking. Hum Mol Genet 23**:** 3579-3595.

Farrer, M. J., M. M. Hulihan, J. M. Kachergus, J. C. Dachsel, A. J. Stoessl *et al.*, 2009 DCTN1 mutations in Perry syndrome. Nat Genet 41**:** 163-165.

Farrugia Wismayer, M., R. Borg, A. Farrugia Wismayer, K. Bonavia, M. Vella *et al.*, 2021 Occupation and amyotrophic lateral sclerosis risk: a case-control study in the isolated island population of Malta. Amyotroph Lateral Scler Frontotemporal Degener**:** 1-7.

Feiler, M. S., B. Strobel, A. Freischmidt, A. M. Helferich, J. Kappel *et al.*, 2015 TDP-43 is intercellularly transmitted across axon terminals. J Cell Biol 211**:** 897-911.

Felice, K. J., and W. A. North, 1998 Creatine kinase values in amyotrophic lateral sclerosis. J Neurol Sci 160 Suppl 1**:** S30-32.

Figley, M. D., G. Bieri, R. M. Kolaitis, J. P. Taylor and A. D. Gitler, 2014 Profilin 1 associates with stress granules and ALS-linked mutations alter stress granule dynamics. J Neurosci 34**:** 8083-8097.

Figley, M. D., W. Gu, J. D. Nanson, Y. Shi, Y. Sasaki *et al.*, 2021 SARM1 is a metabolic sensor activated by an increased NMN/NAD(+) ratio to trigger axon degeneration. Neuron 109**:** 1118-1136 e1111.

Filimonenko, M., S. Stuffers, C. Raiborg, A. Yamamoto, L. Malerod *et al.*, 2007 Functional multivesicular bodies are required for autophagic clearance of protein aggregates associated with neurodegenerative disease. J Cell Biol 179**:** 485-500.

Finkel, R. S., E. Mercuri, B. T. Darras, A. M. Connolly, N. L. Kuntz *et al.*, 2017 Nusinersen versus Sham Control in Infantile-Onset Spinal Muscular Atrophy. N Engl J Med 377**:** 1723-1732.

Floeter, M. K., and R. Mills, 2009 Progression in primary lateral sclerosis: a prospective analysis. Amyotroph Lateral Scler 10**:** 339-346.

Forbes, R. B., S. Colville, J. Parratt and R. J. Swingler, 2007 The incidence of motor nueron disease in Scotland. J Neurol 254**:** 866-869.

Forbes, R. B., S. Colville, R. J. Swingler and A. L. S. M. N. D. R. Scottish, 2004 The epidemiology of amyotrophic lateral sclerosis (ALS/MND) in people aged 80 or over. Age Ageing 33**:** 131-134.

Foust, K. D., E. Nurre, C. L. Montgomery, A. Hernandez, C. M. Chan *et al.*, 2009 Intravascular AAV9 preferentially targets neonatal neurons and adult astrocytes. Nat Biotechnol 27**:** 59-65.

Foust, K. D., D. L. Salazar, S. Likhite, L. Ferraiuolo, D. Ditsworth *et al.*, 2013 Therapeutic AAV9-mediated suppression of mutant SOD1 slows disease progression and extends survival in models of inherited ALS. Mol Ther 21**:** 2148-2159.

Free, R. B., L. A. Hazelwood and D. R. Sibley, 2009 Identifying novel protein-protein interactions using co-immunoprecipitation and mass spectroscopy. Curr Protoc Neurosci Chapter 5**:** Unit 5 28.

Freischmidt, A., T. Wieland, B. Richter, W. Ruf, V. Schaeffer *et al.*, 2015 Haploinsufficiency of TBK1 causes familial ALS and fronto-temporal dementia. Nat Neurosci 18**:** 631-636.

Gaj, T., D. S. Ojala, F. K. Ekman, L. C. Byrne, P. Limsirichai *et al.*, 2017 In vivo genome editing improves motor function and extends survival in a mouse model of ALS. Sci Adv 3**:** eaar3952.

Gallo, V., H. B. Bueno-De-Mesquita, R. Vermeulen, P. M. Andersen, A. Kyrozis *et al.*, 2009 Smoking and risk for amyotrophic lateral sclerosis: analysis of the EPIC cohort. Ann Neurol 65**:** 378-385.

Gallo, V., N. Vanacore, H. B. Bueno-de-Mesquita, R. Vermeulen, C. Brayne *et al.*, 2016 Physical activity and risk of Amyotrophic Lateral Sclerosis in a prospective cohort study. Eur J Epidemiol 31**:** 255-266.

Gary, J. D., T. K. Sato, C. J. Stefan, C. J. Bonangelino, L. S. Weisman *et al.*, 2002 Regulation of Fab1 phosphatidylinositol 3-phosphate 5-kinase pathway by Vac7 protein and Fig4, a polyphosphoinositide phosphatase family member. Mol Biol Cell 13**:** 1238-1251.

Gellera, C., N. Ticozzi, V. Pensato, L. Nanetti, A. Castucci *et al.*, 2012 ATAXIN2 CAG-repeat length in Italian patients with amyotrophic lateral sclerosis: risk factor or variant phenotype? Implication for genetic testing and counseling. Neurobiol Aging 33**:** 1847 e1815-1821.

Georgoulopoulou, E., M. Vinceti, F. Bonvicini, P. Sola, C. A. Goldoni *et al.*, 2011 Changing incidence and subtypes of ALS in Modena, Italy: A 10-years prospective study. Amyotroph Lateral Scler 12**:** 451-457.

Gerards, M., G. Cannino, J. M. Gonzalez de Cozar and H. T. Jacobs, 2018 Intracellular vesicle trafficking plays an essential role in mitochondrial quality control. Mol Biol Cell 29**:** 809-819.

Gibson, S. B., J. M. Downie, S. Tsetsou, J. E. Feusier, K. P. Figueroa *et al.*, 2017 The evolving genetic risk for sporadic ALS. Neurology 89**:** 226-233.

Gibson, S. B., E. J. Kasarskis, N. Hu, S. M. Pulst, M. S. Mendiondo *et al.*, 2015 Relationship of creatine kinase to body composition, disease state, and longevity in ALS. Amyotroph Lateral Scler Frontotemporal Degener 16**:** 473-477.

Gobba, F., F. Cavalleri, D. Bontadi, P. Torri and R. Dainese, 1995 Peripheral neuropathy in styrene-exposed workers. Scand J Work Environ Health 21**:** 517-520.

Gowell, M., I. Baker, O. Ansorge and M. Husain, 2020 Young-onset frontotemporal dementia with FUS pathology. Pract Neurol.

Greenway, M. J., P. M. Andersen, C. Russ, S. Ennis, S. Cashman *et al.*, 2006 ANG mutations segregate with familial and 'sporadic' amyotrophic lateral sclerosis. Nat Genet 38**:** 411-413.

Gregory, J. M. F., D.; Phatnani, H.; Harms, M. B., 2020 Genetics of Amyotrophic Lateral Sclerosis. Current Genetic Medicine Reports 8**:** 121-131.

Guil, S., and J. F. Caceres, 2007 The multifunctional RNA-binding protein hnRNP A1 is required for processing of miR-18a. Nat Struct Mol Biol 14**:** 591-596.

Gunnarsson, L. G., G. Lindberg, B. Soderfeldt and O. Axelson, 1991 Amyotrophic lateral sclerosis in Sweden in relation to occupation. Acta Neurol Scand 83**:** 394-398.

Gurney, M. E., H. Pu, A. Y. Chiu, M. C. Dal Canto, C. Y. Polchow *et al.*, 1994 Motor neuron degeneration in mice that express a human Cu,Zn superoxide dismutase mutation. Science 264**:** 1772-1775.

Haase, G., and C. Rabouille, 2015 Golgi Fragmentation in ALS Motor Neurons. New Mechanisms Targeting Microtubules, Tethers, and Transport Vesicles. Front Neurosci 9**:** 448.

Haghnia, M., V. Cavalli, S. B. Shah, K. Schimmelpfeng, R. Brusch *et al.*, 2007 Dynactin is required for coordinated bidirectional motility, but not for dynein membrane attachment. Mol Biol Cell 18**:** 2081-2089.

Hamidou, B., P. Couratier, C. Besancon, M. Nicol, P. M. Preux *et al.*, 2014 Epidemiological evidence that physical activity is not a risk factor for ALS. Eur J Epidemiol 29**:** 459-475.

Hand, C. K., R. S. Devon, F. Gros-Louis, D. Rochefort, J. Khoris *et al.*, 2003 Mutation screening of the ALS2 gene in sporadic and familial amyotrophic lateral sclerosis. Arch Neurol 60**:** 1768-1771.

Henriques, A., C. Pitzer and A. Schneider, 2010 Neurotrophic growth factors for the treatment of amyotrophic lateral sclerosis: where do we stand? Front Neurosci 4**:** 32.

Highley, J. R., J. Kirby, J. A. Jansweijer, P. S. Webb, C. A. Hewamadduma *et al.*, 2014 Loss of nuclear TDP-43 in amyotrophic lateral sclerosis (ALS) causes altered expression of splicing machinery and widespread dysregulation of RNA splicing in motor neurones. Neuropathol Appl Neurobiol 40**:** 670-685.

Hirano, M., C. M. Quinzii, H. Mitsumoto, A. P. Hays, J. K. Roberts *et al.*, 2011 Senataxin mutations and amyotrophic lateral sclerosis. Amyotroph Lateral Scler 12**:** 223-227.

Hirokawa, N., S. Niwa and Y. Tanaka, 2010 Molecular motors in neurons: transport mechanisms and roles in brain function, development, and disease. Neuron 68**:** 610-638.

Hogden, A., G. Foley, R. D. Henderson, N. James and S. M. Aoun, 2017 Amyotrophic lateral sclerosis: improving care with a multidisciplinary approach. J Multidiscip Healthc 10**:** 205-215.

Hoglinger, G. U., N. M. Melhem, D. W. Dickson, P. M. Sleiman, L. S. Wang *et al.*, 2011 Identification of common variants influencing risk of the tauopathy progressive supranuclear palsy. Nat Genet 43**:** 699-705.

Hou, N., Y. Yang, I. C. Scott and X. Lou, 2017 The Sec domain protein Scfd1 facilitates trafficking of ECM components during chondrogenesis. Dev Biol 421**:** 8-15.

Howe, K. L., P. Achuthan, J. Allen, J. Allen, J. Alvarez-Jarreta *et al.*, 2021 Ensembl 2021. Nucleic Acids Res 49**:** D884-D891.

Howes, S. C., G. M. Alushin, T. Shida, M. V. Nachury and E. Nogales, 2014 Effects of tubulin acetylation and tubulin acetyltransferase binding on microtubule structure. Mol Biol Cell 25**:** 257-266.

Howland, R. H., 1990 Schizophrenia and amyotrophic lateral sclerosis. Compr Psychiatry 31**:** 327-336.

Hu, J., J. Liu, L. Li, K. T. Gagnon and D. R. Corey, 2015 Engineering Duplex RNAs for Challenging Targets: Recognition of GGGGCC/CCCCGG Repeats at the ALS/FTD C9orf72 Locus. Chem Biol 22**:** 1505-1511.

Hu, J., F. Rigo, T. P. Prakash and D. R. Corey, 2017 Recognition of c9orf72 Mutant RNA by Single-Stranded Silencing RNAs. Nucleic Acid Ther 27**:** 87-94.

Huisman, M. H., S. W. de Jong, P. T. van Doormaal, S. S. Weinreich, H. J. Schelhaas *et al.*, 2011 Population based epidemiology of amyotrophic lateral sclerosis using capture-recapture methodology. J Neurol Neurosurg Psychiatry 82**:** 1165-1170.

Huisman, M. H., M. Seelen, S. W. de Jong, K. R. Dorresteijn, P. T. van Doormaal *et al.*, 2013 Lifetime physical activity and the risk of amyotrophic lateral sclerosis. J Neurol Neurosurg Psychiatry 84**:** 976-981.

Iacoangeli, A., A. Al Khleifat, A. R. Jones, W. Sproviero, A. Shatunov *et al.*, 2019 C9orf72 intermediate expansions of 24-30 repeats are associated with ALS. Acta Neuropathol Commun 7**:** 115.

Ikenaka, K., M. Katsuno, K. Kawai, S. Ishigaki, F. Tanaka *et al.*, 2012 Disruption of axonal transport in motor neuron diseases. Int J Mol Sci 13**:** 1225-1238.

Ikenaka, K., K. Kawai, M. Katsuno, Z. Huang, Y. M. Jiang *et al.*, 2013 dnc-1/dynactin 1 knockdown disrupts transport of autophagosomes and induces motor neuron degeneration. PLoS One 8**:** e54511.

Ilieva, H., M. Polymenidou and D. W. Cleveland, 2009 Non-cell autonomous toxicity in neurodegenerative disorders: ALS and beyond. J Cell Biol 187**:** 761-772.

Ilzecka, J., and Z. Stelmasiak, 2003 Creatine kinase activity in amyotrophic lateral sclerosis patients. Neurol Sci 24**:** 286-287.

Imbert, G., F. Saudou, G. Yvert, D. Devys, Y. Trottier *et al.*, 1996 Cloning of the gene for spinocerebellar ataxia 2 reveals a locus with high sensitivity to expanded CAG/glutamine repeats. Nat Genet 14**:** 285-291.

Infante, J., J. Berciano, V. Volpini, J. Corral, J. M. Polo *et al.*, 2004 Spinocerebellar ataxia type 2 with Levodopa-responsive parkinsonism culminating in motor neuron disease. Mov Disord 19**:** 848-852.

Ingre, C., P. M. Roos, F. Piehl, F. Kamel and F. Fang, 2015 Risk factors for amyotrophic lateral sclerosis. Clin Epidemiol 7**:** 181-193.

Irwin, D. J., C. T. McMillan, E. Suh, J. Powers, K. Rascovsky *et al.*, 2014 Myelin oligodendrocyte basic protein and prognosis in behavioral-variant frontotemporal dementia. Neurology 83**:** 502-509.

Ito, H., R. Wate, J. Zhang, S. Ohnishi, S. Kaneko *et al.*, 2008 Treatment with edaravone, initiated at symptom onset, slows motor decline and decreases SOD1 deposition in ALS mice. Exp Neurol 213**:** 448-455.

Iwasaki, Y., K. Ikeda and M. Kinoshita, 1995 Vitamin A and E levels are normal in amyotrophic lateral sclerosis. J Neurol Sci 132**:** 193-194.

Jawaid, A., S. B. Murthy, A. M. Wilson, S. U. Qureshi, M. J. Amro *et al.*, 2010 A decrease in body mass index is associated with faster progression of motor symptoms and shorter survival in ALS. Amyotroph Lateral Scler 11**:** 542-548.

Ji, J., J. Sundquist and K. Sundquist, 2016 Association of alcohol use disorders with amyotrophic lateral sclerosis: a Swedish national cohort study. Eur J Neurol 23**:** 270-275.

Jiang, J., Q. Zhu, T. F. Gendron, S. Saberi, M. McAlonis-Downes *et al.*, 2016 Gain of Toxicity from ALS/FTD-Linked Repeat Expansions in C9ORF72 Is Alleviated by

Antisense Oligonucleotides Targeting GGGGCC-Containing RNAs. Neuron 90**:** 535-550.

Johansson, L., X. Guo, M. Waern, S. Ostling, D. Gustafson *et al.*, 2010 Midlife psychological stress and risk of dementia: a 35-year longitudinal population study. Brain 133**:** 2217-2224.

Johnson, B. S., D. Snead, J. J. Lee, J. M. McCaffery, J. Shorter *et al.*, 2009 TDP-43 is intrinsically aggregation-prone, and amyotrophic lateral sclerosis-linked mutations accelerate aggregation and increase toxicity. J Biol Chem 284**:** 20329-20339.

Johnson, J. O., J. Mandrioli, M. Benatar, Y. Abramzon, V. M. Van Deerlin *et al.*, 2010 Exome sequencing reveals VCP mutations as a cause of familial ALS. Neuron 68**:** 857-864.

Johnson, J. O., E. P. Pioro, A. Boehringer, R. Chia, H. Feit *et al.*, 2014 Mutations in the Matrin 3 gene cause familial amyotrophic lateral sclerosis. Nat Neurosci 17**:** 664-666.

Jun, K. Y., J. Park, K. W. Oh, E. M. Kim, J. S. Bae *et al.*, 2019 Epidemiology of ALS in Korea using nationwide big data. J Neurol Neurosurg Psychiatry 90**:** 395-403.

Kacem, I., I. Sghaier, S. Bougatef, A. Nasri, A. Gargouri *et al.*, 2020 Epidemiological and clinical features of amyotrophic lateral sclerosis in a Tunisian cohort. Amyotroph Lateral Scler Frontotemporal Degener 21**:** 131-139.

Kamel, F., D. M. Umbach, R. S. Bedlack, M. Richards, M. Watson *et al.*, 2012 Pesticide exposure and amyotrophic lateral sclerosis. Neurotoxicology 33**:** 457-462.

Kamel, F., D. M. Umbach, T. L. Munsat, J. M. Shefner and D. P. Sandler, 1999 Association of cigarette smoking with amyotrophic lateral sclerosis. Neuroepidemiology 18**:** 194-202.

Kanekura, K., I. Nishimoto, S. Aiso and M. Matsuoka, 2006 Characterization of amyotrophic lateral sclerosis-linked P56S mutation of vesicle-associated membrane protein-associated protein B (VAPB/ALS8). J Biol Chem 281**:** 30223-30233.

Kang, H., E. S. Cha, G. J. Choi and W. J. Lee, 2014 Amyotrophic lateral sclerosis and agricultural environments: a systematic review. J Korean Med Sci 29**:** 1610-1617.

Karam, C., S. N. Scelsa and D. J. Macgowan, 2010 The clinical course of progressive bulbar palsy. Amyotroph Lateral Scler 11**:** 364-368.

Karcher, R. L., S. W. Deacon and V. I. Gelfand, 2002 Motor-cargo interactions: the key to transport specificity. Trends Cell Biol 12**:** 21-27.

Kaspar, B. K., J. Llado, N. Sherkat, J. D. Rothstein and F. H. Gage, 2003 Retrograde viral delivery of IGF-1 prolongs survival in a mouse ALS model. Science 301**:** 839-842.

Keleman, K., Micheler T., VDRC project members., 2009 RNAi-phiC31 construct and insertion data submitted by the Vienna Drosophila RNAi Center. FlyBase.

Kenna, K. P., R. L. McLaughlin, S. Byrne, M. Elamin, M. Heverin *et al.*, 2013 Delineating the genetic heterogeneity of ALS using targeted high-throughput sequencing. J Med Genet 50**:** 776-783.

Kenna, K. P., P. T. van Doormaal, A. M. Dekker, N. Ticozzi, B. J. Kenna *et al.*, 2016 NEK1 variants confer susceptibility to amyotrophic lateral sclerosis. Nat Genet 48**:** 1037-1042.

Kim, D., and J. Rossi, 2008 RNAi mechanisms and applications. Biotechniques 44**:** 613-616.

Kim, H. J., N. C. Kim, Y. D. Wang, E. A. Scarborough, J. Moore *et al.*, 2013 Mutations in prion-like domains in hnRNPA2B1 and hnRNPA1 cause multisystem proteinopathy and ALS. Nature 495**:** 467-473.

Kim, S., J. H. Jhong, J. Lee and J. Y. Koo, 2017 Meta-analytic support vector machine for integrating multiple omics data. BioData Min 10**:** 2.

Kim, W. K., X. Liu, J. Sandner, M. Pasmantier, J. Andrews *et al.*, 2009 Study of 962 patients indicates progressive muscular atrophy is a form of ALS. Neurology 73**:** 1686-1692.

Ko, H. S., T. Uehara, K. Tsuruma and Y. Nomura, 2004 Ubiquilin interacts with ubiquitylated proteins and proteasome through its ubiquitin-associated and ubiquitin-like domains. FEBS Lett 566**:** 110-114.

Kollewe, K., U. Mauss, K. Krampfl, S. Petri, R. Dengler *et al.*, 2008 ALSFRS-R score and its ratio: a useful predictor for ALS-progression. J Neurol Sci 275**:** 69-73.

Konermann, S., P. Lotfy, N. J. Brideau, J. Oki, M. N. Shokhirev *et al.*, 2018 Transcriptome Engineering with RNA-Targeting Type VI-D CRISPR Effectors. Cell 173**:** 665-676 e614.

Korner, S., J. Kammeyer, A. Zapf, M. Kuzma-Kozakiewicz, M. Piotrkiewicz *et al.*, 2019 Influence of Environment and Lifestyle on Incidence and Progress of Amyotrophic Lateral Sclerosis in A German ALS Population. Aging Dis 10**:** 205-216.

Krishnan, G., Y. Zhang, Y. Gu, M. W. Kankel, F. B. Gao *et al.*, 2020 CRISPR deletion of the C9ORF72 promoter in ALS/FTD patient motor neurons abolishes production of dipeptide repeat proteins and rescues neurodegeneration. Acta Neuropathol 140**:** 81-84.

Kuzma-Kozakiewicz, M., A. Chudy, B. Kazmierczak, D. Dziewulska, E. Usarek *et al.*, 2013 Dynactin Deficiency in the CNS of Humans with Sporadic ALS and Mice with Genetically Determined Motor Neuron Degeneration. Neurochem Res.

Kwiatkowski, T. J., Jr., D. A. Bosco, A. L. Leclerc, E. Tamrazian, C. R. Vanderburg *et al.*, 2009 Mutations in the FUS/TLS gene on chromosome 16 cause familial amyotrophic lateral sclerosis. Science 323**:** 1205-1208.

Kyotani, A., Y. Azuma, I. Yamamoto, H. Yoshida, I. Mizuta *et al.*, 2016 Knockdown of the Drosophila FIG4 induces deficient locomotive behavior, shortening of motor neuron, axonal targeting aberration, reduction of life span and defects in eye development. Exp Neurol 277**:** 86-95.

Lacomblez, L., G. Bensimon, P. N. Leigh, P. Guillet and V. Meininger, 1996 Dose-ranging study of riluzole in amyotrophic lateral sclerosis. Amyotrophic Lateral Sclerosis/Riluzole Study Group II. Lancet 347**:** 1425-1431.

Lagier-Tourenne, C., M. Baughn, F. Rigo, S. Sun, P. Liu *et al.*, 2013 Targeted degradation of sense and antisense C9orf72 RNA foci as therapy for ALS and frontotemporal degeneration. Proc Natl Acad Sci U S A 110**:** E4530-4539.

Lagier-Tourenne, C., M. Polymenidou, K. R. Hutt, A. Q. Vu, M. Baughn *et al.*, 2012 Divergent roles of ALS-linked proteins FUS/TLS and TDP-43 intersect in processing long pre-mRNAs. Nat Neurosci 15**:** 1488-1497.

Lai, C., C. Xie, H. Shim, J. Chandran, B. W. Howell *et al.*, 2009 Regulation of endosomal motility and degradation by amyotrophic lateral sclerosis 2/alsin. Mol Brain 2**:** 23.

Laird, F. M., M. H. Farah, S. Ackerley, A. Hoke, N. Maragakis *et al.*, 2008 Motor neuron disease occurring in a mutant dynactin mouse model is characterized by defects in vesicular trafficking. J Neurosci 28**:** 1997-2005.

LaMonte, B. H., K. E. Wallace, B. A. Holloway, S. S. Shelly, J. Ascano *et al.*, 2002 Disruption of dynein/dynactin inhibits axonal transport in motor neurons causing late-onset progressive degeneration. Neuron 34**:** 715-727.

Lattante, S., H. de Calbiac, I. Le Ber, A. Brice, S. Ciura *et al.*, 2015 Sqstm1 knock-down causes a locomotor phenotype ameliorated by rapamycin in a zebrafish model of ALS/FTLD. Hum Mol Genet 24**:** 1682-1690.

Lee, E. B., V. M. Lee and J. Q. Trojanowski, 2011 Gains or losses: molecular mechanisms of TDP43-mediated neurodegeneration. Nat Rev Neurosci 13**:** 38-50.

Lee, J., M. Kim, T. Q. Itoh and C. Lim, 2018 Ataxin-2: A versatile posttranscriptional regulator and its implication in neural function. Wiley Interdiscip Rev RNA 9**:** e1488.

Lee, J. H., and J. G. Gleeson, 2010 The role of primary cilia in neuronal function. Neurobiol Dis 38**:** 167-172.

Lee, J. R., J. F. Annegers and S. H. Appel, 1995 Prognosis of amyotrophic lateral sclerosis and the effect of referral selection. J Neurol Sci 132**:** 207-215.

Lehmer, C., P. Oeckl, J. H. Weishaupt, A. E. Volk, J. Diehl-Schmid *et al.*, 2017 Poly-GP in cerebrospinal fluid links C9orf72-associated dipeptide repeat expression to the asymptomatic phase of ALS/FTD. EMBO Mol Med 9**:** 859-868.

Leighton, D. J., J. Newton, L. J. Stephenson, S. Colville, R. Davenport *et al.*, 2019 Changing epidemiology of motor neurone disease in Scotland. J Neurol 266**:** 817-825.

Levine, T. P., R. D. Daniels, A. T. Gatta, L. H. Wong and M. J. Hayes, 2013 The product of C9orf72, a gene strongly implicated in neurodegeneration, is structurally related to DENN Rab-GEFs. Bioinformatics 29**:** 499-503.

Levy, J. R., C. J. Sumner, J. P. Caviston, M. K. Tokito, S. Ranganathan *et al.*, 2006 A motor neuron disease-associated mutation in p150Glued perturbs dynactin function and induces protein aggregation. J Cell Biol 172**:** 733-745.

Leyton-Jaimes, M. F., J. Kahn and A. Israelson, 2019 AAV2/9-mediated overexpression of MIF inhibits SOD1 misfolding, delays disease onset, and extends survival in mouse models of ALS. Proc Natl Acad Sci U S A 116**:** 14755-14760.

Li, J. Z., D. M. Absher, H. Tang, A. M. Southwick, A. M. Casto *et al.*, 2008 Worldwide human relationships inferred from genome-wide patterns of variation. Science 319**:** 1100-1104.

Li, Y., P. Ray, E. J. Rao, C. Shi, W. Guo *et al.*, 2010 A Drosophila model for TDP-43 proteinopathy. Proc Natl Acad Sci U S A 107**:** 3169-3174.

Lian, L., M. Liu, L. Cui, Y. Guan, T. Liu *et al.*, 2019 Environmental risk factors and amyotrophic lateral sclerosis (ALS): A case-control study of ALS in China. J Clin Neurosci 66**:** 12-18.

Lima, A. F., T. Evangelista and M. de Carvalho, 2003 Increased creatine kinase and spontaneous activity on electromyography, in amyotrophic lateral sclerosis. Electromyogr Clin Neurophysiol 43**:** 189-192.

Lin, J. S., and E. M. Lai, 2017 Protein-Protein Interactions: Co-Immunoprecipitation. Methods Mol Biol 1615**:** 211-219.

Ling, J. P., O. Pletnikova, J. C. Troncoso and P. C. Wong, 2015 TDP-43 repression of nonconserved cryptic exons is compromised in ALS-FTD. Science 349**:** 650-655.

Littleton, J. T., 2000 A genomic analysis of membrane trafficking and neurotransmitter release in Drosophila. J Cell Biol 150**:** F77-82.

Liu, J. L., 2017 Sparks of the CRISPR explosion: Applications in medicine and agriculture. J Genet Genomics 44**:** 413-414.

Liu, Y. T., M. Laura, J. Hersheson, A. Horga, Z. Jaunmuktane *et al.*, 2014 Extended phenotypic spectrum of KIF5A mutations: From spastic paraplegia to axonal neuropathy. Neurology 83**:** 612-619.

Liu-Yesucevitz, L., A. Bilgutay, Y. J. Zhang, T. Vanderweyde, A. Citro *et al.*, 2010 Tar DNA binding protein-43 (TDP-43) associates with stress granules: analysis of cultured cells and pathological brain tissue. PLoS One 5**:** e13250.

Livak, K. J., and T. D. Schmittgen, 2001 Analysis of relative gene expression data using real-time quantitative PCR and the 2(-Delta Delta C(T)) Method. Methods 25**:** 402-408.

Lloyd, T. E., J. Machamer, K. O'Hara, J. H. Kim, S. E. Collins *et al.*, 2012 The p150(Glued) CAP-Gly domain regulates initiation of retrograde transport at synaptic termini. Neuron 74**:** 344-360.

Logroscino, G., E. Beghi, S. Zoccolella, R. Palagano, A. Fraddosio *et al.*, 2005 Incidence of amyotrophic lateral sclerosis in southern Italy: a population based study. J Neurol Neurosurg Psychiatry 76**:** 1094-1098.

Logroscino, G., B. J. Traynor, O. Hardiman, A. Chio, P. Couratier *et al.*, 2008 Descriptive epidemiology of amyotrophic lateral sclerosis: new evidence and unsolved issues. J Neurol Neurosurg Psychiatry 79**:** 6-11.

Logroscino, G., B. J. Traynor, O. Hardiman, A. Chio, D. Mitchell *et al.*, 2010 Incidence of amyotrophic lateral sclerosis in Europe. J Neurol Neurosurg Psychiatry 81**:** 385-390.

Longinetti, E., and F. Fang, 2019 Epidemiology of amyotrophic lateral sclerosis: an update of recent literature. Curr Opin Neurol 32**:** 771-776.

Longinetti, E., D. Mariosa, H. Larsson, W. Ye, C. Ingre *et al.*, 2017 Neurodegenerative and psychiatric diseases among families with amyotrophic lateral sclerosis. Neurology 89**:** 578-585.

Longinetti, E., A. Regodon Wallin, K. Samuelsson, R. Press, A. Zachau *et al.*, 2018 The Swedish motor neuron disease quality registry. Amyotroph Lateral Scler Frontotemporal Degener 19**:** 528-537.

Lopez-Gonzalez, R., D. Yang, M. Pribadi, T. S. Kim, G. Krishnan *et al.*, 2019 Partial inhibition of the overactivated Ku80-dependent DNA repair pathway rescues neurodegeneration in C9ORF72-ALS/FTD. Proc Natl Acad Sci U S A 116**:** 9628-9633.

Lorenzoni, P. J., R. D. Ducci, G. O. Dalledone, C. S. K. Kay, S. M. de Almeida *et al.*, 2018 Motor neuron disease in patients with HIV infection: Report of two cases and brief review of the literature. Clin Neurol Neurosurg 171**:** 139-142.

Louwerse, E. S., C. E. Visser, P. M. Bossuyt and G. J. Weverling, 1997 Amyotrophic lateral sclerosis: mortality risk during the course of the disease and prognostic factors. The Netherlands ALS Consortium. J Neurol Sci 152 Suppl 1**:** S10-17.

Luna, J., M. Diagana, L. Ait Aissa, M. Tazir, L. Ali Pacha *et al.*, 2019 Clinical features and prognosis of amyotrophic lateral sclerosis in Africa: the TROPALS study. J Neurol Neurosurg Psychiatry 90**:** 20-29.

Magnus, T., M. Beck, R. Giess, I. Puls, M. Naumann *et al.*, 2002 Disease progression in amyotrophic lateral sclerosis: predictors of survival. Muscle Nerve 25**:** 709-714.

Majoor-Krakauer, D., R. Ottman, W. G. Johnson and L. P. Rowland, 1994 Familial aggregation of amyotrophic lateral sclerosis, dementia, and Parkinson's disease: evidence of shared genetic susceptibility. Neurology 44**:** 1872-1877.

Malek, A. M., A. Barchowsky, R. Bowser, T. Heiman-Patterson, D. Lacomis *et al.*, 2015 Exposure to hazardous air pollutants and the risk of amyotrophic lateral sclerosis. Environ Pollut 197**:** 181-186.

Malek, A. M., A. Barchowsky, R. Bowser, A. Youk and E. O. Talbott, 2012 Pesticide exposure as a risk factor for amyotrophic lateral sclerosis: a meta-analysis of epidemiological studies: pesticide exposure as a risk factor for ALS. Environ Res 117**:** 112-119.

Mandrioli, J., S. Biguzzi, C. Guidi, E. Sette, E. Terlizzi *et al.*, 2015 Heterogeneity in ALSFRS-R decline and survival: a population-based study in Italy. Neurol Sci 36**:** 2243-2252.

Mandrioli, J., S. Biguzzi, C. Guidi, E. Venturini, E. Sette *et al.*, 2014 Epidemiology of amyotrophic lateral sclerosis in Emilia Romagna Region (Italy): A population based study. Amyotroph Lateral Scler Frontotemporal Degener 15**:** 262-268.

Marangi, G., S. Lattante, P. N. Doronzio, A. Conte, G. Tasca *et al.*, 2017 Matrin 3 variants are frequent in Italian ALS patients. Neurobiol Aging 49**:** 218 e211-218 e217.

Marin, B., B. Hamidou, P. Couratier, M. Nicol, A. Delzor *et al.*, 2014 Population-based epidemiology of amyotrophic lateral sclerosis (ALS) in an ageing Europe--the French register of ALS in Limousin (FRALim register). Eur J Neurol 21**:** 1292-1300, e1278-1299.

Marsli, S., F. Mouni, A. Araqi, B. Elmoutawakil, H. Elotmani *et al.*, 2020 Can pregnancy decompensate an amyotrophic lateral sclerosis (ALS)? Case report and review of literature. Rev Neurol (Paris) 176**:** 216-217.

Mattsson, P., I. Lonnstedt, I. Nygren and H. Askmark, 2012 Physical fitness, but not muscle strength, is a risk factor for death in amyotrophic lateral sclerosis at an early age. J Neurol Neurosurg Psychiatry 83**:** 390-394.

McDonald, K. K., A. Aulas, L. Destroismaisons, S. Pickles, E. Beleac *et al.*, 2011 TAR DNA-binding protein 43 (TDP-43) regulates stress granule dynamics via differential regulation of G3BP and TIA-1. Hum Mol Genet 20**:** 1400-1410.

McGrail, M., J. Gepner, A. Silvanovich, S. Ludmann, M. Serr *et al.*, 1995 Regulation of cytoplasmic dynein function in vivo by the Drosophila Glued complex. J Cell Biol 131**:** 411-425.

McGuire, V., W. T. Longstreth, Jr., L. M. Nelson, T. D. Koepsell, H. Checkoway *et al.*, 1997 Occupational exposures and amyotrophic lateral sclerosis. A population-based case-control study. Am J Epidemiol 145**:** 1076-1088.

McGurk, L., A. Berson and N. M. Bonini, 2015 Drosophila as an In Vivo Model for Human Neurodegenerative Disease. Genetics 201**:** 377-402.

McKee, A. C., B. E. Gavett, R. A. Stern, C. J. Nowinski, R. C. Cantu *et al.*, 2010 TDP-43 proteinopathy and motor neuron disease in chronic traumatic encephalopathy. J Neuropathol Exp Neurol 69**:** 918-929.

McLaughlin, R. L., D. Schijven, W. van Rheenen, K. R. van Eijk, M. O'Brien *et al.*, 2017 Genetic correlation between amyotrophic lateral sclerosis and schizophrenia. Nat Commun 8**:** 14774.

Medical Research Council, 1943 Aids to the invesigation of the peripheral nervous system, pp., edited by L. H. M. s. S. Office. Medcial Research Council.

Mehta, P., W. Kaye, J. Raymond, R. Punjani, T. Larson *et al.*, 2018 Prevalence of Amyotrophic Lateral Sclerosis - United States, 2015. MMWR Morb Mortal Wkly Rep 67**:** 1285-1289.

Mendell, J. R., S. Al-Zaidy, R. Shell, W. D. Arnold, L. R. Rodino-Klapac *et al.*, 2017 Single-Dose Gene-Replacement Therapy for Spinal Muscular Atrophy. N Engl J Med 377**:** 1713-1722.

Meng, E., S. Yu, J. Dou, W. Jin, X. Cai *et al.*, 2016 Association between alcohol consumption and amyotrophic lateral sclerosis: a meta-analysis of five observational studies. Neurol Sci 37**:** 1203-1208.

Meyer, H., M. Bug and S. Bremer, 2012 Emerging functions of the VCP/p97 AAA-ATPase in the ubiquitin system. Nat Cell Biol 14**:** 117-123.

Michal Freedman, D., R. W. Kuncl, S. J. Weinstein, N. Malila, J. Virtamo *et al.*, 2013 Vitamin E serum levels and controlled supplementation and risk of amyotrophic lateral sclerosis. Amyotroph Lateral Scler Frontotemporal Degener 14**:** 246-251.

Mili, S., H. J. Shu, Y. Zhao and S. Pinol-Roma, 2001 Distinct RNP complexes of shuttling hnRNP proteins with pre-mRNA and mRNA: candidate intermediates in formation and export of mRNA. Mol Cell Biol 21**:** 7307-7319.

Miller, T., M. Cudkowicz, P. J. Shaw, P. M. Andersen, N. Atassi *et al.*, 2020 Phase 1-2 Trial of Antisense Oligonucleotide Tofersen for SOD1 ALS. N Engl J Med 383**:** 109-119.

Miller, T. M., A. Pestronk, W. David, J. Rothstein, E. Simpson *et al.*, 2013 An antisense oligonucleotide against SOD1 delivered intrathecally for patients with SOD1 familial amyotrophic lateral sclerosis: a phase 1, randomised, first-in-man study. Lancet Neurol 12**:** 435-442.

Mitchell, J., P. Paul, H. J. Chen, A. Morris, M. Payling *et al.*, 2010a Familial amyotrophic lateral sclerosis is associated with a mutation in D-amino acid oxidase. Proc Natl Acad Sci U S A 107**:** 7556-7561.

Mitchell, J. D., P. Callagher, J. Gardham, C. Mitchell, M. Dixon *et al.*, 2010b Timelines in the diagnostic evaluation of people with suspected amyotrophic lateral sclerosis (ALS)/motor neuron disease (MND)--a 20-year review: can we do better? Amyotroph Lateral Scler 11**:** 537-541.

Moghadam-Kia, S., C. V. Oddis and R. Aggarwal, 2016 Approach to asymptomatic creatine kinase elevation. Cleve Clin J Med 83**:** 37-42.

Montague, P., A. S. McCallion, R. W. Davies and I. R. Griffiths, 2006 Myelin-associated oligodendrocytic basic protein: a family of abundant CNS myelin proteins in search of a function. Dev Neurosci 28**:** 479-487.

Morotz, G. M., K. J. De Vos, A. Vagnoni, S. Ackerley, C. E. Shaw *et al.*, 2012 Amyotrophic lateral sclerosis-associated mutant VAPBP56S perturbs calcium homeostasis to disrupt axonal transport of mitochondria. Hum Mol Genet 21**:** 1979-1988.

Morrow, J. M., and M. M. Reilly, 2011 The Babinski sign. Br J Hosp Med (Lond) 72**:** M157-159.

Mueller, C., J. D. Berry, D. M. McKenna-Yasek, G. Gernoux, M. A. Owegi *et al.*, 2020 SOD1 Suppression with Adeno-Associated Virus and MicroRNA in Familial ALS. N Engl J Med 383**:** 151-158.

Mukherjee, A., and A. Chakravarty, 2010 Spasticity mechanisms - for the clinician. Front Neurol 1**:** 149.

Munch, C., A. Rosenbohm, A. D. Sperfeld, I. Uttner, S. Reske *et al.*, 2005 Heterozygous R1101K mutation of the DCTN1 gene in a family with ALS and FTD. Ann Neurol 58**:** 777-780.

Murlidharan, G., R. J. Samulski and A. Asokan, 2014 Biology of adeno-associated viral vectors in the central nervous system. Front Mol Neurosci 7**:** 76.

Nakajima, K., X. Yin, Y. Takei, D. H. Seog, N. Homma *et al.*, 2012 Molecular motor KIF5A is essential for GABA(A) receptor transport, and KIF5A deletion causes epilepsy. Neuron 76**:** 945-961.

Nakamura, R., N. Atsuta, H. Watanabe, A. Hirakawa, H. Watanabe *et al.*, 2013 Neck weakness is a potent prognostic factor in sporadic amyotrophic lateral sclerosis patients. J Neurol Neurosurg Psychiatry 84**:** 1365-1371.

Nanetti, L., R. Fancellu, C. Tomasello, C. Gellera, D. Pareyson *et al.*, 2009 Rare association of motor neuron disease and spinocerebellar ataxia type 2 (SCA2): a new case and review of the literature. J Neurol 256**:** 1926-1928.

Naqvi, U., and A. Sherman, 2018 Muscle Strength Grading in *StatPearls*, Treasure Island (FL).

National Statistics Office, 2014 Malta Population and Migration Statistics, pp.

Neumann, M., R. Rademakers, S. Roeber, M. Baker, H. A. Kretzschmar *et al.*, 2009 A new subtype of frontotemporal lobar degeneration with FUS pathology. Brain 132**:** 2922-2931.

Neumann, M., D. M. Sampathu, L. K. Kwong, A. C. Truax, M. C. Micsenyi *et al.*, 2006 Ubiquitinated TDP-43 in frontotemporal lobar degeneration and amyotrophic lateral sclerosis. Science 314**:** 130-133.

Nguyen, H. P., C. Van Broeckhoven and J. van der Zee, 2018 ALS Genes in the Genomic Era and their Implications for FTD. Trends Genet 34**:** 404-423.

Nicolas, A., K. P. Kenna, A. E. Renton, N. Ticozzi, F. Faghri *et al.*, 2018 Genome-wide Analyses Identify KIF5A as a Novel ALS Gene. Neuron 97**:** 1268-1283 e1266.

Nishimura, A. L., M. Mitne-Neto, H. C. Silva, A. Richieri-Costa, S. Middleton *et al.*, 2004 A mutation in the vesicle-trafficking protein VAPB causes late-onset spinal muscular atrophy and amyotrophic lateral sclerosis. Am J Hum Genet 75**:** 822-831.

Nogueira, C., P. Erlmann, J. Villeneuve, A. J. Santos, E. Martinez-Alonso *et al.*, 2014 SLY1 and Syntaxin 18 specify a distinct pathway for procollagen VII export from the endoplasmic reticulum. Elife 3**:** e02784.

Nolle, M., Axisa, N., Vella, L., 2005 State of the Environment Report for Malta 2005 - Background Report on Air Quality, pp. Environment & Resources Authority, Ambient Air Quality Publications.

Nonhoff, U., M. Ralser, F. Welzel, I. Piccini, D. Balzereit *et al.*, 2007 Ataxin-2 interacts with the DEAD/H-box RNA helicase DDX6 and interferes with P-bodies and stress granules. Mol Biol Cell 18**:** 1385-1396.

Norris, F., R. Shepherd, E. Denys, K. U, E. Mukai *et al.*, 1993 Onset, natural history and outcome in idiopathic adult motor neuron disease. J Neurol Sci 118**:** 48-55.

O'Brien, M., T. Burke, M. Heverin, A. Vajda, R. McLaughlin *et al.*, 2017 Clustering of Neuropsychiatric Disease in First-Degree and Second-Degree Relatives of Patients With Amyotrophic Lateral Sclerosis. JAMA Neurol 74**:** 1425-1430.

O'Toole, O., B. J. Traynor, P. Brennan, C. Sheehan, E. Frost *et al.*, 2008 Epidemiology and clinical features of amyotrophic lateral sclerosis in Ireland between 1995 and 2004. J Neurol Neurosurg Psychiatry 79**:** 30-32.

Oakes, J. A., M. C. Davies and M. O. Collins, 2017 TBK1: a new player in ALS linking autophagy and neuroinflammation. Mol Brain 10**:** 5.

Okamoto, K., T. Kihira, T. Kondo, G. Kobashi, M. Washio *et al.*, 2009 Lifestyle factors and risk of amyotrophic lateral sclerosis: a case-control study in Japan. Ann Epidemiol 19**:** 359-364.

Okumura, H., L. T. Kurland and S. C. Waring, 1995 Amyotrophic lateral sclerosis and polio: is there an association? Ann N Y Acad Sci 753**:** 245-256.

Orlacchio, A., C. Babalini, A. Borreca, C. Patrono, R. Massa *et al.*, 2010 SPATACSIN mutations cause autosomal recessive juvenile amyotrophic lateral sclerosis. Brain 133**:** 591-598.

Paisan-Ruiz, C., O. Dogu, A. Yilmaz, H. Houlden and A. Singleton, 2008 SPG11 mutations are common in familial cases of complicated hereditary spastic paraplegia. Neurology 70**:** 1384-1389.

Palese, F., A. Sartori, L. Verriello, S. Ros, P. Passadore *et al.*, 2019 Epidemiology of amyotrophic lateral sclerosis in Friuli-Venezia Giulia, North-Eastern Italy, 2002-2014: a retrospective population-based study. Amyotroph Lateral Scler Frontotemporal Degener 20**:** 90-99.

Pampel, F. C., 2006 Global Patterns and Determinants of Sex Differences in Smoking. Int J Comp Sociol 47**:** 466-487.

Pamphlett, R., and A. Rikard-Bell, 2013 Different occupations associated with amyotrophic lateral sclerosis: is diesel exhaust the link? PLoS One 8**:** e80993.

Parkin Kullmann, J. A., S. Hayes and R. Pamphlett, 2018 Is psychological stress a predisposing factor for amyotrophic lateral sclerosis (ALS)? An online international case-control study of premorbid life events, occupational stress, resilience and anxiety. PLoS One 13**:** e0204424.

Pei, J., R. Sadreyev and N. V. Grishin, 2003 PCMA: fast and accurate multiple sequence alignment based on profile consistency. Bioinformatics 19**:** 427-428.

Perrone, B., and F. L. Conforti, 2020 Common mutations of interest in the diagnosis of amyotrophic lateral sclerosis: how common are common mutations in ALS genes? Expert Rev Mol Diagn 20**:** 703-714.

Peters, S., A. E. Visser, F. D'Ovidio, J. Vlaanderen, L. Portengen *et al.*, 2019 Effect modification of the association between total cigarette smoking and ALS risk by intensity, duration and time-since-quitting: Euro-MOTOR. J Neurol Neurosurg Psychiatry.

Peters, S., A. E. Visser, F. D'Ovidio, J. Vlaanderen, L. Portengen *et al.*, 2020 Effect modification of the association between total cigarette smoking and ALS risk by intensity, duration and time-since-quitting: Euro-MOTOR. J Neurol Neurosurg Psychiatry 91**:** 33-39.

Petri, S., and G. Meister, 2013 siRNA design principles and off-target effects. Methods Mol Biol 986**:** 59-71.

Pfohl, S. R., R. B. Kim, G. S. Coan and C. S. Mitchell, 2018 Unraveling the Complexity of Amyotrophic Lateral Sclerosis Survival Prediction. Front Neuroinform 12**:** 36.

Phukan, J., M. Elamin, P. Bede, N. Jordan, L. Gallagher *et al.*, 2012 The syndrome of cognitive impairment in amyotrophic lateral sclerosis: a population-based study. J Neurol Neurosurg Psychiatry 83**:** 102-108.

Pilling, A. D., D. Horiuchi, C. M. Lively and W. M. Saxton, 2006 Kinesin-1 and Dynein are the primary motors for fast transport of mitochondria in Drosophila motor axons. Mol Biol Cell 17**:** 2057-2068.

Pinto, S., and M. de Carvalho, 2008 Motor responses of the sternocleidomastoid muscle in patients with amyotrophic lateral sclerosis. Muscle Nerve 38**:** 1312-1317.

Pinto, S., M. Gromicho and M. de Carvalho, 2019 Assessing upper limb function with ALSFRS-R in amyotrophic lateral sclerosis patients. Amyotroph Lateral Scler Frontotemporal Degener 20**:** 445-448.

Polymenidou, M., C. Lagier-Tourenne, K. R. Hutt, S. C. Huelga, J. Moran *et al.*, 2011 Long pre-mRNA depletion and RNA missplicing contribute to neuronal vulnerability from loss of TDP-43. Nat Neurosci 14**:** 459-468.

Pradas, J., T. Puig, R. Rojas-Garcia, M. L. Viguera, I. Gich *et al.*, 2013 Amyotrophic lateral sclerosis in Catalonia: a population based study. Amyotroph Lateral Scler Frontotemporal Degener 14**:** 278-283.

Prasad, A., V. Bharathi, V. Sivalingam, A. Girdhar and B. K. Patel, 2019 Molecular Mechanisms of TDP-43 Misfolding and Pathology in Amyotrophic Lateral Sclerosis. Front Mol Neurosci 12**:** 25.

Pringle, C. E., A. J. Hudson, D. G. Munoz, J. A. Kiernan, W. F. Brown *et al.*, 1992 Primary lateral sclerosis. Clinical features, neuropathology and diagnostic criteria. Brain 115 (Pt 2)**:** 495-520.

Project MinE, E. A. L. S. S. C., 2018 Project MinE: study design and pilot analyses of a large-scale whole-genome sequencing study in amyotrophic lateral sclerosis. Eur J Hum Genet 26**:** 1537-1546.

Pugliatti, M., L. D. Parish, P. Cossu, S. Leoni, A. Ticca *et al.*, 2013 Amyotrophic lateral sclerosis in Sardinia, insular Italy, 1995-2009. J Neurol 260**:** 572-579.

Puls, I., C. Jonnakuty, B. H. LaMonte, E. L. Holzbaur, M. Tokito *et al.*, 2003 Mutant dynactin in motor neuron disease. Nat Genet 33**:** 455-456.

Pupillo, E., E. Bianchi, A. Chio, F. Casale, C. Zecca *et al.*, 2018 Amyotrophic lateral sclerosis and food intake. Amyotroph Lateral Scler Frontotemporal Degener 19**:** 267-274.

Rafiq, M. K., E. Lee, M. Bradburn, C. J. McDermott and P. J. Shaw, 2016 Creatine kinase enzyme level correlates positively with serum creatinine and lean body mass, and is a prognostic factor for survival in amyotrophic lateral sclerosis. Eur J Neurol 23**:** 1071-1078.

Ragonese, P., E. Cellura, P. Aridon, M. D'Amelio, R. Spataro *et al.*, 2012 Incidence of amyotrophic lateral sclerosis in Sicily: A population based study. Amyotroph Lateral Scler 13**:** 284-287.

Rainier, S., J. H. Chai, D. Tokarz, R. D. Nicholls and J. K. Fink, 2003 NIPA1 gene mutations cause autosomal dominant hereditary spastic paraplegia (SPG6). Am J Hum Genet 73**:** 967-971.

Ralser, M., M. Albrecht, U. Nonhoff, T. Lengauer, H. Lehrach *et al.*, 2005 An integrative approach to gain insights into the cellular function of human ataxin-2. J Mol Biol 346**:** 203-214.

Ratner, M. H., J. F. Jabre, W. M. Ewing, M. Abou-Donia and L. C. Oliver, 2018 Amyotrophic lateral sclerosis-A case report and mechanistic review of the

association with toluene and other volatile organic compounds. Am J Ind Med 61**:** 251-260.

Ravits, J. M., and A. R. La Spada, 2009 ALS motor phenotype heterogeneity, focality, and spread: deconstructing motor neuron degeneration. Neurology 73**:** 805-811.

Reid, E., M. Kloos, A. Ashley-Koch, L. Hughes, S. Bevan *et al.*, 2002 A kinesin heavy chain (KIF5A) mutation in hereditary spastic paraplegia (SPG10). Am J Hum Genet 71**:** 1189-1194.

Renna, M., C. Schaffner, A. R. Winslow, F. M. Menzies, A. A. Peden *et al.*, 2011 Autophagic substrate clearance requires activity of the syntaxin-5 SNARE complex. J Cell Sci 124**:** 469-482.

Renton, A. E., A. Chio and B. J. Traynor, 2014 State of play in amyotrophic lateral sclerosis genetics. Nat Neurosci 17**:** 17-23.

Renton, A. E., E. Majounie, A. Waite, J. Simon-Sanchez, S. Rollinson *et al.*, 2011 A hexanucleotide repeat expansion in C9ORF72 is the cause of chromosome 9p21-linked ALS-FTD. Neuron 72**:** 257-268.

Rentzsch, P., D. Witten, G. M. Cooper, J. Shendure and M. Kircher, 2019 CADD: predicting the deleteriousness of variants throughout the human genome. Nucleic Acids Res 47**:** D886-D894.

Richards, S., N. Aziz, S. Bale, D. Bick, S. Das *et al.*, 2015 Standards and guidelines for the interpretation of sequence variants: a joint consensus recommendation of the American College of Medical Genetics and Genomics and the Association for Molecular Pathology. Genet Med 17**:** 405-424.

Riviere, M., V. Meininger, P. Zeisser and T. Munsat, 1998 An analysis of extended survival in patients with amyotrophic lateral sclerosis treated with riluzole. Arch Neurol 55**:** 526-528.

Robertson, J., M. M. Doroudchi, M. D. Nguyen, H. D. Durham, M. J. Strong *et al.*, 2003 A neurotoxic peripherin splice variant in a mouse model of ALS. J Cell Biol 160**:** 939-949.

Rodriguez-Beato, F. Y., and O. De Jesus, 2021 Physiology, Deep Tendon Reflexes in *StatPearls*, Treasure Island (FL).

Roman, G. C., 1996 Neuroepidemiology of amyotrophic lateral sclerosis: clues to aetiology and pathogenesis. J Neurol Neurosurg Psychiatry 61**:** 131-137.

Roos, E., D. Mariosa, C. Ingre, C. Lundholm, K. Wirdefeldt *et al.*, 2016 Depression in amyotrophic lateral sclerosis. Neurology 86**:** 2271-2277.

Rose, L., D. McKim, D. Leasa, M. Nonoyama, A. Tandon *et al.*, 2019 Trends in incidence, prevalence, and mortality of neuromuscular disease in Ontario, Canada: A population-based retrospective cohort study (2003-2014). PLoS One 14**:** e0210574.

Rosen, D. R., 1993 Mutations in Cu/Zn superoxide dismutase gene are associated with familial amyotrophic lateral sclerosis. Nature 364**:** 362.

Rosenblum, L. T., and D. Trotti, 2017 EAAT2 and the Molecular Signature of Amyotrophic Lateral Sclerosis. Adv Neurobiol 16**:** 117-136.

Rosenbohm, A., M. Liu, G. Nagel, R. S. Peter, B. Cui *et al.*, 2018 Phenotypic differences of amyotrophic lateral sclerosis (ALS) in China and Germany. J Neurol 265**:** 774-782.

Ross, O. A., N. J. Rutherford, M. Baker, A. I. Soto-Ortolaza, M. M. Carrasquillo *et al.*, 2011 Ataxin-2 repeat-length variation and neurodegeneration. Hum Mol Genet 20**:** 3207-3212.

Rowe, T., C. Dascher, S. Bannykh, H. Plutner and W. E. Balch, 1998 Role of vesicle-associated syntaxin 5 in the assembly of pre-Golgi intermediates. Science 279**:** 696-700.

Rowland, L. P., 1991 Ten central themes in a decade of ALS research. Adv Neurol 56**:** 3-23.

Rutter-Locher, Z., M. R. Turner, P. N. Leigh and A. Al-Chalabi, 2016 Analysis of terms used for the diagnosis and classification of amyotrophic lateral sclerosis and motor neuron disease. Amyotroph Lateral Scler Frontotemporal Degener 17**:** 600-604.

Ryan, M., T. Zaldivar Vaillant, R. L. McLaughlin, M. A. Doherty, J. Rooney *et al.*, 2019 Comparison of the clinical and genetic features of amyotrophic lateral sclerosis across Cuban, Uruguayan and Irish clinic-based populations. J Neurol Neurosurg Psychiatry 90**:** 659-665.

Saccon, R. A., R. K. Bunton-Stasyshyn, E. M. Fisher and P. Fratta, 2013 Is SOD1 loss of function involved in amyotrophic lateral sclerosis? Brain 136**:** 2342-2358.

Said, E., J. X. Chong, M. Hempel, J. Denecke, P. Soler *et al.*, 2017 Survival beyond the perinatal period expands the phenotypes caused by mutations in GLE1. Am J Med Genet A 173**:** 3098-3103.

Salton, M., R. Elkon, T. Borodina, A. Davydov, M. L. Yaspo *et al.*, 2011 Matrin 3 binds and stabilizes mRNA. PLoS One 6**:** e23882.

Sanmarti, R., A. Collado, J. Gratacos, B. E. Herrera, J. Font *et al.*, 1996 Reduced serum creatine kinase activity in inflammatory rheumatic diseases. J Rheumatol 23**:** 310-312.

Sareen, D., J. G. O'Rourke, P. Meera, A. K. Muhammad, S. Grant *et al.*, 2013 Targeting RNA foci in iPSC-derived motor neurons from ALS patients with a C9ORF72 repeat expansion. Sci Transl Med 5**:** 208ra149.

Sasayama, D., H. Hori, N. Yamamoto, S. Nakamura, T. Teraishi *et al.*, 2014 ITIH3 polymorphism may confer susceptibility to psychiatric disorders by altering the expression levels of GLT8D1. J Psychiatr Res 50**:** 79-83.

Saul, A., A. L. Ponsonby, R. M. Lucas, B. V. Taylor, S. Simpson, Jr. *et al.*, 2017 Stressful life events and the risk of initial central nervous system demyelination. Mult Scler 23**:** 1000-1007.

Saunders, W. B., 2002 Muscle and Nerve, pp. in *Motor Neuron Disease*, edited by R. W. Kuncl. Wiley Periodicals, Inc. , London.

Scarlino, S., T. Domi, L. Pozzi, A. Romano, G. B. Pipitone *et al.*, 2020 Burden of Rare Variants in ALS and Axonal Hereditary Neuropathy Genes Influence Survival in ALS: Insights from a Next Generation Sequencing Study of an Italian ALS Cohort. Int J Mol Sci 21.

Schmid, B., A. Hruscha, S. Hogl, J. Banzhaf-Strathmann, K. Strecker *et al.*, 2013 Loss of ALS-associated TDP-43 in zebrafish causes muscle degeneration, vascular dysfunction, and reduced motor neuron axon outgrowth. Proc Natl Acad Sci U S A 110**:** 4986-4991.

Schnorrer, F., C. Schonbauer, C. C. Langer, G. Dietzl, M. Novatchkova *et al.*, 2010 Systematic genetic analysis of muscle morphogenesis and function in Drosophila. Nature 464**:** 287-291.

Schoch, K. M., and T. M. Miller, 2017 Antisense Oligonucleotides: Translation from Mouse Models to Human Neurodegenerative Diseases. Neuron 94**:** 1056-1070.

Schroer, T. A., 2004 Dynactin. Annu Rev Cell Dev Biol 20**:** 759-779.

Scialo, C., G. Novi, M. Bandettini di Poggio, A. Canosa, M. P. Sormani *et al.*, 2016 Clinical epidemiology of amyotrophic lateral sclerosis in Liguria, Italy: An update of LIGALS register. Amyotroph Lateral Scler Frontotemporal Degener 17**:** 535-542.

Shalom, O., N. Shalva, Y. Altschuler and B. Motro, 2008 The mammalian Nek1 kinase is involved in primary cilium formation. FEBS Lett 582**:** 1465-1470.

Shang, Y., and E. J. Huang, 2016 Mechanisms of FUS mutations in familial amyotrophic lateral sclerosis. Brain Res 1647**:** 65-78.

Sherrington, C. S., 1898 Decerebrate Rigidity, and Reflex Coordination of Movements. J Physiol 22**:** 319-332.

Siddiqi, S., J. N. Foo, A. Vu, S. Azim, D. L. Silver *et al.*, 2014 A novel splice-site mutation in ALS2 establishes the diagnosis of juvenile amyotrophic lateral sclerosis in a family with early onset anarthria and generalized dystonias. PLoS One 9**:** e113258.

Simossis, V. A., and J. Heringa, 2005 PRALINE: a multiple sequence alignment toolbox that integrates homology-extended and secondary structure information. Nucleic Acids Res 33**:** W289-294.

Simossis, V. A., J. Kleinjung and J. Heringa, 2005 Homology-extended sequence alignment. Nucleic Acids Res 33**:** 816-824.

Simpkins, J. W., and M. Singh, 2008 More than a decade of estrogen neuroprotection. Alzheimers Dement 4**:** S131-136.

Skibinski, G., N. J. Parkinson, J. M. Brown, L. Chakrabarti, S. L. Lloyd *et al.*, 2005 Mutations in the endosomal ESCRTIII-complex subunit CHMP2B in frontotemporal dementia. Nat Genet 37**:** 806-808.

Skowronska-Krawczyk, D., Q. Ma, M. Schwartz, K. Scully, W. Li *et al.*, 2014 Required enhancer-matrin-3 network interactions for a homeodomain transcription program. Nature 514**:** 257-261.

Smith, B. N., S. Newhouse, A. Shatunov, C. Vance, S. Topp *et al.*, 2013 The C9ORF72 expansion mutation is a common cause of ALS+/-FTD in Europe and has a single founder. Eur J Hum Genet 21**:** 102-108.

Smith, B. N., N. Ticozzi, C. Fallini, A. S. Gkazi, S. Topp *et al.*, 2014 Exome-wide rare variant analysis identifies TUBA4A mutations associated with familial ALS. Neuron 84**:** 324-331.

Smith, B. N., C. Vance, E. L. Scotter, C. Troakes, C. H. Wong *et al.*, 2015 Novel mutations support a role for Profilin 1 in the pathogenesis of ALS. Neurobiol Aging 36**:** 1602 e1617-1627.

Smith, R. A., T. M. Miller, K. Yamanaka, B. P. Monia, T. P. Condon *et al.*, 2006 Antisense oligonucleotide therapy for neurodegenerative disease. J Clin Invest 116**:** 2290-2296.

St Johnston, D., 2002 The art and design of genetic screens: Drosophila melanogaster. Nat Rev Genet 3**:** 176-188.

Stambler, N., M. Charatan and J. M. Cedarbaum, 1998 Prognostic indicators of survival in ALS. ALS CNTF Treatment Study Group. Neurology 50**:** 66-72.

Stocker, H., and P. Gallant, 2008 Getting started : an overview on raising and handling Drosophila. Methods Mol Biol 420**:** 27-44.

Stoica, L., S. H. Todeasa, G. T. Cabrera, J. S. Salameh, M. K. ElMallah *et al.*, 2016 Adeno-associated virus-delivered artificial microRNA extends survival and delays paralysis in an amyotrophic lateral sclerosis mouse model. Ann Neurol 79**:** 687-700.

Stoica, R., K. J. De Vos, S. Paillusson, S. Mueller, R. M. Sancho *et al.*, 2014 ER-mitochondria associations are regulated by the VAPB-PTPIP51 interaction and are disrupted by ALS/FTD-associated TDP-43. Nat Commun 5**:** 3996.

Strong, M. J., K. Volkening, R. Hammond, W. Yang, W. Strong *et al.*, 2007 TDP43 is a human low molecular weight neurofilament (hNFL) mRNA-binding protein. Mol Cell Neurosci 35**:** 320-327.

Stucki, G., P. Bruhlmann, T. Stoll, S. Stucki, B. Willer *et al.*, 1996 Low serum creatine kinase activity is associated with muscle weakness in patients with rheumatoid arthritis. J Rheumatol 23**:** 603-608.

Subramanian, V., and Y. Feng, 2007 A new role for angiogenin in neurite growth and pathfinding: implications for amyotrophic lateral sclerosis. Hum Mol Genet 16**:** 1445-1453.

Sugama, S., K. Sekiyama, T. Kodama, Y. Takamatsu, T. Takenouchi *et al.*, 2016 Chronic restraint stress triggers dopaminergic and noradrenergic neurodegeneration: Possible role of chronic stress in the onset of Parkinson's disease. Brain Behav Immun 51**:** 39-46.

Suzuki, H., K. Kanekura, T. P. Levine, K. Kohno, V. M. Olkkonen *et al.*, 2009 ALS-linked P56S-VAPB, an aggregated loss-of-function mutant of VAPB, predisposes motor neurons to ER stress-related death by inducing aggregation of co-expressed wild-type VAPB. J Neurochem 108**:** 973-985.

Swash, M., 2012 Why are upper motor neuron signs difficult to elicit in amyotrophic lateral sclerosis? J Neurol Neurosurg Psychiatry 83**:** 659-662.

Synofzik, M., W. Maetzler, T. Grehl, J. Prudlo, J. M. Vom Hagen *et al.*, 2012 Screening in ALS and FTD patients reveals 3 novel UBQLN2 mutations outside the PXX domain and a pure FTD phenotype. Neurobiol Aging 33**:** 2949 e2913-2947.

Tai, H., L. Cui, Y. Guan, M. Liu, X. Li *et al.*, 2017 Correlation of Creatine Kinase Levels with Clinical Features and Survival in Amyotrophic Lateral Sclerosis. Front Neurol 8**:** 322.

Tai, H., L. Cui, M. Liu, Y. Guan, X. Li *et al.*, 2018 Creatine kinase level and its relationship with quantitative electromyographic characteristics in amyotrophic lateral sclerosis. Clin Neurophysiol 129**:** 926-930.

Takahashi, Y., Y. Fukuda, J. Yoshimura, A. Toyoda, K. Kurppa *et al.*, 2013 ERBB4 mutations that disrupt the neuregulin-ErbB4 pathway cause amyotrophic lateral sclerosis type 19. Am J Hum Genet 93**:** 900-905.

Talbot, K., 2011 Familial versus sporadic amyotrophic lateral sclerosis--a false dichotomy? Brain 134**:** 3429-3431.

Talbott, E. O., A. M. Malek and D. Lacomis, 2016 The epidemiology of amyotrophic lateral sclerosis. Handb Clin Neurol 138**:** 225-238.

Taliun, D., S. P. Chothani, S. Schonherr, L. Forer, M. Boehnke *et al.*, 2017 LASER server: ancestry tracing with genotypes or sequence reads. Bioinformatics 33**:** 2056-2058.

Tanaka, M., T. Sakata, J. Palumbo and M. Akimoto, 2016 A 24-Week, Phase III, Double-Blind, Parallel-Group of Edaravone (MCI-186) for Treatment of Amyotrophic Laeral Sclerosis (ALS) (P3.189). Neurology 86.

Tanaka, R., 1986 [The Hoffmann reflex]. Nihon Seirigaku Zasshi 48**:** 719-734.

Tanguy, Y., M. G. Biferi, A. Besse, S. Astord, M. Cohen-Tannoudji *et al.*, 2015 Systemic AAVrh10 provides higher transgene expression than AAV9 in the brain and the spinal cord of neonatal mice. Front Mol Neurosci 8**:** 36.

Tanner, N. K., and P. Linder, 2001 DExD/H box RNA helicases: from generic motors to specific dissociation functions. Mol Cell 8**:** 251-262.

Tazelaar, G. H. P., A. M. Dekker, J. van Vugt, R. A. van der Spek, H. J. Westeneng *et al.*, 2019 Association of NIPA1 repeat expansions with amyotrophic lateral sclerosis in a large international cohort. Neurobiol Aging 74**:** 234 e239-234 e215.

Tefera, T. W., and K. Borges, 2016 Metabolic Dysfunctions in Amyotrophic Lateral Sclerosis Pathogenesis and Potential Metabolic Treatments. Front Neurosci 10**:** 611.

Tefera, T. W., K. N. Tan, T. S. McDonald and K. Borges, 2017 Alternative Fuels in Epilepsy and Amyotrophic Lateral Sclerosis. Neurochem Res 42**:** 1610-1620.

Tegeder, I., K. Thiel, S. Erkek, P. D. Johann, J. Berlandi *et al.*, 2019 Functional relevance of genes predicted to be affected by epigenetic alterations in atypical teratoid/rhabdoid tumors. J Neurooncol 141**:** 43-55.

Testa, D., R. Lovati, M. Ferrarini, F. Salmoiraghi and G. Filippini, 2004 Survival of 793 patients with amyotrophic lateral sclerosis diagnosed over a 28-year period. Amyotroph Lateral Scler Other Motor Neuron Disord 5**:** 208-212.

Thiel, C., K. Kessler, A. Giessl, A. Dimmler, S. A. Shalev *et al.*, 2011 NEK1 mutations cause short-rib polydactyly syndrome type majewski. Am J Hum Genet 88**:** 106-114.

Thomsen, G. M., G. Gowing, J. Latter, M. Chen, J. P. Vit *et al.*, 2014 Delayed disease onset and extended survival in the SOD1G93A rat model of amyotrophic lateral sclerosis after suppression of mutant SOD1 in the motor cortex. J Neurosci 34**:** 15587-15600.

Traynor, B. J., M. B. Codd, B. Corr, C. Forde, E. Frost *et al.*, 2000 Clinical features of amyotrophic lateral sclerosis according to the El Escorial and Airlie House diagnostic criteria: A population-based study. Arch Neurol 57**:** 1171-1176.

Tripolszki, K., D. Torok, D. Goudenege, K. Farkas, A. Sulak *et al.*, 2017 High-throughput sequencing revealed a novel SETX mutation in a Hungarian patient with amyotrophic lateral sclerosis. Brain Behav 7**:** e00669.

Tsang, H. T., T. L. Edwards, X. Wang, J. W. Connell, R. J. Davies *et al.*, 2009 The hereditary spastic paraplegia proteins NIPA1, spastin and spartin are inhibitors of mammalian BMP signalling. Hum Mol Genet 18**:** 3805-3821.

Turgut, N., G. Varol SaraCoglu, S. Kat, K. Balci, G. U. B *et al.*, 2019 An epidemiologic investigation of amyotrophic lateral sclerosis in Thrace, Turkey, 2006-2010. Amyotroph Lateral Scler Frontotemporal Degener 20**:** 100-106.

Turner, B. J., and K. Talbot, 2008 Transgenics, toxicity and therapeutics in rodent models of mutant SOD1-mediated familial ALS. Prog Neurobiol 85**:** 94-134.

Turner, M. R., R. Goldacre, K. Talbot and M. J. Goldacre, 2016 Psychiatric disorders prior to amyotrophic lateral sclerosis. Ann Neurol 80**:** 935-938.

Tysnes, O. B., S. E. Vollset and J. A. Aarli, 1991 Epidemiology of amyotrophic lateral sclerosis in Hordaland county, western Norway. Acta Neurol Scand 83**:** 280-285.

Uemura, M., T. Kosaka, T. Shimohata, M. Ishikawa, Y. Nishihira *et al.*, 2013 Dropped head syndrome in amyotrophic lateral sclerosis. Amyotroph Lateral Scler Frontotemporal Degener 14**:** 232-233.

Uenal, H., A. Rosenbohm, J. Kufeldt, P. Weydt, K. Goder *et al.*, 2014 Incidence and geographical variation of amyotrophic lateral sclerosis (ALS) in Southern Germany--completeness of the ALS registry Swabia. PLoS One 9**:** e93932.

Umapathi, T., V. Chaudhry, D. Cornblath, D. Drachman, J. Griffin *et al.*, 2002 Head drop and camptocormia. J Neurol Neurosurg Psychiatry 73**:** 1-7.

Urwin, H., K. A. Josephs, J. D. Rohrer, I. R. Mackenzie, M. Neumann *et al.*, 2010 FUS pathology defines the majority of tau- and TDP-43-negative frontotemporal lobar degeneration. Acta Neuropathol 120**:** 33-41.

van Blitterswijk, M., M. DeJesus-Hernandez and R. Rademakers, 2012 How do C9ORF72 repeat expansions cause amyotrophic lateral sclerosis and

frontotemporal dementia: can we learn from other noncoding repeat expansion disorders? Curr Opin Neurol 25**:** 689-700.

van Blitterswijk, M., B. Mullen, A. Wojtas, M. G. Heckman, N. N. Diehl *et al.*, 2014 Genetic modifiers in carriers of repeat expansions in the C9ORF72 gene. Mol Neurodegener 9**:** 38.

Van Damme, P., J. H. Veldink, M. van Blitterswijk, A. Corveleyn, P. W. van Vught *et al.*, 2011 Expanded ATXN2 CAG repeat size in ALS identifies genetic overlap between ALS and SCA2. Neurology 76**:** 2066-2072.

van der Spek, R. A. A., W. van Rheenen, S. L. Pulit, K. P. Kenna, L. H. van den Berg *et al.*, 2019 The project MinE databrowser: bringing large-scale whole-genome sequencing in ALS to researchers and the public. Amyotroph Lateral Scler Frontotemporal Degener 20**:** 432-440.

van Es, M. A., H. J. Schelhaas, P. W. van Vught, N. Ticozzi, P. M. Andersen *et al.*, 2011 Angiogenin variants in Parkinson disease and amyotrophic lateral sclerosis. Ann Neurol 70**:** 964-973.

van Es, M. A., J. H. Veldink, C. G. Saris, H. M. Blauw, P. W. van Vught *et al.*, 2009 Genome-wide association study identifies 19p13.3 (UNC13A) and 9p21.2 as susceptibility loci for sporadic amyotrophic lateral sclerosis. Nat Genet 41**:** 1083-1087.

van Gijn, J., 1995 The Babinski reflex. Postgrad Med J 71**:** 645-648.

van Rheenen, W., A. Shatunov, A. M. Dekker, R. L. McLaughlin, F. P. Diekstra *et al.*, 2016 Genome-wide association analyses identify new risk variants and the genetic architecture of amyotrophic lateral sclerosis. Nat Genet 48**:** 1043-1048.

Vance, C., B. Rogelj, T. Hortobagyi, K. J. De Vos, A. L. Nishimura *et al.*, 2009 Mutations in FUS, an RNA processing protein, cause familial amyotrophic lateral sclerosis type 6. Science 323**:** 1208-1211.

Vanden Broeck, L., M. Naval-Sanchez, Y. Adachi, D. Diaper, P. Dourlen *et al.*, 2013 TDP-43 loss-of-function causes neuronal loss due to defective steroid receptor-mediated gene program switching in Drosophila. Cell Rep 3**:** 160-172.

Varoqueaux, F., M. S. Sons, J. J. Plomp and N. Brose, 2005 Aberrant morphology and residual transmitter release at the Munc13-deficient mouse neuromuscular synapse. Mol Cell Biol 25**:** 5973-5984.

Vasta, R., M. C. Torrieri, F. D'Ovidio, A. Circiello, F. De Mattei *et al.*, 2021 Neck flexor weakness at diagnosis predicts respiratory impairment in amyotrophic lateral sclerosis. Eur J Neurol 28**:** 1181-1187.

Villarroya-Beltri, C., C. Gutierrez-Vazquez, F. Sanchez-Cabo, D. Perez-Hernandez, J. Vazquez *et al.*, 2013 Sumoylated hnRNPA2B1 controls the sorting of miRNAs into exosomes through binding to specific motifs. Nat Commun 4**:** 2980.

Visser, A. E., F. D'Ovidio, S. Peters, R. C. Vermeulen, E. Beghi *et al.*, 2019 Multicentre, population-based, case-control study of particulates, combustion products and amyotrophic lateral sclerosis risk. J Neurol Neurosurg Psychiatry 90**:** 854-860.

Visser, J., R. M. van den Berg-Vos, H. Franssen, L. H. van den Berg, J. H. Wokke *et al.*, 2007 Disease course and prognostic factors of progressive muscular atrophy. Arch Neurol 64**:** 522-528.

Voigt, A., D. Herholz, F. C. Fiesel, K. Kaur, D. Muller *et al.*, 2010 TDP-43-mediated neuron loss in vivo requires RNA-binding activity. PLoS One 5**:** e12247.

Walker, C., S. Herranz-Martin, E. Karyka, C. Liao, K. Lewis *et al.*, 2017 C9orf72 expansion disrupts ATM-mediated chromosomal break repair. Nat Neurosci 20**:** 1225-1235.

Walker, H. K., 1990 Deep Tendon Reflexes in *Clinical Methods: The History, Physical, and Laboratory Examinations*, edited by rd, H. K. Walker, W. D. Hall and J. W. Hurst, Boston.

Wallimann, T., M. Wyss, D. Brdiczka, K. Nicolay and H. M. Eppenberger, 1992 Intracellular compartmentation, structure and function of creatine kinase isoenzymes in tissues with high and fluctuating energy demands: the 'phosphocreatine circuit' for cellular energy homeostasis. Biochem J 281 (Pt 1)**:** 21-40.

Wang, C., X. Zhan, J. Bragg-Gresham, H. M. Kang, D. Stambolian *et al.*, 2014 Ancestry estimation and control of population stratification for sequence-based association studies. Nat Genet 46**:** 409-415.

Wang, H., E. J. O'Reilly, M. G. Weisskopf, G. Logroscino, M. L. McCullough *et al.*, 2011a Vitamin E intake and risk of amyotrophic lateral sclerosis: a pooled analysis of data from 5 prospective cohort studies. Am J Epidemiol 173**:** 595-602.

Wang, H., E. J. O'Reilly, M. G. Weisskopf, G. Logroscino, M. L. McCullough *et al.*, 2011b Smoking and risk of amyotrophic lateral sclerosis: a pooled analysis of 5 prospective cohorts. Arch Neurol 68**:** 207-213.

Wang, L. J., Y. Y. Lu, S. Muramatsu, K. Ikeguchi, K. Fujimoto *et al.*, 2002 Neuroprotective effects of glial cell line-derived neurotrophic factor mediated by an adeno-associated virus vector in a transgenic animal model of amyotrophic lateral sclerosis. J Neurosci 22**:** 6920-6928.

Wang, W., W. Duan, Y. Wang, D. Wen, Y. Liu *et al.*, 2017 Intrathecal Delivery of ssAAV9-DAO Extends Survival in SOD1(G93A) ALS Mice. Neurochem Res 42**:** 986-996.

Wang, X., W. R. Shaw, H. T. Tsang, E. Reid and C. J. O'Kane, 2007 Drosophila spichthyin inhibits BMP signaling and regulates synaptic growth and axonal microtubules. Nat Neurosci 10**:** 177-185.

Wang, Z., M. Gerstein and M. Snyder, 2009 RNA-Seq: a revolutionary tool for transcriptomics. Nat Rev Genet 10**:** 57-63.

Watanabe, Y., T. Nakagawa, T. Akiyama, M. Nakagawa, N. Suzuki *et al.*, 2020 An Amyotrophic Lateral Sclerosis-Associated Mutant of C21ORF2 Is Stabilized by NEK1-Mediated Hyperphosphorylation and the Inability to Bind FBXO3. iScience 23**:** 101491.

Wiggans, S. T., J., 2016 Nerve damage associated with a spinal or epidural injection, pp. Royal College of Anaesthetists.

Williams, K. L., S. Topp, S. Yang, B. Smith, J. A. Fifita *et al.*, 2016 CCNF mutations in amyotrophic lateral sclerosis and frontotemporal dementia. Nat Commun 7**:** 11253.

Wong, P. C., C. A. Pardo, D. R. Borchelt, M. K. Lee, N. G. Copeland *et al.*, 1995 An adverse property of a familial ALS-linked SOD1 mutation causes motor neuron disease characterized by vacuolar degeneration of mitochondria. Neuron 14**:** 1105-1116.

Wu, C. H., C. Fallini, N. Ticozzi, P. J. Keagle, P. C. Sapp *et al.*, 2012 Mutations in the profilin 1 gene cause familial amyotrophic lateral sclerosis. Nature 488**:** 499-503.

Xu, L., J. Li, L. Tang, N. Zhang and D. Fan, 2016 MATR3 mutation analysis in a Chinese cohort with sporadic amyotrophic lateral sclerosis. Neurobiol Aging 38**:** 218 e213-218 e214.

Xu, Z., M. Poidevin, X. Li, Y. Li, L. Shu *et al.*, 2013 Expanded GGGGCC repeat RNA associated with amyotrophic lateral sclerosis and frontotemporal dementia causes neurodegeneration. Proc Natl Acad Sci U S A 110**:** 7778-7783.

Yamaguchi, T., I. Dulubova, S. W. Min, X. Chen, J. Rizo *et al.*, 2002 Sly1 binds to Golgi and ER syntaxins via a conserved N-terminal peptide motif. Dev Cell 2**:** 295-305.

Yang, C. P., X. Li, Y. Wu, Q. Shen, Y. Zeng *et al.*, 2018 Comprehensive integrative analyses identify GLT8D1 and CSNK2B as schizophrenia risk genes. Nat Commun 9**:** 838.

Yoshino, H., 2019 Edaravone for the treatment of amyotrophic lateral sclerosis. Expert Rev Neurother 19**:** 185-193.

Zatloukal, K., C. Stumptner, A. Fuchsbichler, H. Heid, M. Schnoelzer *et al.*, 2002 p62 Is a common component of cytoplasmic inclusions in protein aggregation diseases. Am J Pathol 160**:** 255-263.

Zhang, K., J. G. Daigle, K. M. Cunningham, A. N. Coyne, K. Ruan *et al.*, 2018 Stress Granule Assembly Disrupts Nucleocytoplasmic Transport. Cell 173**:** 958-971 e917.

Zhao, J., D. S. Matthies, E. J. Botzolakis, R. L. Macdonald, R. D. Blakely *et al.*, 2008 Hereditary spastic paraplegia-associated mutations in the NIPA1 gene and its Caenorhabditis elegans homolog trigger neural degeneration in vitro and in vivo through a gain-of-function mechanism. J Neurosci 28**:** 13938-13951.

Zhou, H., G. Chen, C. Chen, Y. Yu and Z. Xu, 2012 Association between extremely low-frequency electromagnetic fields occupations and amyotrophic lateral sclerosis: a meta-analysis. PLoS One 7**:** e48354.

Zhou, M., N. Goto, J. Goto, H. Moriyama and H. J. He, 2000 Gender dimorphism of axons in the human lateral corticospinal tract. Okajimas Folia Anat Jpn 77**:** 21-27.

Zhou, S., Y. Zhou, S. Qian, W. Chang, L. Wang *et al.*, 2018 Amyotrophic lateral sclerosis in Beijing: Epidemiologic features and prognosis from 2010 to 2015. Brain Behav 8**:** e01131.

Zhou, X., M. N. Edmonson, M. R. Wilkinson, A. Patel, G. Wu *et al.*, 2016 Exploring genomic alteration in pediatric cancer using ProteinPaint. Nat Genet 48**:** 4-6.

Zhu, G., C. J. Wu, Y. Zhao and J. D. Ashwell, 2007 Optineurin negatively regulates TNFalpha- induced NF-kappaB activation by competing with NEMO for ubiquitinated RIP. Curr Biol 17**:** 1438-1443.

Zimmerman, B., and J. B. Hubbard, 2019 Clonus in *StatPearls*, Treasure Island (FL).

Zimmerman, B., and J. B. Hubbard, 2021 Deep Tendon Reflexes in *StatPearls*, Treasure Island (FL).

Zoing, M. C., D. Burke, R. Pamphlett and M. C. Kiernan, 2006 Riluzole therapy for motor neurone disease: an early Australian experience (1996-2002). J Clin Neurosci 13**:** 78-83.

Zou, Z. Y., Z. R. Zhou, C. H. Che, C. Y. Liu, R. L. He *et al.*, 2017 Genetic epidemiology of amyotrophic lateral sclerosis: a systematic review and meta-analysis. J Neurol Neurosurg Psychiatry 88**:** 540-549.

CHAPTER 6
APPENDIX

6.1 APPENDIX I: STUDY PARTICIPANT QUESTIONNAIRE AND CLINICAL DATA FORM

ALS/MND BIOBANK PROJECT

Malta ALS/MND Research Programme

Centre for Molecular Medicine & Biobanking

Faculty of Medicine & Surgery

University of Malta
Università ta' Malta

CODE NUMBER:	
PATIENT ID:	
GENDER:	
CURRENT AGE:	
ETHNICITY & ANCESTRY: MOTHER'S & FATHER'S NATIONALITY	
AFFECTATION STATUS: PATIENT/PARENT/SIB/CONTROL	
CLINICAL DIAGNOSIS:	
DIFFERENTIAL DIAGNOSIS	

CLINICAL HISTORY

AGE AT PRESENTATION:	
SITE OF PRESENTATION: (E.G. WEAKNESS, FLICKERS, SPASMS…ETC)	
DOMINANT HAND	
SOCIAL HISTORY **A) TRAVEL HISTORY** CONTINENT VISITED? VACCINATIONS? **B) SPORTS HISTORY** PROFFESIONAL VS. AMATEUR? TYPE OF SPORTS? FREQUENCY? **C) SEXUAL HISTORY** BI/HOMO/HETEROSEXUAL? NUMBER OF MALE/FEMALE PARTNERS? SEXUALLY TRANSMITTED DISEASE – HIV?	
FAMILY HISTORY: (Including ALS/MND, Parkinson's disease, Alzheimer's disease, Dementia, Psychosis, other neurological/neuromuscular conditions)	

OTHER INFORMATION

CURRENT/PREVIOUS OCCUPATION:

STRENUOUS LABOUR?

EXPOSURE TO TOXIC

PARTICLES/CHEMICALS/DUST?

DIET:

OMNIVORE/ VEGETERARIAN/VEGAN?

SMOKING HABITS:

YEAR STARTED/STOPPED?

AMOUNT PER DAY?

EXCESSIVE ALCOHOL CONSUMPTION/DRUG ABUSE:

YEAR STARTED/STOPPED?

AMOUNT PER DAY?

RESIDENCE:

YEARS LIVING IN SAME LOCATION?

CHANGE IN LOCATION?

FAMILY PEDIGREE

CURRENT MEDICATIONS

DRUG	DOSE	FREQUENCY	NOTES

In the case of disease modifying medications/drugs, date started and notes

ALS-FRS SCORE

1. SPEECH

- ☐ Normal speech processes
- ☐ Detectable speech disturbance
- ☐ Intelligible with repeating
- ☐ Speech combined with non-vocal communication
- ☐ Loss of useful speech

2. SALIVATION

- ☐ Normal
- ☐ Slight but definite excess of saliva in mouth; may have night-time drooling
- ☐ Moderate excessive saliva; may have minimal drooling
- ☐ Marked excess of saliva with some drooling
- ☐ Marked drooling; requires constant tissue or handkerchief

3. SWALLOWING

- ☐ Normal eating habits
- ☐ Early eating problems - occasional choking
- ☐ Dietary consistency changes
- ☐ Needs supplemental tube feeding
- ☐ NPO (exclusively parenteral or enteral feeding)

4. HANDWRITING

- ☐ Normal
- ☐ Slow or sloppy; all words are legible

- ☐ Not all words are legible
- ☐ Able to grip pen but unable to write
- ☐ Unable to grip pen

5. CUTTING FOOD

- ☐ Normal
- ☐ Somewhat slow and clumsy, but no help needed
- ☐ Can cut most foods, although clumsy and slow; some help needed
- ☐ Food must be cut by someone, but can still feed slowly
- ☐ Needs to be fed

6. DRESSING AND HYGIENE

- ☐ Normal function
- ☐ Independent and complete self-care with effort or decreased efficiency
- ☐ Intermittent assistance or substitute methods
- ☐ Needs attendant for self-care
- ☐ Total dependence

7. TURNING IN BED

- ☐ Normal
- ☐ Somewhat slow and clumsy, but no help needed
- ☐ Can turn alone or adjust sheets, but with great difficulty
- ☐ Can initiate, but not turn or adjust sheets alone
- ☐ Helpless

8. WALKING

- ☐ Normal
- ☐ Early ambulation difficulties
- ☐ Walks with assistance
- ☐ Non-ambulatory functional movement only
- ☐ No purposeful leg movement

9. CLIMBING STAIRS

- ☐ Normal
- ☐ Slow
- ☐ Mild unsteadiness or fatigue
- ☐ Needs assistance
- ☐ Cannot do

10. DYSPNOEA

- ☐ None
- ☐ Occurs when walking
- ☐ Occurs when one or more of the following: eating, bathing, dressing
- ☐ Occurs at rest, difficulty breathing when either sitting or lying
- ☐ Significant difficulty, considering using mechanical respiratory support

11. ORTHOPNOEA

- ☐ None

- ☐ Some difficulty sleeping at night due to shortness of breath. Does not routinely use more than two pillows
- ☐ Needs extra pillow in order to sleep (>2)
- ☐ Can only sleep sitting up
- ☐ Unable to sleep

12. RESPIRATORY INSUFFICIENCY

- ☐ None
- ☐ Intermittent use of BiPAP
- ☐ Continuous use of BiPAP
- ☐ Continuous use of BiPAP during the day and the night
- ☐ Invasive mechanical ventilation by intubation or tracheostomy

13. HOW MANY YEARS SINCE ONSET OF SYMPTOMS? _____

PHYSICAL EXAMINATION:

BREATHING RATE: **HEART RATE:**

MUSCLE TONE	
RUL:	LUL:
RLL:	LLL:

MRC SCORES

	RIGHT	LEFT
NECK FLEXION		
NECK EXTENSION		
SHOULDER ABDUCTION		
ELBOW FLEXION		
ELBOW EXTENSION		
WRIST FLEXION		
WRIST EXTENSION		
THUMB ABDUCTION		
HIP FLEXION		
KNEE FLEXION		
KNEE EXTENSION		
ANKLE DORSIFLEXION		
ANKLE PLANTAR FLEXION		

REFLEXES

	RIGHT	LEFT
BICEPS		
TRICEPS		
SUPPINATOR		
HOFFMANN'S		
SUPRAPATELLAR		
KNEE		
CROSSED ADDUCTOR		
ANKLE		
PLANTAR		

Others (e.g. fasciculations)

_____ _____ _____

Project Researcher: Full Name Signature Date

Malta ALS/MND Research Programme

Centre for Molecular Medicine & Biobanking

Faculty of Medicine & Surgery

University of Malta

6.2 APPENDIX II: STUDY CONSENT FORM

Malta ALS/MND Research Programme

Centre for Molecular Medicine & Biobanking

Faculty of Medicine & Surgery

University of Malta

Università ta' Malta

We would like to invite you to participate in this original research study. You should only participate if you want to. Choosing not to take part will not disadvantage you in any way.

Before you decide whether you want to take part, it is important for you to understand why the research is being done and what your participation will involve. Please take time to read the following information carefully and discuss it with others if you wish. Ask us if there is anything that is not clear or if you would like more information.

Title of the research project

The ALS/MND BioBank Project

Purpose of the research

Amyotrophic Lateral Sclerosis (ALS) or Motor Neuron Disease (MND) is a rapidly progressive rare neurodegenerative disease that affects the brain and spinal cord, which unfortunately is usually fatal approximately 2-5 years after symptom onset.

The main aim of the ALS/MND BioBank is the identification of the genetic factors that may play a role in causing or modifying the disease. The broader objectives of the bank are to help in the development of technologies that might lead to disease diagnosis and treatment.

To reach these goals we need the participation of Maltese donors to donate blood and/or tissue samples to be stored, preserved in appropriate conditions and used for further medical research

Procedures

If you agree to participate in this project, a sample of saliva or a sample of blood (3ml) will be taken by venipuncture from your arm by a qualified and experienced doctor or his/her assistant. The sample will be used for blood and genetic analysis. The blood and extracted DNA samples will be stored in the Malta ALS/MND BioBank as part of the Malta BioBank. You would also be required to answer some questions regarding your condition and family history. A physical examination will also be carried out to assess for function, strength and other signs of this condition.

We also wish to assess family members as well as partners and collect a sample of saliva or blood (3ml) from them in order to study the inheritance pattern of the disorder.

It is our aim to develop this activity with the respect due to individual rights in accordance with the internationally accepted ethical rules, ensuring you that all the research to be carried out will be under the supervision of the University of Malta Research Ethics Committee (UREC), that will ensure the observance of the mentioned regulations.

For the above reasons we request your voluntary collaboration.

Identification of the sample

The sample collection will be an "identifiable collection" as the biological samples, although unidentified for research means, can be linked to their sources through the use of a code. The biological samples and personal data will be stored separately. All working stock will be partially anonymized by coding and can only be linked to the information through this code. Only the Data Custodian (Dr. R. Cauchi) or his delegate/s (including Ms. R. Borg) will have access to this link thus ensuring your privacy, and de-codification will only be made when required. The Malta ALS/MND BioBank would not like to have complete anonymization as it might be in the interest of the participating donor that important results of tests are known to the donor and can be traced back should medication or an intervention be required.

Length of storage

By providing your consent, you agree to the storage of any samples collected for an initial period of ten (10) years or longer, subject to EU guidelines and re-evaluation by UREC. This period may be extended if approved by UREC.

Due to the expense and effort involved in the establishment and maintenance of collections and databases, it is important and useful to store these for a significant period of time[1]. These collections are invaluable for the development of personalized medicine. Once samples are stored in the Malta ALS/MND BioBank, these will be under the responsibility of the Principal Investigator, Dr. R Cauchi and / or his delegates (including Ms. R. Borg).

Samples use

Since the University of Malta does not have the resources to independently identify genetic factors, the coded samples may be transferred to International Research Institutes so that the necessary analyses can be performed subject to approval by the UREC.

We cannot predict all the future uses of your samples. However, the use of your samples will be regulated by the Malta BioBank which is itself regulated by the UREC

European Society of Human, G., 2003 Data storage and DNA banking for biomedical research: technical, social and ethical issues. Eur J Hum Genet 11 Suppl 2**:** S8-10.

Benefits

It should be noted that this is an altruistic donation, therefore no economic benefit shall be obtained. You will not gain financially by participating in this project (e.g. if research leads to commercial development of a new treatment). It is possible that this study will result in a test/tests that may someday be used in genetic diagnosis of the disorder. If such a test is developed, you have no right for compensation. A third party might benefit from this development.

The information gathered may be useful for you or your relatives. Furthermore, we hope that the results obtained will enable us to improve our understanding of ALS/MND.

Physical risks

Although the drawing of blood causes no serious problems for most people, it can cause some bleeding, bruising, and / discomfort at the injection site. A physical exam and assessment of muscle function can lead to fatigue.

Confidentiality

The creation of a BioBank means the existence of a file containing your personal and medical data. This file will be treated in accordance with the national regulations on data protection (Data Protection Act 2002). Both the information gathered from you and the research results will be treated confidentially. The information will be under lock and key and will be coded to add another level of protection. Samples will also be coded and researchers will not have access to personal data.

Data obtained will only be published in an anonymous and aggregated way, such as percentages or numerical data without identification of the participant. Under no circumstances will data be provided in an individualized way. As a result, your privacy will be ensured and respected.

Unless you provide us with specific authorization, personal results will not be made available to third parties such as employers, governmental organizations, insurance companies or educational institutions. This also applies to spouses, partners, or members of your family, and your family doctor.

Freedom of participation and right of withdrawal

Participation in this project is voluntary and you may withdraw your consent at any time. The Data Protection Act grants the right of access and the donor's right to rectify or withdraw. You have the right to decide whether the material already collected can remain part of the study or destroyed. Should you wish to withdraw your data or your samples from the laboratory you will be free to do so without further explanation.

Resource persons

Should you need additional information regarding the progress of the research project, wish to communicate any change of address, or wish to withdraw your participation you can contact Ms. R. Borg on 79900471 or by email: rebecca.borg.09@um.edu.mt during office hours.

Final Words

It is up to you to decide whether or not to take part. If you do decide to take part you will be given this information sheet to keep and will be asked to sign a consent form. If you decide to take part you are still free to withdraw at any time and without giving a reason.

_____	_____	_____
Project Researcher: Full Name	Signature	Date

Malta ALS/MND Research Programme
Centre for Molecular Medicine & Biobanking
Faculty of Medicine & Surgery
University of Malta

Informed Consent (to be kept by the Malta ALS/MND BioBank)

Code:

To be filled in by the interviewer

Date of Interview:		
Interviewer:		
Donor's details		
Name: **(Block Capital)**	*Name of Legal Representative in the case of minors or mentally infirm donors*	
Surname: **(Block Capital)**		
I.D. card no.		
Gender:	**Male** ☐	**Female** ☐
Age of subject:		
Address:	*N.B. I will inform the principal researcher of any change of address.*	
Tel. / Mobile no.		
Email:		

Researcher's Name (Block Capital)	**Date**	**Signature**
Donor's Name (Block Capital)	**Date**	**Signature of donor or his/her legal representative**

By agreeing to take part in the study: "**The ALS/MND BioBank Project**" you are giving your consent:

1. To the Principal Investigator and his delegates to make the appropriate observations and/or tests and to take the necessary Blood/Saliva/DNA samples.

2. To the Principal Investigator and his delegates to gain access to medical and other health-related records and for the long-term storage and use of this and other information for health-related research purposes (even after your incapacity or death). This information will be treated with the utmost confidentiality and will be stored in a secure location.

		Yes	No
1.	I have read and understood what the project titled "**The ALS/MND BioBank Project**" is about and have had the opportunity to ask questions.	☐	☐
2.	I agree to take part in "**The ALS/MND BioBank Project**".	☐	☐
3.	I give my permission for my samples to be stored in the Malta BioBank.	☐	☐
4.	**Use of Samples:** I provide permission for the use of my samples in other ethically approved research projects.	☐	☐

_____	_____	_____
Full Name (Mother)	Signature	Date

_____	_____	_____
Full Name (Father)	Signature	Date

_____	_____	_____
Full Name (Researcher)	Signature	Date

6.3 APPENDIX III: RNAi SEQUENCE LOCATION

Stock Name	*CG9279-IR^{ME9}*
Lab Name	ME-9
Transgene	*UAS.CG9279*-RNAi
Inserted Chromosome	3
Source	Vienna Drosophila Resource Center
VDRC ID	45052
FlyBase Annotation	CG9279
Description	*UAS*-RNAi transgene used for *Drosophila* CG9279 knockdown (3.6.1) studies.

Stock Name	*CG9279-IR^{ME10}*
Lab Name	ME-10
Transgene	*UAS.CG9279*-RNAi
Inserted Chromosome	2
Source	Vienna Drosophila Resource Center
VDRC ID	105109
FlyBase Annotation	CG9279
Description	*UAS*-RNAi transgene used for *Drosophila* CG9279 knockdown (3.6.1) studies.

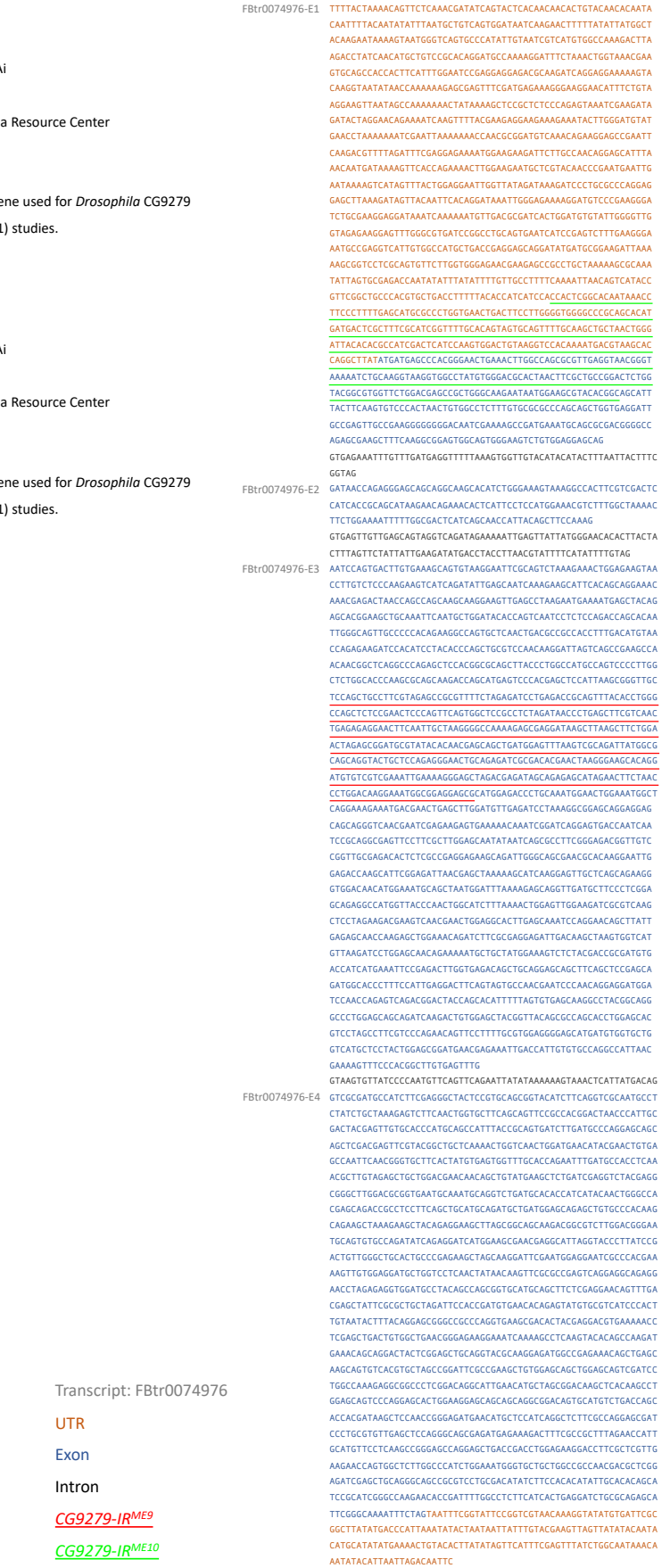

Stock Name	*DCTN1 p150-IR^{ME18}*
Lab Name	ME-18
Transgene	*UAS.DCTN1 p150*-RNAi
Inserted Chromosome	2
Source	Vienna Drosophila Resource Center
VDRC ID	3785
FlyBase Annotation	CG9206
Description	*UAS*-RNAi transgene used for *Drosophila* DCTN1 p150 knockdown (3.6.1) studies.

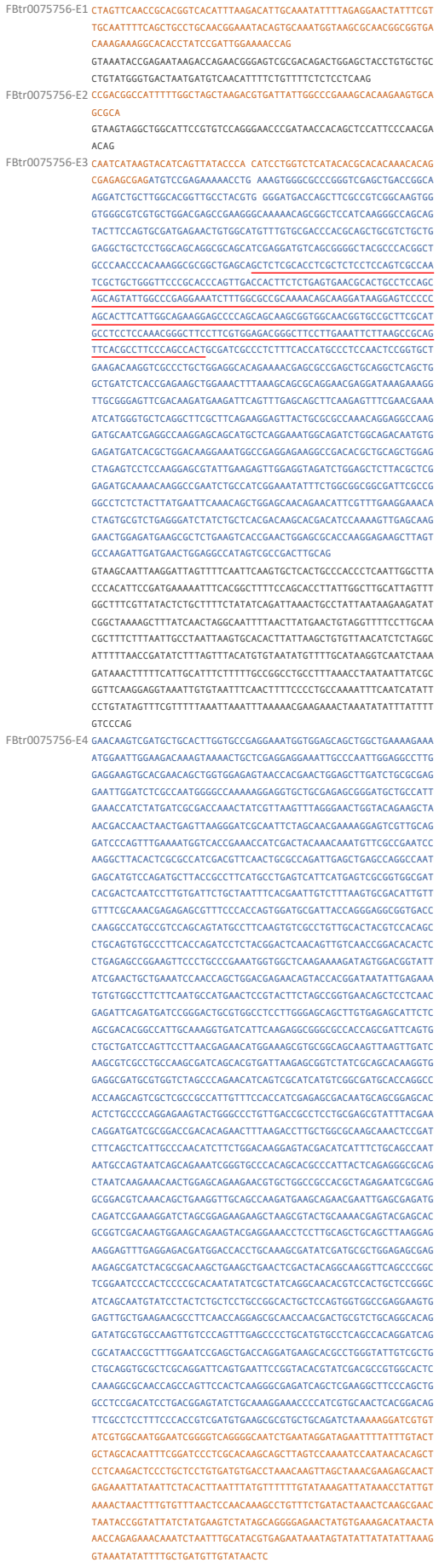

Stock Name	*Slh-IR^{ME2}*
Lab Name	ME-2
Transgene	*UAS.Slh*-RNAi
Inserted Chromosome	2
Source	Vienna Drosophila Resource Center
VDRC ID	51840
FlyBase Annotation	CG3539
Description	*UAS*-RNAi transgene used for *Drosophila* Slh knockdown (3.6.2) studies.

Stock Name	*Slh-IR^{ME3}*
Lab Name	ME-3
Transgene	*UAS.Slh*-RNAi
Inserted Chromosome	2
Source	Vienna Drosophila Resource Center
VDRC ID	105669
FlyBase Annotation	CG3539
Description	*UAS*-RNAi transgene used for *Drosophila* Slh knockdown (3.6.2) studies.

Stock Name	*Slh-IR^{ME4}*
Lab Name	ME-4
Transgene	*UAS.Slh*-RNAi
Inserted Chromosome	2
Source	Vienna Drosophila Resource Center
VDRC ID	108778
FlyBase Annotation	CG3539
Description	*UAS*-RNAi transgene used for *Drosophila* Slh knockdown (3.6.2) studies.

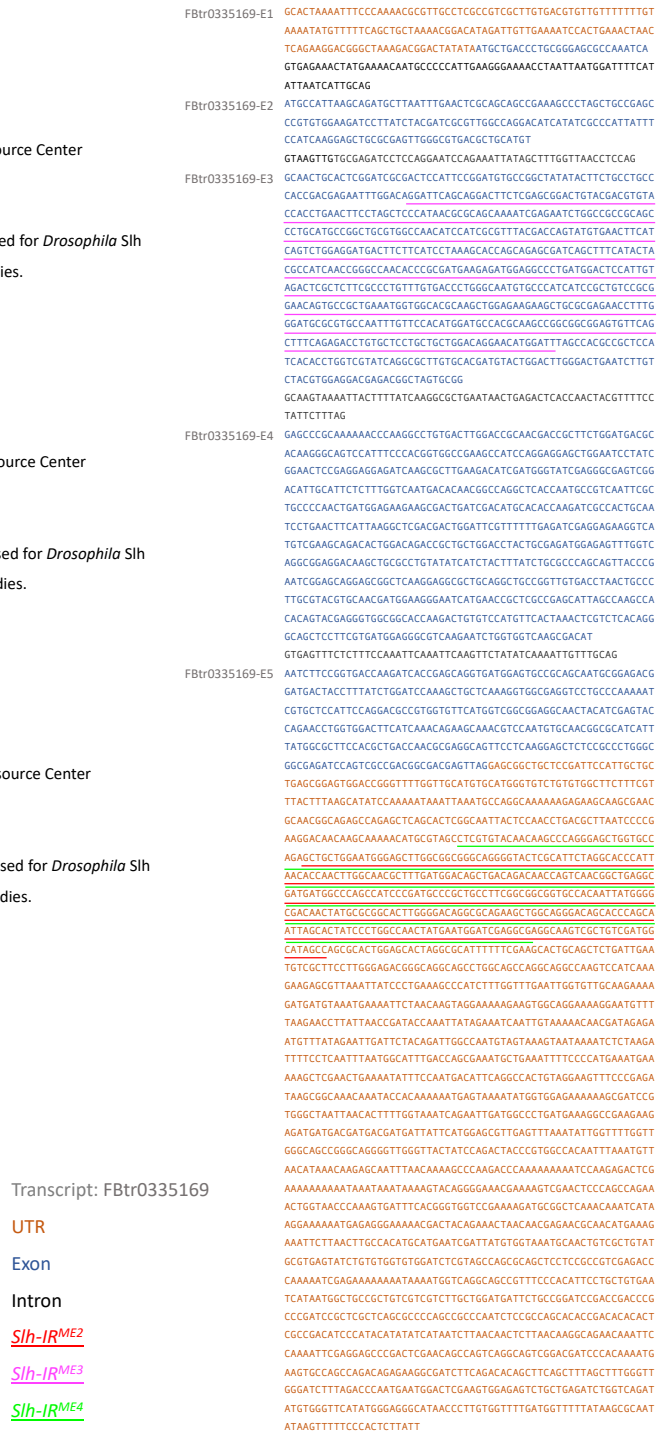

6.4 APPENDIX IV: FLY STOCKS

6.4.1 Ubiquitous GAL4 Drivers

Stock Name	*Act5C*-GAL4
Lab Stock Number	MT-50C
Genotype	*y[1] w*; P{Act5C-GAL4}25FO1/CyO*
Chromosome	1; 2
Source	Bloomington Drosophila Stock Center
Description	Embryonic and larval stage ubiquitous GAL4 expression (ITO *et al.* 1997; LANG *et al.* 2012) Utilised for knockdown (3.6.1, 3.6.2) studies.

Stock Name	*da*-GAL4
Lab Stock Number	RC-108C
Genotype	*w*; P{GAL4-da.G32}UH1*
Chromosome	1; 3
Source	Bloomington Drosophila Stock Center
Description	Embryonic, larval and adult stage ubiquitous GAL4 expression (WODARZ *et al.* 1995; LANG *et al.* 2012; PAIK *et al.* 2012). Utilised in knockdown (3.6.1, 3.6.2) studies.

Stock Name	*tubP*-GAL4
Lab Stock Number	RC-110C
Genotype	*y^1w*; P{tubP-GAL4}LL7/MKRS*
Chromosome	1; 3
Source	Bloomington Drosophila Stock Center
Description	Embryonic and adult stage ubiquitous GAL4 expression (LEE AND LUO 1999; LIU AND LEHMANN 2008). Utilised for knockdown (3.6.2) studies

6.4.2 Muscle-specific GAL4 Drivers

Stock Name	*Mef2*-GAL4
Lab Stock Number	RC-130
Genotype	*y^1w*; P{Mef2-GAL4}*
Chromosome	1; 3
Source	Gift from Barry Dickson, Research Institute of Molecular Pathology, Vienna, Austria
Description	Embryonic and larval stage muscle-specific GAL4 expression (LILLY *et al.* 1994). Utilised for knockdown (3.6.1, 3.6.2) studies.

Stock Name	*Mef2*-GAL4>Dicer-2
Lab Stock Number	MT-6
Genotype	*P{UAS-Dcr-2.D}1, w^{1118}; P{GAL4-Mef2.R}R1*
Chromosome	1; 3
Source	Bloomington Drosophila Stock Center
Description	Enhanced embryonic and larval stage muscle-specific GAL4 expression (LILLY *et al.* 1994). Utilised for knockdown (3.6.1, 3.6.2) studies.

Stock Name	*C179*-GAL4
Lab Stock Number	RC-101B
Genotype	*w*; P{GawB}c179*
Chromosome	1; 2
Source	Bloomington Drosophila Stock Center
Description	Embryonic and adult stage mesoderm and muscle-specific GAL4 expression (MANSEAU *et al.* 1997; PESAH *et al.* 2004). Utilised for knockdown (3.6.2) studies.

Stock Name	*how*-GAL4
Lab Stock Number	RC-111
Genotype	*w*; P{GawB}how^{24B}*
Chromosome	1; 3
Source	Bloomington Drosophila Stock Center
Description	Late embryonic, larval and adult stage somatic muscle-specific GAL4 expression (STAEHLING-HAMPTON *et al.* 1994; WODARZ *et al.* 1995; SCHUSTER *et al.* 1996). Utilised for knockdown (3.6.2) studies.

Stock Name	*C57*-GAL4
Lab Stock Number	RC-48
Genotype	*w*; P{GawB}C57*
Chromosome	1; 3
Source	Gift from Vivian Budnik, University of Massachusetts, USA
Description	Third instar larval stage somatic muscle-specific GAL4 expression (PACKARD *et al.* 2002). Utilised for knockdown (3.6.2) studies.

Stock Name	*G7*-GAL4
Lab Stock Number	RC-53B
Genotype	*w*; P{GAL4}G7/ In(2LR)Gla, wg[Gla-1] Bc[1]*
Chromosome	1; 2
Source	Gift from A. DiAntonio, Washington University, St. Louis, Missouri, USA
Description	Embryonic and larval stage somatic muscle-specific GAL4 expression (ARAVAMUDAN AND BROADIE 2003). Utilised for knockdown (3.6.2) studies.

Stock Name	*MHC*-GAL4
Lab Stock Number	RC-127B
Genotype	*P{Mhc-GAL4.K}1, w[*]/FM7c*
Chromosome	X
Source	Gift from Frank Schnorrer, University of Marseille, France
Description	Larval stage muscle-specific GAL4 expression (SCHNORRER 2014). Utilised for knockdown (3.6.2) studies.

Stock Name	*G14*-GAL4
Lab Stock Number	MT-132
Genotype	*w*; P{GAL4}G14/CyO*
Chromosome	1; 2
Source	Gift from Brian McCabe Columbia University, NY, USA
Description	Embryonic and larval stage somatic muscle-specific GAL4 expression (SHISHIDO *et al.* 1998; HAGHIGHI *et al.* 2003). Utilised for knockdown (3.6.2) studies.

6.4.3 Brain/neuron-specific GAL4 Drivers

Stock Name	*elav*-GAL4
Lab Stock Number	MT-116
Genotype	$P\{GawB\}elav^{C155}$
Chromosome	X
Source	Bloomington Drosophila Stock Center
Description	Embryonic, larval and adult stage pan-neuronal GAL4 expression (ZHANG *et al.* 2002; AGRAWAL *et al.* 2005; WANG *et al.* 2011). Utilised for knockdown (3.6.2) studies.

Stock Name	*elav*-GAL4>Dicer-2
Lab Stock Number	MT-1
Genotype	$P\{GawB\}elav^{C155}\ w^{1118}$; P{UAS-Dcr-2.D}2*
Chromosome	X; 2
Source	Bloomington Drosophila Stock Center

Description	Enhanced embryonic, larval and adult stage pan-neuronal GAL4 expression (ZHANG *et al.* 2002; AGRAWAL *et al.* 2005; WANG *et al.* 2011). Utilised for knockdown (3.6.1, 3.6.2) studies.

Stock Name	*1407*-GAL4
Lab Stock Number	RC-73B
Genotype	*w*; P{GawB}insc^{Mz1407}/ In(2LR)Gla, wg[Gla-1] Bc[1]*
Chromosome	1; 2
Source	Bloomington Drosophila Stock Center
Description	Embryonic, larval and adult stage pan-neuronal GAL4 expression (CONNOLLY *et al.* 1996; FERGESTAD AND BROADIE 2001; KRAFT *et al.* 2016). Utilised for knockdown (3.6.2) studies.

Stock Name	*OK6*-GAL4
Lab Stock Number	RC-126C
Genotype	P{GawB}*OK6/In(2LR)Gla, wg[Gla-1] Bc[1]*
Chromosome	2
Source	Gift from Cahir O'Kane, University of Cambridge, UK
Description	Embryonic, and larval stage motor neuron-specific GAL4 expression (LANDGRAF *et al.* 2003; MCCABE *et al.* 2004). Utilised for knockdown (3.6.2) studies.

Stock Name	*OK6*-GAL4>Dicer-2
Lab Stock Number	MT-124
Genotype	*P{UAS-Dcr-2.D}1 w^{1118}; P{GawB}OK6/CyO*
Chromosome	1; 2
Source	Gift from Cahir O'Kane, University of Cambridge, UK

Description	Enhanced embryonic, and larval stage motor neuron-specific GAL4 expression (LANDGRAF *et al.* 2003; MCCABE *et al.* 2004). Utilised for knockdown (3.6.2) studies.
Stock Name	*Nrv*-GAL4
Lab Stock Number	RC-103B
Genotype	*w*; P{nrv2-GAL4.S}8*
Chromosome	1; 3
Source	Gift from Paul Salvaterra, City of Hope National Medical Center, Duarte, California, USA.
Description	Embryonic, larval and adult stage pan-neuronal GAL4 expression (SUN *et al.* 1999). Utilised for knockdown (3.6.2) studies.
Stock Name	*D42*-GAL4
Lab Stock Number	RC-104
Genotype	*w*; P{GawB}D42*
Chromosome	1; 3
Source	Bloomington Drosophila Stock Center
Description	Larval and adult stage motor neuron-specific GAL4 expression (YEH *et al.* 1995; WITTMANN *et al.* 2001). Utilised for knockdown (3.6.2) studies.
Stock Name	*nSyb*-GAL4
Lab Stock Number	RC-165B
Genotype	*y[1] w*; P{nSyb-GAL4.S}3/In(2LR)Gla, wg[Gla-1] Bc[1]*
Chromosome	1; 3
Source	Gift from Brian McCabe Columbia University, NY, USA
Description	Adult stage pan-neuronal GAL4 expression (BUSHEY *et al.* 2009; YU *et al.* 2010). Utilised for knockdown (3.6.2) studies.

Stock Name	*Cha*-GAL4
Lab Stock Number	MT-125
Genotype	*w^{1118}; P{ChAT-GAL4.7.4}19B*
Chromosome	1; 2
Source	Bloomington Drosophila Stock Center
Description	Embryonic, larva and adult stage cholinergic neuron-specific GAL4 expression (BAINES *et al.* 2002; DANIELS *et al.* 2008; BOERNER AND DUCH 2010). Utilised for knockdown (3.6.2) studies.

Stock Name	*VGlut*-GAL4
Lab Stock Number	MT-126C
Genotype	*w^{1118}; P{GawB}VGlut^{OK371}*
Chromosome	1; 2
Source	Bloomington Drosophila Stock Center
Description	Larval and adult stage glutamatergic neuron-specific GAL4 expression(LEE AND THOMAS 2011). Utilised for knockdown (3.6.2) studies.

6.4.4 Other GAL4 Drivers

Stock Name	*GMR*-GAL4
Lab Stock Number	MT-42
Genotype	*w^{1118}; P{GMR-GAL4.w-}2/CyO*
Chromosome	1; 2
Source	Bloomington Drosophila Stock Center
Description	Larval stage eye disc post-photoreceptor GAL4 expression (DE HARO *et al.* 2010; KING *et al.* 2017). Utilised for knockdown (3.6.2) studies.

6.5 APPENDIX V: REFERENCES

Agrawal, N., J. Pallos, N. Slepko, B. L. Apostol, L. Bodai *et al.*, 2005 Identification of combinatorial drug regimens for treatment of Huntington's disease using Drosophila. Proc Natl Acad Sci U S A 102**:** 3777-3781.

Aravamudan, B., and K. Broadie, 2003 Synaptic Drosophila UNC-13 is regulated by antagonistic G-protein pathways via a proteasome-dependent degradation mechanism. J Neurobiol 54**:** 417-438.

Baines, R. A., L. Seugnet, A. Thompson, P. M. Salvaterra and M. Bate, 2002 Regulation of synaptic connectivity: levels of Fasciclin II influence synaptic growth in the Drosophila CNS. J Neurosci 22**:** 6587-6595.

Boerner, J., and C. Duch, 2010 Average shape standard atlas for the adult Drosophila ventral nerve cord. J Comp Neurol 518**:** 2437-2455.

Bushey, D., G. Tononi and C. Cirelli, 2009 The Drosophila fragile X mental retardation gene regulates sleep need. J Neurosci 29**:** 1948-1961.

Connolly, J. B., I. J. Roberts, J. D. Armstrong, K. Kaiser, M. Forte *et al.*, 1996 Associative learning disrupted by impaired Gs signaling in Drosophila mushroom bodies. Science 274**:** 2104-2107.

Daniels, R. W., M. V. Gelfand, C. A. Collins and A. DiAntonio, 2008 Visualizing glutamatergic cell bodies and synapses in Drosophila larval and adult CNS. J Comp Neurol 508**:** 131-152.

de Haro, M., I. Al-Ramahi, J. Benito-Sipos, B. Lopez-Arias, B. Dorado *et al.*, 2010 Detailed analysis of leucokinin-expressing neurons and their candidate functions in the Drosophila nervous system. Cell Tissue Res 339**:** 321-336.

European Society of Human, G., 2003 Data storage and DNA banking for biomedical research: technical, social and ethical issues. Eur J Hum Genet 11 Suppl 2**:** S8-10.

Fergestad, T., and K. Broadie, 2001 Interaction of stoned and synaptotagmin in synaptic vesicle endocytosis. J Neurosci 21**:** 1218-1227.

Haghighi, A. P., B. D. McCabe, R. D. Fetter, J. E. Palmer, S. Hom *et al.*, 2003 Retrograde control of synaptic transmission by postsynaptic CaMKII at the Drosophila neuromuscular junction. Neuron 39**:** 255-267.

Ito, K., W. Awano, K. Suzuki, Y. Hiromi and D. Yamamoto, 1997 The Drosophila mushroom body is a quadruple structure of clonal units each of which contains a virtually identical set of neurones and glial cells. Development 124**:** 761-771.

King, A. N., A. F. Barber, A. E. Smith, A. P. Dreyer, D. Sitaraman *et al.*, 2017 A Peptidergic Circuit Links the Circadian Clock to Locomotor Activity. Curr Biol 27**:** 1915-1927 e1915.

Kraft, K. F., E. M. Massey, D. Kolb, U. Walldorf and R. Urbach, 2016 Retinal homeobox promotes cell growth, proliferation and survival of mushroom body neuroblasts in the Drosophila brain. Mech Dev 142**:** 50-61.

Landgraf, M., N. Sanchez-Soriano, G. M. Technau, J. Urban and A. Prokop, 2003 Charting the Drosophila neuropile: a strategy for the standardised characterisation of genetically amenable neurites. Dev Biol 260**:** 207-225.

Lang, M., C. L. Braun, M. R. Kanost and M. J. Gorman, 2012 Multicopper oxidase-1 is a ferroxidase essential for iron homeostasis in Drosophila melanogaster. Proc Natl Acad Sci U S A 109**:** 13337-13342.

Lee, S. K., and G. H. Thomas, 2011 Rac1 modulation of the apical domain is negatively regulated by beta (Heavy)-spectrin. Mech Dev 128**:** 116-128.

Lee, T., and L. Luo, 1999 Mosaic analysis with a repressible cell marker for studies of gene function in neuronal morphogenesis. Neuron 22**:** 451-461.
Lilly, B., S. Galewsky, A. B. Firulli, R. A. Schulz and E. N. Olson, 1994 D-MEF2: a MADS box transcription factor expressed in differentiating mesoderm and muscle cell lineages during Drosophila embryogenesis. Proc Natl Acad Sci U S A 91**:** 5662-5666.
Liu, Y., and M. Lehmann, 2008 A genomic response to the yeast transcription factor GAL4 in Drosophila. Fly (Austin) 2**:** 92-98.
Manseau, L., A. Baradaran, D. Brower, A. Budhu, F. Elefant *et al.*, 1997 GAL4 enhancer traps expressed in the embryo, larval brain, imaginal discs, and ovary of Drosophila. Dev Dyn 209**:** 310-322.
McCabe, B. D., S. Hom, H. Aberle, R. D. Fetter, G. Marques *et al.*, 2004 Highwire regulates presynaptic BMP signaling essential for synaptic growth. Neuron 41**:** 891-905.
Packard, M., E. S. Koo, M. Gorczyca, J. Sharpe, S. Cumberledge *et al.*, 2002 The Drosophila Wnt, wingless, provides an essential signal for pre- and postsynaptic differentiation. Cell 111**:** 319-330.
Paik, D., Y. G. Jang, Y. E. Lee, Y. N. Lee, R. Yamamoto *et al.*, 2012 Misexpression screen delineates novel genes controlling Drosophila lifespan. Mech Ageing Dev 133**:** 234-245.
Pesah, Y., T. Pham, H. Burgess, B. Middlebrooks, P. Verstreken *et al.*, 2004 Drosophila parkin mutants have decreased mass and cell size and increased sensitivity to oxygen radical stress. Development 131**:** 2183-2194.
Schnorrer, F., 2014 New Mhc-GAL4 construct., pp., FlyBase.
Schuster, C. M., G. W. Davis, R. D. Fetter and C. S. Goodman, 1996 Genetic dissection of structural and functional components of synaptic plasticity. I. Fasciclin II controls synaptic stabilization and growth. Neuron 17**:** 641-654.
Shishido, E., M. Takeichi and A. Nose, 1998 Drosophila synapse formation: regulation by transmembrane protein with Leu-rich repeats, CAPRICIOUS. Science 280**:** 2118-2121.
Staehling-Hampton, K., P. D. Jackson, M. J. Clark, A. H. Brand and F. M. Hoffmann, 1994 Specificity of bone morphogenetic protein-related factors: cell fate and gene expression changes in Drosophila embryos induced by decapentaplegic but not 60A. Cell Growth Differ 5**:** 585-593.
Sun, B., P. Xu and P. M. Salvaterra, 1999 Dynamic visualization of nervous system in live Drosophila. Proc Natl Acad Sci U S A 96**:** 10438-10443.
Wang, W., W. Liu, Y. Wang, L. Zhou, X. Tang *et al.*, 2011 Notch signaling regulates neuroepithelial stem cell maintenance and neuroblast formation in Drosophila optic lobe development. Dev Biol 350**:** 414-428.
Wittmann, C. W., M. F. Wszolek, J. M. Shulman, P. M. Salvaterra, J. Lewis *et al.*, 2001 Tauopathy in Drosophila: neurodegeneration without neurofibrillary tangles. Science 293**:** 711-714.
Wodarz, A., U. Hinz, M. Engelbert and E. Knust, 1995 Expression of crumbs confers apical character on plasma membrane domains of ectodermal epithelia of Drosophila. Cell 82**:** 67-76.
Yeh, E., K. Gustafson and G. L. Boulianne, 1995 Green fluorescent protein as a vital marker and reporter of gene expression in Drosophila. Proc Natl Acad Sci U S A 92**:** 7036-7040.

Yu, J. Y., M. I. Kanai, E. Demir, G. S. Jefferis and B. J. Dickson, 2010 Cellular organization of the neural circuit that drives Drosophila courtship behavior. Curr Biol 20**:** 1602-1614.
Zhang, Y. Q., C. K. Rodesch and K. Broadie, 2002 Living synaptic vesicle marker: synaptotagmin-GFP. Genesis 34**:** 142-145.

6.6 APPENDIX VI: LIST OF PUBLICATIONS AND PRESENTATIONS

PEER-REVIEWED PUBLICATIONS

Borg R, Farrugia Wismayer M, Bonavia K, Farrugia Wismayer A, Vella M, van Vugt JJFA, Kenna BJ, Kenna KP, Vassallo N, Veldink JH, Cauchi RJ. Genetic analysis of ALS cases in the isolated island population of Malta. Eur J Hum Genet. 2021 Apr;29(4):604-614. doi: 10.1038/s41431-020-00767-9. Epub 2021 Jan 7. PMID: 33414559; PMCID: PMC8115635.

Farrugia Wismayer M, Borg R, Farrugia Wismayer A, Bonavia K, Vella M, Pace A, Vassallo N, Cauchi RJ. Occupation and amyotrophic lateral sclerosis risk: a case-control study in the isolated island population of Malta. Amyotroph Lateral Scler Frontotemporal Degener. 2021 Apr 6:1-7. doi: 10.1080/21678421.2021.1905847. Epub ahead of print. PMID: 33821701.

SYMPOSIA/SUMMITS

- 29th International Symposium on ALS/MND, 2018
- Virtual 31st International Symposium on ALS/MND, 2020
- University of Malta ALS/MND Summit, March 2021
- University of Malta ALS/MND Summit 2.0, September 2021

FUNDING

- 'Bjorn Formosa Scholarship for Advanced Research into ALS/MND' funded by the non-profit organization, ALS Malta Foundation, facilitated by the Research Trust (RIDT) of the University of Malta.
- Excellence in the Life Sciences (EMBO) short-term fellowship to visit Jan Herman Veldink's laboratory in Utrecht, The Netherlands.